



**HAL**  
open science

# Investigation of Polyhedral Oligomeric Silsesquioxanes for improved fire retardancy of hybrid epoxy-based polymer systems

Suzanne Laik

► **To cite this version:**

Suzanne Laik. Investigation of Polyhedral Oligomeric Silsesquioxanes for improved fire retardancy of hybrid epoxy-based polymer systems. Materials. INSA de Lyon, 2014. English. NNT : 2014ISAL0126 . tel-01149062

**HAL Id: tel-01149062**

**<https://theses.hal.science/tel-01149062>**

Submitted on 6 May 2015

**HAL** is a multi-disciplinary open access archive for the deposit and dissemination of scientific research documents, whether they are published or not. The documents may come from teaching and research institutions in France or abroad, or from public or private research centers.

L'archive ouverte pluridisciplinaire **HAL**, est destinée au dépôt et à la diffusion de documents scientifiques de niveau recherche, publiés ou non, émanant des établissements d'enseignement et de recherche français ou étrangers, des laboratoires publics ou privés.

N° d'ordre : 2014 ISAL 0126

Année 2014

Thèse

# INVESTIGATION OF POLYHEDRAL OLIGOMERIC SILSESQUIOXANES FOR IMPROVED FIRE RETARDANCY OF HYBRID EPOXY-BASED POLYMER SYSTEMS

Présentée devant  
L'Institut National des Sciences Appliquées (INSA) de Lyon

Pour obtenir le grade de  
Docteur

Ecole Doctorale Matériaux de Lyon  
Spécialité : Matériaux Polymères et Composites

Par  
**Suzanne LAIK**  
(Ingénieur Matériaux Polytech'Montpellier, Master of Sciences in Advanced Materials of Cranfield University)

Soutenue le 12 décembre 2014 devant la Commission d'Examen

Jury

<i>Referee</i>	Ivana Partridge	Professor, Faculty of Engineering, University of Bristol (UK)
<i>Referee</i>	Sophie Duquesne	Professor, UMET, Université de Lille (France)
<i>Examiner</i>	Giovanni Camino	Professor, Politecnico di Torino – Sede di Alessandria (Italy)
<i>Examiner</i>	Sophie Cozien-Cazuc	Doctor, Far-UK Ltd, Nottingham (UK)
<i>PhD supervisor</i>	Jocelyne Galy	Doctor, IMP UMR CNRS 5223, INSA Lyon (France)
<i>PhD supervisor</i>	Jean-François Gérard	Professor, IMP UMR CNRS 5223, INSA Lyon (France)



SIGLE	ECOLE DOCTORALE	NOM ET COORDONNEES DU RESPONSABLE
<b>CHIMIE</b>	<b>CHIMIE DE LYON</b> <a href="http://www.edchimie-lyon.fr">http://www.edchimie-lyon.fr</a>  Sec : Renée EL MELHEM Bat Blaise Pascal 3 <sup>e</sup> etage 04 72 43 80 46 Insa : R. GOURDON	<b>M. Jean Marc LANCELIN</b> Université de Lyon – Collège Doctoral Bât ESCPE 43 bd du 11 novembre 1918 69622 VILLEURBANNE Cedex Tél : 04.72.43 13 95 directeur@edchimie-lyon.fr
<b>E.E.A.</b>	<b>ELECTRONIQUE, ELECTROTECHNIQUE, AUTOMATIQUE</b> <a href="http://edeea.ec-lyon.fr">http://edeea.ec-lyon.fr</a>  Sec : M.C. HAVGOUDOUKIAN <a href="mailto:eea@ec-lyon.fr">eea@ec-lyon.fr</a>	<b>M. Gérard SCORLETTI</b> Ecole Centrale de Lyon 36 avenue Guy de Collongue 69134 ECULLY Tél : 04.72.18 60.97 Fax : 04 78 43 37 17 Gerard.scorletti@ec-lyon.fr
<b>E2M2</b>	<b>EVOLUTION, ECOSYSTEME, MICROBIOLOGIE, MODELISATION</b> <a href="http://e2m2.universite-lyon.fr">http://e2m2.universite-lyon.fr</a>  Sec : Safia AIT CHALAL Bat Darwin - UCB Lyon 1 04.72.43.28.91 Insa : H. CHARLES <a href="mailto:Safia.ait-chalal@univ-lyon1.fr">Safia.ait-chalal@univ-lyon1.fr</a>	<b>Mme Gudrun BORNETTE</b> CNRS UMR 5023 LEHNA Université Claude Bernard Lyon 1 Bât Forel 43 bd du 11 novembre 1918 69622 VILLEURBANNE Cédex Tél : 06.07.53.89.13 <a href="mailto:e2m2@univ-lyon1.fr">e2m2@univ-lyon1.fr</a>
<b>EDISS</b>	<b>INTERDISCIPLINAIRE SCIENCES-SANTE</b> <a href="http://www.ediss-lyon.fr">http://www.ediss-lyon.fr</a>  Sec : Safia AIT CHALAL Hôpital Louis Pradel - Bron 04 72 68 49 09 Insa : M. LAGARDE <a href="mailto:Safia.ait-chalal@univ-lyon1.fr">Safia.ait-chalal@univ-lyon1.fr</a>	<b>Mme Emmanuelle CANET-SOULAS</b> INSERM U1060, CarMeN lab, Univ. Lyon 1 Bâtiment IMBL 11 avenue Jean Capelle INSA de Lyon 696621 Villeurbanne Tél : 04.72.68.49.09 Fax :04 72 68 49 16 <a href="mailto:Emmanuelle.canet@univ-lyon1.fr">Emmanuelle.canet@univ-lyon1.fr</a>
<b>INFOMATHS</b>	<b>INFORMATIQUE ET MATHÉMATIQUES</b> <a href="http://infomaths.univ-lyon1.fr">http://infomaths.univ-lyon1.fr</a>  Sec :Renée EL MELHEM Bat Blaise Pascal 3 <sup>e</sup> etage <a href="mailto:infomaths@univ-lyon1.fr">infomaths@univ-lyon1.fr</a>	<b>Mme Sylvie CALABRETTO</b> LIRIS – INSA de Lyon Bat Blaise Pascal 7 avenue Jean Capelle 69622 VILLEURBANNE Cedex Tél : 04.72. 43. 80. 46 Fax 04 72 43 16 87 <a href="mailto:Sylvie.calabretto@insa-lyon.fr">Sylvie.calabretto@insa-lyon.fr</a>
<b>Matériaux</b>	<b>MATERIAUX DE LYON</b> <a href="http://ed34.universite-lyon.fr">http://ed34.universite-lyon.fr</a>  Sec : M. LABOUNE PM : 71.70 –Fax : 87.12 Bat. Saint Exupéry <a href="mailto:Ed.materiaux@insa-lyon.fr">Ed.materiaux@insa-lyon.fr</a>	<b>M. Jean-Yves BUFFIERE</b> INSA de Lyon MATEIS Bâtiment Saint Exupéry 7 avenue Jean Capelle 69621 VILLEURBANNE Cedex Tél : 04.72.43 71.70 Fax 04 72 43 85 28 <a href="mailto:Ed.materiaux@insa-lyon.fr">Ed.materiaux@insa-lyon.fr</a>
<b>MEGA</b>	<b>MECANIQUE, ENERGETIQUE, GENIE CIVIL, ACOUSTIQUE</b> <a href="http://mega.universite-lyon.fr">http://mega.universite-lyon.fr</a>  Sec : M. LABOUNE PM : 71.70 –Fax : 87.12 Bat. Saint Exupéry <a href="mailto:mega@insa-lyon.fr">mega@insa-lyon.fr</a>	<b>M. Philippe BOISSE</b> INSA de Lyon Laboratoire LAMCOS Bâtiment Jacquard 25 bis avenue Jean Capelle 69621 VILLEURBANNE Cedex Tél : 04.72 .43.71.70 Fax : 04 72 43 72 37 <a href="mailto:Philippe.boisse@insa-lyon.fr">Philippe.boisse@insa-lyon.fr</a>
<b>ScSo</b>	<b>ScSo*</b> <a href="http://recherche.univ-lyon2.fr/scso/">http://recherche.univ-lyon2.fr/scso/</a>  Sec : Viviane POLSINELLI Brigitte DUBOIS Insa : J.Y. TOUSSAINT <a href="mailto:viviane.polsinelli@univ-lyon2.fr">viviane.polsinelli@univ-lyon2.fr</a>	<b>Mme Isabelle VON BUELTZINGLOEWEN</b> Université Lyon 2 86 rue Pasteur 69365 LYON Cedex 07 Tél : 04.78.77.23.86 Fax : 04.37.28.04.48

\*ScSo : Histoire, Géographie, Aménagement, Urbanisme, Archéologie, Science politique, Sociologie, Anthropologie

---

# ACKNOWLEDGEMENTS

---

First of all, I would like to gratefully thank Prof. Ivana Partridge and Prof. Sophie Duquesne for accepting to refer this manuscript and allowing me to defend. I also acknowledge the examiners of the jury, Dr Sophie Cozien-Cazuc and Prof. Giovanni Camino, who accepted the chairmanship of the Examination Commission. I thank them all for the interest they showed for my work. I also take the opportunity to say (write) here that I was personally happy to defend before a jury where the parity was more than respected.

I sincerely and greatly acknowledge my supervisor, Jocelyne Galy, for her guidance during these three years, her help, support and her confidence in me. It was a great pleasure and enrichment to work with her, and she gave me the opportunity to take part to various congresses and external collaborations. I also thank my co-supervisor, Jean-François Gérard, who took the time to make useful corrections to this manuscript.

I would like to thank all the members of the Fire-Resist project, the Fire-Resistors, for their contribution to my work through useful discussions during scientific and technical meetings, or during conferences, always in a really nice and pleasant atmosphere. I dedicate special thanks to those partners I had the chance to collaborate with more closely:

- Gianni Camino and Marco Monti, from Politecnico of Torino and Proplast, respectively, for the nice discussions about our cone calorimeter results, for their availability and their kindness which made my stays in Alessandria so pleasant, and for their contribution to the full paper (not published to this day) and conference abstracts ;
- Sophie Cozien-Cazuc, formerly from Cytec, for her useful comments during scientific meetings, her help and kindness, and Ian Aspin, for his nice scientific collaboration and the mechanical experiments carried out at Cytec ;
- Patrik Fernberg and Spyros Tsampas, from Sicomp, for the useful discussions during the WP2 and WP4 meetings, as well as during conferences.
- Peter Nordström, from APC, for the production of composite parts from our polymer systems, and the nice collaboration it led to ;
- Per Blomqvist, for the cone calorimeter testing of the composite parts.

I also would like to acknowledge my colleagues from the laboratory IMP@INSA-Lyon for their help and kindness, either for the experiments or during useful scientific discussions about the techniques and the results obtained. They are almost as numerous as the number of people of our laboratory, so I will quote only a few people here: Nicolas Laforet and Damien Montarnal for

their help as concerns the NIRS, Aymeric Genest and Loïc Picard for their help with chemistry, Hynek Benes for its contribution to sol-gel and solid NMR experiments, Prof. Pascault for the nice discussions about phase separation, Guilhem Quintard and Julien Chatard for helping me carrying out some of my experiments. I greatly acknowledge Pierre Alcouffe, from the IMP@Lyon1 laboratory, for the SEM and TEM pictures, for his time, his work of great quality and the nice discussions it led to. I am not forgetting Isabelle Polo and Mallaouia Bengoua for the logistical (but not only) support.

Working in the IMP@INSA laboratory was a great pleasure, it meant three years of good and friendly atmosphere with nice moments – both inside and outside the laboratory – which contributed greatly to the completion of this work. Finally, I would like to thank all the people – colleagues, friends, family – who gave me their support, in very different ways but all valuables.



---

## ABSTRACT

---

Thermoset polymer composite materials are used in a number of application domains, amongst which the transport sector, but they suffer from poor fire resistance which limits their use for obvious safety and security issues. With the increasingly demanding restrictions from the European Commission, there is a real need to seek for alternative solutions. Recent studies have found the Polyhedral Oligomeric Silsesquioxane (POSS) compounds promising as fire retardant agents, particularly the POSS bearing phenyl ligands. The present work aimed at investigating how the fire retardancy of hybrid epoxy networks can be improved by incorporating Polyhedral Oligomeric Silsesquioxanes (POSS).

In this study, the nature of the epoxy-amine comonomers was varied, as well as the POSS structure. An inert POSS and two multifunctional POSS were selected in order to generate various morphologies. The aim was to answer the question: does a structure-property relationship exist as concerns the fire behaviour of epoxy networks? Particular attention was dedicated to systems containing the trisilanolphenyl POSS (POSSOH) for which different processes of dispersion were implemented.

The POSS dispersion state was shown to be greatly influenced by the type of POSS ligands, but also by the epoxy prepolymer nature in the case of the versatile POSSOH. In particular, intricate, never-observed morphologies were discovered in the networks based on Tetraglycidyl(diaminodiphenyl) methane (TGDDM) and containing POSSOH. The study of functional POSS-involving interactions and epoxy-amine kinetics in the model systems revealed the high catalytic power of the combined presence of POSSOH and an aluminium-based catalyst in the model epoxy networks, as well as the occurrence of homopolymerisation. The thermo-mechanical properties were not significantly modified by the addition of POSS. Finally, spectacular improvements in fire retardancy were obtained in some cases, in particular when the POSSOH and the Al-based catalyst were introduced in combination. The fire protection mechanism was attributed to intumescence in the TGDDM-based networks. The addition of POSSOH and the Al-catalyst was found to be efficient in all the epoxy-amine network types, which could not be clearly related to the POSSOH structures but was rather attributed to a chemical synergistic effect.



---

# CONTENTS

---



---

<b>GENERAL INTRODUCTION.....</b>	<b>15</b>
----------------------------------	-----------

---

<b>CHAPTER I.FIRE BEHAVIOUR OF THERMOSET POLYMERS: CURRENT SITUATION AND NEW SOLUTIONS .....</b>	<b>19</b>
--	-----------

---

<b>1. INTRODUCTION – FIRE AND NEEDS IN FIRE RETARDANTS: DAMAGES AND REGULATIONS .....</b>	<b>20</b>
<b>2. GENERALITIES ON FIRE, FIRE TESTING AND CONVENTIONAL FIRE RETARDANTS.....</b>	<b>21</b>
2.1. Combustion, flame and fire in polymers .....	21
2.1.a. <i>Thermolysis.....</i>	22
2.1.b. <i>Ignition and flame spread .....</i>	24
2.1.c. <i>Extinguishment and char production .....</i>	26
2.2. Means to investigate the fire behaviour of polymers.....	27
2.2.a. <i>Different tests for different purposes.....</i>	27
2.2.b. <i>Focus on UL94 and cone calorimeter tests: characteristics and correlations.</i>	28
2.2.c. <i>Thermal stability assessed via Thermogravimetric Analysis (TGA).....</i>	35
2.3. Intrinsic flammability of polymers.....	37
2.4. Conventional flame retardants.....	38
2.4.a. <i>Modes of action.....</i>	39
2.4.b. <i>Fire retardants for epoxies .....</i>	42
2.4.c. <i>Regulations and restrictions for conventional flame retardant compounds ....</i>	43
<b>3. POLYSILSESQUIOXANES: A FIRE-RETARDANT ALTERNATIVE FOR EPOXY/AMINE NETWORKS?.</b>	<b>44</b>
3.1. Epoxy networks and Polysilsesquioxanes: an introduction .....	44
3.1.a. <i>Epoxy networks.....</i>	44
3.1.b. <i>Polysilsesquioxane compounds .....</i>	45

3.2.	Epoxy networks fire retarded with silicon-based compounds .....	47
3.2.a.	<i>Silicon-based nanoclays for fire retardancy of epoxy networks</i> .....	48
3.2.b.	<i>Epoxy networks containing silica-based glass domains</i> .....	50
3.2.c.	<i>Cage-structure polysilsesquioxanes: a promising route towards flame retardancy?</i> .....	54
3.2.d.	<i>POSS used in synergy with other elements</i> .....	60
<b>4.</b>	<b>CONCLUSION</b> .....	<b>62</b>

---

**CHAPTER II. POSS-CONTAINING THERMOSET NETWORKS: PROCESSING AND ASSESSING THE MORPHOLOGY** .....

---

<b>1.</b>	<b>MATERIALS</b> .....	<b>64</b>
1.1.	Model systems.....	64
1.1.a.	<i>Selected epoxy prepolymers and comonomers</i> .....	64
1.1.b.	<i>Epoxy-amine crosslinking reactions</i> .....	66
1.2.	Commercial epoxy system.....	67
1.3.	Polyhedral Oligomeric Silsesquioxane specifications.....	68
1.4.	An aluminium-based catalyst .....	70
<b>2.</b>	<b>PROCESSING THE NEAT AND HYBRID EPOXY NETWORKS</b> .....	<b>70</b>
2.1.	Preparation of epoxy-based reactive systems.....	70
2.1.a.	<i>Reference epoxy networks</i> .....	70
2.1.b.	<i>POSS-containing epoxy networks</i> .....	71
2.2.	Curing, composition, and nomenclature.....	72
<b>3.</b>	<b>MORPHOLOGIES OF FULLY-CURED MODEL EPOXY-AMINE NETWORKS</b> .....	<b>73</b>
3.1.	Non-reactive POSS .....	73
3.2.	Functionalized POSS.....	76
3.2.a.	<i>Networks containing PhenylAminoPropyl POSS</i> .....	76
3.2.b.	<i>Networks containing triSilanolPhenyl POSS</i> .....	77
<b>4.</b>	<b>MORPHOLOGY DEVELOPMENT IN THE POSS-CONTAINING NETWORKS THROUGH CURE</b> .....	<b>87</b>
4.1.	Reaction Induced Phase Separation phenomena .....	87

4.2. Investigation of the morphology development during cure in the TM-POSSOH-Al system.....	90
<b>5. CONCLUSIONS ON THE NETWORKS' MORPHOLOGIES.....</b>	<b>93</b>
<hr/>	
<b>CHAPTER III.FUNCTIONAL POSS IN THE MODEL EPOXY NETWORKS: DEVELOPMENT OF INTERACTIONS DURING THE PROCESS AND WITHIN THE FULLY-CURED NETWORKS .....</b>	<b>95</b>
<hr/>	
<b>1. DEVELOPMENT OF REACTIVE POSS INTERACTIONS DURING CURE AND INFLUENCE ON THE DGEBA-BASED MODEL NETWORK BUILD-UP MECHANISM.....</b>	<b>96</b>
1.1. N-phenylaminopropyl POSS as a crosslinker in the epoxy network.....	97
1.2. Trisilanolphenyl POSS and aluminium-based catalyst: influence on the epoxy-amine crosslinking reactions .....	101
1.2.a. <i>Background on the use of silanol-containing compounds and metallic catalysts in epoxy systems.....</i>	<i>101</i>
1.2.b. <i>Study of reactions between POSSOH-DGEBA.....</i>	<i>104</i>
1.2.c. <i>Influence of POSSOH and aluminium acetate catalyst on the polymerization of a DGEBA-MDEA system.....</i>	<i>107</i>
<b>2. POSS-INVOLVING INTERACTIONS IN THE FINAL-STATE NETWORKS.....</b>	<b>121</b>
2.1. Dynamic Mechanical Analysis (DMA).....	121
2.2. Indirect analysis via SEC.....	123
2.3. Solid state <sup>29</sup> Si Nuclear Magnetic Resonance (NMR).....	124
<b>3. CONCLUSION.....</b>	<b>126</b>
<hr/>	
<b>CHAPTER IV.DEGRADATION AND FIRE BEHAVIOUR OF ORGANIC/INORGANIC HYBRID POLYMER MATERIALS.....</b>	<b>129</b>
<hr/>	
<b>1. PRELIMINARY CONSIDERATIONS ON TECHNIQUES AND DATA TREATMENT .....</b>	<b>130</b>
<b>2. THERMAL STABILITY AND FIRE BEHAVIOUR OF EPOXY-AMINE NETWORKS: COMPARISON OF THREE NEAT MATRICES .....</b>	<b>131</b>
<b>3. THERMAL DEGRADATION AND FIRE BEHAVIOUR OF HYBRID ORGANIC/INORGANIC NETWORKS ...</b>	<b>134</b>

3.1.	Networks containing poorly-dispersed non-functional POSS (iOPOSS).....	135
3.2.	Networks containing functional POSS dispersed at a molecular scale (AmPOSS).... .....	137
3.3.	The particular case of POSSOH: degradation and fire behaviour of epoxy networks of different natures .....	140
	3.3.a. <i>Influence of the dispersion process</i> .....	140
	3.3.b. <i>Influence of the addition of an aluminium-containing catalyst – effect of the nature of the epoxy matrix</i> .....	143
<b>4.</b>	<b>CONCLUSION</b> .....	<b>152</b>
<hr/>		
	<b>CHAPTER V.CASE STUDY: POSSOH AS A FIRE RETARDANT FOR A COMPLEX THERMOSET/THERMOPLASTIC FORMULATION</b> .....	<b>155</b>
<hr/>		
<b>1.</b>	<b>PROCESS OF PHASE SEPARATION IN A THERMOSET/THERMOPLASTIC BLEND</b> .....	<b>158</b>
<b>2.</b>	<b>SELECTION OF MATERIALS AND PREPARATION OF PEI-CONTAINING EPOXY NETWORKS</b> .....	<b>161</b>
2.1.	Materials.....	161
2.2.	Preparation of PEI-containing epoxy networks.....	163
	2.2.a. <i>PEI percentage in the networks and stoichiometric ratio</i> .....	163
	2.2.b. <i>Preparation of TGDDM/Curative Fibre-based networks and the reference systems</i> .....	164
<b>3.</b>	<b>THERMAL AND MORPHOLOGICAL CHARACTERISATION</b> .....	<b>168</b>
3.1.	Influence of the Curative Fibre content on the glass-transition temperature of the TCF networks .....	168
3.2.	Phase separation in thermoset/thermoplastic blends .....	171
	3.2.a. <i>Influence of the PEI content on the phase separation and inversion phenomena in PEI-containing epoxy networks</i> .....	172
	3.2.b. <i>Influence of the introduction of POSSOH and Al catalyst on the phase separation and inversion phenomena in PEI-containing epoxy networks</i> .....	173
<b>4.</b>	<b>INVESTIGATION OF THERMAL STABILITY AND FIRE RETARDANCY OF A COMPLEX THERMOSET/ THERMOPLASTIC FORMULATION CONTAINING POSS</b> .....	<b>180</b>
4.1.	Influence of the Curative Fibre on the thermal stability and the fire performance of epoxy networks.....	180

4.2. Influence of additives on the thermal stability and the fire performance of epoxy networks.....	183
<b>5. CONCLUSION.....</b>	<b>185</b>
<hr/>	
<b>CONCLUSIONS AND OUTLOOKS .....</b>	<b>189</b>
<hr/>	
<b>APPENDIX A – EXPERIMENTAL TECHNIQUES.....</b>	<b>195</b>
<hr/>	
<b>APPENDIX B – COMPLEMENTARY RESULTS RELATED TO TGDDM-BASED NETWORKS .....</b>	<b>199</b>
<hr/>	
<b>APPENDIX C – CALIBRATION AND COMPLEMENTARY RESULTS RELATED TO THE NIRS PRESENTED IN CHAPTER III .....</b>	<b>202</b>
<hr/>	
<b>APPENDIX D – RESULTS RELATED TO COMPOSITES BASED ON EPOXY FORMULATIONS .....</b>	<b>206</b>
<hr/>	
<b>EXTENDED ABSTRACT IN FRENCH .....</b>	<b>217</b>
<hr/>	
<b>REFERENCES.....</b>	<b>241</b>
<hr/>	



---

## GENERAL INTRODUCTION

---

Over the last century, the use of synthetic polymers has kept increasing and they are now part of most of the consumer goods, but also find applications in very specific domains. In particular, their use as matrices in composite parts in the transport sector has gathered growing interest over the last decades as such materials allow considerable weight savings with improved stiffness, chemical and fatigue resistance. Their use is thus highly desirable as it allows fuel efficiency and sustainability as compared to conventional steel and aluminium structures, which results in more economical and environmentally friendly vehicles.

There is, however, one major factor hindering the more widespread use of composites in transport: their lack of adequate fire performance. Fires in vehicles often lead to catastrophic consequences, both on the human and economic point of view. Vehicles often constitute a closed environment where flash-over – fully developed fire – is a non-survivable condition. The main strategy thus consists of delaying the flash-over to provide the passengers with sufficient time to evacuate. One has to note though that evacuation times are usually short in vehicles (such as aircraft) as compared to buildings for which other strategies, e.g. compartmenting or fire fighting, are implemented.

Polymers for composite matrices are selected for their mechanical and chemical properties, and processability. One example of a multipurpose material among the thermoset polymers is epoxy resin. The issue of the missing fire-retardant property of such polymers has been tackled through the use of conventional fire retardants, including additives and chemically modified comonomers, that can, however, be detrimental for other material properties in certain cases. As research on the subject progressed, studies have highlighted issues of human and environmental toxicity for certain of these fire retardants, leading to an evolution of the legislation towards more drastic directives. Therefore, there is still nowadays a need for efficient, economic, safe, and environmentally friendly fire-retardant solutions. As a consequence, intensive scientific research has been carried out on seeking new fire retardants, but also understanding better the combustion phenomenon in polymers. Inorganic compounds

in particular have attracted growing interest as fire retardants, with promising results but also issues e.g. in processability, that still remain to be addressed.

The work presented here was incorporated within the framework of a FP7-NMP project funded by the European Commission – FP7 = Seventh Framework Programme and NMP = Nanosciences, Nanotechnologies, Materials and New Production Technologies. This project, called “Fire-Resist: Developing Novel Fire-Resistant High Performance Composites”, is registered under the project reference 246037 within the subprogramme NMP-2009-2.5-1: Light high-performance composites.

The Fire-Resist project general aim is to develop novel fire-resistant high performance composites for the transport sector. The project is sub-divided into eight workpackages (WP), either aiming at developing new fire-retardant materials, or related to fire modelling, upscaling of the materials developed in the four first WP, assessing the innovation risks and environmental impacts, and disseminating the results in the scientific community. In particular, the present study is related to the WP2 and WP4, whose objectives are:

- WP2: developing hybrid thermoset composites that provide a step-change improvement in fire behaviour;
- WP4: developing particle-doped polymer fibres for fire-retarded commingled composites.

The project includes many partners from both industrial and academic fields, which allows to combine varied expertise areas:

- material researchers and developers: *University of Newcastle*, UK (coordinator, material research and modelling); *INSA-Lyon*, France (polymer science and technology); *Proplast*, Italy (polymer science and technology); *Gaiker*, Spain (polymer and composite science and technology), *Swerea SICOMP*, Sweden (polymer composite research); *TransFurans Chemicals*, Belgium (furan resins);
- composite manufacturers: *Cytec Industrial Materials*, UK (formulation and prepregs); *Amorim Cork Composites*, Portugal (cork-containing composites); *Anthony, Patrick and Murta Exportação*, Portugal (composite production); *APC composites* (composite production);
- end-users of the transport sectors: *EADS-Innovation Works*, Germany (aeronautics); *Bombardier*, UK (railway); *Flensburger Schiffbau-Gesellschaft*, Germany (maritime); *Germanischer Lloyd*, Germany (ship quality and safety);

- fire expertise, risk and environment assessment: *BALance Technology Consulting*, Germany (risk and environment assessment); *SP*, Sweden (technical evaluation, testing and certification); *VTT*, Finland (fire safety, modelling).

In the framework of the present study, closer collaboration was developed with Proplast as concerns fire testing; with APC, who manufactured the composite materials based on certain formulations developed at INSA-Lyon; with Cytec, who performed the mechanical tests on the composite materials but also provided the epoxy prepolymers; with SP, who performed fire testing on the composite materials.

In this work, focus was placed on epoxy/amine-based systems which will be used as matrices for carbon fibre-based materials. Two model systems and one commercial formulation were investigated. One model system was based on the most used epoxy type, the Diglycidyl Ether of Bisphenol A (DGEBA), both for industrial applications and in the scientific research field. The other model system was designed for high performance structural composite matrices and was based on the Tetraglycidyl(diaminodiphenyl)methane (TGDDM) prepolymer. In addition, the most promising solutions developed in the model systems were implemented in a commercial formulation designed for structural composite parts produced by the infusion process. Finally, a fourth system consisting of a high T<sub>g</sub> thermoplastic-modified epoxy system was examined. The solution implemented to achieve good fire retardancy of these formulations consisted of the addition of organic/inorganic compounds, namely the Polyhedral Oligomeric Silsesquioxanes (POSS). Introducing inorganic objects in polymers has proved to be an interesting way towards the improvement of their fire retardancy. The interest of POSS, as compared to other inorganic fillers, relies on the versatility of its organic parts. From an appropriate selection of the POSS architecture, the dispersion of POSS in the organic matrix could be enhanced and/or strong interactions with the polymer could be generated via functional groups, allowing the control of the morphology of the networks. In this framework, the main objectives of the study consisted of:

- assessing the influence of the POSS type and experimental conditions on the morphology developed within the epoxy/amine networks, and understanding the interactions POSS/polymer matrix;
- analyzing and understanding the fire behaviour of the produced networks and how it is influenced by the chemical structure of POSS and/or the morphology of the networks.

The present report proceeds in five main parts. Chapter I is aimed at providing the reader with a general background on polymers and fire. It will be structured as follows: after a brief introduction justifying the need for novel fire-retardant solutions, a first part will be dedicated to the description of the fire phenomenon in polymers and the way implemented nowadays to evaluate it. Considerations about the intrinsic flammability of polymers and the ways conventionally used to fire retard them will also be expounded in this part. A second main section will aim at providing information on the polysilsesquioxanes and the introduction of silicon-based additives in epoxy-based polymers as alternative fire-retardant solutions.

After this introductory chapter, experimental results will be reported. In chapter II, the materials and process implemented to produce hybrid POSS-containing epoxy networks will be detailed, and the morphology obtained in the final materials will be examined. The development of the morphology will be considered, both through theoretical and experimental approaches.

Because complex systems were studied where the use of reactive compounds – epoxy, crosslinking agent, functional POSS – offered a range of possibilities in terms of reactions, Chapter III will focus on the interactions developing between the different system constituents.

Chapter IV will be related to the heart of the study with the results on the thermal stability and fire behaviour of the systems presented in Chapter II, with an insight on the mode of fire protection for the most promising systems.

Finally, the Chapter V constitutes an independent study focused on thermoplastic/epoxy networks. After detailing the material and processes, considerations on phase separation and morphology will be presented and eventually the fire behaviour will be examined.

Appendices will come as a support, with a first one detailing the techniques implemented (devices and parameters), the second and the third presenting experimental results that were not included in the chapters, while the fourth appendix is dedicated to the results that were obtained on composite materials.

---

**CHAPTER I. FIRE BEHAVIOUR OF THERMOSET  
POLYMERS: CURRENT SITUATION  
AND NEW SOLUTIONS**

---

## **1. INTRODUCTION – FIRE AND REQUIREMENTS IN FIRE RETARDANTS: DAMAGE AND REGULATIONS**

Fire is a well-known phenomenon that results from the rapid exothermic oxidation of a material, in presence of an oxidizer – usually oxygen from air – and a source of energy. The combustion occurs when certain conditions are achieved: a close-to-stoichiometry oxidizer/combustible ratio, a quantity of energy equal or superior to the flash point of the oxidizer/combustible mixture, and an exothermic chain reaction able to sustain the flame. Combustion is characterized by a large heat release, leading to high temperatures, the presence of a flame and emission of smokes resulting from the degradation of the material under gas and particles. The most remarkable phenomena in a fire may be the light and heat produced, but one must keep in mind that smokes are usually the major risk when living beings are involved in a fire scenario. Due to their toxicity and opacity, smokes can provoke death or sequelae by suffocation or poisoning, and/or prevent people from escaping, respectively.

Arguing about the needs in flame retardants is not needed anymore: the damage, on the human, environmental and economic aspects, is obvious and generally accepted. The European Fire Retardant Association (EFRA) reports 12 deaths and over 120 injuries related to fire in Europe every day, and the World Health Organisation recorded about 300.000 related-to-fire deaths per year in the world [1]. However, the collection of data regarding death, injuries and economic weight of fire is still not harmonized between countries and assessing the fire risks remains a delicate issue.

Fire protection can be classified in three categories: (i) the fire prevention, which involves education of public, owners and users, and means to reduce the fire risks by displaying the emergency procedures or suppressing ignition sources; (ii) the passive fire protection, which aims at limiting the fire ignition and spread by using fire-retardant materials and/or compartmenting the space in order to allow more time for evacuation; (iii) the active fire protection, which consists of all automated or manual means to fight a fire, such as the fire detection systems, firefighting through fire sprinklers, fire extinguishers or firemen intervention. Using fire retardants is thus part of the passive fire protection strategy. It is adopted in almost all applications domains involving flammable materials. Certain sectors are most subjected to fire risks. This is the case for materials in electronics applications, or in the building sector where many situations can be the starting point of a fire scenario. The demand in fire retardants is then the highest in these sectors.

Regulations about fire protection remain disparate between countries. They also depend strongly on the targeted application domain, because the requirements are not the same –

different evacuation times, different concentrations of people. More global regulations have arisen lately in certain domains such as the transport sector, where the heterogeneity of legislation between countries can be a problem given the policy of free movement of goods and persons in Europe. For example, the European directive 95/28/EC gives specifications concerning the burning behaviour of interior materials in certain motor vehicle categories [2]. Regulations on the fire retardants chemical compounds, from a health and environmental point of view, also exist at the European level, with the European regulation REACH – Regulation, Evaluation, Authorisation and Restriction of Chemicals – in particular.

The present chapter is not intended to be an exhaustive review of the fire behaviour and retardancy of all materials, but rather aims at providing the reader with relevant information for a better understanding of the next chapters. Generalities on fire, fire testing and current fire-retardant solutions will be presented, before focusing on the particular case of epoxy-based materials. In particular, existing works dealing with the use of Polyhedral Oligomeric Silsesquioxanes (POSS) and related compounds as fire retardants in epoxy polymers will be investigated in order to provide a background for the work carried out in the present study.

## 2. GENERALITIES ON FIRE, FIRE TESTING AND CONVENTIONAL FIRE RETARDANTS

### 2.1. COMBUSTION, FLAME AND FIRE IN POLYMERS

A fire is characterized by a succession of phases that can be defined through the temperature profile, as a function of time (Figure I-1). A fire always comprises a time during which no flame is present, i.e. before the ignition, a short low-combustion phase, followed by the flash-over and the fully developed fire characterized by a high temperature plateau, and finally extinguishment, with a possible glowing of embers.

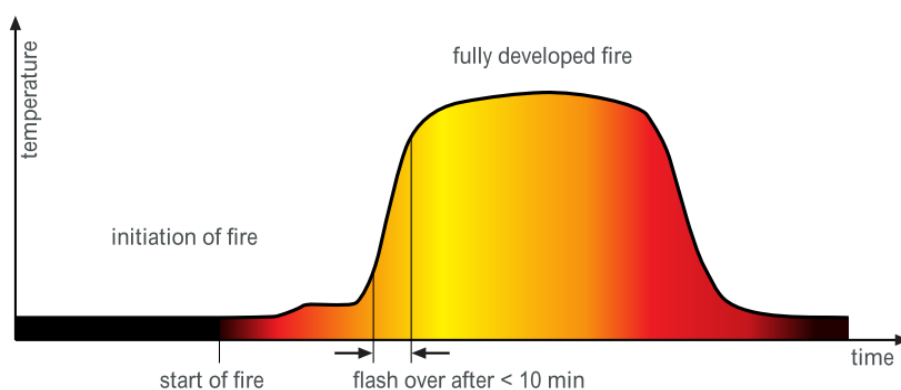


Figure I-1 Fire scenario as observed from its temperature profile [3]

The combustion of a material is a complex phenomenon that involves thermal, chemical, and fluid dynamics processes. Fire is an association of mechanisms occurring both in the condensed phase and in the gas phase (Figure I-2). The processes detailed thereafter are involved in the combustion of most materials, but they will be treated here from the point of view of polymer materials. The steps of the fire process described in the boxes (a) and (b) in Figure I-2 will be discussed in further details in the next subsections 2.1.a. and 2.1.b. , respectively.

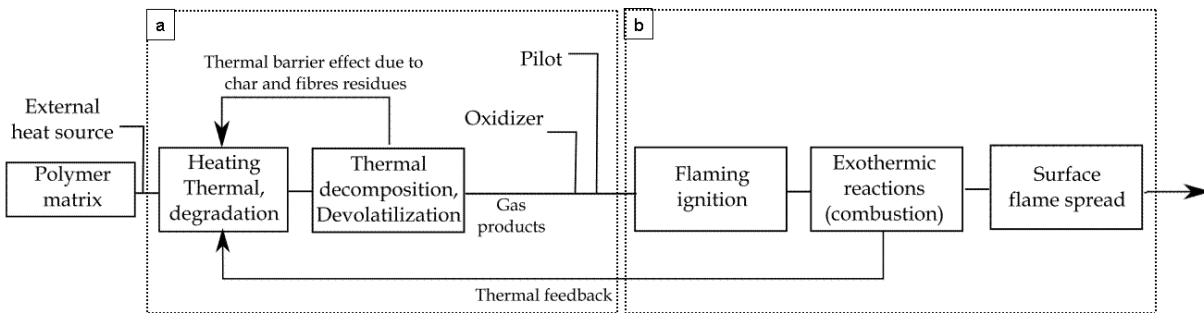
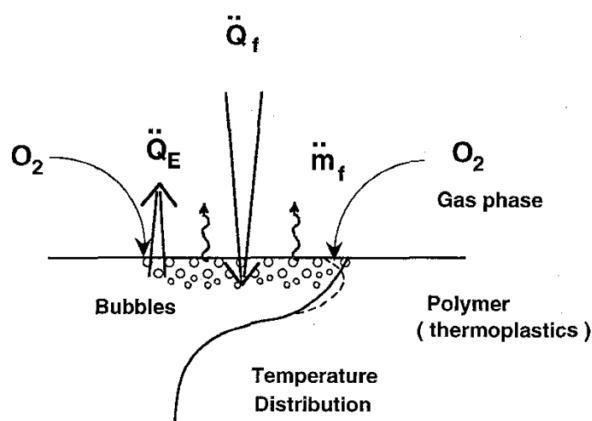


Figure I-2 General reaction to fire processes of polymers [4]

### 2.1.a. Thermolysis

The process of combustion starts in the solid phase with the decomposition and degradation of the material due to energy absorption of the material from an external heat source. This stage, the thermolysis, occurs when the polymer reaches a high temperature. Various chemical processes – such as random or end-chain scission, elimination of pendant groups or crosslinking – are involved which then influence greatly the combustion processes [4], [5].

Thermolysis results in the production of – more or less – small fragments of polymers, leading to: (i) production of flammable volatiles and radicals that migrate to the gas phase and will then act as combustibles for the flame ; (ii) a decrease of the solid phase viscosity through the breakage of polymer chains, which will help the volatiles reaching the surface faster and possibly cause dripping of the material ; (iii) production of a carbonaceous char, stable until reaching higher temperatures and mainly due to crosslinking of small molecules in polyaromatic arrays [6], [7]. A schematic illustration of the gasification of a thermoplastic polymer can be found in Figure I-3.



**Figure I-3 Gasification of a thermoplastic polymer subjected to heat ( $Q_f$ ) in presence of oxygen. The solid and the dash lines represent the temperature profile through the thickness of an opaque and diathermic material, respectively [6]**

The thermolysis can be either oxidative or purely thermal (pyrolysis), depending on whether the material decomposes in presence of oxygen or not, respectively. In most of the real cases of fire, the thermolysis starts in an oxidative media, at the surface of the polymer, where oxygen from air is present. However, when the decomposition front reaches the inside of the material, as the temperature rises due to thermal conduction in the sample, the oxygen is less and less present, also because the production of volatiles tends to blow the oxygen away from the decomposition zone. Stuetz and al. [8] investigated the presence of oxygen at the surface of a burning sample of polypropylene and found a well-defined oxygen-containing layer developed under the material surface, contributing to a certain amount of oxidative decomposition inside the material. However, similar experiments conducted by Brauman [9], on polypropylene, showed that this was likely to be a measurement artefact, as he also observed this oxygen-rich layer in quenched samples subjected to pyrolysis under nitrogen atmosphere, i.e. where oxygen should not be present. Nevertheless, he acknowledged the role of oxygen in combustion or thermolysis under air as a promoter for the thermal degradation at the sample surface. An interesting point is that he did not find this correspondence between the combustion behaviour and the presence or not of oxygen for PMMA samples, leading to the conclusion that not in all polymers has the oxygen an influence on the degradation pathways.

The thermolysis occurring during the combustion of polymers can then be regarded as a complex combination of thermal and oxidative decomposition, which is highly dependent on the polymer chemistry.

### 2.1.b. Ignition and flame spread

- Ignition and gas phase mechanisms

Firstly, ignition will occur when two conditions are fulfilled: (i) the concentration of flammable volatiles above the surface sample must be comprised between the Low Flammability Limit (LFL) and the Upper Flammability Limit (UFL); (ii) the external heat source must provide either enough thermal energy to set fire to the oxygen-volatiles mixture, thus carrying it at a temperature at least equal to its flashpoint, or a rich source of radicals, e.g. a flame or a spark.

Depending on the polymer chemistry – nature of bonds, presence of heteroatoms – the mechanisms involved in the gas phase will differ. Generally, the reactions are exothermic and allow for the flame to self-sustain by feeding back the material with energy, which leads to the formation of more fuel volatiles. The gases produced by the thermolysis are generally highly reactive, radical volatiles that produce radiative energy by reacting with oxygen (Figure I-4).

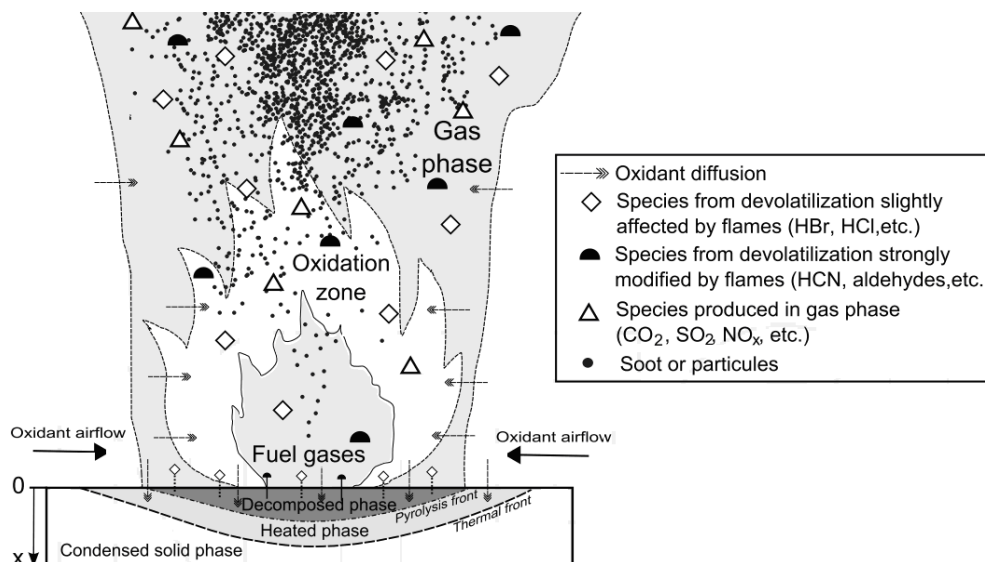


**Figure I-4 Schematic representation of a flame: reactive gaseous species from devolatilization process of solid phase, feeding the flame after ignition [4]**

- Parameters influencing the time to ignition and the flame spread

The ignition of a polymer and the flame spread will depend on various intrinsic and extrinsic parameters, i.e. specific of the material or external, respectively.

The ignition time will depend on the capacity of the material to absorb the energy from the heat source. A high absorption coefficient will result in heating quickly the surface layer of the material, leading to a fast degradation and production of volatiles, and thus a short time of

ignition. On the contrary, a low absorption coefficient will favour a slow heating of the polymer over a larger depth, thus reducing the time to ignition [6].

The concentration of oxygen which is controlled by the gas flux – usually the speed of air wind or ventilation – will be determining for ignition and for flame spread and feed. Stuetz et al. evidenced the influence of oxygen-related extrinsic parameters in a model configuration on the behaviour of a diffusion flame [10]. They also demonstrated the influence of these parameters, i.e. the oxygen concentration, the air flow direction as compared to the fuel stream direction – which can be related to the fire configuration – and the sample diameter in the case of cylindrical polymer samples [11]. In particular, they defined the flammability of a polymer as the combination of its intrinsic combustibility resulting from its chemical structure, and the interference of external parameters. In other words, the fire configuration and environment will have a strong effect on the combustion behaviour.

Another physical intrinsic parameter involved in the process of combustion is the viscosity of the molten/degraded polymer when it reaches high temperatures. This factor will play two roles: it will control the diffusion coefficient of low molar mass species in the molten state of the polymer, and determine the propensity of the material to drip. Kashiwagi et al. studied the gasification in a thermoplastic material as a function of heat flux and oxygen content of the surrounding atmosphere [12]. They found that increasing the oxygen concentration decreased the viscosity of the molten polymer and increased the mass flux of degradation volatiles. One of their conclusions was that bubbling is an important mass transfer mechanism that cannot be expressed simply as a function of the surface temperature, but depends on various intrinsic and extrinsic parameters. On the other side, viscosity of the heated material controls dripping, which constitutes another type of flame spread mechanism. One can easily understand that the lower the viscosity of the degraded polymer, the higher its tendency to drip. However, whether the dripping is beneficial or not is not so obvious. A polymer releasing flaming drops will enhance the propagation of fire by igniting surrounding materials. On the other side, a polymer releasing non-flaming drops will not propagate the fire, and the dripping will allow it to evacuate heat and potential fuel material that would have fed the flame instead.

Finally, the propagation of the flame will depend on the orientation of the burning material. Different scenaria are possible, as depicted in Figure I-5.

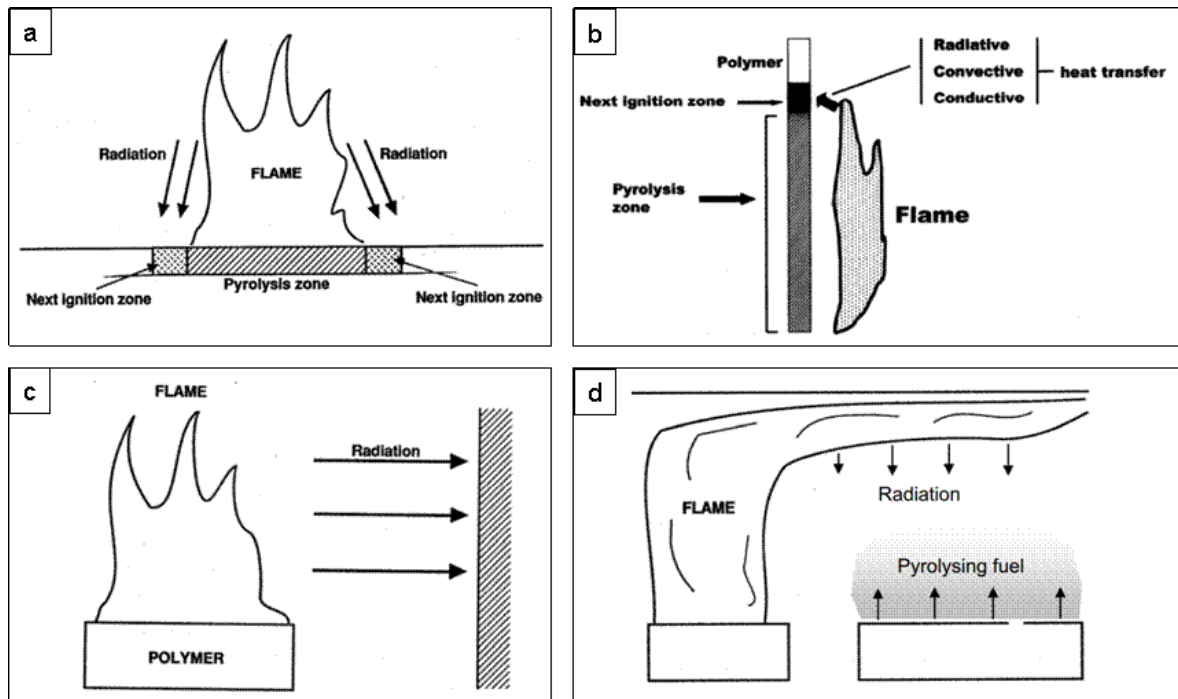


Figure I-5 Fire propagation in different scenarii, a) horizontal propagation (slow), b) vertical propagation (rapid), c) ignition at a distance, d) flashover conditions [13]

Thus, the fire configuration – horizontal or vertical orientation of the polymer, distance to surrounding material – will play a determining role as to the propagation of a fire. Based on these considerations, one can already foresee the issue of assessing the flammability of a material. This will be discussed in section 2.2. with considerations about fire testing.

### 2.1.c. Extinguishment and char production

Extinguishment of a polymer subjected to fire requires that at least one of the following conditions is fulfilled: (i) suppression of the oxygen supply, (ii) suppression of the fuel supply, (iii) suppression of the heat supply. The first condition will be met when a depletion of the oxygen in the surrounding atmosphere is achieved, either by suppressing the oxygen source, or by preventing the oxygen to access the burning material, which can be the case when the fuel stream at the polymer surface is high enough to counter the oxygen flux. This can be achieved for a polymer releasing volatiles by bursting [14], though this phenomenon must be strong enough to cause local quenching of the flame, and spread enough to lead to complete extinguishment of the fire. Another physical phenomenon leading to reduction of the oxygen access to the polymer surface is the production of a consistent enough char, which will be discussed hereafter. The suppression of the fuel supply will be achieved when no more combustible material is left to burn, or by blocking the mass transfer of the combustible volatiles to the gas phase, or else by stopping the polymer material from degrading, which actually

involves that the third condition – the suppression of the heat supply – is fulfilled. This last condition can be achieved either by ‘simply’ removing the energy source – which involves active fire protection if the fire has developed – or by blocking the heat transfer to the combustible material.

These conditions for extinguishment are obviously interdependent, and one of the commonly suggested mechanism for achieving one or the other of these conditions is the production of a protective char layer on top of the burning polymer. Some polymers can indeed produce a solid residue when combusting. As mentioned in the section presenting the thermolysis, various chemical processes yield small molecules and fragments that either volatilize and participate to the flame feed, or that can recombine through various crosslinking reactions, involving creation of unsaturated bonds and appearance of polyaromatic structures that are more stable than the virgin polymer.

Depending on the polymer nature, the char yield will be more or less important. Also, the structure and thermal stability of the char will play a strong role in terms of protection of the material. The appearance of a char layer will act physically on different parameters of the combustion process [6]. Firstly, it will block the mass transfer, i.e. the migration of volatiles to the gas phase, via a mechanism of entrapment. Similarly, the migration of oxygen towards the degrading polymer will be prevented, stopping the oxidative degradation of the material. However, these protective mechanisms can be effective only if the char reaches a sufficient degree of cohesiveness: obviously, a porous or crackled char will not prevent gases to pass through. Secondly, the char can have a thermally insulating effect, leading to decreasing the temperature of the virgin underlying material and preventing it from further degradation. These aspects are usually exploited for fire protection via production of intumescent materials [15].

Understanding the mechanisms of fire and the possible ways for fire extinguishment is key for designing fire retardant solutions. In section 2.4. , examples of usual fire retardants for polymers will be mentioned, together with their action mechanisms.

## **2.2. MEANS TO INVESTIGATE THE FIRE BEHAVIOUR OF POLYMERS**

### **2.2.a. Different tests for different purposes**

There exist different ways to characterize a material behaviour in fire conditions. The first observations can be related to how the material reacts, i.e. how long it stands fire conditions without igniting, how fast it propagates the flame, if it releases drops or not, how much smoke and heat it emits, etc. On the other hand, testing can be carried on how a material conserves its integrity when subjected to fire. The norm ISO13943:2008 thus defined: (i) the fire reaction, as

"the response of a material in contributing by its own decomposition to a fire to which it is exposed under specified conditions", and (ii) the fire resistance as "the ability of an item to fulfil for a stated period of time the required stability and/or integrity and/or thermal insulation, and/or other expected duty specified in a standard fire-resistance test". Resistance to fire is particularly relevant when considering part assemblies.

The reaction or the resistance to fire will be assessed by different tests. Indeed, fire tests can be classified by considering the scale of the sample, and consequently their 'degree of reality' as related to a real fire scenario: bench-scale, medium-scale or full-scale tests. It remains very difficult to extrapolate the fire behaviour of a material tested at a particular scale and in a specific configuration because reaction to fire is not a fully intrinsic characteristic of a material and it depends on many external parameters.

Lots of fire tests actually exist that usually provide a product classification for industrial purposes – i.e. the material, part or component passes the test or not. While some tests aim at simulating a fire in the real conditions of use of the material, the purpose of other tests is to provide understanding of the fire behaviour of a material. The latter are usually bench-scale tests that assess the reaction-to-fire of samples.

In this study, the UL94 and the cone calorimeter tests – which are reaction-to-fire tests – were used to assess the fire retardancy of the hybrid epoxy networks. They will be described in details in the next section, with particular attention to the parameters they evaluate and efforts to correlate the results of these two tests that were made up to now.

As explained in the previous section, the combustion phenomenon starts with the thermolysis of a material. Understanding the thermal decomposition of polymers is thus considered as a key element and the scientific community has been investigating this issue through various techniques. In the present study, the thermal stability of the networks was assessed via the technique of thermogravimetric analysis. This method was widely used for investigation of the thermolysis phenomenon, and can be coupled with analysis techniques such as Infrared or Mass Spectroscopy. Section 2.2.c. will focus on the TGA and the efforts that have been made to correlate the TGA results to results obtained with fire testing.

### **2.2.b. Focus on UL94 and cone calorimeter tests: characteristics and correlations**

- UL 94 test

The UL 94 is a fire test released by Underwriters Laboratories and harmonized via the ASTM standard D3801 [16]. It is a bench-scale fire test where samples of 125 x 13 mm<sup>2</sup> are used – the

thickness can vary. Both horizontal and vertical configurations exist, but the present study will focus on the vertical test set-up, as depicted in Figure I-6. The UL 94 test is designed for assessing the fire response of a material to an ignition by a flame and its propensity to self-extinguish. The standard describes thoroughly the testing procedure and specifies a classification of tested materials based upon the following criteria: the flaming and afterflame times through the successive ignitions of the sample, and the potential releasing of flaming drops (Table I-1). The classification is given for a certain thickness of the material.

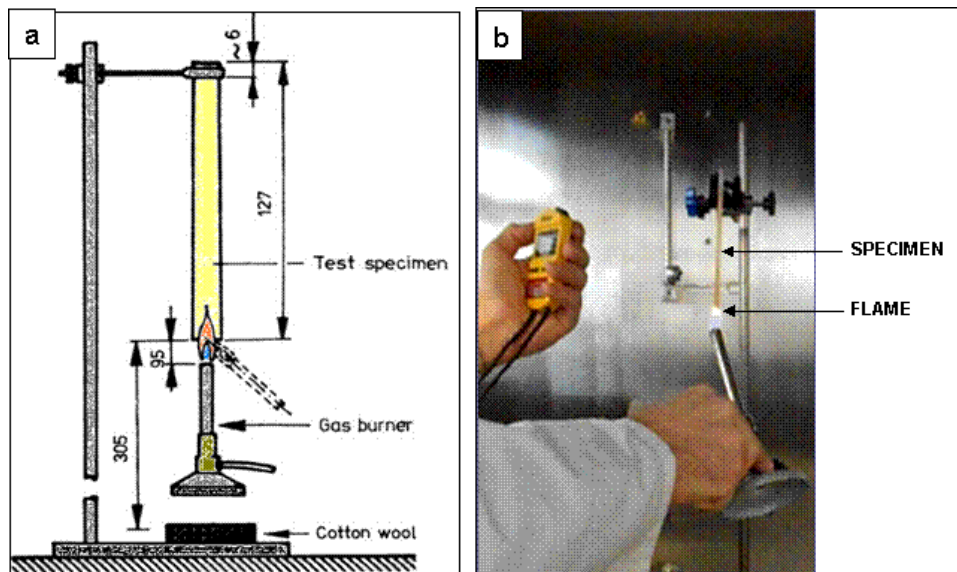


Figure I-6 UL 94 test: a) scheme of the vertical burning set-up [17] and b) ignition of an epoxy sample

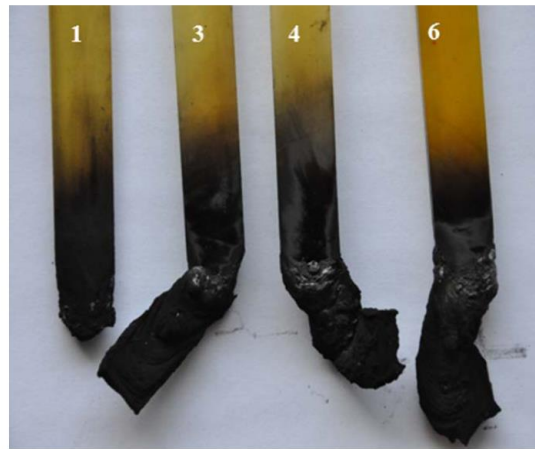
Criteria Conditions	V-0	V-1	V-2
Afterflame time for each individual specimen, $t_1$ or $t_2$	$\leq 10$ s	$\leq 30$ s	$\leq 30$ s
Total afterflame time for any condition set ( $t_1$ plus $t_2$ for the five specimens)	$\leq 50$ s	$\leq 250$ s	$\leq 250$ s
Afterflame plus afterglow time for each individual specimen after the second flame application ( $t_2 + t_3$ )	$\leq 30$ s	$\leq 60$ s	$\leq 60$ s
Afterflame or afterglow of any specimen up to the holding clamp	No	No	No
Cotton indicator ignited by flaming particles or drops	No	No	Yes

Table I-1 Criteria for material classification [16]

While the classification is mainly intended to provide guidance for industrial qualification of materials for commercial applications, the test can also provide the operator with useful information on the fire behaviour of a material in this particular configuration. Information could be obtained from visual observation, such as the flame propagation length – to correlate with

the time of flaming to obtain the propagation speed –, the residual mass, the propensity of the material to drip without igniting the cotton indicator, its propensity to swell, to intumesce or release fuel gases by bursting.

An example of residues images of UL 94 samples based on epoxy-amine networks with or without a novel phosphorus/nitrogen-containing flame retardant is displayed in Figure I-7 [18]. Such pictures provided information about the charring and deformation propensity of the fire-retarded systems under fire conditions, which would not have been available if only a classification table was provided by the authors, as it is usually done in the literature.



**Figure I-7 Pictures of UL 94 residues of DGEBA/DDS-based epoxy networks with or without a novel phosphorus/nitrogen-containing flame retardant (TNTP); 1) reference sample; 3) with 5 wt% TNTP; 4) with 10 wt% TNTP; 6) with 20 wt% TNTP [18]**

The UL 94 is thus a test assessing qualitatively the reaction to fire of a specific material under specific conditions. This test is thus not adequate for predicting the fire behaviour of large pieces of materials, but can give an insight of the resistance to ignition of a specific material as compared to a reference system.

- Cone calorimeter

The cone calorimeter test was first proposed by Babrauskas in 1984 and is based on the measurement of the oxygen consumption during the combustion of a material [19]. It was then harmonized through the ISO 5660 standard in 1993 which was revised several times since then [20]. The horizontal configuration of the test is depicted in Figure I-8.

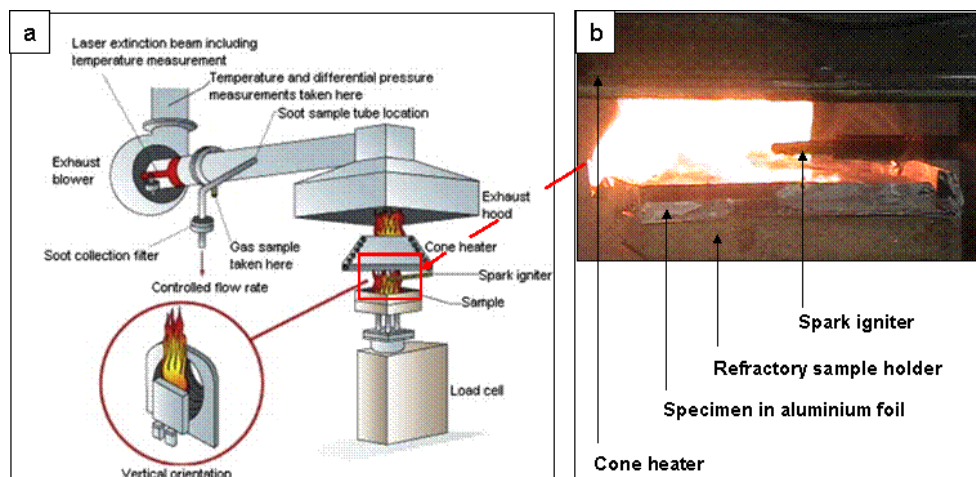


**Figure I-8 Cone calorimeter test: (a) horizontal set-up [21] (b) ignition of an epoxy sample**

The cone calorimeter, unlike the UL 94 test, is a forced-convection test, i.e. a constant heat flux is applied to the sample during all the test duration. As in the UL 94 test, visual observation can provide information on the mode of burning of the material, especially if the samples tend to intumesce, but most of the data are numerical and based on various measurements from which are derived the following main parameters:

- Time To Ignition (TTI, s)
- Heat-related parameters: Heat Release Rate (HRR, kW/m<sup>2</sup>), peak of Heat Release Rate (pHRR, kW/m<sup>2</sup>), Total Heat Released (THR, MJ/m<sup>2</sup>)
- Smoke-related parameters: Total Smoke Released (TSR, m<sup>2</sup>/m<sup>2</sup>), average carbon monoxide yield (CO yield, kg/kg), average carbon dioxide yield (CO<sub>2</sub> yield, kg/kg)
- Mass-related parameters: Residual Weight (RW, %) and Mass Loss Rate (MLR, %/s)

In particular, HRR as a function of the test time has been shown to be a parameter of utmost importance in a fire. Simulations have demonstrated that, while the toxicity, opacity and corrosiveness of the smoke were generally the cause of death, HRR was the decisive parameter as concerns the fire hazard, assessed through the times to incapacitation and death [22]. The pHRR is thus the most commented cone calorimeter data by far. An example of a HRR curves obtained for different neat and flame-retarded epoxy networks are displayed in Figure I-9 [23], where the pHRR was highlighted.

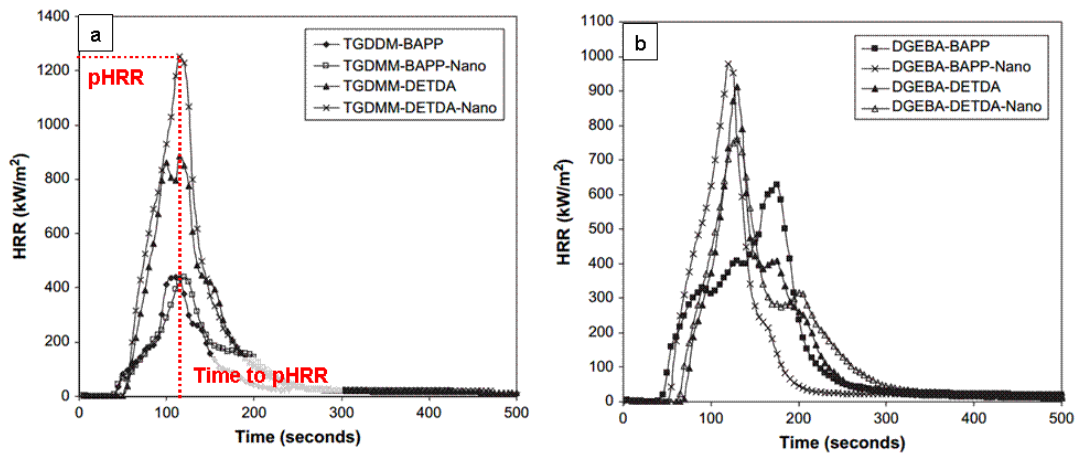


**Figure I-9** Examples of HRR curves for epoxy systems cured with either a classical amine curing agent (DETDA) or a phosphorus-containing crosslinking agent (BAPP), and with and without a fire-retardant nanoclay; a) TGDDM-based, and b) DGEBA-based epoxy systems [23]

In these systems, the applied heat flux was of 50 kW/m<sup>2</sup> and the sample dimensions were of 100 mm x 100 mm x 2.1 mm. The influence of such parameters will be discussed later on in this section. The maximum HRR value (pHRR), ranged from 400 kW/m<sup>2</sup> for fire-retarded systems to 1200 kW/m<sup>2</sup> for reference networks, which is a classical range of value for epoxies, considering the test parameters of the study.

The HRR curves can display different shapes that are usually related to the combustion behaviour of the material, as shown in Figure I-10.

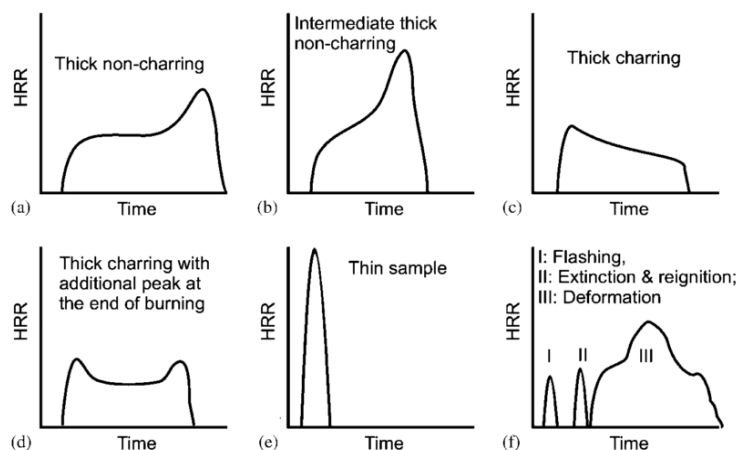


**Figure I-10** Typical HRR curves for different characteristic burning behaviours [24]

The cone calorimeter is thus a more comprehensive method that can quantitatively assess the reaction-to-fire of a specific material under specific burning conditions – in the limit of the 10% experimental error. However, it has eventually proved delicate to compare materials when the

test parameters were varied. ScharTEL et al. produced a document aiming at providing guidance for the interpretation of cone calorimeter data [24], in which the authors highlighted the influence of parameters such as:

- heat flow and distance 'cone heater to sample': they are usually in the range of 25 to 70 kW/m<sup>2</sup> and 2.5 to 6 cm, respectively [20], [24], [25]. In addition to increasing the heat release rate, a high heat flow and/or a low distance to the sample would reduce the time to ignition by increasing significantly the temperature of the sample;
- sample holder material: the thermal conduction of the sample holder will play a role on the thermal feedback on the sample when the degradation front reaches the bottom sample surface;
- nature of the samples: cone calorimeter was originally designed for bulky flammable materials. For other types of materials, such as textiles or thin films, some data can be inaccurate or not measurable;
- size and shape of the sample: generally, square samples of 100 x 100 mm<sup>2</sup> are used,. Another size and shape of the sample allows a different distribution and value of the heat flow over the sample surface. The thickness of the sample plays a particularly important role. It will affect the HRR profile, due to thermal conductivity considerations;
- deformation, swelling and dripping: the deformation and swelling will change the distance to the cone heater, possibly causing the sample to touch the cone resistance. Grids may be used to hinder the deformation but thus change the material fire behaviour. Dripping will cause artefacts in the mass measurement.

Numerical data provided by the cone calorimeter test can be implemented in simulations, and models have been developed which aim at predicting fire hazard in different fire configurations and/or other fire tests results – usually larger-scale tests – with increasing success. These models are based also on other characteristics of the material, e.g. the thermal conduction of the virgin and the char materials, or other test data from e.g. fire-under-load testing or thermogravimetric analysis.

- Correlations

From the different characteristics presented above, one can easily understand that the UL 94 and the cone calorimeter tests will not assess the same features of a given material, as regards its fire behaviour. Apart from the fact that the ignition modes, the external heat flux and the sample dimensions are different, the possible occurrence of dripping in the UL 94 test will have an important influence on the variations between both tests. Nevertheless, predicting the UL 94

classification of some materials, based on their cone calorimeter results, has been attempted with more or less success.

In particular, Morgan et al. [26] studied the potential correlation of cone calorimeter results with UL 94 classification of several commercial flame-retarded thermoplastic formulations, and the corresponding non flame-retarded materials. Several thicknesses and heat fluxes were implemented. An artificial parameter,  $HRR_0$ , the critical HRR for a nil heat flux, was then introduced. It was determined by extrapolating the linear dependency between the experimental pHRR measured for three different heat flux and taking the value of pHRR for a heat flux value of zero. This empirical notion was first proposed by Lyon [27], who used HRR values during steady burning, rather than pHRR values. A tendency seemed to emerge that could allow to correlate  $HRR_0$  values and the UL 94 ratings: V0 and V1-rated materials generally had a  $HRR_0$  below  $400\text{kW/m}^2$ , the value being higher as concerns the non-rated and V2-rated polymers. Another study carried out on a wide range of non flame-retarded polymers found out that an unsteady or self-extinguishing burning behaviour of a material in the UL 94 test generally corresponded to a value of  $HRR_0$  of less than about  $90\text{kW/m}^2$  [28]. However, one should account for the uncertainties in the  $HRR_0$  determination, coming from the different HRR curve shapes. A statistical study revealed that the average Heat Release Rate (HRR) values taken 60s after the Time To Ignition (TTI), the peak of Heat Release Rate (pHRR), in a lesser extent, and finally the Fire Growth Rate index, or FIGRA (ratio of pHRR over TTI), were the parameters somehow correlated with the UL 94-rating of the polymers, though the correlation became rougher – to say the least – when the applied heat flux increased. Only at a heat flux of  $30\text{kW/m}^2$  the correlation seemed to appear (Figure I-11).

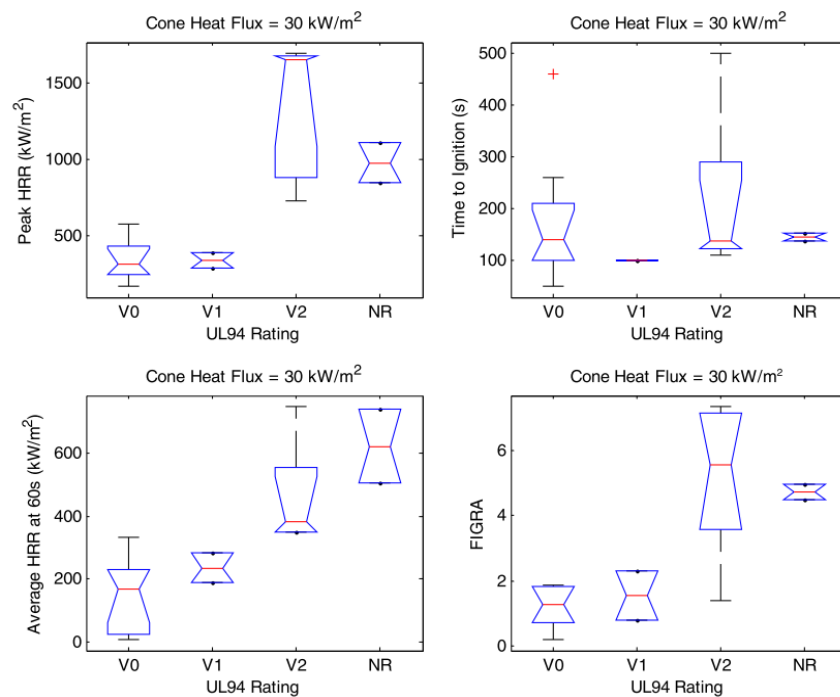


**Figure I-11 Relationships between UL 94 V rating and 30kW/m² heat flux cone calorimeter data [26]**

It still remains difficult to correlate UL 94 ratings and cone calorimeter parameters. Even if the fire behaviour of the same material is tested, the two tests simulate different fire scenarios and thus provide the investigator with different fire characteristics that can be somehow considered as complementary.

### 2.2.c. Thermal stability assessed via Thermogravimetric Analysis (TGA)

One of the most wide spread means to investigate the thermal behaviour of polymers is thermogravimetric analysis (TGA), which consists of recording the weight changes a mg-size polymer sample undergoes as a function of the temperature. Isothermal or dynamic scans, with a ramp speed of usually no more than 10 K.s<sup>-1</sup>, can be performed, either under oxidative or inert atmosphere.

Information about the onset temperature of degradation, the maximum degradation rate temperature(s), the number of degradation steps, the residual weight at a certain temperature – usually when no more evolution is observed – can be obtained from the resulting weight/temperature curves and their derivatives. The temperatures at 95% and 50% of residual weight are also sometimes given.

The mechanisms of degradation depend not only on the material but also on the atmosphere the test is carried out in. In particular, it is classical to observe several degradation steps due to

the active oxidative role of oxygen in air. The work carried out by Mustafa et al. [29] gave a clear example of the differences in the degradation pathways due either to the atmosphere or the chemical structure of the networks (Figure I-12). They investigated the thermal stability of epoxy networks copolymerized with a new pyridine-containing curing agent (PDD), and/or with a classical curing agent, the diamino diphenyl methane (DDM). Comparing the TGDDM/DDM matrix under oxidative or inert atmosphere, the occurrence of several degradation steps under air, as compared to a single step under argon, proved the existence of different degradation pathways. The first and second steps were attributed to the thermal degradation and the oxidative degradation of the products, respectively. On the other hand, the introduction of the PDD crosslinker in the networks seemed to complicate the degradation pathways as observed from the multiplication of degradation steps as compared to the TGDDM/DDM matrix, in both atmospheres.

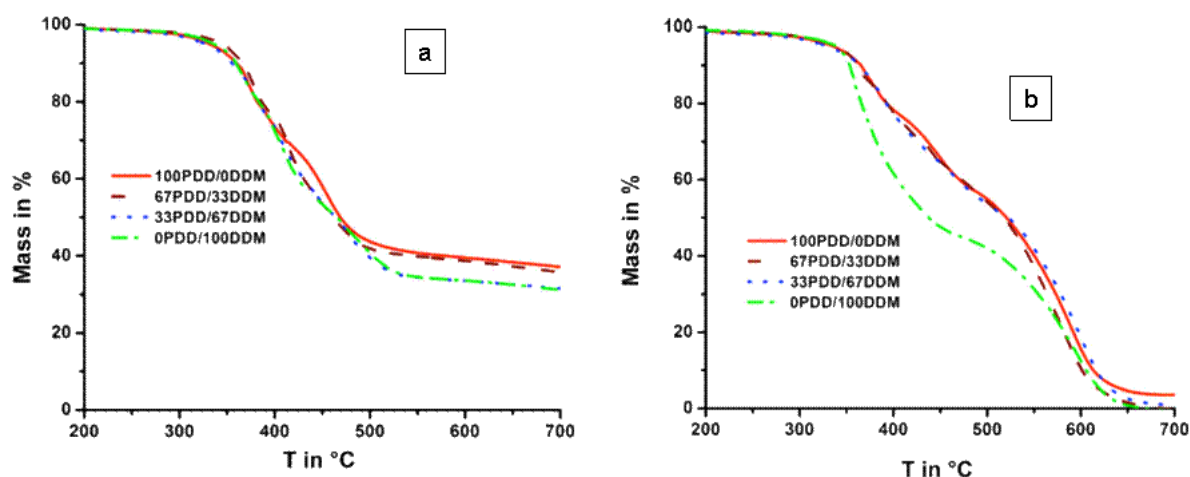


**Figure I-12 TG curves of TGDDM-based networks cured with a pyridine-containing crosslinker (PDD) and/or an aromatic diamine (DDM) crosslinker a) in inert (Ar) atmosphere and b) in oxidative (air) atmosphere [29]**

Coupling the TGA with a spectrometric technique could allow to identify to a certain extent the volatiles resulting from each degradation step and trace back to the chemical mechanisms. Apart from the investigation of degradation mechanisms, attempts have been made to correlate TGA measurements and fire performance. In particular, parameters such as the onset of degradation or the char residue amount are thought to be representative of the thermal stability of a material. Liu et al. [23] compared char residue values of neat or fire-retarded epoxy networks, from cone calorimeter experiments and TGA measurements under both inert and air atmosphere. They found a rough correlation between the char residue amounts from the cone calorimeter and the TGA experiments under inert atmosphere, which could promote the hypothesis according to which the thermolysis in a fire is mostly anaerobic (Table I-2).

Sample	% Char yield at 850 °C in air (TGA)	% Char yield at 850 °C in N <sub>2</sub> (TGA)	% Mass after combustion (cone calorimetry)
DGEBA/BAPP	4.27	27.37	24.5
DGEBA/BAPP/Nano	12.73	32.13	27.8
DGEBA/DETDA	2.95	14.02	19.8
DGEBA/DETDA/Nano	5.95	10.03	19.7
TGDDM/BAPP	8.69	37.39	30
TGDDM/BAPP/Nano	11.51	37.42	42.8
TGDDM/DETDA	6.09	17.62	21.5
TGDDM/DETDA/Nano	6.89	23.3	20.4

**Table I-2 Comparison of char yields obtained from TGA and cone calorimeter ; BAPP is a phosphonate hardener and 'Nano' designates an organo-modified polymeric layered silicate [23]**

However, correlations between thermal stability as assessed by the TGA and fire test results are rare in the literature. While sometimes authors rely on the TGA results to extrapolate on the fire performance of their systems [29], [30], some works have proven that such shortcuts could not be made automatically and often not all the TG parameters – char residue, degradation temperature onset – indicate the same trend as concerns the thermal stability [31]. As one can understand, the simplification of the degradation of a limited amount of material, in a fixed atmosphere, at a constant temperature or heating rate, cannot faithfully describe the thermolysis phenomenon when it takes place in the context of a fire.

### 2.3. INTRINSIC FLAMMABILITY OF POLYMERS

As seen in the previous section, the fire behaviour of a polymer depends on many external parameters, but the chemistry of the polymer is the first determining intrinsic parameter for its flammability. Stuetz et al. [11] defined the intrinsic combustibility of a polymer as the minimum oxygen demand for sustained combustion, i.e. the Limit Oxygen Index (LOI). The experiment used for such a measurement is based on adjusting the oxygen concentration in a closed environment in order to have a self-sustained combustion of a polymer bar in a candle-like configuration. As reminded by Camino et al. [32], the test parameters, even in a simple configuration as the one of the LOI test, have an influence on the results.

Walters and Lyon [33] proposed a semi-empirical theory to derive the Heat Release Capacity (HRC) of polymers from the measured contributions of molar groups constituting the repeat units of these polymers. The HRC showed good correlations with the average Heat Release Rate (aHRR) as measured by the cone calorimetry, for a wide range of polymers (Figure I-13 a). Correlations were also highlighted between the HRC and results from the LOI and the UL 94

tests, which allowed the authors to conclude that the HRC was a reasonably good parameter to characterize the relative flammability of different polymers.

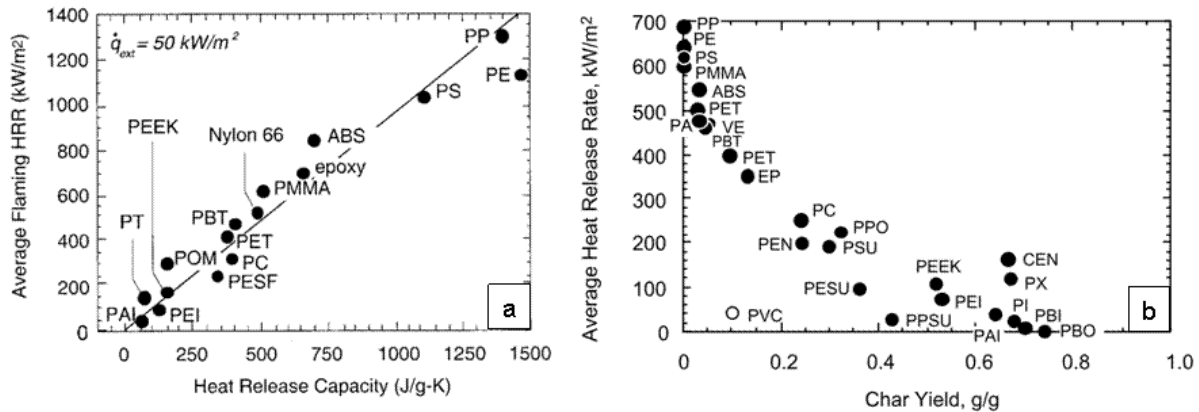


**Figure I-13 a) Average flaming Heat Release Rate (aHRR) from cone calorimetry versus the Heat-Release Capacity (HRC) for several polymers [33] ; b) Average flaming HRR from cone calorimetry versus Char Yield for several polymers ('EP' stands for 'epoxy') [34]**

In Figure I-13 a), several polymers were classified according to the relevant HRC parameter identified by Walters and Lyon. High performance thermoplastic polymers such as PEI or PEEK show the lowest value of HRC while common thermoplastic polymers – PP, PE, PS – present the worst flammability property. The epoxies are located in the middle range, with HRC and aHRR values of about 650 J/g.K and 750 kW/m<sup>2</sup>, respectively. It is interesting to note that the aHRR parameter was related to the char yield and as expected (Figure I-13 b), less flammable polymers tended to yield more char.

Selecting poorly flammable polymers for a given application is one of the strategies for fire protection. However, other aspects must be taken into account for material selection, such as mechanical properties, chemical resistance or cost, and this solution is often not applicable. Hence the need to enhance the fire resistance of polymers suitable for a given application, without modifying the key properties they have been selected for.

## 2.4. CONVENTIONAL FLAME RETARDANTS

The scope of the study being the flame retardancy of polymers in their bulkiness, other fire-retardant strategies, such as coatings, will not be mentioned here, in order to focus on the flame-retardant additives.

A flame retardant compound cannot make a flammable polymer completely non-combustible. Strategies must be developed by targeting and inhibiting, via the addition of a particular flame retardant, one of the mechanisms involved in the combustion cycle. The substance can thus

have an effect on the time to ignition, or the developing phase of the fire, in which case the aim is to delay and/or reduce the flash-over.

Flame retardants can be classified in different classes that refer to their chemistry: halogenated, phosphorus-containing, nitrogen-containing and inorganic flame retardants. The modes of actions of these compounds can be classified according to their chemical or physical nature. However, often the flame retardants act through various mechanisms that are interdependent. Also, several flame retardants in a same material are often used to create synergistic effects.

The next section will present the main modes of actions of the commercial flame retardants, with examples and a summarizing table, but does not aim at providing an exhaustive review or a precise description of the chemical mechanisms. More information can be found in [3], [35]–[37].

#### **2.4.a. Modes of action**

Flame retardants act through one or various mechanisms. Such mechanisms can be present in the condensed or the gas phase, and be either chemical or physical.

- Flame retardants acting in the condensed phase

A chemical mechanism of flame retardancy of certain compounds is their decomposition via endothermic reactions. The reaction can also target the volatilization of non-flammable compounds, such as water. These reactions will consume energy and provoke a cooling of the polymer material, thus preventing – or retarding – its degradation.

Some flame retardants will favour reactions in the condensed phase that will promote char formation, having a double effect: it provides less combustible for the gas phase, but also leads to the formation of a char layer that helps protecting the underlying material, by reducing the gas exchanges of fuel combustible and oxygen between the condensed and the gas phases. Also, this carbonaceous layer provides thermal insulation, leading to less thermal degradation of the virgin material. This is particularly the case of intumescent materials where several substances are used to obtain a synergistic effect leading to a swelling of the burnt material.

- FR compounds acting in the gas phase

In the gas phase, the chemical action of certain flame retardants targets the exothermic reactions prompted by free radicals. Their mechanism is based on scavenging high energy radicals such as  $H^{\bullet}$  and  $OH^{\bullet}$ , and producing non-flammable gases or less reactive radicals. Also, certain flame retardants, when decomposing, release non-flammable gases which results in a physical mechanism of dilution of the combustible volatiles in the gas phase. It reduces the

concentration of exothermic reactions in the gas phase and thus disturbs the self-sustainable fire mechanism.

- Overview of the existing commercial flame retardants for polymers and their modes of action

In Table I-3 are summarized the different types of commercial flame retardants and their modes of action. Selection of a particular substance must be guided by careful knowledge of the polymer chemistry and processing, the mode of action of the flame retardant and the targeted application, i.e. the potential fire scenario the material is likely to be subjected to. As an example, careful attention must be given to the temperature of activation of the flame retardant selected, which should be in the same range of the degradation temperature of the polymer, but higher than the polymer processing temperature.

In terms of tonnage, halogenated flame retardants and mineral fillers represent most of the flame retardant market (Figure I-14). Aluminium TriHydrate (ATH) is indeed a very cost-effective compound which represents nearly half of the European tonnage and is needed in high loadings to achieve satisfactory levels of flame retardancy in polymeric materials. Halogen-containing compounds are up-to-now the most commercially effective flame retardants. In terms of value, they actually represent the greatest part of the flame retardant market.

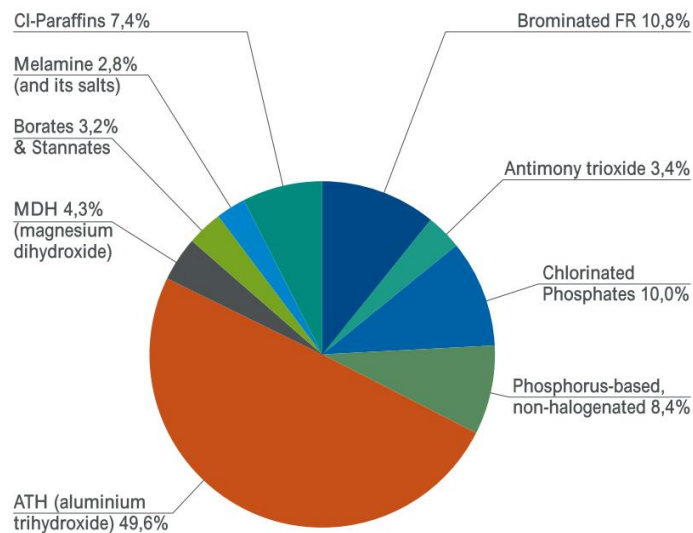


Figure I-14 2005 European flame retardant market consumption, on a tonnage basis [3]

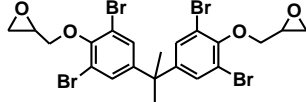
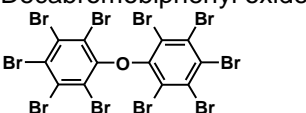
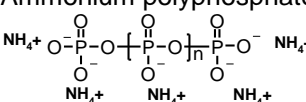
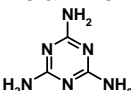
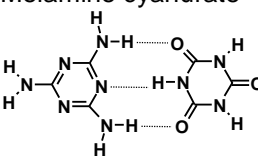
Category	Examples	Modes of action	Comments
Halogenated compounds: reactive (brominated oligomers...) and inert additives	Diglycidyl Ether of TetraBromoBisphenol A 	- In the gas phase (chemical): entrapment of H <sup>•</sup> and OH <sup>•</sup> radicals	- Br FR are more effective than Cl FR - Antimony trioxide is often used as synergist
	Decabromobiphenyl oxide 		
Phosphorus-containing compounds	Chlorinated paraffins		
	Phosphine oxides 	- In the condensed phase (chemical and physical): dehydration of the polymer → char formation and intumescence if used in combination with other compounds - In the gas phase (physical): dilution of fuel volatiles by releasing water	- Adequate for oxygen-containing polymers, e.g. epoxies, polyesters, polyurethanes, polycarbonates, phenolics
	Phosphonates 		
	Ammonium polyphosphate 		
Red phosphorus			
Nitrogen-containing compounds	Melamine 	- In the gas phase (physical): dilution of fuel volatiles → intumescence, in combination with phosphorus-containing FR	- Limited applications in polymers
	Melamine cyanurate 		
Inorganic compounds	Mineral fillers: Al and Mg hydroxides	- In the condensed phase (physical): cooling by endothermic dehydration and protective ceramic containing Al or Mg - In the gas phase (chemical and physical): dilution of gases by water release	- Al(OH)3 is the most widely used FR - High loadings are required (40-60%)
	Borates: borax, boric acids, zinc borate	In the condensed phase (physical): cooling by endothermic dehydration and protective glassy char formation	- 'Niche' FR: adequate for specific polymer systems
	Stannates: zinc stannates	- Smoke reduction in combination with halogenated FR	- Usually used in combination with other FR
	Silicates	- Formation of a protective ceramic barrier	

Table I-3 General information on commercial flame retardants (FR), based on [35]–[37]

### **2.4.b. Fire retardants for epoxies**

Epoxy polymers are found in a wide range of applications, from structural composites for aeronautics to printed circuit boards and adhesives. Each application domain has its own requirements in terms of fire safety, but often the epoxy components are found in situations where probabilities of fire are not negligible, e.g. contact with electric and electronic components, thermal stresses. Among the different classes of fire retardants presented in the previous section, mainly halogenated and phosphorus-containing substances are commercially available for thermoset polymers nowadays [38], [39].

- Halogen-containing flame retardants

The halogenated compounds used in epoxies polymers comprise diphenyl oxides, brominated resins mainly derived from DGEBA, and chlorinated paraffins used in combination with antimony trioxide. In particular, the decabromobiphenyl (see Table I-3 above for chemical structure), the TetraBromoBisPhenol A (TBBPA) and its reactive derivatives, such as the Diglycidyl Ether of TetraBromoBisphenol A (Table I-3), are often used. The latter is particularly interesting as they are reactive compounds that can bond to the polymer backbone, which is thought to limit their release in the environment during the lifetime of the polymer. Bromine contents are approximately of 20 wt% in epoxy systems for electrical applications such as circuit boards [40]. Changes in physical properties of the networks were observed resulting from the use of such modified monomers – higher coefficient of thermal expansion, lower thermal stability, higher viscosity [41].

The efficiency of brominated flame retardants is established and most of the recent studies now focus on the potential hazards caused by such compounds. In particular, they examine the propensity of bromine-containing compounds to be released in the environment and absorbed by living beings, as well as the toxicity of such compounds and of their smoke [40], [42], [43].

- Phosphorus-containing flame retardants

Epoxy resins can also be flame-retarded with Ammonium Polyphosphate (APP), phosphines oxides such as triphenyl phosphine oxide or red phosphorus, the latter being particularly suited for electronic applications. Cyclic phosphonates or polyphosphates are compatible with epoxy systems as well. Organo-phosphorus compounds and reactive phosphorus-containing oligomers are also used. In particular, phosphorus-containing amine hardeners provide a certain synergistic effect due to the combined presence of P and N elements. Research on this track has been particularly active in the last decades as solutions remain to be developed that

must be suitable for commercial applications in terms of materials' properties and process [23], [44]–[47].

However, phosphorus-containing flame retardants can be detrimental for the polymer properties or processing. For example, the phosphorus-containing additives tend to act as plasticizers in these systems. Red phosphorus also causes issues in terms of handling and processing safety [38].

#### **2.4.c. Regulations and restrictions for conventional flame retardant compounds**

As seen before, the main commercial flame retardants available for thermosetting systems are based on halogenated or phosphorus-containing compounds, sometimes used in synergy with other substances. In general, if selected rightly, brominated compounds can provide a good compromise as they are good flame retardants while they usually allow the polymer to maintain its physical and mechanical properties.

However, they have been confronted by more demanding regulations, in particular through the European directive REACH (Registration, Evaluation, Authorization and restriction of Chemicals). This directive was first implemented in 2007 and aims at regulating the production and sale of the substances listed as SVHC (Substances of Very High Concern) and the products containing these compounds within Europe. The European Chemical Agency (ECHA) is the organisation in charge of helping companies to conform to the REACH directive. As concerns brominated compounds, the REACH directive has identified several molecules as potentially harmful for the human health or the environment, and listed conditions of use and marketing of these substances in its Annex XVII [48]. Such restrictions are based on the results of a Risk Assessment procedure that is carried out systematically for substances listed as SVHC. The RoHS directive (Restriction of Hazardous Substances) also targets certain brominated compounds used as flame retardants for electronic and electrical applications: polybromobiphenyls (PBB), which are not used anymore, and polybromodiphenyl ethers (PBDE). As an example, products such as octabromodiphenyl and pentabromodiphenyl ethers are limited to 0.1 wt% in concentration, while decabromodiphenyl ether is not included in the directive [49]. Also, TBBPA was subjected to a Risk Assessment procedure, whose results were published in the Official Journal of the European Union in 2008, and which stated that no concerns for human health were to be foreseen, despite a potential effect on the water and terrestrials environments [50].

Therefore, as concerns halogenated flame retardants, even if certain compounds are still authorized for use and commercialization, alternatives must be found that, ideally, do not

significantly change the material properties, do not allow migration of the compounds, are not harmful for health and limit the smoke production in case of a fire. This challenge has been addressed through the last decades with particular attention to nanostructured hybrid polymers. The use of silicate layers such as montmorillonite, or carbon nanotubes has been thoroughly investigated. However, one must keep in mind that nanomaterials are to be eventually registered within REACH, and for this purpose, the European Commission has launched a public consultation on transparency measures for nanomaterials on the market, closing on 5 August 2014. The global nanomaterials market was estimated to 11 million tonnes at a market value of 20 billion euros (all application fields), but a lack of information remains on the nature and the potential impacts of these materials upon human health and environment [51].

### **3. POLYSILSESQUIOXANES: A FIRE-RETARDANT ALTERNATIVE FOR EPOXY/AMINE NETWORKS?**

#### **3.1. EPOXY NETWORKS AND POLYSILSESQUIOXANES: AN INTRODUCTION**

##### **3.1.a. Epoxy networks**

Epoxyes are a type of thermoset polymers, i.e. insoluble and infusible 3D networks. The term epoxy refers to monomers containing oxirane rings that open to polymerize either through homopolymerization or by copolymerization with a comonomer – the crosslinking agent or hardener. A wide range of epoxyes and hardeners are available, making it possible to tailor the final properties of these networks. Epoxyes differ in their chemical structure and composition, the molar mass of monomers and their functionality [52]. The most widely commercialised epoxy prepolymer is the Diglycidyl Ether of Bisphenol A, and it is also commonly used as a model compound in most of the scientific studies. A tetrafunctional epoxy prepolymer, the Tetraglycidyl(diaminodiphenyl)methane (TGDDM), is preferably used in high-performance applications such as in the aeronautical sector. The crosslinking agents include mainly different types of polyfunctional amine compounds, but also acids, anhydrides, phenols, alcohols, and thiols [53]. Amine compounds can be either aliphatic or aromatic, which control their reactivity, together with their substituents' nature. In the present work, aromatic epoxyes with glycidyl groups and a low molar mass aromatic primary diamine were used as comonomers (Figure I-15). Details on the copolymerization reactions will be given in the next chapter.

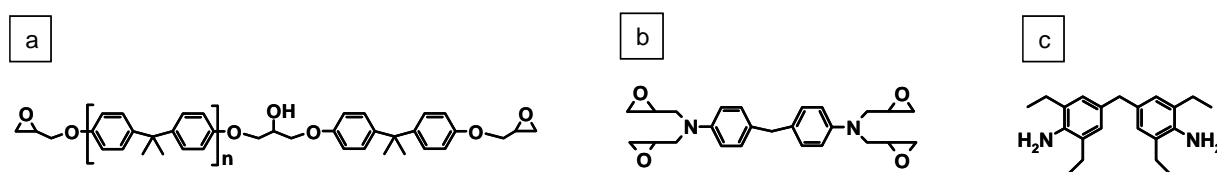


**Figure I-15 Comonomers' chemical structure a) Diglycidyl Ether of Bisphenol A (DGEBA); b) Tetraglycidyl(diaminodiphenyl)methane (TGDDM); c) 4,4' methylene bis(2,6-diethylaniline) (MDEA)**

Because of the large range of chemistries and structures of the comonomers, epoxy-based networks can target many applications and are fitted for many different processing techniques. Their properties can fulfil specific requirements depending on the application sector, such as improved mechanical performance, high chemical resistance, excellent electrical or adhesion properties, etc. However, one of their drawbacks is their poor intrinsic fire behaviour.

### 3.1.b. Polysilsesquioxane compounds

- Polysilsesquioxanes, an adjustable organic/inorganic class of materials

Polysilsesquioxanes are a class of materials of general formula  $(\text{RSiO}_{3/2})_n$ . They are thus organic/inorganic molecules and present a wide variety of structures and properties. They exist under various forms, either bi-dimensional with a ladder-like structure, or tridimensional with random or cage-like organisation (Figure I-16). They can be found as resins or as crystalline or non-crystalline powders, depending on their structure and purity. The peculiarity of polysilsesquioxanes lies in their high versatility: numerous polysilsesquioxanes have been developed with a great range of substituents, which allows to tailor a wide range of properties of these molecules and of the polymers they are included in.

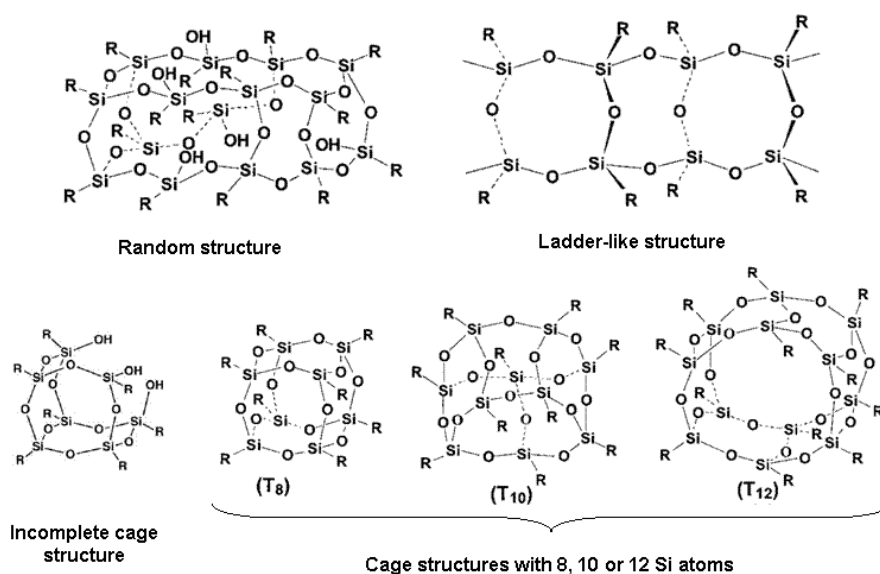


**Figure I-16 Possible structures of polysilsesquioxanes**

- The particular case of POSS

The cage-like molecule constitutes a particular type of polysilsesquioxane known as Polyhedral Oligomeric Silsesquioxanes (POSS), which has been subjected lately to a growing interest of the research community. More than 800 patents and 2300 papers involving POSS are currently available [54]. They are made of an inorganic Si-O cage – 6, 8, 10, 12, or more silicon atoms – and organic ligands. Synthesis of such compounds has gathered a lot of efforts of research in the last decade [55]–[57]. As a result, a number of POSS are now commercially available from the Hybrid Plastics Company, Fountain Valley, CA (USA) [58], and many other POSS compounds are available to be synthesised for research purposes.

The interest of the POSS lays in two main characteristics:

- their molecular character: each POSS is a molecule of nanometric dimension (see Figure I-17) and can be potentially dispersed as such in a polymer matrix;

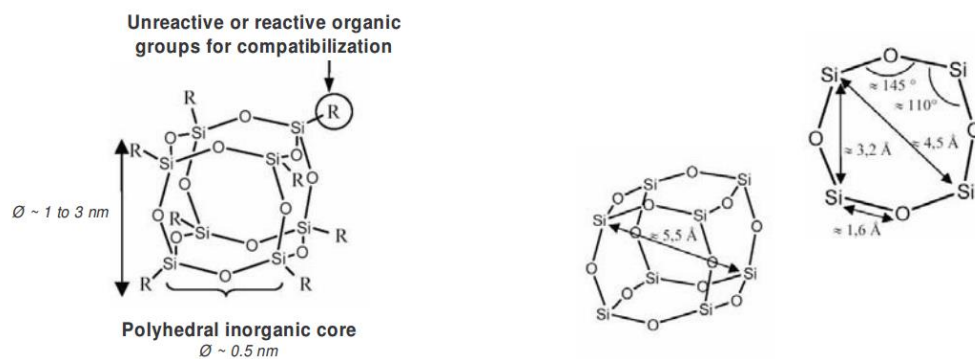


**Figure I-17 Schematic structure of  $T_8$ -POSS and its dimensions (values determined by molecular modelling) [59]**

- the versatility of the organic tethers allowing compatibilization and nanostructuration through a range of POSS-matrix interactions (Figure I-18): depending on their functionality  $f$ , the POSS molecules can act as inert fillers and the organic groups will control its solubility in the matrix through physical interactions ( $f=0$ ); they can be included as pendant groups ( $f=1$ ), comonomers ( $f=2$ ) or crosslinking points ( $f>2$ ), providing the functions born by the POSS can react with a functional group of the polymer matrix.

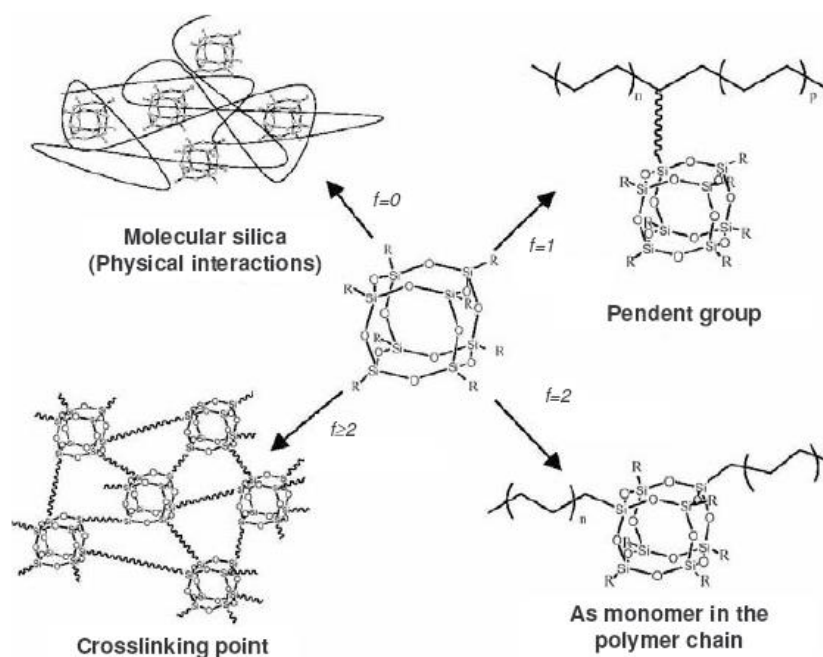


Figure I-18 Possible POSS-polymer matrix interactions depending on POSS functionality

### 3.2. EPOXY NETWORKS FIRE RETARDED WITH SILICON-BASED COMPOUNDS

Introducing silicon-based inorganic domains in polymers is a strategy that has been widely investigated with the general purpose of enhancing a wide range of properties in a number of polymers. In particular such an approach has been found to have a certain potential as concerns the fire behaviour of polymers. The field related to the fire retardancy of thermoset polymers and epoxies in particular constitutes a narrow research domain which has, however, been attracting growing interest. It is also worth noting that many studies rely on results from small-scale simple tests such as the UL94 or the LOI (briefly explained in section 2.3. ), the latter being considered as a relative measurement of the intrinsic flammability of the polymer. The cone calorimeter being a more recent technique, it has only progressively become accessible to research laboratories. In the next sections, focus will be made on studies presenting results of fire tests such as the ones mentioned previously. A number of works relying on thermal degradation data to extrapolate on the fire behaviour of the materials they investigate are available, but as discussed in section 2.2.c. , a lack of correlation exist that makes difficult to reach conclusions on the base of these studies.

The nature and the form of these silicon-based objects are varied: from ready-to-use particles to *in-situ* generation of inorganic-rich domains, the wide range of possibilities allows many different processes that lead to varied morphologies and properties of the final networks.

### 3.2.a. Silicon-based nanoclays for fire retardancy of epoxy networks

Amongst the strategies based on the introduction of silicon-containing objects in epoxy networks, one consists in introducing nanoclays. These nanoparticles consist of an arrangement of silica and magnesia or alumina layers. The interest of such objects lays in their nanometric size and their high aspect ratio. The two main nanoclay types investigated as concerns the fire retardancy of polymers are the montmorillonite and the sepiolite, which are crystalline layered silicates, under the form of flakes and needles, respectively. One of the drawbacks of such clays, contrary to the polysilsesquioxanes previously described, is their poor compatibility with organic matrix and they are thus generally surface-modified in order to improve their dispersion. Franchini [60] studied the influence of surface modification of sepiolite via ion exchange or silane grafting upon its effect on the fire retardancy of DGEBA/MDEA-based networks. The maximum pHRR reduction – as compared to the reference system – was obtained in the case of the epoxy networks containing 6 wt% of non-modified sepiolite. The reduction was no more than 17%, which is not significant considering the uncertainty margin of about 10% inherent to the cone calorimeter experiment. The study demonstrated that the amount of sepiolite used, no matter its dispersion state or the interaction it developed with the matrix, failed to promote a fire-retardant mechanism robust enough for truly improving the fire performance of the epoxy networks. Better results were found in the case of Cloisite 30B – which is a type of functionalised montmorillonite – as compared to other montmorillonite clays [61]. In this paper, Camino et al. reported cone calorimeter results of epoxy/anhydride networks modified with 21 wt% of several kinds of montmorillonite (Figure I-19).

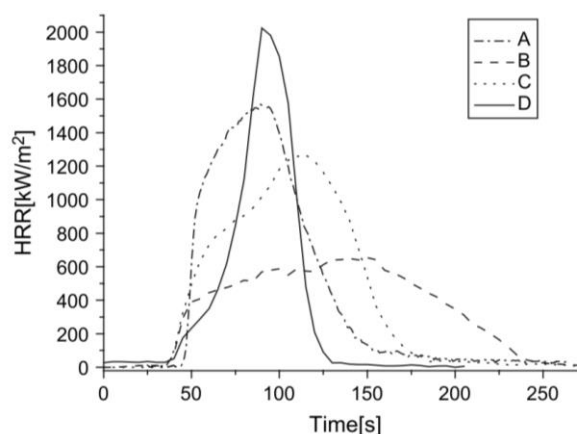


**Figure I-19 Cone calorimeter analysis of neat epoxy (D) and epoxy composites with (A) Cloisite 25A (dimethyl hydrogenated-tallow (2-ethylhexyl) ammonium montmorillonite) ; (B) Cloisite 30B (methyl tallow bis(2-hydroxyethyl) ammonium montmorillonite) ; (C) Nanofil 848 (octadecyl ammonium-modified montmorillonite) [61]**

The spectacular reduction of pHRR – 68% as compared to the neat epoxy network – was attributed to a predominant chemical role of the clay – an increased charring catalysis during combustion – as compared to the dispersion state, the Nanofil 848 filler being better exfoliated than the Cloisite 30B in the epoxy networks. While large improvements were highlighted in this work, one has to keep in mind that the loadings were as high as about 20 wt%. Thermomechanical properties of the final composite networks were not assessed in this study.

Mechanical properties of DGEBA/amine networks filled with surface-modified montmorillonites at low content levels – 0.5, 1, 2, or 3 wt% – were investigated by Kaynak et al. [62]. As concerns the flexural strength, strain at rupture, modulus and the fracture toughness, an improvement was observed by introducing long alkyl ammonium ions-substituted montmorillonites – with the best results found for 0.5 wt% of nanoclay. The flame retardancy was investigated by measuring the LOI of the networks. Limited improvements were observed with a maximum increase of LOI from 20.9% for the neat epoxy to 23.2% in the best case, found for a 2 wt% loading of dodecyl trimethylammonium montmorillonite. The increase was attributed to aggregation of nanoclays at the polymer surface during combustion, leading to the formation of protective layer impeding the oxygen and volatiles transfer. Katsoulis et al. [63] investigated the influence of 5 wt% of montmorillonites (Cloisite 30B and octadecyl ammonium ion-modified montmorillonite, I.30E) on the flammability of high performance TGDDM-based networks. No improvements were highlighted in terms of reduction of pHRR or classification, with the cone calorimeter or the UL 94 test, respectively. A slight increase of the LOI was observed for the montmorillonite-containing networks, from 27.8 for the neat epoxy system, to 30.0 and 30.8 with I.30E and 30B respectively. The same study based on low-temperature curing bifunctional epoxy resin showed no improvements as compared to the fire behavior of the neat network.

Based on the studies carried out on the use of nanoclays in epoxy networks, it seemed that layered silicates should be introduced in sufficient amount to obtain a significant beneficial effect on the fire behavior of these networks. The mechanism of fire retardancy was attributed to a physical effect of the particles, namely their aggregation at the burning surface of the samples, due to combustion of the surrounding polymer material. The hypothesis of the nanoclays migrating towards the polymer surface (illustrated in Figure I-20) has also been proposed in thermoplastic polymers [64]. This mechanism of fire retardancy is potentially valid for other nano-particles, even if the platelet shape of the nanoclays renders them more efficient. One can thus easily understand that a certain volume fraction and exfoliation degree of clays are required in order to produce a layer able to stop the gas transfer.

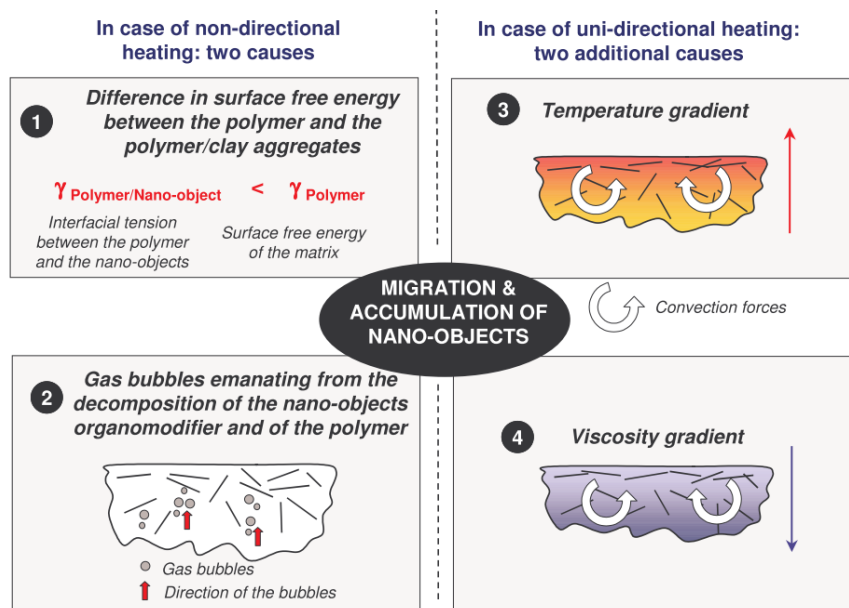


**Figure I-20 Phenomena suggested to explain the migration and accumulation of nanofillers on the surface during burning of a thermoplastic polymer [60], [64]**

### **3.2.b. Epoxy networks containing silica-based glass domains**

Another strategy for the fire retardancy of epoxies is to introduce silica nano-particles within the networks. Commercial epoxy resins containing such fillers are available commercially, such as the one used by Katsoulis et al. [63]. The resin was the Bakelite EPR 486, and was based on TGDDM filled with 30 wt% of nano-silica particles and cured using 4,4-diaminodimethyl sulfone (DDS) as a curing agent. The morphology obtained in the final network was a rather homogeneous dispersion of particles of a few tens of nanometres in diameter. Despite a rather high filler content, the epoxy-based network containing the silica particles displayed no significant improvement as observed from cone calorimeter experiments. Only a slight delay of the time to ignition and the time to the peak was noticed, as compared to the neat TGDDM/DDS network. The LOI was increased from 27.8 to 29.4% and the silica nanoparticles allowed the epoxy network to reach a V-1 classification – the reference system failing to satisfy the minimum requirements for classification. The influence of the addition of a commercial multi-element glass, the Ceepree glass (grade B200U, average particle size D50 of 3-8  $\mu\text{m}$  and a maximum particle size of 30  $\mu\text{m}$ ) was also investigated in epoxy systems based on bisphenol A diglycidyl ether epoxy and an anhydride (MMHPA) as curing agent [65], [66]. A loading of 10 or 15 wt% of the glass in the networks caused a decrease of T<sub>g</sub> of 10 °C. A reduction of pHRR between 50% and 63% was obtained, depending on the irradiation level implemented in the cone calorimeter experiments, and an increase of the LOI from 21% to 25% was observed.

In similar epoxy networks, Scharrel's research group also investigated the influence of a silica glass on the fire performance [67], [68]. They, however, synthesized the Si-based glass by the hydrolysis/condensation of phenyltriethoxysilane, which was further heat treated to obtain a higher condensation degree and confer the glass a better thermal stability in terms of degradation temperature onset and amount of residue – as seen from TGA measurements [67]. This resulted in the production of a mixture of polysilsesquioxanes of different structures (Figure I-21).

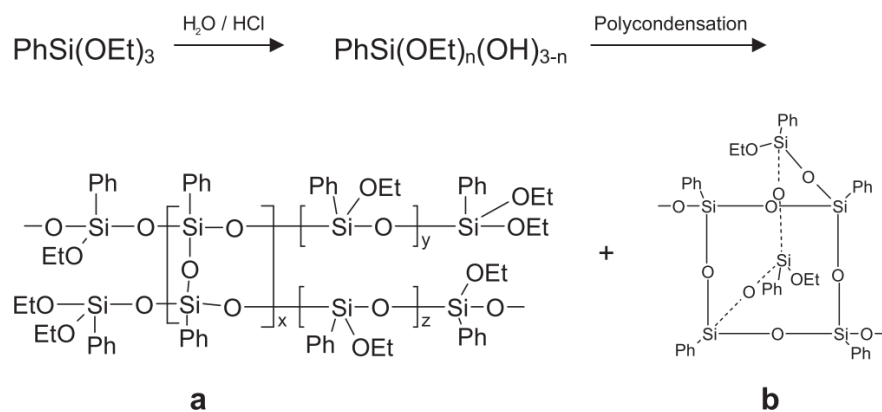


**Figure I-21 Preparation of a phenyl-containing silica glass from  $\text{PhSi(OEt)}_3$  through hydrolysis and polycondensation. Illustration of chemical structures of the glass containing a) ladder structure and b) partially reacted hexasisesquioxane structure [67]**

The idea was to take advantage of the low-melting characteristic of such a glass to favour the formation of continuous silica protective layer during the combustion. Networks based on bisphenol A diglycidyl ether epoxy and an anhydride (MMHPA) as curing agent were filled with 5, 10 or 15 wt% of inorganic glass. Synergy with tetraphenylphosphonium montmorillonite (TPPMMT) was also investigated. While no improvements were reported as concerns the LOI of glass-containing networks and their UL94 classification [68], results from the cone calorimeter experiments showed a beneficial effect of the silica glass in terms of reduction of pHRR and Total Heat Released (THR) (Figure I-22).

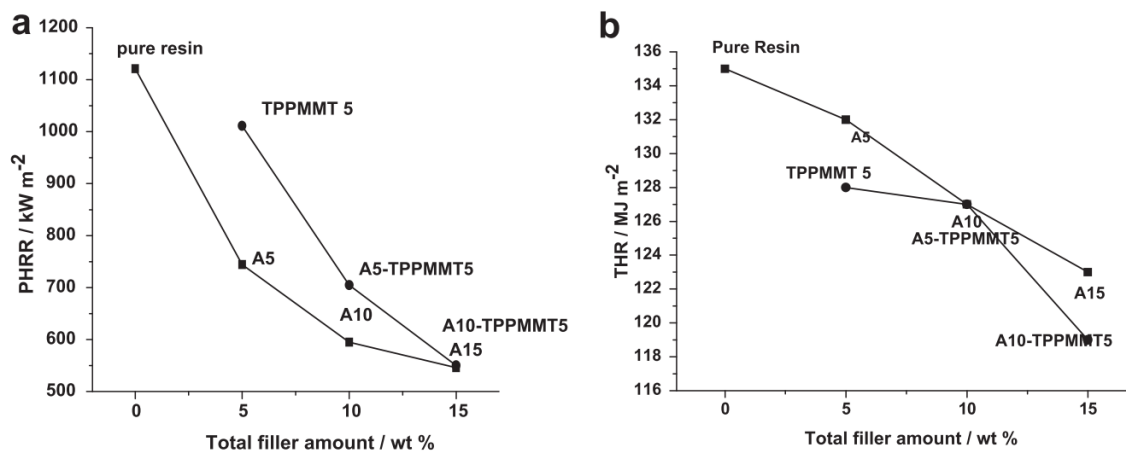


**Figure I-22** Dependence of a) peak of Heat Release Rate and b) Total Heat Released on total filler content. 'A' stands for the heat-treated glass, 'TPPMMT' for the tetraphenyl phosphonium montmorillonite and the numbers '5', '10' or '15' or the weight percentage of the fillers [67]

Such a positive effect of the silica glass on the pHRR was explained by a thorough observation of the char residues. Visual observation revealed a consistent but crackled glassy coating on top of the residue. Observation by Transmission Electron Microscope (TEM) of a sample extinguished just after ignition showed glass particles starting to coalesce. It was assumed that they softened and/or melted and thus entrapped the bubbles of volatiles from matrix decomposition which enhanced the transport of glass to the sample surface (Figure I-23).

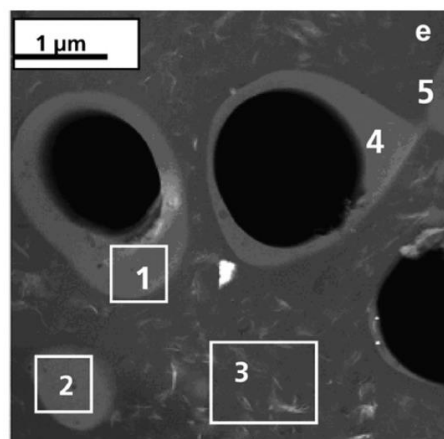


**Figure I-23** TEM images of A5-TPPMMT5 residue after burning test (nomenclature is the same as in Figure I-22). Zones 1 and 2 are attributed to silica glass while zone 3 is regarded as TPPMMT dispersed in the epoxy matrix. The phenomenon of entrapment of gas bubbles (in black) by the silica glass (grey rings) is visible close to zone 1 [68]

The use of ladder-like polysilsesquioxanes in epoxy networks was also reported by Zhang et al. [69]. Polyphenyl silsesquioxane was introduced in DGEBA/m-phenylene diamine networks at a level of 4.1 wt%. The LOI was increased from 25% to 27.1% by the addition of polyphenyl

silsesquioxane, but the UL 94 samples failed to pass the minimum requirements for classification, just like the unfilled epoxy network. As for the cone calorimeter results, pHRR was actually increased of about 10% as compared to that of the neat epoxy network. The increase may not be significant but it clearly showed the absence of a fire-retardant behavior from the ladder-like polyphenyl silsesquioxanes, which was unexpected, especially given the good thermal stability of these compounds, assessed via TGA. Moreover, the epoxy/silsesquioxane system displayed a clearly intumescent behavior which should have protected the virgin material. The reason provided by the authors for the poor fire performance of this network was the brittleness of the char, based on Scanning Electron Microscopy observation. Nonetheless, an interesting point of the study is the comparison of such a network with a system filled with 4.1 wt% of the equivalent cage-structure polysilsesquioxanes, namely the octaphenyl polyhedral silsesquioxane. The case of POSS will be discussed in the next section, but it is worth noting that, in this study, the use of the POSS allowed to obtain similar results of LOI and UL 94 but above all, a relative enhancement of the cone calorimeter results through a significant decrease of the pHRR (Figure I-24).

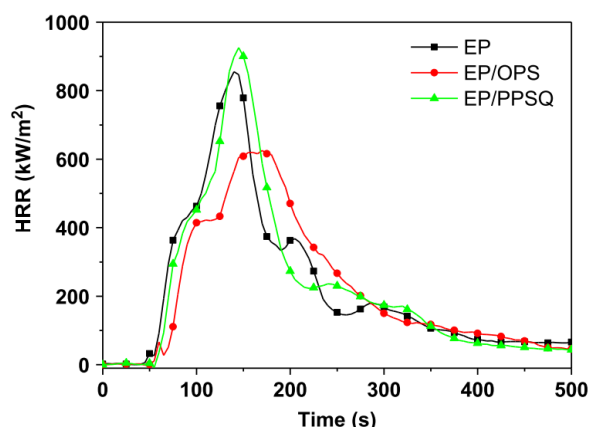


**Figure I-24 HRR curves of the neat epoxy network (EP) and epoxy composites containing octaphenyl polyhedral silsesquioxane (OPS) or polyphenyl silsesquioxane (PPSQ) [69]**

Thus, silica glasses and organic/inorganic silica-based glasses proved to be an interesting strategy to investigate for the fire retardancy of epoxies, with, however, mitigated results. Schartel et al. highlighted an interesting new possible fire-retardant mechanism that relied greatly on the physical properties of their organic/inorganic glass. While the chemical composition may also be of importance – especially the phenyl presence – results with similar compounds reported by Zhang et al. did not confirm the beneficial effect showed by the former. More investigation is thus needed in this field to clearly identify the critical parameters influencing the success of the use of such compounds in epoxy networks.

### 3.2.c. Cage-structure polysilsesquioxanes: a promising route towards flame retardancy?

As previously highlighted, POSS with a large range of tethers are available for modifying the fire behaviour of epoxy polymers. While several parameters, such as the dispersion process, will influence the final properties of the networks – in particular their morphology and fire performance – this section will focus on the influence of the POSS structure, in terms of composition and reactivity of the organic groups.

- Functional POSS versus unreactive POSS

Franchini et al. [70] published a work in 2009 in which they investigated precisely the functionality of POSS as a parameter influencing the morphology and the fire behaviour of DGEBA/MDEA-based epoxy networks. The study was carried out on epoxy networks containing about 4 wt% of POSS with phenyl groups. The POSS were either surrounded by eight phenyl groups, i.e. OctaPhenyl POSS, or by seven phenyl groups and a glycidyl function, i.e. GlycidylPhenyl POSS (Figure I-25).

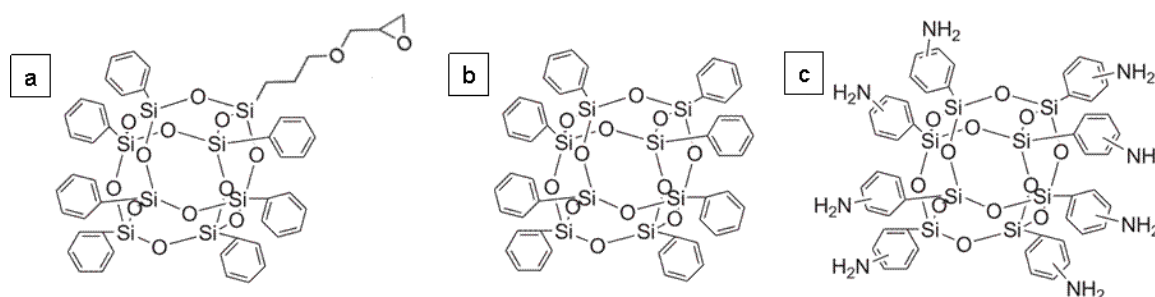


**Figure I-25 Structure of: a) GlycidylPhenyl POSS; b) OctaPhenyl POSS; c) OctaAminoPhenyl POSS**

The latter was prereacted with the amine hardener before introduction in the epoxy and curing of the formulation, allowing the POSS to be grafted to the epoxy/amine network. While phase separation of the POSS actually occurred in both cases, it seemed that the prereaction step enhanced the dispersion of POSS in the network, while the OctaPhenyl POSS-containing network exhibited a certain extent of crystallinity, meaning that the POSS may have aggregated and organized with a certain order. As concerns the fire performance, both networks failed to reach minimum requirements in the UL 94 test, but exhibited self-extinguishment leading to large residue – 96% – when the neat network burnt entirely. From the cone calorimeter experiment, a large improvement was also reported, with reductions of 34% and 40% of the pHRR when introducing OctaPhenyl POSS or GlycidylPhenyl POSS, respectively (Figure I-26). Thus a slightly superior improvement was obtained in the case of the pre-reacted

monofunctional POSS as compared with the inert POSS, but the difference between both POSS-containing networks was not remarkable.

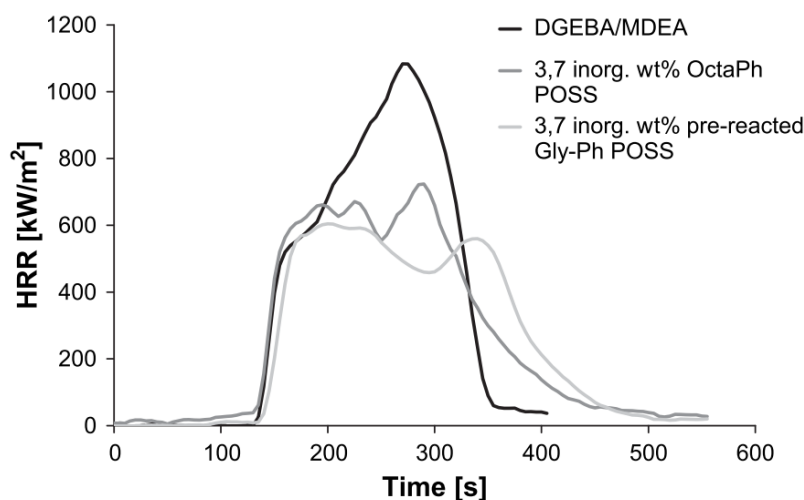


**Figure I-26 Heat Release Rate curves of neat epoxy network and networks containing POSS. ‘OctaPh POSS’ stands for OctaPhenyl POSS and ‘Gly-Ph POSS’ for GlycidylPhenyl POSS [70]**

Epoxy networks loaded with OctaPhenyl POSS were also investigated by Zhang et al. who confirmed this positive tendency with loadings of 2.5 wt%, 4.1 wt% and 5 wt% of this POSS in a DGEBA/m-PDA network [14], [71]. Comparison of these systems can be made with similar networks containing a phenyl-bearing octa-functional POSS, the OctaAminoPhenyl POSS (see Figure I-25 above). This POSS could potentially act as a crosslinking point by reacting with the oxirane of the epoxy prepolymer. Networks based on DGEBA and m-PDA with 4.6 wt% of this multifunctionalPOSS were studied by Zhang et al. [71], and Yang et al. investigated the fire properties of a DGEBA/DDM epoxy with a 10.28 wt% loading of POSS [72]. In both cases the POSS was first dispersed within the epoxy prepolymer, but no analytical or morphological studies were carried out to prove that the POSS actually reacted with the DGEBA. A comparison of results from networks containing OctaPhenyl POSS and OctaAminoPhenyl POSS is given in Table I-4, using the data from [14], [71], [72].

	D-mPDA	2.5 wt% OPS in D-mPDA	4.1 wt% OPS in D-mPDA	5 wt% OPS in D-mPDA	4.6 wt% OAPS in D-mPDA	D-DDM	10.28 wt% OAPS in D- DDM
TTI (s)	45	-	55	60	57	-	-
pHRR (kW/m <sup>2</sup> )	855	-	626 (-27)	712 (-17)	635 (-26)	-	-
THR (MJ/m <sup>2</sup> )	112	-	112 (0)	103 (-8)	110 (-2)	-	-
TSR (m <sup>2</sup> /m <sup>2</sup> )	4182	-	3729 (-11)	3192 (-24)	3753 (-10)	-	-
UL 94	NR	NR	NR	NR	NR	-	-
LOI (%)	25.0	26.8 (+7)	27.2 (+8)	27.6 (+9)	27.0 (+8)	22.0	24.5 (+11)

**Table I-4 Cone calorimeter, UL94 and LOI data derived from [14], [71], [72]. Values in brackets are for the difference percentage as compared with the neat corresponding matrix. 'D-mPDA' stands for DGEBA/m-PDA, 'D-DDM' for 'DGEBA/DDM', 'OPS' for 'OctaPhenyl POSS' and 'OAPS' for 'OctaAminoPhenyl POSS'. 'NR' stands for 'Not Rated'. For the cone parameter abbreviations, please see section 2.2.b. Unfilled boxes correspond to non available data**

Once again, close results were obtained when comparing networks containing functional POSS and unreactive POSS with organic groups of similar structure. In the light of these comparisons, it seemed that, for similar inert groups, the reactivity of the tethers is not a critical parameter for the fire retardancy of the POSS-containing epoxy networks.

- Influence of the inert organic groups

The influence of the non reactive organic groups surrounding the POSS cage can be determined by comparing similar POSS with different tethers. Franchini et al. studied the combustion of DGEBA/MDEA-based networks containing 9.19 wt% of OctaPhenyl POSS [70], and Gérard et al. investigated epoxy systems based on DGEBA-DETA with 5 wt% of OctaMethyl POSS [15]. The morphology was assessed in both cases, and better dispersion was achieved in the case of OctaMethyl where rod-like clusters of about 0.5-1  $\mu\text{m}$  were observed, while the OctaPhenyl POSS constituted rough, large, crystalline phases in Franchini's networks. Results of cone calorimeter are reported in Table I-5 for comparison. In both studies the heat flux was fixed at 35 kW/m<sup>2</sup>, but the samples' dimensions and shape were different.

	D-DETA	5 wt% oMeP in D-DETA	D-MDEA	9.19 wt% OPS in D-MDEA
TTI (s)	49	50	133	140
pHRR (kW/m <sup>2</sup> )	813	731 (-10)	1040	689 (-34)
THR (MJ/m <sup>2</sup> )	33	36 (+9)	139	131 (-6)
RW (%)	4	3	1	10

**Table I-5 Cone calorimeter data from [15], [70]. <sup>1</sup> Values in brackets are for the difference percentage as compared with the neat corresponding matrix. 'D-DETA' stands for 'DGEBA-DETA', 'D-MDEA' for 'DGEBA-MDEA', 'oMeP' for 'OctaMethyl POSS', and 'OPS' for 'OctaPhenyl POSS'**

Addition of OctaMethyl POSS to the epoxy network brought insignificant improvements that lay within the error margin of the cone experiment. The phenyl-bearing POSS proved more efficient in decreasing the pHRR and increasing the residual weight, even when considering that twice more OctaPhenyl POSS than OctaMethyl POSS was introduced in the epoxy network. When comparing the Si content in both networks, they were comparable (2.0 wt% for OctaPhenyl POSS, 2.03 wt% for OctaMethyl POSS).

Similar comparison can be made on POSS containing reactive ligands. Franchini et al. compared two POSS containing one glycidylpropyl tether, and bearing either phenyl or isobutyl groups on the seven other silicon atoms [70]. HRR curves are displayed in Figure I-27. The peaks of HRR were diminished of 40% and 25% by the presence of phenyl- or isobutyl-bearing POSS, respectively. This tendency was confirmed by the UL 94 results: while the epoxy containing Glycidylisobutyl POSS burnt entirely, showing no improvement as compared to the neat matrix, the GlycidylPhenyl POSS caused the epoxy network to self-extinguish, leaving a mass residue of 96%. In this case again, the phenyl tethers were the cause of a larger improvement, as compared with non-aromatic groups.

<sup>1</sup>Some data related to neat and OctaPhenyl POSS-containing DGEBA/MDEA networks were not published neither in Franchini's paper nor in her PhD thesis [60], [70]. However, access to the data was granted as the authors of the present study belong to the same research group as Franchini's.

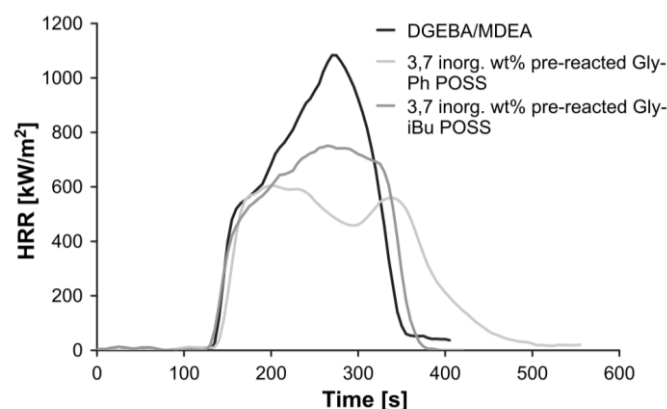


**Figure I-27 HRR curves of neat DGEBA/MDEA based network and hybrids containing GlycidylPhenyl POSS (Gly-Ph POSS) or Glycidylisobutyl POSS (Gly-iBu POSS) [70]**

The particular case of trisilanol POSS, with its incomplete cage structure, has been frequently studied as it is used as a precursor in the synthesis of tailored monofunctional POSS. In particular, the trisilanol POSS bearing isobutyl or phenyl tethers are amongst the cheapest POSS [58]. These compounds were studied for the flame retardancy of epoxy networks in [31], [73], [74]. A slightly different POSS, the CyclohexylDisilanol POSS, was studied in [75] and will be included for comparison. The POSS structures are displayed in Figure I-28.

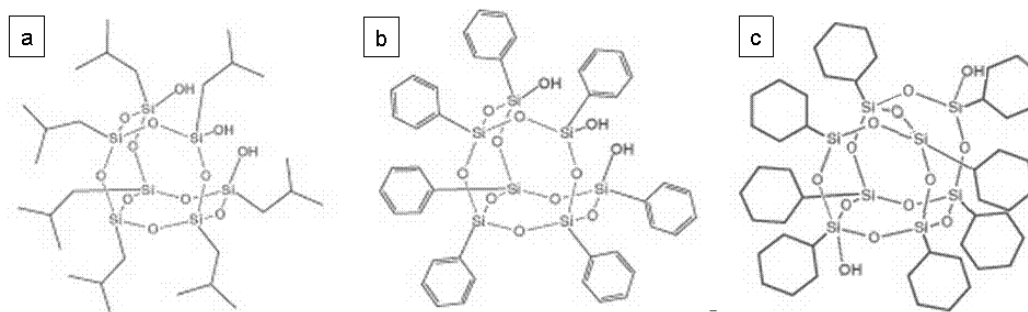


**Figure I-28 Chemical structure of a) Trisilanollisobutyl POSS; b) TrisilanolPhenylPOSS; c) DisilanolCyclohexyl POSS**

In Table I-6 are displayed the LOI results of neat and POSS-containing epoxy networks, gathered from [31], [75], [76]. Unexpectedly, the network containing 5 wt% of Trisilanollisobutyl POSS showed the best improvement. This could possibly come from the type of resin. The network where the phenyl-bearing POSS was introduced was composed of aliphatic epoxy and amines. It may be more difficult to fire-retard as compared to systems containing aromatic groups, such as DGEBA-, BSA- and DDS-based networks. It is thus difficult to conclude on the influence of the POSS ligands in this example.

	Aliph. EP	PhPOSS(OH) <sub>3</sub> in Aliph. EP 10 wt%	D-BSA	iBuPOSS(OH) <sub>3</sub> in D-BSA 5 wt%	D-DDS	CyPOSS(OH) <sub>2</sub> in D-DDS	
						5 wt%	10 wt%
LOI (%)	19.8	20.7 (+5)	22.6	25.7 (+14)	26	26.5 (+2)	27.3 (+5)

**Table I-6 LOI results compiled from [31], [75], [76]. Values in brackets are for the difference percentage as compared with the neat corresponding matrix. 'Aliph. EP' stands for 'aliphatic epoxy' (1,4-butanediol diglycidylether and modified cycloaliphatic amines), D-BSA' for 'DGEBA-BSA' and 'D-DDS' for 'DGEBA-DDS'**

An interesting point, more related to the reactivity of the POSS than to the inert tethers structure, is that in [73], [75], a metal compound was used as a catalyst to enhance the grafting of Silanol POSS. In particular, Wu et al. showed that the use of Aluminium triacetylacetonate resulted in smaller POSS domains of about 0.5  $\mu\text{m}$  in diameter, as compared to 5  $\mu\text{m}$  when the catalyst was not present. The authors did not perform any study aiming at verifying the actual grafting of POSS on the epoxy network. As concerns the fire behaviour of the DGEBA-DETDA network, there was a larger improvement when the catalyst was introduced in combination with the POSS, as compared to the network with only POSS (Figure I-29). In particular, a reduction of the pHRR of 12% and 33% was found for the networks containing either the POSS only, or the POSS and the catalyst, respectively.

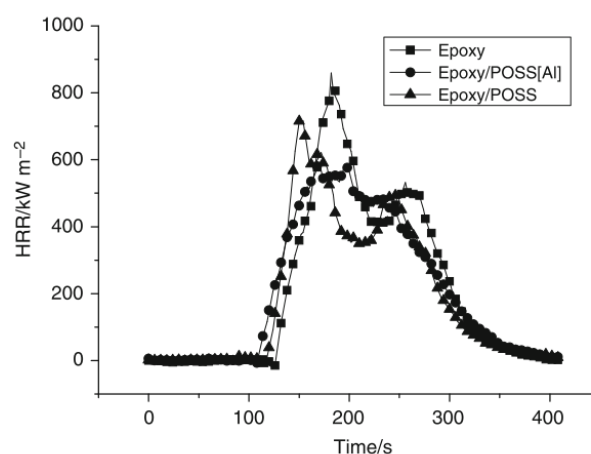


**Figure I-29 HRR curves of DGEBA-DETDA networks containing 10 wt% of TrisilanolPhenyl POSS, with or without 0.6phr of Aluminium triacetylacetonate as a catalyst [73]**

Concluding on the influence of the inert tethers in the light of the reported results is not an easy process, as between the different studies, other parameters were varying. Nonetheless, a beneficial effect of aromatic tethers is to be forecast, as compared to aliphatic or cycloaliphatic organic groups.

### 3.2.d. POSS used in synergy with other elements

The question of the effect of using POSS in synergy with other elements and/or nano-objects to improve the fire retardancy of epoxy networks is a subject slightly beyond the scope of the present study. However, this is a way which has been widely investigated and thus deserves to be mentioned.

Amongst the many studies on the subject, particular interest has been focused on the synergy between POSS and phosphorus-containing compounds. Gérard et al. [77] reported the use of Ammonium PolyPhosphate (APP) in combination of OctaMethyl POSS in a DGEBA-diethylenetriamine network. A clear synergistic effect of both POSS and APP was indeed observed via cone calorimetry, as compared with networks containing one or the other compound (Figure I-30).

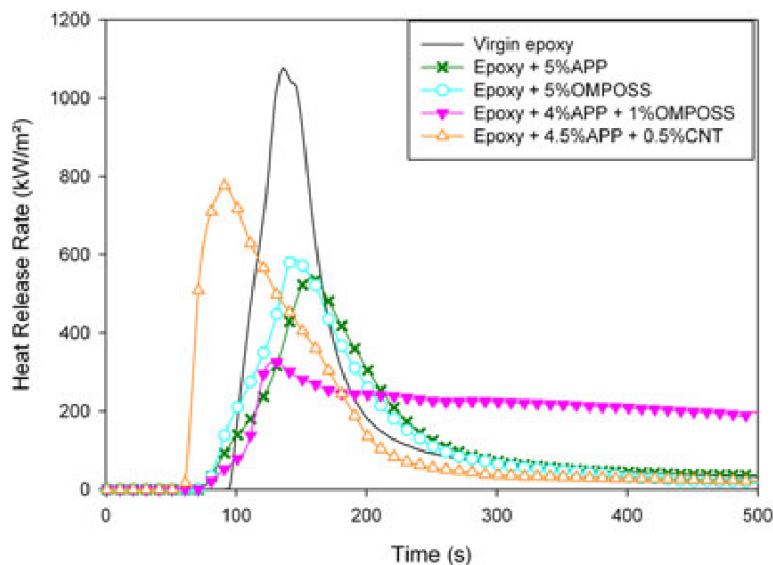


**Figure I-30 HRR curves of DGEBA-triethylenetriamine networks with OctaMethyl POSS and/or APP**  
[77]

The epoxy network containing both APP and POSS displayed a large reduction of pHRR, but also a quasi-constant HRR after the flash-over, corresponding to slow and constant burning. This was due to a phenomenon of intumescence: the epoxy polymer started to swell under the action of fire and the surface sample approached the heat resistance during the test, causing the material to keep burning. Swelling is typical for phosphorous-containing systems. Actually, to obtain an intumescent system, there must be three ingredients in presence: an acid source (the APP, in the present study), a char forming agent and a blowing agent [78]. Intumescence is an interesting phenomenon for flame retardancy because it promotes the formation of a thick foam-like char layer made of a crosslinked structure of polyaromatic arrays that provides good

thermal protection and hinders the transfer of volatiles. In this case, the APP-containing networks swelled more than the network with the combination of both compounds (Figure I-31), but the latter exhibited a more solid char with less cracks, certainly providing better protection and barrier properties.

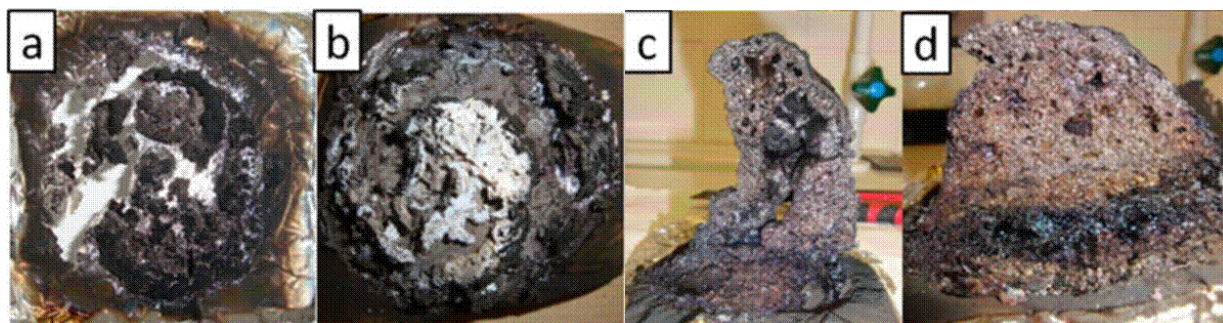


**Figure I-31 Char residue pictures of a) neat epoxy (top view); b) POSS-containing network (top view); c) APP-containing network (cross section); d) network containing both APP and POSS (cross section) [77]**

Zhang et al. investigated the potential synergy of POSS with 9,10-dihydro-9-oxy-10-phosphaphenanthrene-10-oxide (DOPO), the latter being either grafted to the former [79], [80] or used in combination with OctaPhenyl POSS [81]. A peculiar phenomenon, the 'blowing-out' effect, was observed in certain networks containing the DOPO-POSS – the POSS with DOPO grafted as the surrounding tethers [80]. The blowing-out effect is pictured in Figure I-32. It seems that this phenomenon consists in the formation of a porous char and the simultaneous fast release of gas that tend to blow the oxygen away and smother the flame.

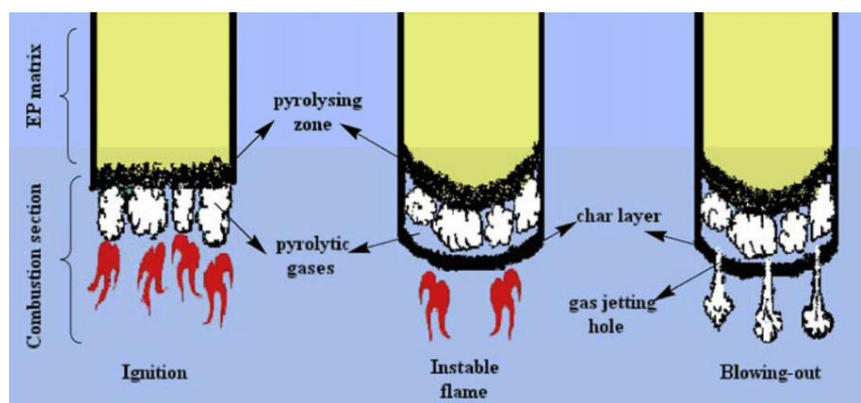


**Figure I-32 Scheme of the principle of the blowing-out effect [80]**

However, the blowing-out effect did not happen systematically. The HRR curves of networks based on different hardeners, i.e. either oligomeric polyamide 650 (PA650) or 4,4'-diaminodiphenylsulphone (DDS) are displayed in Figure I-33. It was clear from these curves that the occurrence of the beneficial effect of DOPO-POSS depended on the matrix chemistry. In the PA650-based network, the authors highlighted the absence of a char, and suggested that

in this system, the crosslinking structures could not be created in the condensed phase until addition of a sufficient DOPO-POSS content. Study of a DGEBA/DDS network containing DOPO and OctaPhenyl POSS – DOPO thus being grafted on the POSS structure – revealed a positive effect similar to the one reported previously [81]. The blowing-out effect thus did not seem to depend on the DOPO being grafted or not.

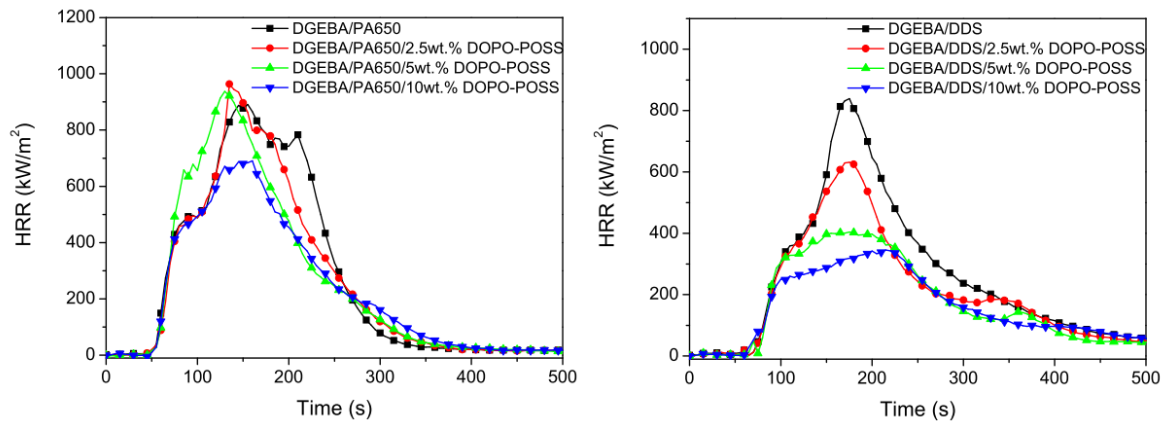


**Figure I-33 HRR curves of epoxy networks cured with two different hardeners and containing various DOPO-POSS contents [80]**

#### 4. CONCLUSION

In the present chapter, an overview of the field related to fire in polymers has been presented. Elements concerning the fire mechanisms and tests have been provided with the aim to guide the reader throughout the rest of this study. An overview of the strategies commercially in use at the present has been presented. What emerges from this is that there is a need for efficient and environmentally acceptable alternatives. In this context, the present study proposes to focus on the use of Polyhedral Oligomeric Silsesquioxane (POSS) as a fire retardant solution for epoxy networks. POSS are silicon-containing, well-defined nano-objects. As highlighted in the last section of this chapter, the strategies involving silicon-based additives for the fire retardancy of epoxies are varied. Silsesquioxanes appeared as a promising way for reducing the flammability of epoxies, though a careful selection of their structure and chemistry should be implemented in order to obtain the best possible improvements.

---

**CHAPTER II. POSS-CONTAINING THERMOSET  
NETWORKS: PROCESSING AND  
ASSESSING THE MORPHOLOGY**

---

The second chapter of this manuscript aimed at presenting the selected epoxy systems (Part 1) and how POSS were dispersed in epoxy matrices, depending on their potential reactive structure (Part 2). Last but not least, the third part of this chapter will focus on investigating the POSS dispersion in the fully cured networks, i.e:

- (i) How did the POSS physically assemble in the network? The dispersion was characterized by X-Ray Diffraction and microscopy. Information about the shape, the size and the overall dispersion of the POSS domains was obtained and will be discussed.
- (ii) How did the morphology develop within the network, during the curing cycle? Investigation was carried out based on cloud-point measurements and Transmission Electron Microscopy. The development of the morphology was expected to be dependent on the network crosslinking kinetics as a reaction-induced phase separation (RIPS) phenomenon was involved.

## 1. MATERIALS

### 1.1. MODEL SYSTEMS

#### 1.1.a. Selected epoxy prepolymers and comonomers

- DGEBA: a widely-used epoxy prepolymer

The Diglycidyl Ether of Bisphenol A (DGEBA) is the most spread type of epoxy resin on the global market, and can be found in a wide range of applications such as in coatings, flooring, adhesives, composite materials, etc. Consequently, in association with various types of curing agents, it constitutes the base of the model system *par excellence* and has been extensively studied in the literature in terms of kinetics, mechanical properties, addition of fillers, morphological characterization, etc. In this study, networks based on DGEBA (Epon 828 from Momentive) were investigated. The DGEBA used in this study was a difunctional epoxy with an equivalent weight epoxy from 185 to 192 g/eq (Figure II-1). The resin was a viscous liquid at room temperature, its viscosity being of 11-15 Pa.s at 25 °C, thus allowing easy handling for dispersion of additives.

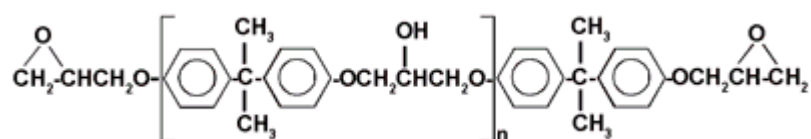
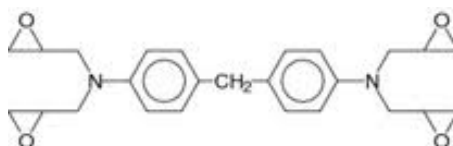


Figure II-1 Chemical structure of Diglycidyl Ether of Bisphenol A (DGEBA) prepolymer

- TGDDM: a high-performance epoxy resin

The Tetraglycidyl(diaminodiphenyl)methane (TGDDM) is an epoxy prepolymer for 'high-performance' materials, i.e. it is mainly used in epoxy formulations where properties of the final networks need to meet high requirements in terms of mechanical strength and moduli, glass transition temperature or thermal stability. TGDDM is then usually found in structural composite applications for the transport and energy sectors. TGDDM is generally included in resin formulations designed for the infusion or prepeg processes of composite manufacturing. The epoxy prepolymer selected was the MY9512 from Huntsman. It was an aromatic tetrafunctional epoxy prepolymer with an equivalent weight epoxy from 117 to 134 g/eq. The simplified chemical structure is reminded in Figure II-2. The resin was a viscous liquid at room temperature, its viscosity being of 110-130 Pa.s at 25 °C.



**Figure II-2 Chemical structure of Tetraglycidyl(diaminodiphenyl)methane (TGDDM) prepolymer**

- MDEA: a low-reactive aromatic amine curing agent

The crosslinker selected was the MDEA (4,4' methylene bis(2,6-diethylaniline)) provided by Lonza, and was a powder at room temperature. It is a primary aromatic diamine (Figure II-3) with low reactivity as compared to aliphatic and cycloaliphatic amines. This implies that high temperatures and long curing times are needed in order to reach crosslinking completion in epoxy-based networks. Thus, cure kinetics being slow, monitoring the epoxy-amine reactions is easily feasible, as well as handling the reactive epoxy-amine formulations at room temperature. The MDEA molecular structure is close to that of MDA (4,4'-diaminodiphenylmethane), which has been widely studied and used in composites in the past, but is highly toxic.

The functionality of the MDEA molecule is equal to 4, which will be taken into account for determining the stoichiometry of the networks.

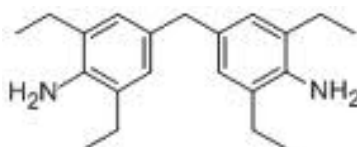


**Figure II-3 Chemical structure of 4,4' methylene bis(2,6-diethylaniline) (MDEA)**

### 1.1.b. Epoxy-amine crosslinking reactions

The build-up of a conventional epoxy system involves three possible well-known reaction pathways (Figure II-4).

- (i) The reaction of a primary amine on an epoxy group. This reaction involves the opening of the epoxy ring and results in the creation of a secondary amine and a hydroxyl function.
- (ii) The reaction of a secondary amine produced by the previous reaction, with an epoxy group. This reaction produces a tertiary amine and a hydroxyether group.
- (iii) The reaction of a hydroxyl group upon an epoxy group. In this case, there is homopolymerization via a reaction of etherification, which consumes one epoxy group and leaves the hydroxyl groups' content unaffected.

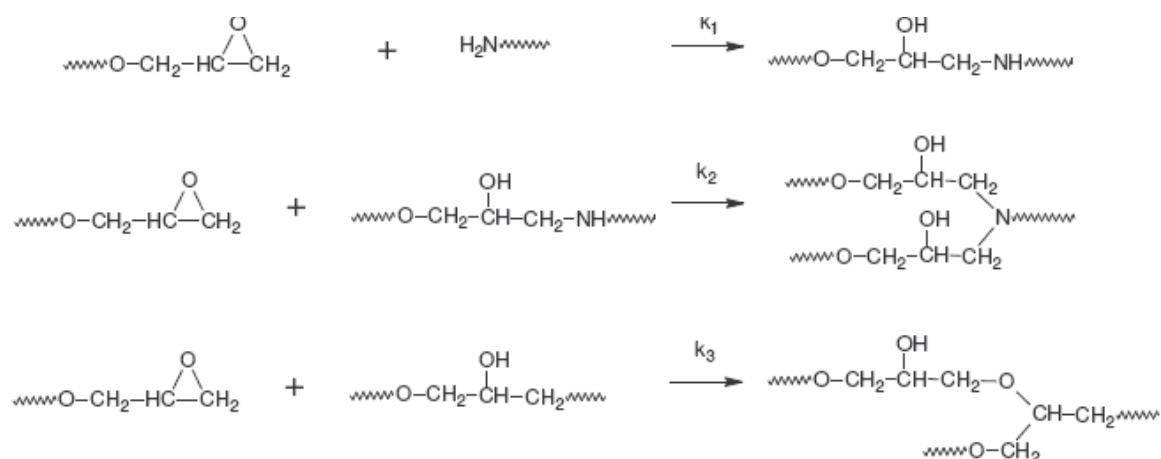


**Figure II-4 Reactions of polyaddition between an epoxy and a primary or secondary amine, and homopolymerization (from top to bottom) [82]**

The copolymerization reactions, with the related kinetic constants  $k_1$  and  $k_2$ , can be defined as a combination of two mechanisms, either catalytic or non-catalytic. Indeed, these reactions are known to be catalysed by the hydroxyl groups existing in the epoxy prepolymer and produced during the polymerization. As any labile hydrogen-containing group, the  $-\text{OH}$  enhances the epoxy ring opening and promotes the nucleophilic addition of the amine, which explains the auto-catalytic nature of the epoxy-amine addition. If  $k_1'$  and  $k_2'$  are the kinetic constants associated to the non-catalytic pathway for the reaction producing the secondary amine and the tertiary amine, respectively, and  $k_1''$  and  $k_2''$  are the kinetic constants associated to the catalytic pathway for the same reactions, then the kinetic equations are as follows:

II-1

$$\frac{-d[NH_2]}{dt} = k_1'[EP][NH_2] + k_1''[EP][NH_2][OH]$$

II-2

$$\frac{-d[TA]}{dt} = k_2'[EP][SA] + k_2''[EP][SA][OH]$$

Where  $[NH_2]$ ,  $[EP]$ ,  $[OH]$ ,  $[TA]$  and  $[SA]$  are the concentrations of the primary amine groups, the epoxy groups, the hydroxyl groups, the tertiary amines, and the secondary amines, respectively.

Liu et al. [83] performed study of kinetics by Near-Infrared Spectroscopy (NIRS) involving various epoxy-aromatic diamine systems and showed that in most cases, the experimental kinetic data fitted the empirical kinetic equation of the catalytic mechanism, i.e. that the catalytic mechanism predominated and the non-catalytic mechanism contribution could be neglected. They also highlighted that the reaction rates of these reactions depended on the reactants' chemistry, in particular on the amine substituents' nature – electronegativity and steric hindrance.

The etherification reaction – defined by the kinetic constant  $k_3$  – is considered as a side reaction in most cases and is known to occur generally at high temperatures and/or in excess of epoxy [84] and/or in presence of a catalyst. This reaction is generally neglected in the kinetic studies focusing on the copolymerization reactions.

## 1.2. COMMERCIAL EPOXY SYSTEM

Epoxy networks based on a commercial formulation for aeronautics, specially designed for the infusion process i.e. RTM, were investigated. Main advantages of this formulation include its low infusion temperature – 70 °C – and its good performance before and after hot/wet conditioning, as stated by the product data sheet. It was supplied by Cytec, UK, as a two-component, namely the resin, MVR444R and the hardener, MVR444H. The two components were provided as a mixture of several epoxy prepolymers or different hardeners, respectively. The resin was a light-brown viscous liquid while the hardener was a brown two-phase component which required heating and mixing before use. The material supplier gave the following – and limited – information: the resin component contained TGDDM, the epoxy-functionalized molecule presented in the previous section, and one of the crosslinking agent of the MVR444H component was 4,4'-methylenebis(2-isopropyl-6-methylaniline) (MMIPA). The chemical

structure of the latter is presented in Figure II-5 and as one can see, its structure is very similar to that of MDEA, the hardener used in the model systems. The MVR444 system thus constitutes a complex system which can be compared to one of the model system of this study, namely the TGDDM-MDEA system.

The material supplier advised a MVR444H:MVR444R weight ratio of 58:100.

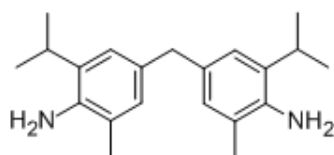


**Figure II-5 Chemical structure of 4,4'-methylenebis(2-isopropyl-6-methylaniline) (MMIPA)**

### 1.3. POLYHEDRAL OLIGOMERIC SILSESQUOXANE SPECIFICATIONS

As mentioned in the previous chapter, POSS ligands can influence a number of properties, from the initial state of dispersion to the mechanical and thermal properties of the final material the POSS are included in. If one cannot yet predict these properties before actually making the material, one can still have a hint of which POSS is more likely to enhance the desired properties. Down-selection of the POSS is thus of importance in the process of optimization of a material. The literature gives useful information as the number of studies related to POSS compounds have greatly increased in the last decades [85].

Thus, it was decided in this study to focus on POSS whose ligands contained aromatic cycles, for two reasons: (i) they showed promising fire-retardant potential [70] and (ii) they are of similar nature as epoxy comonomers which potentially can increase their compatibility. Moreover, the POSS selected were supposed to lead to different dispersion states in the final networks. Indeed, it is believed that the morphology developed may have an influence on the fire behaviour. This is why one non-reactive and two reactive POSS were selected from Hybrid Plastics and used as received. Their chemical structures are displayed in Table II-1.

- isooctylphenyl POSS (iOPOSS)

This POSS was selected for its high concentration of phenyl ligands – seven per molecule – and because the alkyl chain was thought to hinder assembling, i.e. crystallizing, , thus making them possibly easier to disperse in the epoxy-amine system. This POSS being unreactive, it is also referred to as a molecular silica. It is expected to behave like a filler and form aggregates [70].

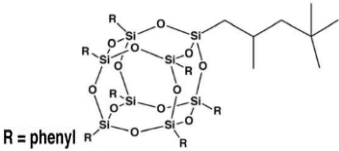
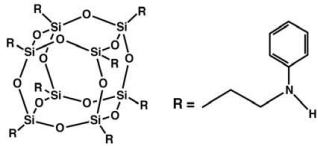
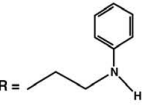
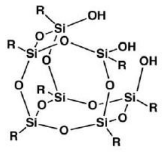
The iOPOSS was solid at room temperature. Full characterization of the product revealed the iOPOSS crystallinity and a high melting temperature equal to 193 °C.

- N-phenylaminopropyl POSS (AmPOSS)

The AmPOSS was a cage mixture, i.e. it contained both  $\text{Si}_8\text{O}_{12}$  and  $\text{Si}_{10}\text{O}_{14}$  cages, in a proportion of ca. 92% and 8% respectively as determined by Size Exclusion Chromatography. This POSS was a highly viscous liquid at room temperature and thus did not cause crystallinity issues. It was chosen for its phenyl content – one aromatic ring on each ligand – and its reactivity: the secondary amine function present on each ligand would allow this POSS to react with the epoxy prepolymer. A kinetic study where the POSS is used as a crosslinker will be presented in a following section of this chapter.

- trisilanolphenyl POSS (POSSOH)

POSSOH was different from the other POSS selected as it consisted in an incomplete, open cage of seven silicon atoms. Three of them bore a silanol function and on all of them was linked an aromatic ring. This POSS could behave differently depending on the possibility of reaction through its silanol functions.

Product	Denomination	Functionality	Schematic structure	Tm (DSC)
isooctylphenyl POSS	iOPOSS	0	 R = phenyl	193 °C
N-phenylaminopropyl POSS	AmPOSS	8	 R = 	-
trisilanolphenyl POSS	POSSOH	3	 R = phenyl	219 °C

**Table II-1 Chemical structures of down-selected POSS; ‘Tm’ stands for ‘melting temperature’**

#### 1.4. AN ALUMINIUM-BASED CATALYST

The aluminium tris(acetylacetonate) was a 99%-purity reactant obtained from Sigma-Aldrich and used as received. It was a white-powder solid at room temperature. Its structure is displayed in Figure II-6.

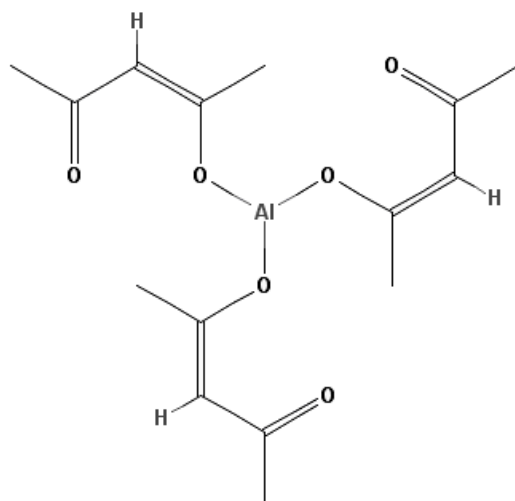


Figure II-6 Chemical structure of aluminium triacetylacetonate

## 2. PROCESSING THE NEAT AND HYBRID EPOXY NETWORKS

### 2.1. PREPARATION OF EPOXY-BASED REACTIVE SYSTEMS

#### 2.1.a. Reference epoxy networks

The neat epoxy networks were synthesized by mixing the epoxy (DGEBA, TGDDM or MVR444R) prepolymer with the crosslinking agent (MDEA or MVR444H) at 90 °C in a glass reactor under vacuum. The epoxy and amine functions were introduced in stoichiometric ratio in the model systems (amino hydrogen-to-epoxy ratio equal to 1) and the hardener-to-epoxy ratio specified by the supplier was respected in the case of the MVR444 networks. The MVR444H (hardener) being heterogeneous at room temperature, it was heated to 70 °C in oven and hand-stirred prior to mixing with the epoxy. About 100 and 300 g of these mixtures were prepared for UL-94 samples and cone calorimeter samples, respectively. The degassing phase was carried out until obtaining a perfectly homogeneous medium and no more visible gas bubbles, which took ca. 20 minutes for DGEBA-MDEA network and ca. 30 minutes for TGDDM-MDEA network.

### **2.1.b. POSS-containing epoxy networks**

For the systems containing POSS, an additional step was carried out, consisting of mixing the POSS with the epoxy prepolymer before adding the required hardener quantity. The degassing step carried out at 90 °C took more time in presence of POSS, being of *ca.* 30 minutes for the DGEBA-based systems and *ca.* 45 minutes for the TGDDM-based networks. Different processes were implemented for the dispersion of POSS.

Because not all the POSS had the same ligands and cage structures, neither the mass ratio nor molar content could correctly allow a right comparison of POSS content in the networks. Thus, it was chosen to introduce the same inorganic weight content – 1.5 inorg.wt% – in all of the final materials. The quantities of all compounds in each system are reported in Table II-2 at the end of the section.

- Dispersion of POSS via heat solubilisation

This process consisted of solubilising POSS in the epoxy prepolymers by mechanical stirring and heating the mixture to different temperatures for each POSS – these temperatures being previously determined by performing small-scale solubility tests. The mixture was then slowly stabilized at 90 °C in order to add a stoichiometric amount of the comonomer.

The initially solid iOPOSS was solubilised in DGEBA at 205 °C. However, the POSS recrystallized before the end of the degassing phase at 90 °C, forming very fine particles which made the solution cloudy. Moreover, the iOPOSS could not be solubilised in the TGDDM prepolymer.

The AmPOSS was also solubilised in the DGEBA prepolymer by heating at 60 °C. As AmPOSS brought a certain amount of amine functions, the quantity of crosslinking agent in this particular epoxy network has been slightly decreased in order to keep the stoichiometric ratio between epoxy and amine functions equal to 1. No network based on TGDDM was made with the AmPOSS.

The POSSOH was solubilised by heating at 130 °C for 30 minutes in the DGEBA, the TGDDM and the MVR444R prepolymers. No recrystallisation of the POSS was observed during the degassing phase.

- Dispersion via high-shear mechanical stirring

POSS clusters were mixed with the epoxy prepolymer using a high-shear mixing device (Rayneri Dissolver), at 2000 rpm for one hour without heating.

The high-shear mechanical mixing was used to disperse the iOPOSS in the TGDDM prepolymer. However, aggregates of various sizes were still visible after the mixing procedure. This process was also implemented to disperse POSSOH in DGEBA and TGDDM. Aggregates, slightly finer though, were also observed. The mixtures were then heated to 90 °C and the proper amount of MDEA was added.

- Dispersion with addition of an aluminium acetate catalyst

The reactivity of the POSSOH was taken into account via the addition of an aluminium acetate catalyst. In the literature [73], [75], [86] it was found that the presence of a metallic catalyst would allow the reaction between silanols and epoxies to occur. The aluminum tri(acetylacetonate) has been chosen in order to graft the POSSOH on the DGEBA or TGDDM monomers. The POSSOH was mixed in the epoxy monomers at 130 °C for 30 minutes, until it finally solubilised and the solution became transparent. After cooling down the mixture to 90 °C, the MDEA was added and the mixture was stirred under vacuum to allow the mixture to degas. Aluminium catalyst (0.6% of the weight resin part) was introduced and the preparation was stirred for further 5 minutes at 90 °C, until the catalyst powder solubilised. Addition of catalyst before addition of MDEA was first attempted but caused the premature gelation of the system in the reactor during the stage of solubilisation of MDEA at 90 °C.

## **2.2. CURING, COMPOSITION, AND NOMENCLATURE**

The mixtures were poured in closed moulds and the crosslinking stage was done in an oven under air atmosphere, according to the curing cycles specified in Table II-2. It is worth noting that a first additional step at 90 °C was carried on for systems containing the aluminium catalyst.

The networks nomenclature is made of three parts:

- The initials of the epoxy prepolymer and the hardener – e.g. ‘DM’ stands for DGEBA-MDEA, ‘MVR’ stands for MVR444R-MVR444H ;
- The POSS abbreviation ;
- A hint on the process of POSS dispersion: a number stands for the temperature of solubilisation of the POSS, dispersed via heating, ‘mix’ refers to the process of POSS dispersion through high-shear mixing, and ‘Al’ stands for aluminium-based catalyst.

As an example, a network named ‘TM-POSSOH-130’ designates a network based on TGDDM and MDEA, containing triSilanolPhenyl POSS, which was solubilised in the TGDDM prepolymer at 130 °C.

	System compositions				Curing cycle
	POSS		hardener	Epoxy	
	[inorg. wt%]	[wt%]	[wt%]	[wt%]	
DM	/	/	29.2	70.8	
DM-AmPOSS-60	1.5	5.2	26.3	68.5	4h @ 135 °C + 4h @ 190 °C
DM-iOPOSS-205	1.5	3.9	28.0	68.1	
DM-POSSOH-mix	1.5	4.1	28.0	67.9	
DM-POSSOH-130	1.5	4.1	28.0	67.9	
DM-POSSOH-Al	1.5	4.1	27.9	67.7	
TM	/	/	38.2	61.8	
TM-iOPOSS-mix	1.5	3.9	36.7	59.4	4h @ 135 °C + 3h @ 200 °C
TM-POSSOH-mix	1.5	4.1	36.6	59.3	
TM-POSSOH-130	1.5	4.1	36.6	59.3	
TM-POSSOH-Al	1.5	4.1	36.5	59.0	
MVR	/	/	36.7	63.3	4h @ 130 °C + 2h @ 180 °C
MVR-POSSOH-130	1.5	4.1	35.2	60.7	
MVR-POSSOH-Al	1.5	4.1	35.1	60.5	2h @ 90 °C + 2h @ 130 °C + 2h @ 180 °C

**Table II-2 System compositions and curing cycles; the networks with the aluminium-based catalyst contained 0.6% of the epoxy prepolymer weight part of this compound (i.e. about 0.4 wt%)**

### 3. MORPHOLOGIES OF FULLY-CURED MODEL EPOXY-AMINE NETWORKS

In this section, the morphology of the final materials will be reported and discussed, based on the results from different techniques: X-Ray Diffraction (XRD) to assess the crystallinity of the POSS-containing networks, observation techniques (Scanning and Transmission Electron Microscopy, SEM and TEM) and an elemental analysis technique, the Energy Dispersive X-ray Spectroscopy (EDXS). Experimental details are given in Appendix A.

#### 3.1. NON-REACTIVE POSS

A non-reactive POSS was added to the networks based on DGEBA or TGDDM epoxy prepolymer with MDEA as crosslinking agent. The isoOctylPhenyl POSS was introduced either by solubilisation at 205 °C or by high-shear mechanical mixing, hence the networks DM-iOPOSS-205 and TM-iOPOSS-mix.

A preliminary visual observation gave a first estimation of the dispersion of the POSS within the networks: DM-iOPOSS-205 was translucent, with visible aggregates and TM-iOPOSS-mix showed big aggregates of POSS on the ‘lower’ surface of the plate – ‘lower’ surface, considering that the closed mould was oriented horizontally in the oven.

The characterization of the neat iOPOSS by X-Ray Diffraction (XRD) revealed its crystalline structure. The diffractograms of the networks containing iOPOSS are given in Figure II-7. XRD was carried out both on the lower and upper faces of the TM-iOPOSS-mix network, considering the differences visually observed between the two surfaces.

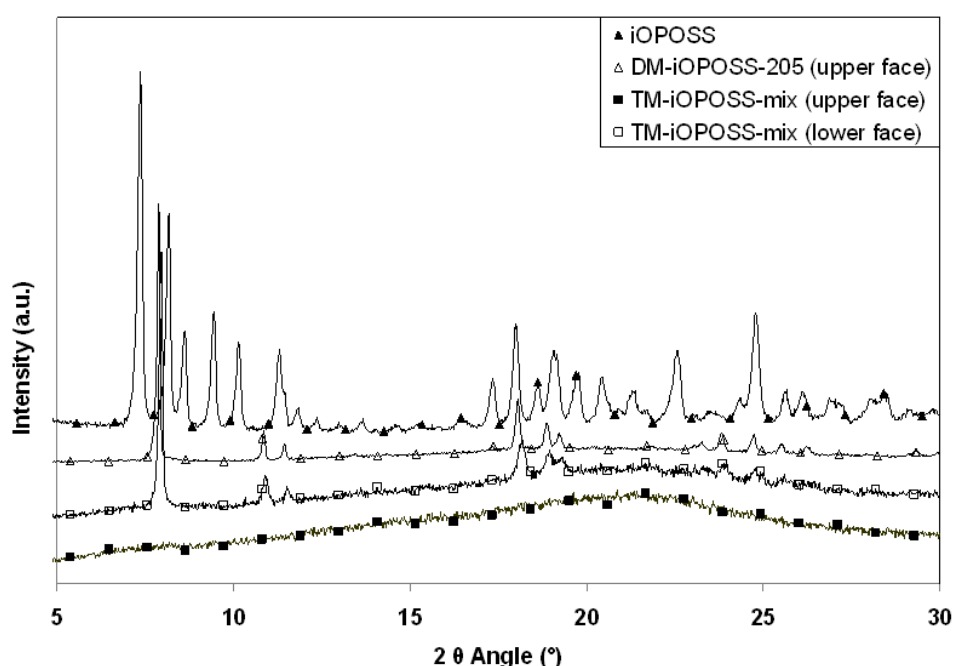


**Figure II-7 XRD spectra of iOPOSS and iOPOSS-containing networks**

The epoxy networks containing iOPOSS clearly displayed patterns of crystalline objects with well-defined peaks, similar in the DM-iOPOSS-205 and TM-iOPOSS-mix (lower face) networks. The upper face of TM-iOPOSS-mix showed an amorphous nature while the lower face displayed crystalline patterns, thus confirming the visual observation: the POSS aggregates settled during the curing stage in TM-iOPOSS-mix. The crystalline pattern observed on the networks did not match perfectly the signature of the iOPOSS, especially for  $2\theta$  lower than  $12^\circ$ , i.e. representative of the correlation distances of about  $10 \text{ \AA}$  or more [87]. This could indicate a change in the POSS morphism between neat structure and the assembled features in the epoxy networks.

Further investigation of the morphology of the networks was carried out by means of Scanning Electron Microscopy (SEM). The images of the cryo-fracture surfaces of the DGEBA-based and

TGDDM-based networks are given in Figure II-8 and Figure II-9 respectively. The neat epoxy networks showed a homogeneous fracture surface, with a well-known stick-slip fracture pattern which led to the formation of thin white threads. The iOPOSS-containing networks showed a poor low dispersion state in both epoxy networks. The POSS was mainly aggregated towards the lower side of the plate and formed angular, i.e. crystalline micro-objects (Figure II-8 b, c) and Figure II-9 b), in agreement with the XRD analysis. The DM-iOPOSS-205 network also presented randomly dispersed smaller aggregates within the thickness of the sample (Figure II-8 d). In the case of TM-iOPOSS-mix, a finer level of dispersion was observed in the sample thickness – in addition to the angular aggregates located at the lower surface – with POSS dispersed particles of diameters ranging from 100nm to 1 $\mu$ m.

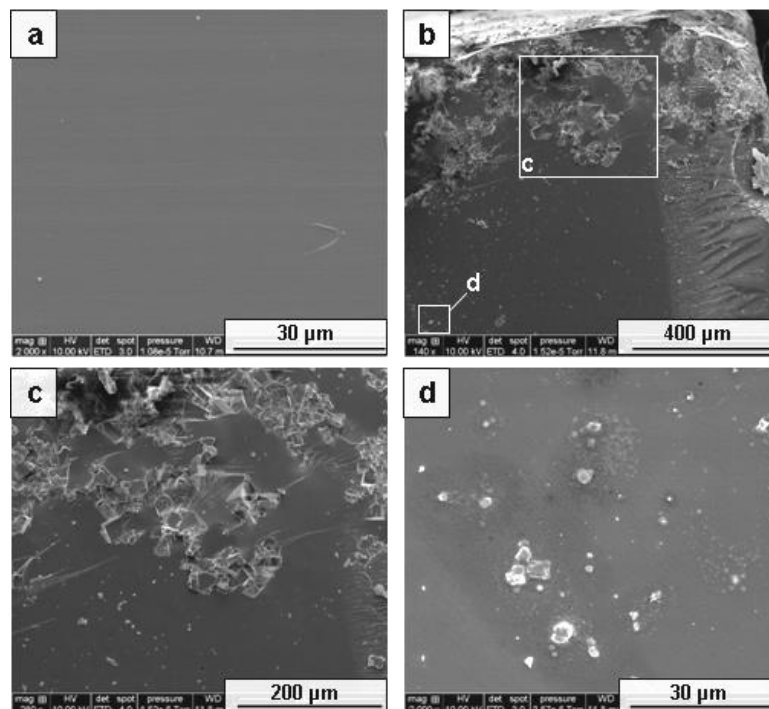


**Figure II-8 SEM images of fracture surfaces of DM (a) and DM-iOPOSS-205 (b,c,d) with b) a view of the sample lower surface and c) and d) being higher magnifications of areas of b)**

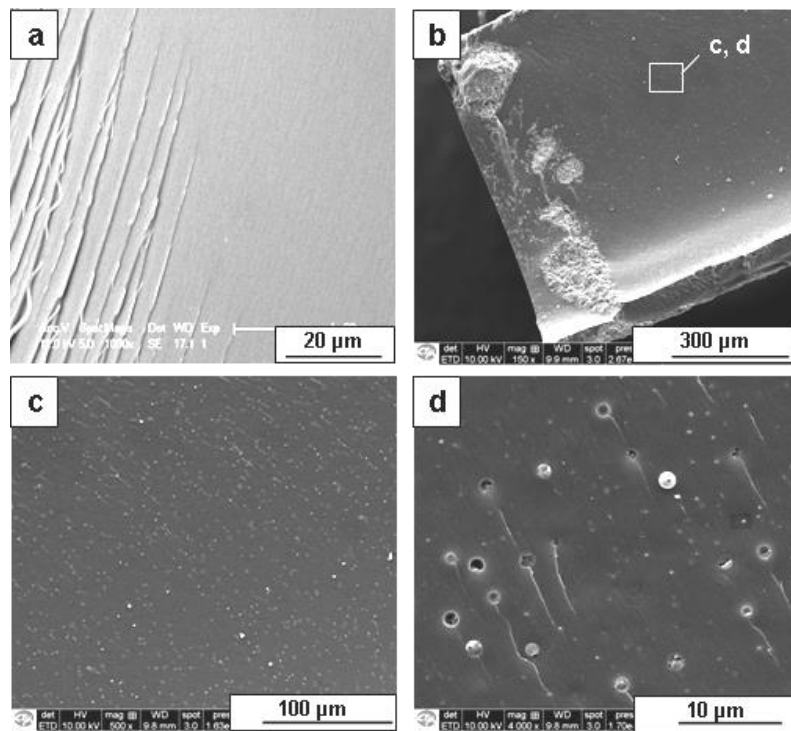


**Figure II-9 SEM images of fracture surfaces of TM (a) and TM-iOPOSS-mix (b,c,d) with b) a view of the sample lower surface and c) and d) being higher magnifications of b)**

The iOPOSS, in addition to problems of processing – difficult solubilisation in the epoxy prepolymers – presented very poor dispersion quality in the final networks. An important segregation of the POSS was observed which could give rise to unequal properties of higher-scale parts in future applications, as well as to stress concentration zones.

## 3.2. FUNCTIONALIZED POSS

### 3.2.a. Networks containing N-PhenylAminoPropyl POSS

The morphology of the DGEBA-based network containing N-PhenylAminoPropyl POSS, the multi-functional POSS, was investigated via SEM (Figure II-10). The fracture surface of the organic/inorganic network was similar to the one of the neat epoxy network, showing no micro phase-separated POSS domains (according to the SEM resolution). Similar results were obtained by Ni et al. for epoxy-amine networks containing AminoPhenyl POSS [88].

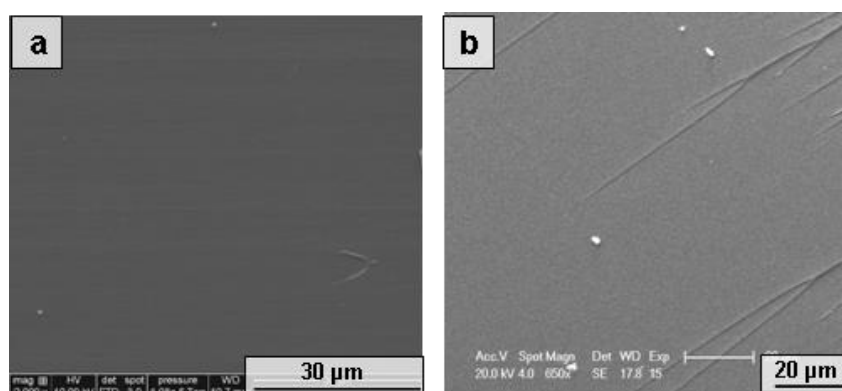


Figure II-10 SEM images of a) DM and b) DM-AmPOSS-60 networks

### 3.2.b. Networks containing triSilanolPhenyl POSS

The POSSOH was a specific case as its three silanols could be potentially involved in different reactions or interactions, which will be discussed in the next chapter. The processes implemented were: (i) solubilisation of POSSOH by heating, (ii) high-shear mixing, (iii) addition of an Al-based catalyst after solubilisation by heating. Model networks (DGEBA- and TGDDM-based) were considered according to these three routes for processing, while only the solubilisation and addition of catalyst processes were implemented as concerns the commercial MVR444-based formulation. Morphology of these networks is displayed in Appendix B. In the present section, the morphology of the model networks was chosen to be compared in such a way as to highlight the influence of the different processes.

- Solubilisation by heating vs. mechanical dispersion via high-shear mixing

The networks denoted as 'POSSOH-130' and 'POSSOH-mix' will be compared in this section. Their XRD spectra are presented in Figure II-11. Neat POSSOH as a powder displayed a crystalline pattern. This pattern was not retrieved in the POSSOH-containing networks, which presented an amorphous halo. However, in the DM-based network, a more-or-less intense peak appeared at  $2\theta$  equal to ca.  $23.9^\circ$  – which did not correspond to a correlation distance of neat POSSOH. This could mean that POSSOH displays different crystalline morphism(s) as a dispersed phase in epoxy networks than as in its neat state. More information could be provided by direct observation of the POSS-containing networks.

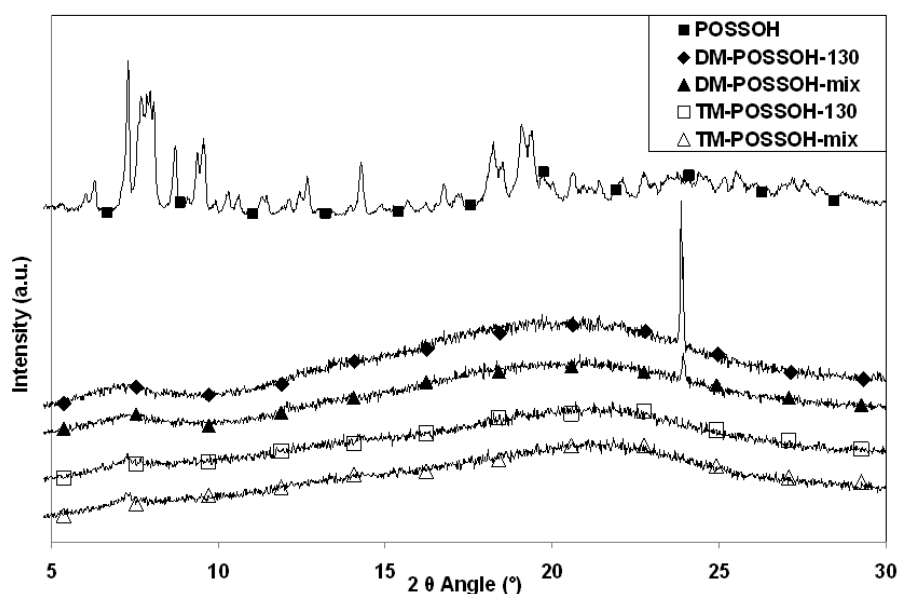


**Figure II-11 XRD spectra of DGEBA- and TGDDM-based networks with POSSOH dispersed either via solubilisation or high-shear mixing**

In this aim, SEM observation was conducted on fracture surfaces of the networks (Figure II-12 Figure II-13). Corresponding Energy Dispersive X-ray spectra are presented opposite to the SEM images (Figure II-14 and Figure II-15). The DGEBA-based systems displayed a conventional morphology with POSSOH dispersed as spherical micro-size nodules in the epoxy matrix. This type of morphology is typical of polymerization-induced phase separation. Similar morphologies were observed in the literature with different types of POSS [86], [89], [90]. The process of high-shear mixing, gave rise to slightly smaller nodules (300 to 500 nm) as compared to solubilisation via heating (600 nm to 1  $\mu\text{m}$ ).

The morphologies were totally different in TGDDM-based networks (Figure II-13) which presented rough fracture surfaces with angular aggregates of a few microns and some small nodules outside the aggregates. These differences of morphology between DGEBA- and TGDDM-based networks highlighted the sensitivity of phase separation with the different epoxy resin chemical structure and/or the thermodynamics of the reactive systems. Various parameters could be at the origin of such dissimilarities: solubility of the POSS in the epoxy prepolymers, POSSOH-matrix interactions, viscosity and/or cure kinetics of the epoxy-amine systems, etc.

Energy dispersive X-ray spectroscopy was performed during SEM analysis of the networks in order to reveal the potential presence of POSSOH in the dispersed objects and in the matrix. The EDX spectroscopy drawback is to actually gather the signal from a larger zone than the one targeted. Thus, signal of elements belonging to non-visible underlying objects can be obtained,

especially when the matrix was analysed. Several measurements for the matrix were performed at different locations to increase the likelihood of obtaining representative spectra. The DGEBA-based networks contained some silicon – representative of the POSSOH – in both the nodules and the matrix (Figure II-14). In DGEBA-POSSOH-130, the relative amount of silicon in the nodule zone was much higher than in the matrix, revealing a high concentration of POSSOH in the nodules, as expected. The not-nil amount of silicon in the matrix revealed that some POSSOH might be well dispersed in the surrounding matrix. In the case of DM-POSSOH-mix, the difference between the matrix and the nodule zone was less significant. Unexpectedly, the nodule zone presented a low amount of silicon, which was likely to be an artefact. The presence of POSSOH outside the nodules was, however, confirmed.

In the case of TGDDM-based networks, the measurements were carried out on surfaced samples – cut with a microtome – in order to avoid issues caused by the rough surface of fractured samples (Figure II-15). The nodules surrounding the aggregates were not visible anymore when surfacing the TGDDM-based networks, but it allowed to obtain information on the structure of the aggregates. Indeed, surfacing caused tearing within the aggregate zone due to the difference of hardness of the materials. Thus, the aggregates were made of both POSSOH and epoxy-amine matrix, the former being harder than the latter. EDX analysis revealed a significant amount of silicon element inside the aggregates for both TGDDM-based networks. The surrounding matrix presented traces of silicon in a much smaller amount. The presence of POSSOH in the matrix seemed confirmed in these networks as well.

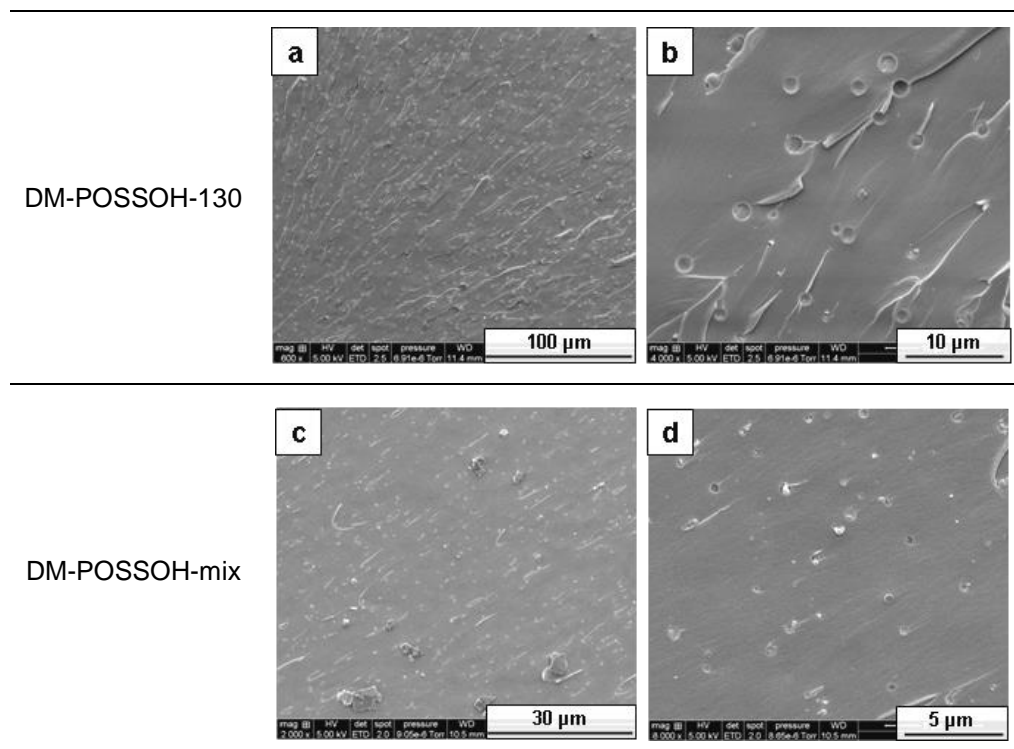


Figure II-12 SEM images of fracture surfaces of DM-POSSOH-130 (a, b) and DM-POSSOH-mix (c,d); b) and d) are higher-magnification images of a) and c), respectively

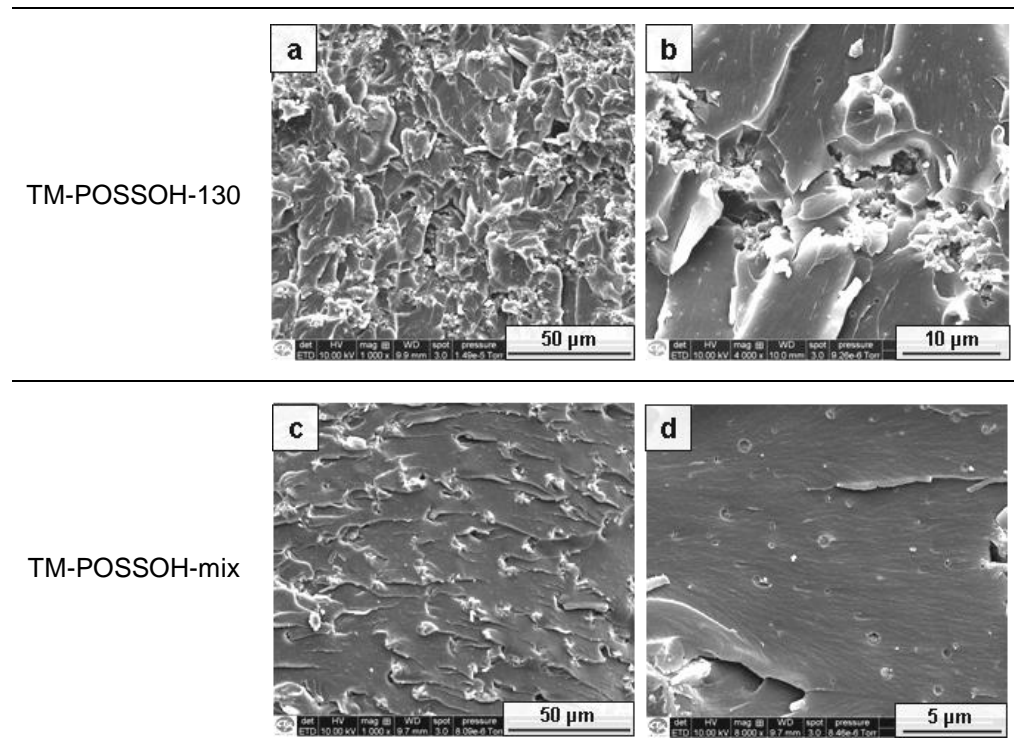


Figure II-13 SEM images of fracture surfaces of TM-POSSOH-130 (a, b) and TM-POSSOH-mix (c,d); b) and d) are higher-magnification images of a) and c), respectively

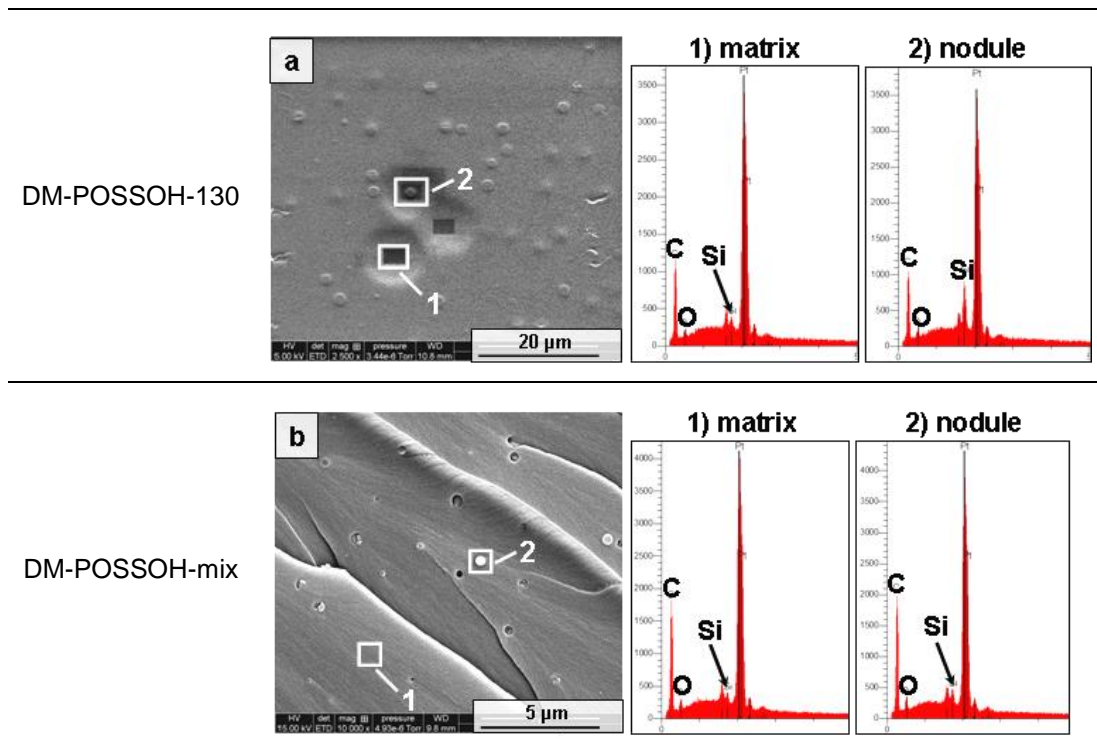


Figure II-14 SEM images and associated EDX spectra of DM-POSSOH-130 (a) and DM-POSSOH-mix (b)

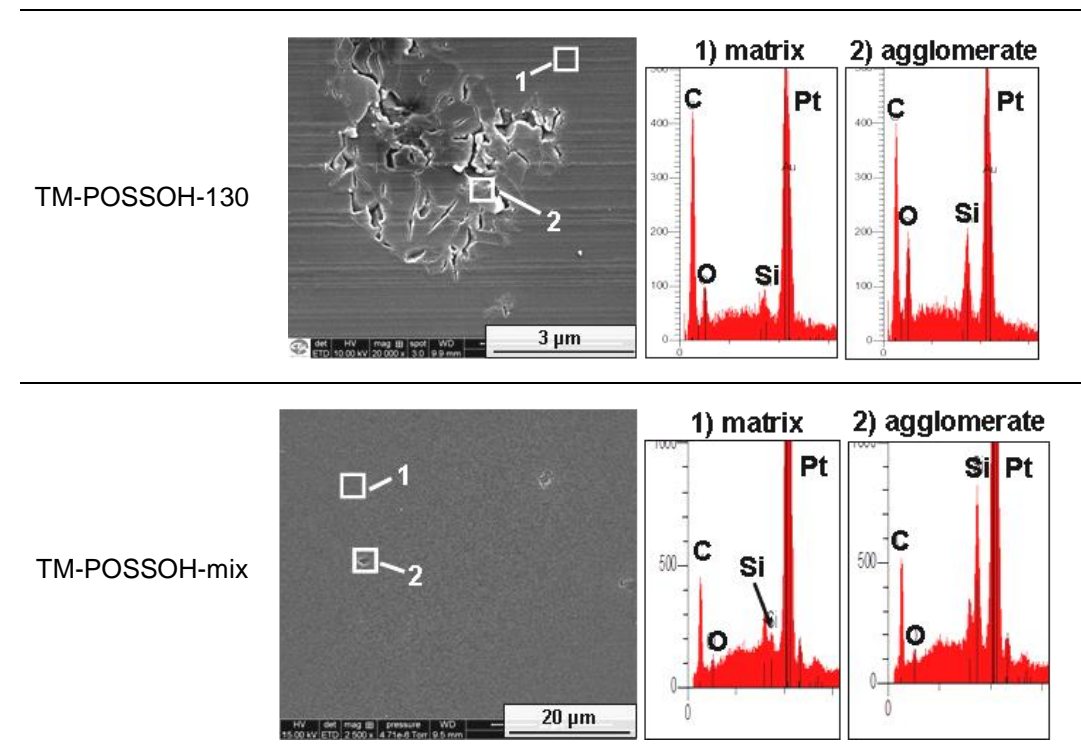
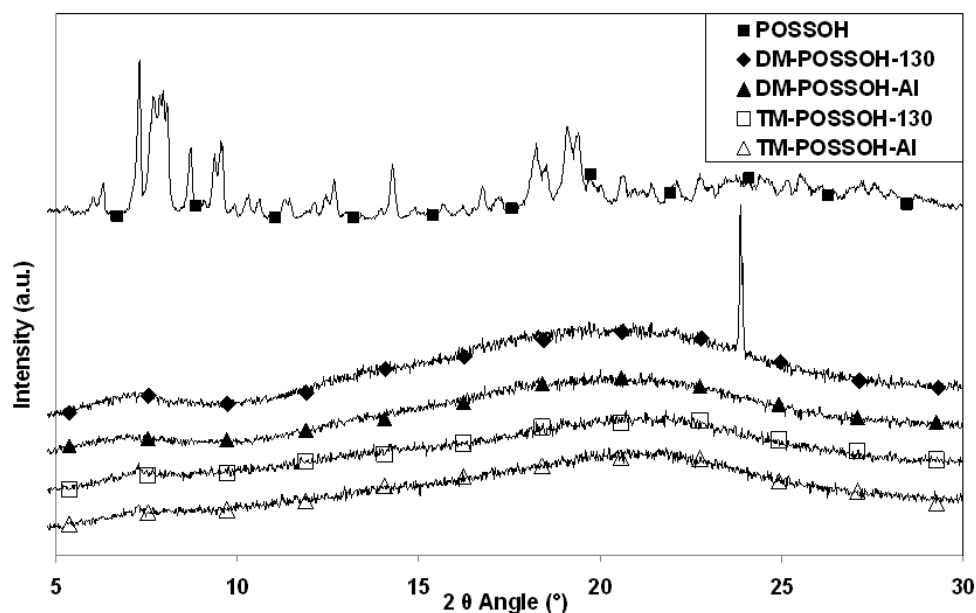


Figure II-15 SEM images and associated EDX spectra of TM-POSSOH-130 (a) and TM-POSSOH-mix (b)

- Influence of the aluminium acetate catalyst addition

The networks denoted as 'POSSOH-130' and 'POSSOH-AI' will be compared in this section.



**Figure II-16 XRD spectra of DGEBA- and TGDDM-based networks with POSSOH dispersed via solubilisation with or without Al-based catalyst**

The XRD spectra of DGEBA- or TGDDM-based networks containing POSSOH with or without the Al-based catalyst revealed the absence of dispersed phase displaying crystallinity, except for the DM-POSSOH-130 network where the uncertainty due to the sharp peak at 23.9° remained, as explained in the previous section.

SEM observation revealed a conventional phase-separation phenomenon of POSSOH as nodules in the DGEBA-based networks (Figure II-17). The addition of Al-based catalyst resulted in a slight reduction of the dispersed phase diameter, i.e. from 0.5-1 μm for DM-POSSOH-130 to 300-800 nm for DM-POSSOH-AI. The overall dispersion of nodules in the samples was homogeneous.

In the TGDDM-based networks, the morphologies were similar to the ones described in the previous section (Figure II-18). The addition of Al-based catalyst allowed to diminish the aggregate size from several tens of microns in TM-POSSOH-130 to about 1 μm in TM-POSSOH-AI.

Similar investigations of the morphologies were conducted by means of Transmission Electron Microscopy (TEM) on the POSSOH-containing networks (Figure II-19 and Figure II-20). The dark zones were attributed to POSSOH, as silicon has a higher atomic number than the hydrocarbon epoxy. The observation of DGEBA-based networks (Figure II-19) confirmed the presence of dispersed phases which were smaller in DM-POSSOH-Al networks. In the case of TGDDM-based networks, the TEM observation revealed the nature of the aggregates observed by SEM in those networks. In both networks, the aggregates were in fact composed of both POSSOH and epoxy matrix, as expected. POSSOH molecules arranged themselves in the form of threads or filaments, forming non-continuous inorganic network-like domains (Figure II-20). In the case of TM-POSSOH-Al network, these domains were denser, the filaments were well defined, and some nodules around 0.1-0.2  $\mu\text{m}$  were present within the 'filament network'. In TM-POSSOH-130 network, there were fewer filaments around diffuse nuclei of POSSOH.

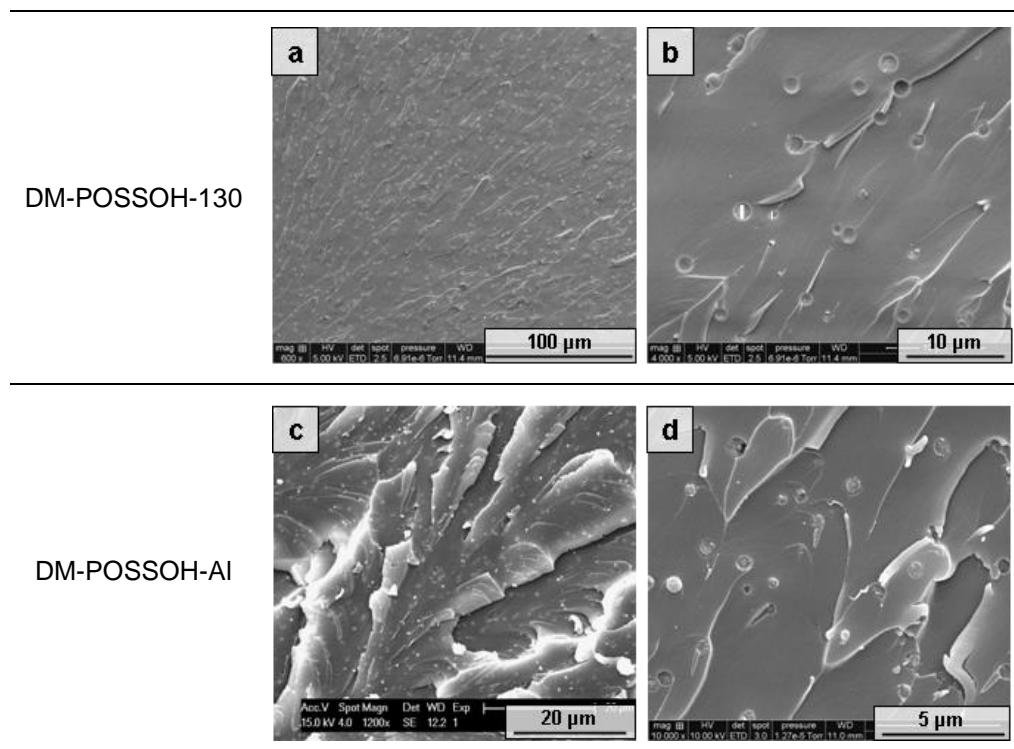


Figure II-17 SEM images of fracture surfaces of DM-POSSOH-130 (a, b) and DM-POSSOH-AI (c,d) ; b) and d) are higher-magnification images of a) and c), respectively

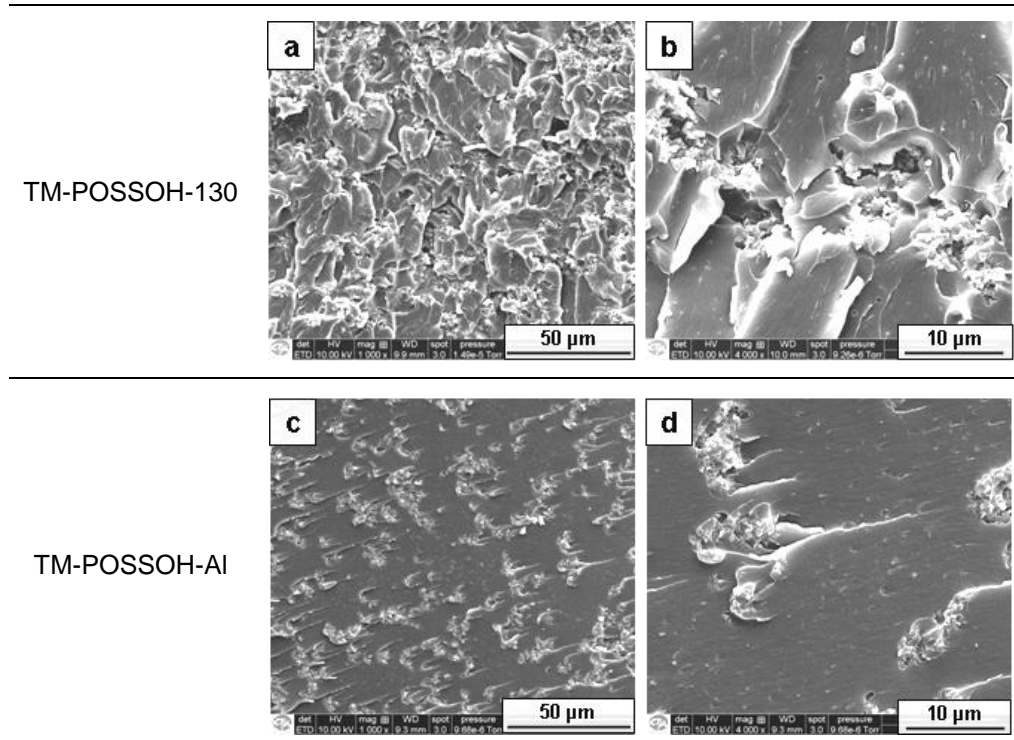
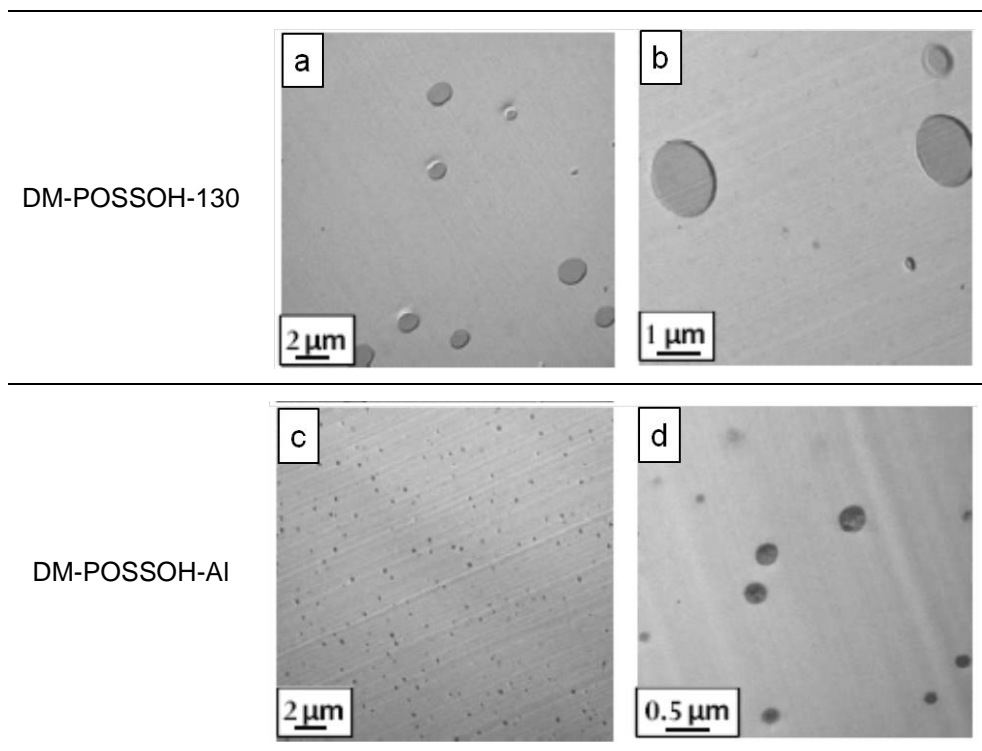
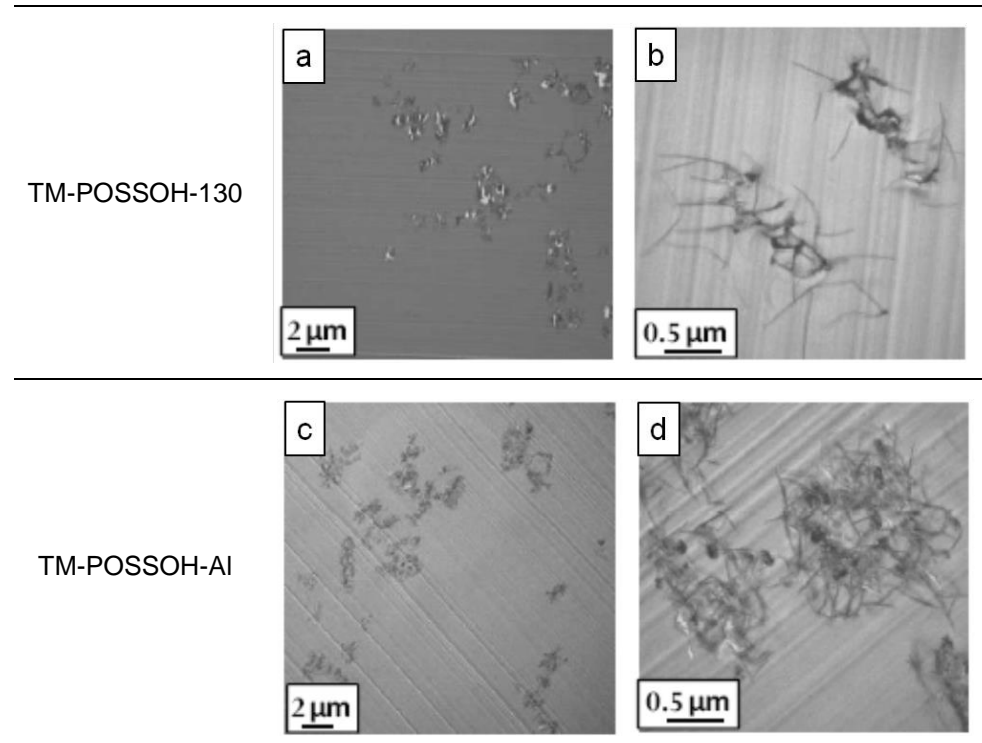


Figure II-18 SEM images of fracture surfaces of TM-POSSOH-130 (a, b) and TM-POSSOH-AI (c,d) ; b) and d) are higher-magnification images of a) and c), respectively



**Figure II-19** TEM images of DM-POSSOH-130 (a, b) and DM-POSSOH-AI (c, d); b) and d) are higher-magnification images of a) and c), respectively



**Figure II-20** TEM images of TM-POSSOH-130 (a, b) and TM-POSSOH-AI (c, d); b) and d) are higher-magnification images of a) and c), respectively

- Conclusions

The process of dispersion of POSS molecules before curing seemed to have low influence on the final morphologies, the POSS structures being only refined when high-shear mixing was implemented, as compared to heat solubilisation. Most of the POSSOH were phase-separated, but the presence of well-dispersed POSS in the matrix could be achieved. Similarly, the addition of the Al-based catalyst cannot induce substantial changes in the morphologies of the POSS-containing networks based on a given epoxy prepolymer (DGEBA or TGDDM). The structures the POSSOH adopted were either classical for DGEBA-based networks, or unexpected in the case of TGDDM-based networks. The type of epoxy prepolymer was indeed the first-order parameter influencing the morphology of the final networks.

In particular, investigation of the networks by TEM revealed a very intricate and previously unseen morphology, with the POSS organizing in filaments and nodules. The filaments' width in this system was equal to about 10 nm (Figure II-21) which corresponded to several POSS units – one POSS molecule dimensions lays between 1 and 3 nm [59]. These filament structures could consist of POSSOH condensing on themselves via their silanol functions.

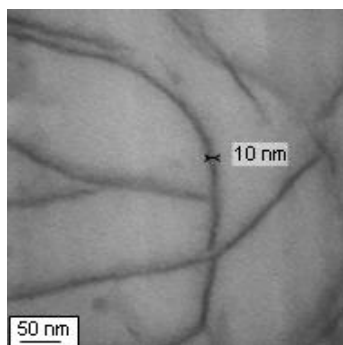


**Figure II-21 TEM high magnification image of a 'thread' in the TM-POSSOH-Al network**

Matejka et al. reported a morphology close to the ones observed in the present study [91]. In this system, a DGEBA-functionalised POSS, and bearing cyclopentyl groups on seven of the eight silicon atoms, was reacted with an aliphatic diamine. The content of POSS (not including the DGEBA part) was equal to 50 wt%. Looking at the TEM image displayed in Figure II-22, one can observe both filaments and platelets with oblong nodule-like aggregates. However, this morphology was attributed to POSS crystalline layers; in the present study, the crystallinity of POSSOH in the networks was dismissed from XRD studies. Moreover, the structures were smaller than the ones from Matejka's study, thus corresponding to organisation of different geometry.

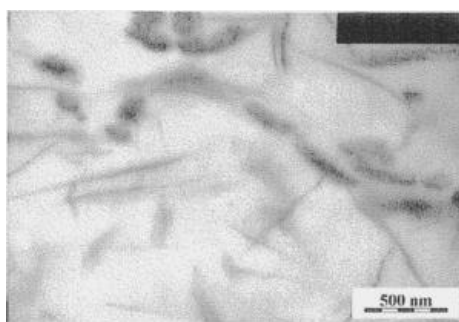


**Figure II-22 TEM micrograph of an epoxy-amine network based on a DGEBA-functionalised POSS and polyoxypropylene diamine D2000 as curing agent. The weight fraction of POSS (not including the DGEBA part) was equal to 50% [91]**

The morphologies developed in the MVR444-based networks were very similar to the ones observed in TGDDM-based networks. The morphological results related to the MVR networks are reported in Appendix B.

#### **4. MORPHOLOGY DEVELOPMENT IN THE POSS-CONTAINING NETWORKS THROUGH CURE**

In the present section, particular attention will be dedicated to the study of the development of the morphologies in the POSSOH-containing networks. In particular, study of the morphology during cure in the TM-POSSOH-Al network, where special POSS structures were observed in the final material, was carried out. The investigations were implemented via cloud-point measurements and Transmission Electron Microscopy. Bearing this in mind, the phenomenon of reaction-induced phase separation (RIPS) will first be reminded.

##### **4.1. REACTION INDUCED PHASE SEPARATION PHENOMENA**

Reaction-induced phase-separation (RIPS) in thermoset materials is a well-known phenomenon that was described in detail by Williams et al. [92]. Starting from a homogeneous blend of comonomers and/or additives, which will form the final polymer material, the RIPS process proceeds through the competition between polymerization and the generation of a phase-separated material during curing. RIPS is thus related to the reaction advancement and will occur as the growing network and the additive component are not chemically compatible anymore. As concerns POSS, the occurrence of RIPS in epoxy-amine systems during polymerization has been reported in a number of works [86], [88], [91], [93]–[95], and first-order parameters influencing the final morphologies were the functionality and reactivity of POSS.

Low contents of modifier and high phase-separation rate as compared to crosslinking kinetics favour the mechanism of nucleation and growth, as opposed to spinodal demixing [92]. In the

first case, the dispersed phase, rich in modifier, takes the most stable shape, i.e. spheres, while the latter mechanism gives rise to bicontinuous morphologies. As concerns the present study, a clear nucleation/growth mechanism dominated in the DGEBA-based systems containing POSSOH, while the case of TGDDM-based systems was more complex: the RIPS was clearly modified, probably by reactions other than polymerization of the epoxy-amine network. The nucleation and growth mechanism is illustrated in Figure II-23.

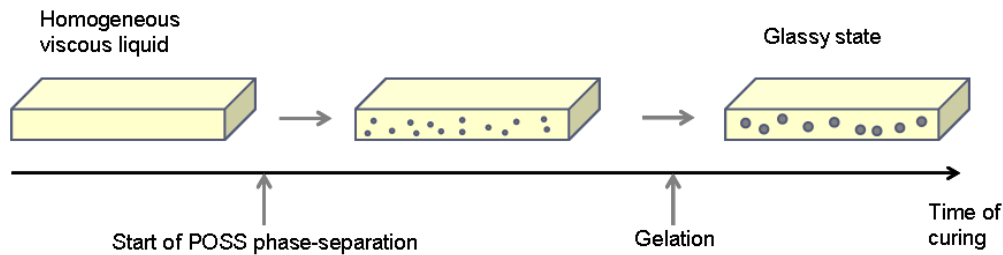


**Figure II-23 Scheme of the nucleation and growth mechanism occurring in the DGEBA-based networks containing POSSOH**

The parameters influencing the development of the RIPS phenomenon in a given modified thermosetting system – apart from polymer-modifier chemical reactions – are the fraction and the molar mass of modifier, the temperature of reaction and the crosslinking state of the thermosetting polymer – the conversion. RIPS can then be described through conversion-modifier fraction phase diagrams. This type of diagram is valid for a fixed reaction temperature. RIPS will occur as the molar masses of the thermosetting polymer increase – i.e. with conversion. It is represented on the diagram by drawing the cloud point curve, which is the limit at which the first phase-separated domains are observed during cure, for a given fraction of modifier in the system (Figure II-24).

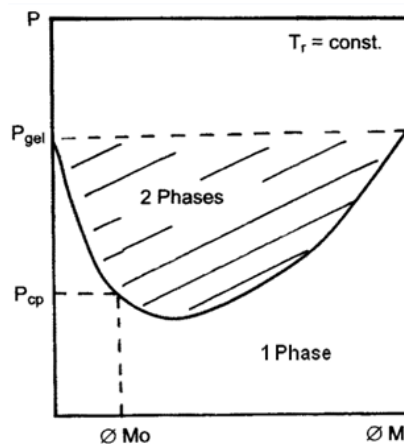


**Figure II-24 Schematic conversion-composition phase diagram (Upper Critical Solution Temperature, UCST) where the solid line represents the cloud-point curve. ‘P’ is the conversion of the thermosetting polymer, ‘ØMo’ the fraction of modifier M and ‘Tr’ the reaction temperature [92]**

Experimentally, the cloud point of the system was determined by a light transmission method (see Appendix A for further details). Considering the wavelength of visible light, only objects having an order of diameter greater than 100 nm will be detected [96], meaning that phase separation starts before the drop in transmitted light intensity. In the following discussion, the phase separation time will be related to time of gelation of each system. It was determined by chemorheology and will be described in further details and discussed in the next chapter.

An example of a transmitted light intensity vs. time curve is given in Figure II-25 for the DM-POSSOH-130 system, recorded at 135 °C. The intensity decrease indicating the growth of POSSOH domains from nodules of ca. 100 nm to their final size (1 $\mu$ m, see Figure II-19 b) started from 1 hour of reaction. It meant that the growth of POSSOH nodules mainly took place very close to gelation of the network, occurring after about one hour at 135 °C as measured via chemorheology – depending on the experimental set-up, gelation time is expected to slightly vary. For the TM-POSSOH-130 system, the phase separation was detected by light transmission from 70 minutes at 135 °C. For this system, the gel time occurred after about 100 minutes at 135 °C. This meant that the RIPS of the POSSOH in this system started well before the gel time, as compared to the DM-POSSOH-130 system.

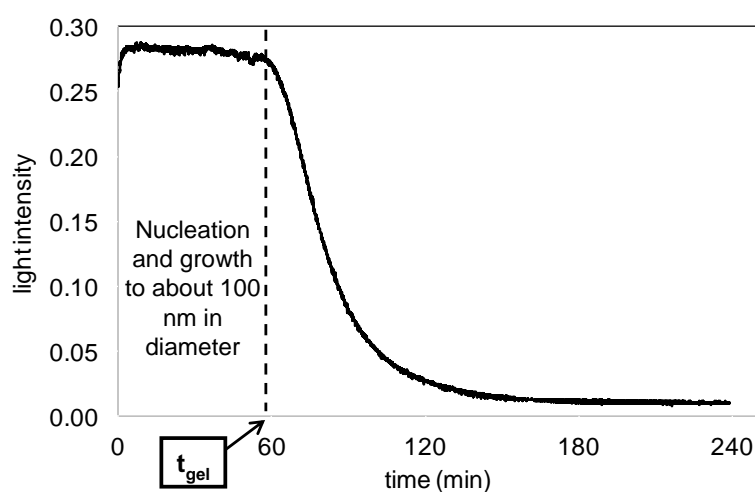


**Figure II-25 Light transmission measurement during curing of DM-POSSOH-130 at 135 °C. The represented gel time on the diagram was determined by chemorheology**

Concerning the systems containing both POSSOH and the Al-based catalyst, analysis of the curves was more delicate. In the case of DM-POSSOH-Al, the cloud point was measured both at 135 °C and 90 °C. The light intensity was already low and clearly in the middle of a drop at the beginning of the experiment at 135 °C, indicating that the RIPS had already started during the stabilization of the system at 135 °C. This was in agreement with the very fast gelation observed by chemorheology at this temperature – less than 2 minutes. The light intensity

displayed a continuous gentle negative slope at the beginning of the measurement performed at 90 °C, indicating a slow and progressive phase separation leading to small objects. Detecting the start of the phase separation with accuracy was therefore not possible with the transmitted light experimental set-up. In the case of TM-POSSOH-Al, the experiment was carried out at 135 °C and the light intensity displayed a clear drop, but the presence of interferences probably due to degassing of the mixture at the beginning of the measurement hindered the interpretation of the curve. The start of phase separation could be situated around 10 minutes.

#### 4.2. INVESTIGATION OF THE MORPHOLOGY DEVELOPMENT DURING CURE IN THE TM-POSSOH-AL SYSTEM

As mentioned earlier, the morphology of the TM-POSSOH networks were totally unexpected. This is why the formation of the POSSOH structures in the TM-POSSOH-Al network was further studied by TEM, and DSC was used to assess the development of the glass transition temperature and the evolution of the reaction exotherm through cure.

Small aluminium cups containing samples of about 10 mg of the uncured TM-POSSOH-Al mixture were subjected to the conventional curing cycle – i.e. 2 hours at 90 °C, 2 hours at 135 °C, and 3 hours at 200 °C. Every 10 minutes all along the curing cycle, one sample was removed from the oven and cooled down externally using iced water in order to stop the polymerization. The conversion of the system was derived from the residual exotherms, and was plotted as a function of time in Figure II-26 together with the glass transition temperature. The conversion curve allowed to determine the gel time, knowing the theoretical conversion at the gel – 33% for this epoxy-amine system, calculated from the Flory-Stockmayer theory (Equation II-3). A value of 230 minutes was found, i.e. 40 min from the beginning of the dwell at 135 °C.

II-3

$$r \cdot \alpha_{gel}^2 = \frac{1}{(f_a - 1)(f_b - 1)}$$

where  $r$  is the ratio between the epoxy and the amino-hydrogen functions – equal to 1 here –  $\alpha_{gel}$  is the conversion at the gel point and  $f_a$  and  $f_b$  are the functionality of TGDDM and MDEA respectively, with  $f_a=4$  and  $f_b=4$ .

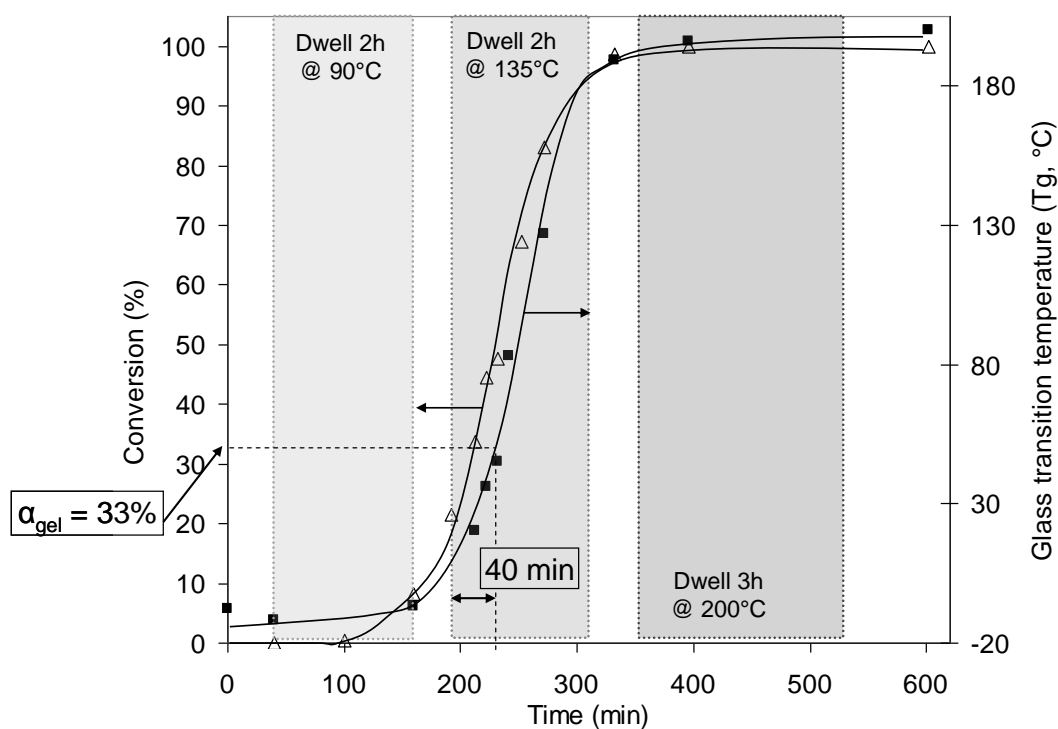


**Figure II-26 Conversion and glass transition evolution as a function of curing time for TM-POSSOH-AI (DSC data)**

Secondly, samples collected close to the gel time were chosen for the TEM observations. The specimens sampled at  $t=0$ ,  $t=20\text{min}$ ,  $t=30\text{min}$ , from the beginning of the dwell at  $135\text{ °C}$ , needed to be microtomed under cryogenic conditions as their glass transition temperature was too close to the ambient temperature.

From the TEM images in Figure II-27, it could be seen that at the beginning of the dwell at a temperature of  $135\text{ °C}$ , phase separation had already begun, forming loose aggregates of a hundred nanometres in diameter. The structure then became better defined with the appearance of the first ‘threads’ and larger nodules as from 20 minutes at  $135\text{ °C}$ . Most of the objects measured about  $100\text{ nm}$  at the beginning of the dwell at  $135\text{ °C}$ . Then, the structures either coalesced or gathered POSSOH that could still be dispersed in the matrix and formed greater clusters (about  $1\text{ }\mu\text{m}$ ). The evolution of the POSSOH structures seemed more limited from 30 minutes at  $135\text{ °C}$ , where they consisted of nodules surrounded by filaments.

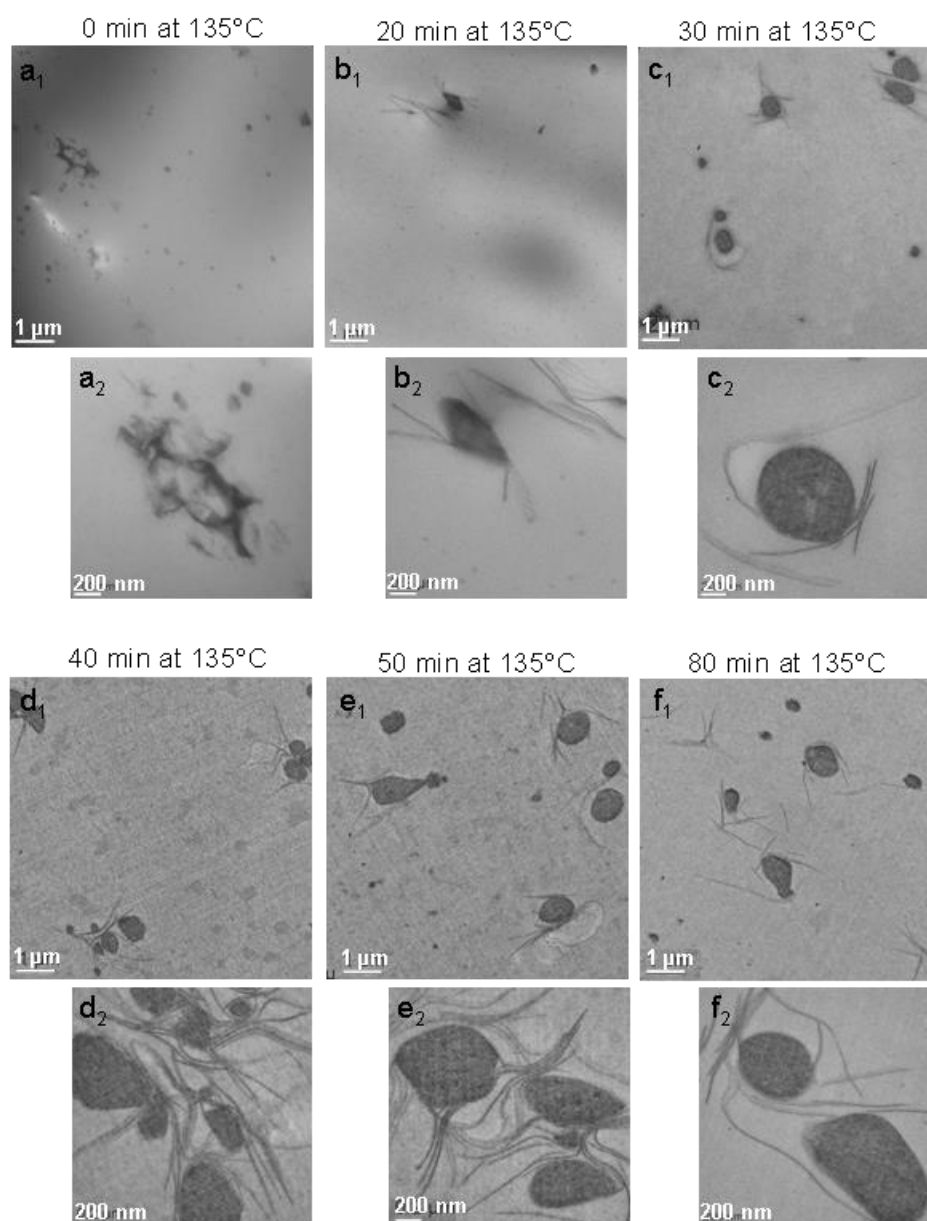


**Figure II-27 TEM images of TM-POSSOH-Al network at different times during the second dwell (135 °C) of the curing cycle ; the images designated as  $x_2$  display details of the overall morphology, shown in the images  $x_1$**

However, some clusters consisting mainly of filaments with some small embedded nodules, rather than in well defined big nodules surrounded by a few filaments, were also observed in these samples for which the curing cycle was interrupted, though they were not predominant. These structures are shown in Figure II-28 a and b. Such an organisation of the POSS was actually closer to the morphology of the final structures, i.e. after completion of the curing cycle with the dwell at 200 °C. This structure in clusters was observed in several samples produced independently (Figure II-28 c, d, e), which evidenced its repeatability. One could thus imagine that the clusters represented a second evolution of the morphology, i.e. from the structures

displayed in Figure II-27 e and f, to the structures represented in Figure II-28. This evolution occurred later in the curing cycle and probably locally, as the POSS movements would be obstructed by the network gelation. The last dwell at 200 °C, i.e. close to the T<sub>g</sub> of the almost final network, could favour the local transformation of the nodules. This further confirmed the evolution of the morphology from initial aggregates and nodules, observed at the beginning of the phase separation, towards filaments 'webs'.

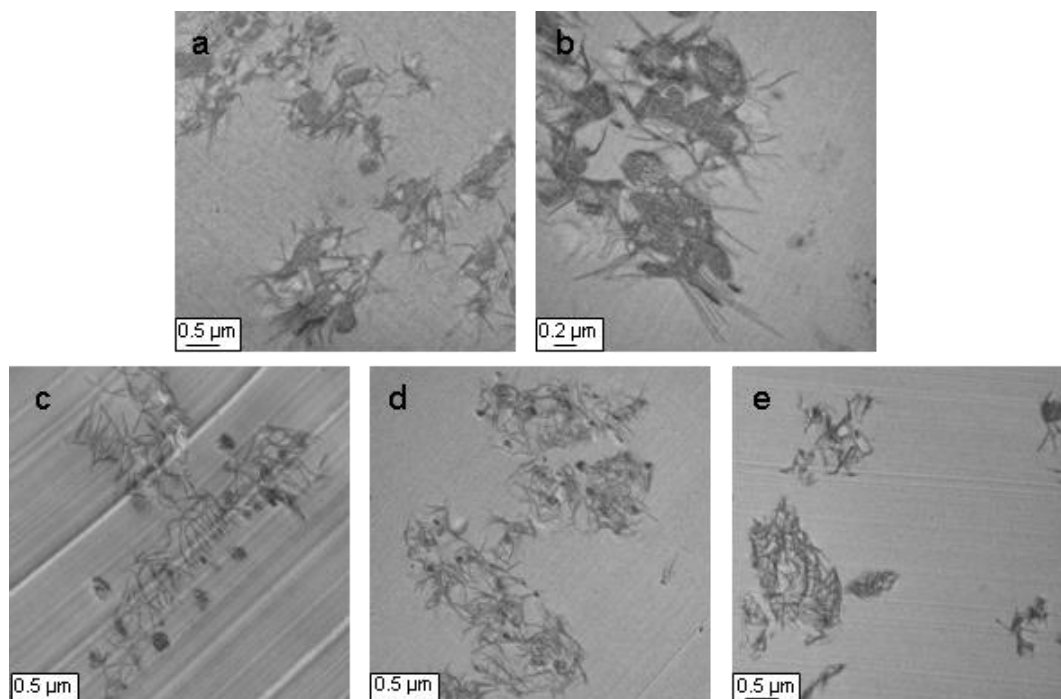


**Figure II-28 TEM images of TM-POSSOH-Al networks for which the curing cycle was interrupted during the dwell at 135 °C after 50 minutes (a) and 80 minutes (b), and fully-cured networks produced independently (c, d, e)**

The TEM observations allowed to actually see the morphology development, even if it did not provide an explanation for such intricate structures. Only, the hypothesis of a mechanism of nucleation and growth as in the DGEBA-based networks, disturbed by POSSOH-POSSOH or POSSOH-epoxy reactions, could be put forward.

## 5. CONCLUSIONS ON THE NETWORK MORPHOLOGIES

Different POSS-containing epoxy-amine networks were produced, using various POSS and two epoxy prepolymers, DGEBA and TGDDM. One non-functional POSS and two polyfunctional POSS were selected, and various processes were implemented for the dispersion of one particular POSS, the trisilanophenyl POSS. The morphologies were then assessed through several techniques (XRD, SEM, TEM, etc). Particular investigation of the morphology

development of the POSSOH- and Al-containing, TGDDM-based network was carried out as special POSSOH structures were discovered by TEM observation in this network.

The morphologies developed in the iOPOSS and AmPOSS-containing networks presented no ambiguity. In the latter case, potentially molecular dispersion of the POSS was achieved – the possibility of a reaction of the amine functions of the POSS with DGEBA will be investigated in the following chapter – while in the former case, almost macroscopic aggregation was observed with maintenance of the crystalline character of the POSS.

Unexpectedly, the POSSOH-containing networks presented morphologies that varied a lot depending on the matrix type. In the DGEBA-based networks, the dispersion of POSSOH in nodules of various size orders depending on the process implemented, revealed a phase-separation mechanism in nucleation and growth, as expected. The TGDDM-based networks displayed very particular and never-seen structures made of clusters nodules and well-defined filaments. An explanation for this particular morphology could be that the POSSOH may have had time to condensate on itself via its silanol functions, thus forming these polyPOSS branched structures. The extent of condensation could be higher when the aluminium catalyst was added as better-defined filaments were observed. Despite its classical nodule-like morphology, a condensation of POSSOH in DGEBA-based networks was not excluded, especially in the Al catalyst-containing system.

Thus, the morphology in these networks was thought to be due to interactions developed by the POSSOH. Bonding to the matrix was not to be neglected either. This topic will be discussed in detail in the next chapter.

---

## **CHAPTER III. FUNCTIONAL POSS IN THE MODEL EPOXY NETWORKS: DEVELOPMENT OF INTERACTIONS DURING THE PROCESS AND WITHIN THE FULLY-CURED NETWORKS**

---

In the previous chapter, the morphology of epoxy-amine networks containing POSS were presented. Among them, different morphologies were observed, depending on:

- (i) the POSS nature, i.e. its potential reactivity and its chemical structure;
- (ii) the matrix type, for the POSSOH-containing networks, namely;
- (iii) the process implemented, and particularly the addition of an aluminium-based catalyst in the POSSOH-containing networks.

Some of the morphologies particularly highlighted the occurrence of interactions developed by the reactive POSS. Thus, this chapter will be aimed at answering the following questions through the implementation of several analytical methods: in the case of reactive POSS, did they create interactions – between themselves or with the epoxy-amine network? To which extent could it be responsible for the observed morphology?

In this chapter, the investigations were carried out on the DGEBA-based model systems. Some results were obtained for the TGDDM- and the MVR444-based systems that are reported in Appendix B.

## **1. DEVELOPMENT OF REACTIVE POSS INTERACTIONS DURING CURE AND INFLUENCE ON THE DGEBA-BASED MODEL NETWORK BUILD-UP MECHANISM**

Among the three different POSS selected in this work, two have functional groups, i.e. they are likely to interact and/or react with a constituent of the epoxy-amine network, or influence the polymerization reactions. Investigation of the reaction between amine functions of AmPOSS with epoxies will first be presented. The study was conducted by Size Exclusion Chromatography (SEC) on a binary system – i.e. without the crosslinking agent. A second part will assess the possibility of the reaction between epoxies and the silanol functions of POSSOH in presence of the aluminium acetate catalyst. SEC analysis was performed on the system without the amine comonomers, thus avoiding gelation and allowed to dissolve the samples. Liquid  $^{29}\text{Si}$ ,  $^{13}\text{C}$ , and  $^1\text{H}$  NMR analyses were performed on the samples used for the SEC study. However, due to a lack of sensitivity of the technique, no information could be collected from these experiments and it was chosen not to report these results herein. Finally, the complete formulation was investigated by means of chemorheology, Dynamic Scanning Calorimetry (DSC), and Near-Infrared spectroscopy (NIRS). Details on the techniques and apparatus are given in Appendix A.

### 1.1. N-PHENYLAMINOPROPYL POSS AS A CROSSLINKER IN THE EPOXY NETWORK

AmPOSS was a reactive POSS with 8 secondary amine functions (see Table II-1), which might react with the epoxy functions of the DGEBA prepolymer, thus competing with the MDEA/epoxy reaction. In the present section will be presented results of SEC and DSC studies, in order to determine if the grafting reaction of the POSS upon the epoxy prepolymer actually occurred. The kinetic study was performed at a constant temperature of 135 °C, which corresponded to the first-dwell temperature of the curing cycle (see Table II-2).

The DGEBA prepolymer and the AmPOSS were mixed in stoichiometric ratio (amino hydrogen-to-epoxy ratio equal to 1) and slightly heated to proceed from a homogeneous mixture, which was then split in equal parts into test tubes. One of the tubes was kept as a control blank whilst the others were subjected to a temperature dwell at 135 °C. Tubes were removed one at a time, periodically, from the thermostated oil bath. The evolution of the system composition was assessed by SEC (Figure III-1) and DSC.

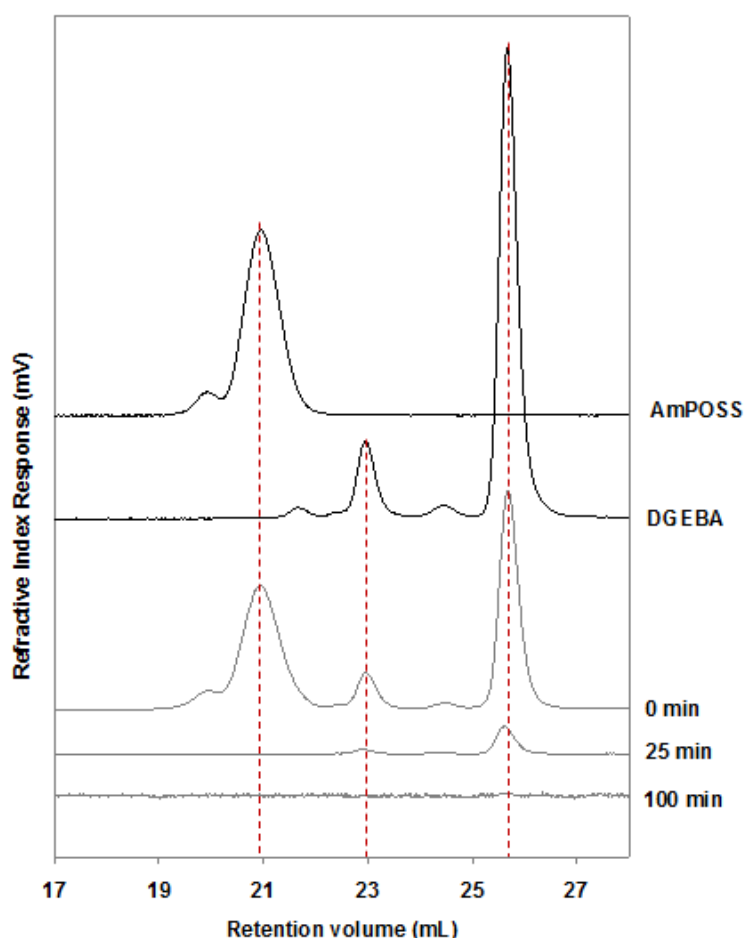


Figure III-1 SEC chromatograms of DGEBA and AmPOSS (black curves) and DGEBA-AmPOSS during curing at 135 °C (grey curves) ( $a/e=1$ )

As a first statement, it was noticed that after 25 minutes of reaction the system had vitrified when brought back to room temperature, and was not fully soluble into THF, which meant that the system reached gelation. At  $t=0\text{min}$ , the DGEBA prepolymer was identified by the four peaks between 22 and 26 mL (retention volume unit) and the AmPOSS by the peaks between 19 and 22 mL. The signals, from 25 minutes of reaction, showed the extinction of all peaks but the most intense one ca. 26 mL, associated to the DGEBA monomer, which decreased strongly. This fact was caused by the consumption of the epoxy functions during curing and the loss of solubility of the samples in THF due to crosslinking. Considering that all the unreacted DGEBA was solubilised in the SEC solutions, one could determine the conversion of epoxy thanks to the evolution of the area of the peak of the DGEBA at 25.6 mL (see Equation III-1) [97].

III-1

$$\alpha_{Ep} = 100 \times \left( 1 - \sqrt{\frac{A_0}{A_t}} \right)$$

where  $\alpha_{ep}$  refers to the epoxy conversion,  $A_0$  to the area of the peak of DGEBA at  $t=0\text{min}$ , and  $A_t$  to the area of the peak at a given time.

At 25 min, the epoxy conversion calculated from the peak area was of 64%. From the Flory-Stockmayer theory (see Equation II-3) [98], it was found that the gel point occurred for a theoretical conversion of ca. 38% (considering a functionality of 8 for the AmPOSS). The conversion after 25 min of reaction was higher than this value, which was in accordance with the preparation being insoluble in THF at this time.

Following the evolution of the glass transition temperature of the system during the experiment is a more sensible technique to monitor the advancement of the reaction above gelation (Figure III-2). The DSC curve of the system DGEBA-AmPOSS before reaction showed the glass transition of the mixture ca. 0 °C and an exothermic large peak corresponding to the reaction between the amine and epoxy functions. This exothermic peak disappeared from 25 minutes of reaction, and the glass transition temperature kept on increasing to finally stabilize around 90 °C after about 100 minutes of reaction at 135 °C.

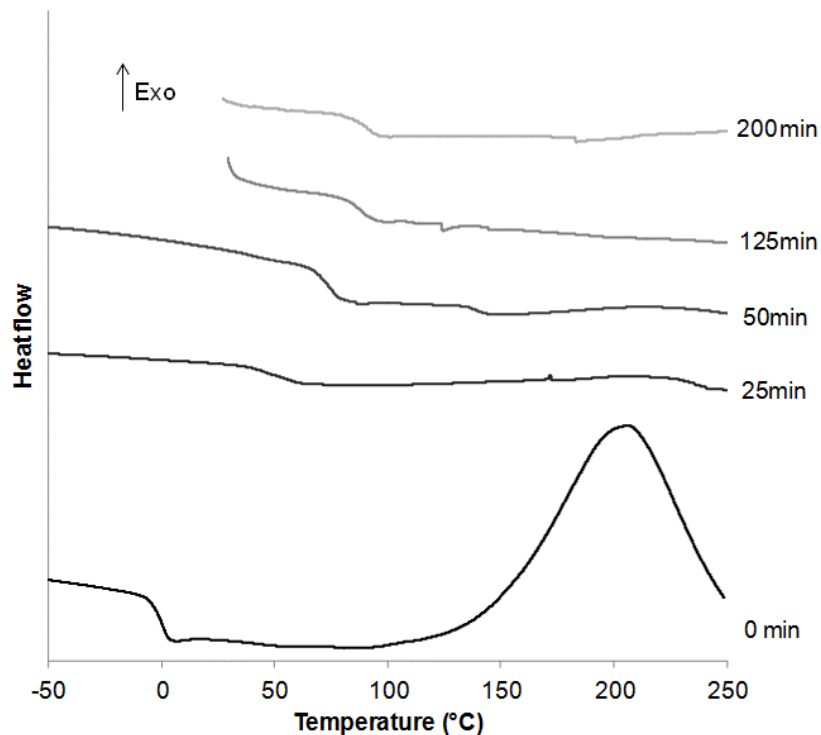


**Figure III-2 DSC curves of the DGEBA-AmPOSS system (stoichiometric ratio) at different times of reaction at 135 °C (10 K.min<sup>-1</sup>)**

The final  $T_g$  being significantly lower than the curing temperature, vitrification was avoided, and it could be assumed that the reaction reached its maximum after 100 minutes of reaction at 135 °C. Considering the reaction as complete – conversion being equal or very close to 1 after 100 minutes of reaction – was a reasonable assumption, though one as to keep in mind that some amine functions might be left unreacted due to steric hindrance around the AmPOSS. The DiBenedetto empirical model modified by Pascault and Williams [99] gives a relationship between the glass transition temperature and the conversion (Equation III-2). Based on the measurements performed via DSC, a conversion-vs-time curve could be plotted (

Figure III-3 a). Knowing that the theoretical conversion at gelation was equal to 38%, the gel time was estimated to about 12 minutes at 135 °C.

**III-2**

$$\frac{T_g - T_{g_0}}{T_{g_\infty} - T_{g_0}} = \frac{\lambda \alpha}{1 - (1 - \lambda)\alpha}$$

where  $T_g$ ,  $T_{g_0}$ , and  $T_{g_\infty}$  are the glass transition temperatures at  $t$ ,  $t=0$ , and at the end of the reaction, respectively ;  $\alpha$  is the conversion and  $\lambda$  is the ratio of the heat capacity at fully cured and uncured states:  $C_{p_\infty}/C_{p_0}$ .

From the DSC measurement and the modified DiBenedetto relation, the conversion after 25 minutes of reaction was equal to 64%, which is in perfect agreement with the conversion calculated from the SEC measurement.

The reaction of epoxy with the amino-functions of the AmPOSS was thus evidenced in the binary DGEBA-AmPOSS system. It remained to determine whether, in the DM-AmPOSS-60 ternary system where the crosslinking agent was present, the POSS could effectively react with the epoxy monomers before the epoxy-amine network built up. Zucchi et al. obtained the conversion-vs-time curve for this system from isothermal DSC measurements at 135 °C (Figure III-3b) [93]. The conversion at 100 minutes in the neat system could thus be estimated to about 50%, which was much lower than the quasi 100%-conversion found for the stoichiometric DGEBA-AmPOSS system after 100 minutes at 135 °C. It could then be concluded that the POSS had a higher reactivity towards DGEBA than the MDEA crosslinking agent, and thus was likely to react first with the DGEBA in the ternary system.

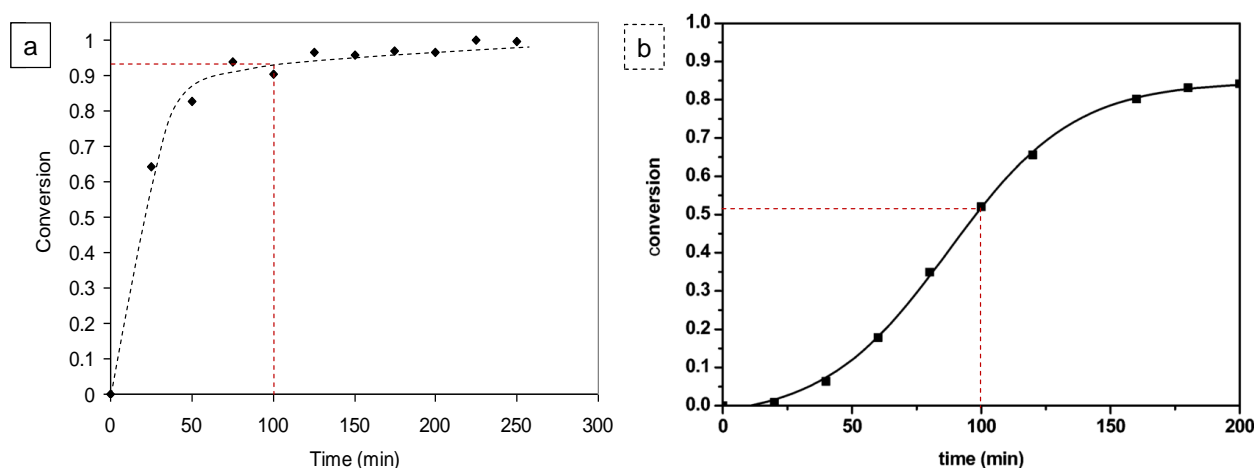


**Figure III-3 Evolution of the conversion in a) DGEBA-AmPOSS during curing at 135 °C (calculated from DSC data and modified DiBenedetto relation, Equation III-2) and b) in DM system (obtained from DSC isothermal runs) [93]**

Finally, the DMA of the DM-AmPOSS-60 network was compared to that of the neat DM network (Figure III-4). The glass transition temperature and width of the network was not influenced by the addition of the AmPOSS, but the glassy and rubbery moduli were slightly increased, which highlighted potentially tighter crosslinking points – but not necessarily more numerous – indicated that the AmPOSS, which had a higher functionality than MDEA, was probably included in the network as a crosslinking point. The effective grafting of AmPOSS through several of its amine functions also explained the absence of phase separation as observed by SEM.

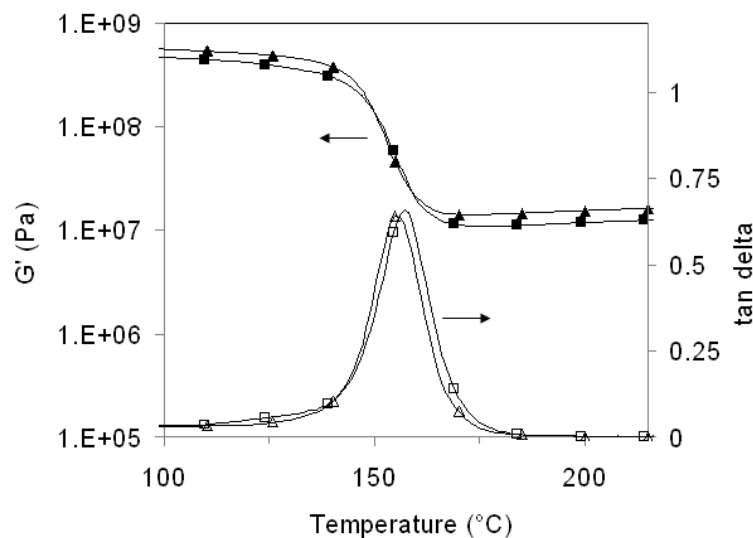


**Figure III-4 Comparison of DMA curves of neat DGEBA matrix and DGEBA-based network containing AmPOSS**

## **1.2. TRISILANOLPHENYL POSS AND ALUMINIUM-BASED CATALYST: INFLUENCE ON THE EPOXY-AMINE CROSSLINKING REACTIONS**

### **1.2.a. Background on the use of silanol-containing compounds and metallic catalysts in epoxy systems**

The aim of introducing an aluminium-based catalyst in the DM or in the TM systems in combination with the POSSOH was to promote the grafting of the POSSOH upon the epoxy monomers. Depending on the number of silanols reacting per molecule, the POSSOH can act as a pendant group, a chain extender, or a crosslinking point, or even as an inert filler if no reaction occurs (see Figure I-18 in Chapter I).

Liu et al. [86] studied the DGEBA/DDM system in which they introduce POSSOH with or without the aluminium acetate catalyst. From the FT-IR study of a model system – Phenyl Glycidyl Ether (PGE), POSSOH with or without the aluminium-based catalyst – they proposed a mechanism for grafting of POSSOH on the epoxy monomers, detailed in Figure III-5. In this reaction, one epoxy is consumed by one silanol of the POSS, thus displacing the stoichiometric ratio. Also, this mechanism implies that the Al catalyst enhance the epoxy ring opening even in absence of the silanol compound, that is, the catalyst alone could favour catalysis of polymerization of epoxy with other compounds than the POSS – i.e. with amine products, or epoxy monomers through homopolymerization.

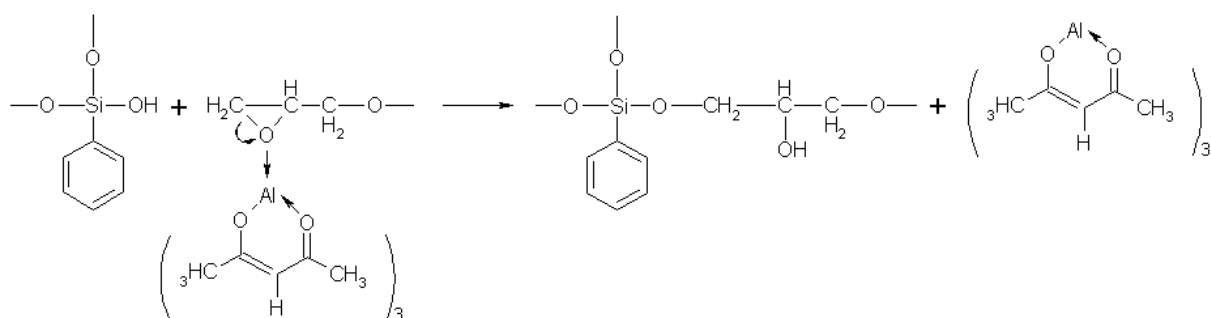


**Figure III-5 Reaction of POSSOH grafting upon DGEBA [86]**

The presence of silanols on the POSS molecule could be the cause of condensation reactions, either between the silanol and the hydroxyl from the epoxy molecule, or between the silanols of two molecules of POSSOH [75]. In both cases, no epoxy is consumed, and water is a by-product.

Silanol condensation is well-known reaction that occurs in the sol-gel process following the hydrolysis step. Such a reaction is favoured in basic conditions [100], for example in presence of amine compounds. It creates Si-O-Si linkages, whereas silanol-hydroxyl condensation produces Si-O-C bonds. Condensation reactions between silanols and hydroxyl groups born by epoxy monomers have been reported in the case of hydroxyl-terminated polydimethylsiloxanes and DGEBA reacted at 130 °C in presence of tetraisopropyl titanate introduced as a catalyst [101], [102]. Lu et al. studied the grafting reaction of CyclohexylDisilanol POSS to DGEBA monomers through a prereaction in presence of Cobalt Naphtanate [75], before subsequent addition of the crosslinking agent. Conclusions of the study were that grafting occurred by condensation with the hydroxyl groups born by the DGEBA when the prereaction was performed at temperatures lower than 150 °C, and by addition on the epoxy functional group for higher temperatures.

Such a mechanism was also highlighted by Manna et al. [103], but for very different reaction conditions. The silanol functions were introduced by silica particles in an epoxy-modified natural rubber, and dispersed via high-shear mixing, with the increase of temperature due to mixing not exceeding 60 °C. In a similar system, the proposed reaction mechanisms involved either condensation of the silanol with hydroxyl groups resulting from opened epoxy cycles, or addition of the silanol upon the epoxy ring (Figure III-6) [104]. In both cases, the Si-O-C linkage was created. The stability of such a chemical bond towards hydrolysis has often been criticized. Indeed, acidic conditions are known to enhance the hydrolysis, for example in the case of alkoxy silane compounds in the sol-gel process. However, the sensitivity of the Si-O-C linkage to hydrolysis decreases when the size of alkoxyde substituents increases [100].

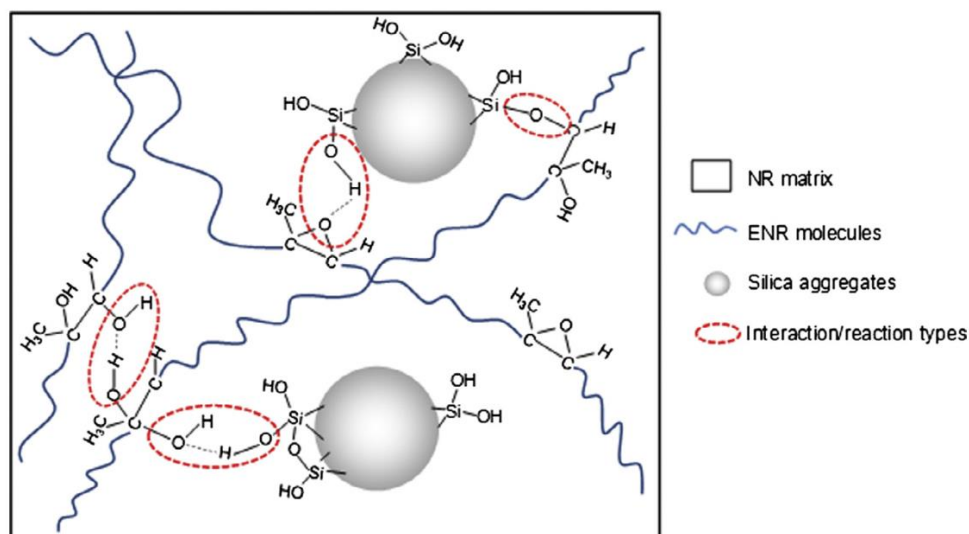


**Figure III-6 Possible interactions and bonding between silica and epoxy-modified natural rubber [104]: hydrogen bonds and/or Si-O-C linkage through condensation with epoxy rings, possibly already opened**

Hayase et al. published a series of works [105]–[110] dealing with the catalytic activity of a model epoxy system containing various types of metal-ligands catalysts and phenol- or silanol-containing compounds. They conducted diverse studies in order to assess the influence of various parameters (silanol acidity, catalyst ligands...) on the catalytic activity, and the properties of the final polymer. In particular, they studied the homopolymerization of a cycloaliphatic epoxy, the cyclohexene oxide, in presence of  $\text{Al}(\text{acac})_3$  and/or  $\text{Ph}_2\text{Si}(\text{OH})_2$  and found out that the combined presence of both compounds catalysed the epoxy polymerization [106]. They also highlighted the occurrence of self-condensation of di-substituted Si compounds in presence of the  $\text{Al}(\text{acac})_3$  alone, concluding that such a reaction is likely to hinder the catalytic effect previously observed. For tri-substituted silanol-containing compounds – such as in the present work – Hayase et al. dismissed the hypothesis of self-condensation but instead proposed that the catalytic activity could be decreased by the Si compounds reacting with the epoxy in certain cases, thus being consumed and no longer available for the catalysis mechanism [108]. This reaction, which involved the inclusion of Si compounds in the final polymer, was proposed as a termination mechanism for the homopolymerization of cyclohexene oxide. However, this phenomenon was only observed for silanol compounds with non-bulky substituents.

The hydroxyl groups are known to enhance the epoxy ring opening. However, in the case of cyclohexene oxide, the presence of either an aluminium catalyst or a silanol-bearing compound did not result in an activation of the polymerization [106], in opposition to the mechanism

proposed by Liu et al. (reported in Figure III-5). The interaction mechanism shown in Figure III-7 was thus proposed in the particular case of  $\text{Al}(\text{acac})_3$  with triphenyl silanol, to explain the catalytic effect observed in the combined presence of these compounds. The homopolymerization of the cyclohexene oxide was then cationically initiated by the separated proton from the Si-OH moiety.

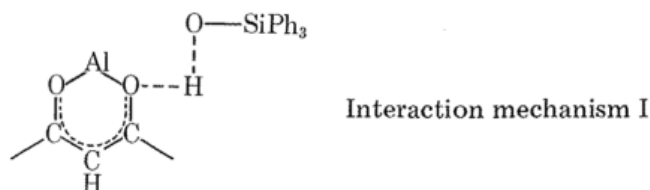


**Figure III-7 Interaction mechanisms between the aluminium catalyst and the Si compound [109]**

The works carried out by Hayase et al. proved the existence of a synergistic catalytic activity which enhanced epoxy ring opening. It is thus reasonable to expect an effect on the polymerization rate and mechanisms in the system under study in the present work, which is however quite different from the one studied by Hayase et al., owing to the epoxy nature and the presence of an amine hardener. This latter compound was not only involved in copolymerization reactions but also brought basicity to the medium, which modified the silanol groups' acidity and could promote condensation reactions as well as stability of Si-O-C bonds.

### **1.2.b. Study of reactions between POSSOH-DGEBA**

A simple experiment was conducted using SEC to determine whether the POSSOH actually grafted on the DGEBA monomers in presence of the Al-based catalyst. For this study, it was chosen not to introduce the amine crosslinking agent in the test procedure, thus avoiding solubility problems. Also, the simplification of the system was an advantage to better understand the role of the combination of the POSSOH and the Al catalyst, though one has to keep in mind that the amine – primary, secondary or tertiary, depending on the polymerization progress – should certainly play a role as mentioned in the previous section.

A sample was prepared that respected the usual proportion of POSSOH towards DGEBA, which corresponded to 5.69 wt% of POSSOH, considering the absence of MDEA in this experiment. The POSSOH was mixed with the epoxy monomer at 130 °C for 30 minutes, until it finally solubilised and the solution became transparent. After cooling down the mixture to 90 °C, 0.6 phr of the Al catalyst was added and the preparation stirred for 50 minutes, sampling being done every 10 minutes. In the same way, a blank DGEBA/Al-based catalyst mixture, i.e. without

POSSOH, was subjected to the same experiment. The catalyst solubilised in the epoxy prepolymer.

In the blank system chromatogram (Figure III-8) the two main peaks of the DGEBA could be observed at ca. 23 and 26 mL, corresponding to its oligomers  $n=1$  and  $n=0$ , respectively. The Al-based catalyst, whose peak was situated ca. 28mL, was in too small quantity to be clearly identified. No decrease of the DGEBA peaks was observed, nor appearance of high molecular weight compounds, thus the Aluminium-based catalyst alone clearly did not cause any homopolymerization.

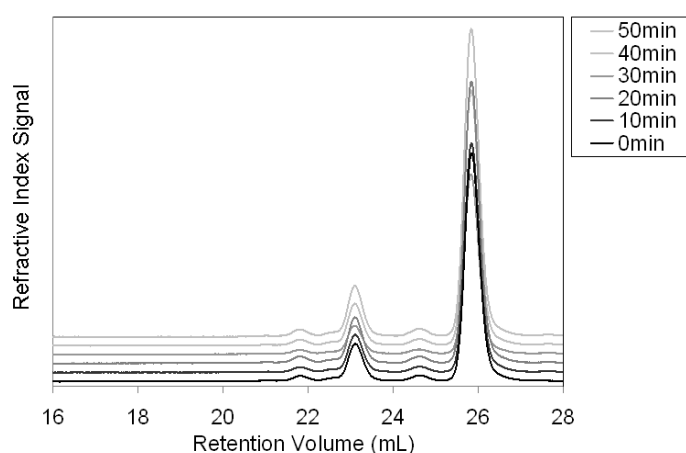


**Figure III-8 SEC chromatograms of the DGEBA-Al catalyst system (blank system) at different times at 90 °C**

In the POSSOH-containing system, the peak of POSSOH coincided with the 23mL-peak of DGEBA ( $n=1$ ). A broad peak, plateau-shaped, appeared between ca. 16.5 and 22 mL as the time of reaction increased, and indicated the formation of larger molecules with highly dispersed molecular weight (Figure III-9). Simultaneously the DGEBA peak decreased. This plateau-shaped peak was not visible on the first spectrum, collected right at the end of the step consisting of mixing the preparation at 130 °C for 30 minutes and before addition of the Al catalyst. This indicated that no products were created, allowing to consider this spectra as a starting point – as the ‘t=0’.

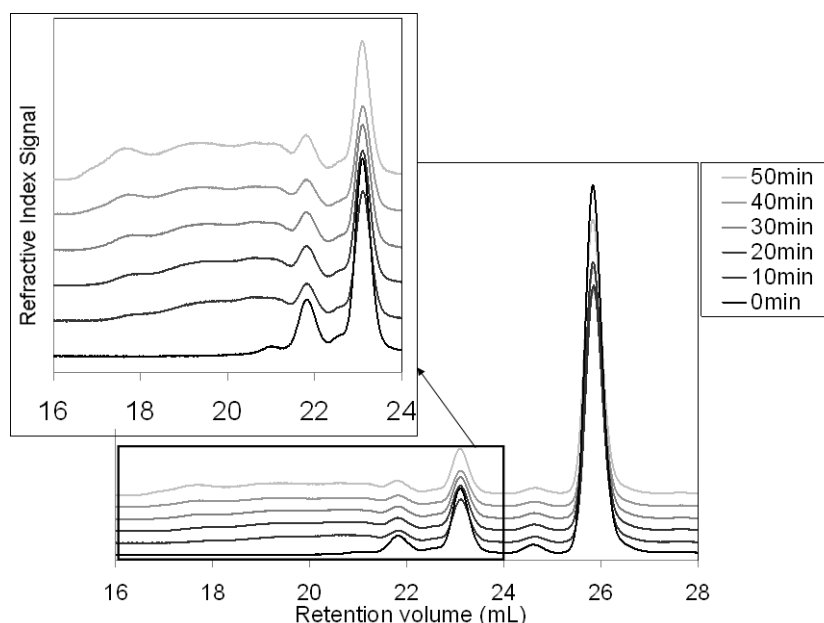


**Figure III-9 SEC chromatograms of the POSSOH-DGEBA-AI catalyst system at different times of reaction at 90 °C**

The conversion of DGEBA could be easily calculated by following the area of the peak at  $V_e=26\text{mL}$  ( $n=0$ ). The conversion in epoxy functions (in %) was calculated according to Equation III-1 [97] and plotted in Figure III-10.

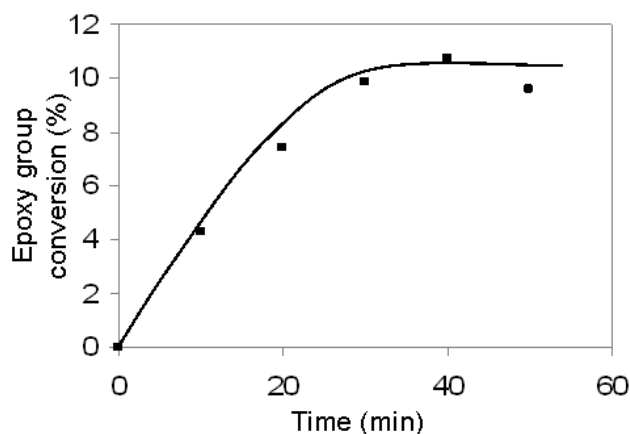


**Figure III-10 Epoxy group conversion in the reactive system as a function of the reaction time at 90 °C**

About 10% of epoxy groups had disappeared at  $t=30$  minutes. The initial epoxy group concentration was equal to 2.50 mol/kg and the initial concentration of silanol groups was of 0.06 mol/kg, which was still less than one tenth of the initial epoxy group concentration – corresponding to the reacted epoxies. Thus, the final conversion of epoxy groups was higher than the maximum conversion it could have reached if epoxy functions reacted only with silanol

groups. Whereas this fact did not allow to conclude on the possible reaction of epoxies with silanols, and at which extent, it highlighted the occurrence of a certain amount of epoxy homopolymerization in presence of both POSSOH and the Al catalyst.

The POSSOH conversion could not be obtained simply because of the overlapping of the POSSOH and DGEBA ( $n=1$ ) peaks at  $V_e=23\text{mL}$ . An attempt was made to estimate the conversion of POSS via a calculus based upon the area of the peak at *ca.* 23 mL, of which the contribution from DGEBA ( $n=1$ ) was subtracted using the pure DGEBA spectrum and the evolution of the area of the peak at *ca.* 26 mL at the different times of the kinetic study. This calculus was based on the hypothesis that the ratio of areas of the peaks of the DGEBA ( $n=0$  and  $n=1$ ) remained constant during the experiment, i.e.: (i) the reactivity of both DGEBA oligomers ( $n=0$  and  $n=1$ ) was similar and (ii) the RI responses of the monomer and the dimer were the same. However, the appearance of the plateau-shaped peak at lower elution volumes disturbed the peak used for POSS conversion calculus *ca.* 23 mL. The results obtained from the POSSOH conversion calculus suffered from a too large variability depending on the baseline and the peak limits settings. They could not be used, leading to aberrant values and are not shown herein.

### **1.2.c. Influence of POSSOH and aluminium acetate catalyst on the polymerization of a DGEBA-MDEA system**

In this part are presented the results obtained for the complete system, i.e. including the MDEA curing agent. Investigations by means of chemorheology, DSC, and NIRS were conducted. The SEC technique was not adapted to investigate the complete formulation, mainly because of solubility issues, but also because of the complexity of the formulation.

- Gelation times

Gelation times were measured at 135 °C, the temperature of the first dwell of the curing cycle. One can notice that the gelation time of the DM system containing either the Al catalyst or the POSSOH, was assessed. Moreover, measurements were performed also at 90 °C, which corresponded to the first-dwell temperature for the DM-POSSOH-Al system (Figure III-11). Results were gathered in Table III-1.

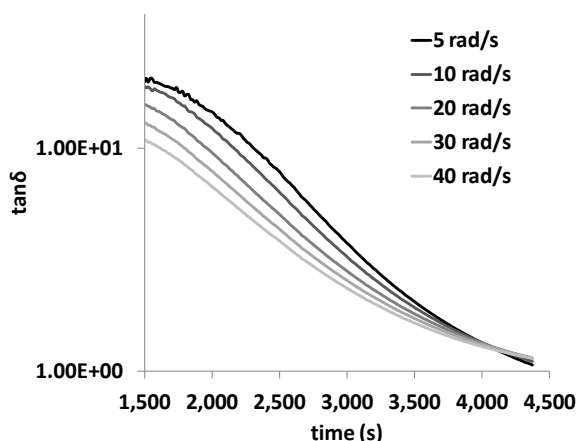


**Figure III-11  $\tan\delta$  curves at different frequencies for DM-POSSOH-AI at 90 °C; the cross point of the curves indicates the gelation time of the system**

Temperature	System	Gelation time
135 °C	DM	59min
	DM-POSSOH	58min
	DM-AI	1h
	DM-POSSOH-AI	< 250s
90 °C	DM-POSSOH-AI	1h 07min
	DM	7h 10 min

**Table III-1 Gelation times of DGEBA-based systems with or without POSSOH and/or aluminium-based catalyst**

While the presence of POSSOH or aluminium acetate catalyst did not have any influence on the gel time of the DGEBA-MDEA system, the combined presence of both compounds decreased greatly this gel time at 135 °C. In this latter case, the gelation was reached too rapidly to obtain a precise measurement – the sensor was overloaded before 250 seconds. At 90 °C, the gel time of DM-POSSOH-AI was measurable and found to be very short as compared to the reference DM system. The higher reactivity of the system containing both POSSOH and the Al catalyst was in accordance with the hypothesis of the formation of a complex between these two compounds, as proposed by Hayase et al. This complex was supposed to enhance epoxy ring opening, which could then be available for reacting with the amine comonomers. The effect of the compound would then result in the decrease of the activation energy of the copolymerization reactions, implying activation temperature and kinetics modifications.

- DSC of reactive formulations

Figure III-12 displays the dynamic scans performed on the reactive systems. The first ramp up to 350 °C revealed the exotherm of the crosslinking reaction. The temperatures and enthalpy exotherms are given in Table III-2. The presence of POSSOH alone did not lower the temperature of exotherm and slightly increased the specific exotherm enthalpy. Combined presence of POSSOH and Al catalyst strongly decreased the temperature of exotherm – revealing a clear catalytic effect. When introduced together, there was a clear synergy between both compounds that possibly modified the polymerization mechanisms.

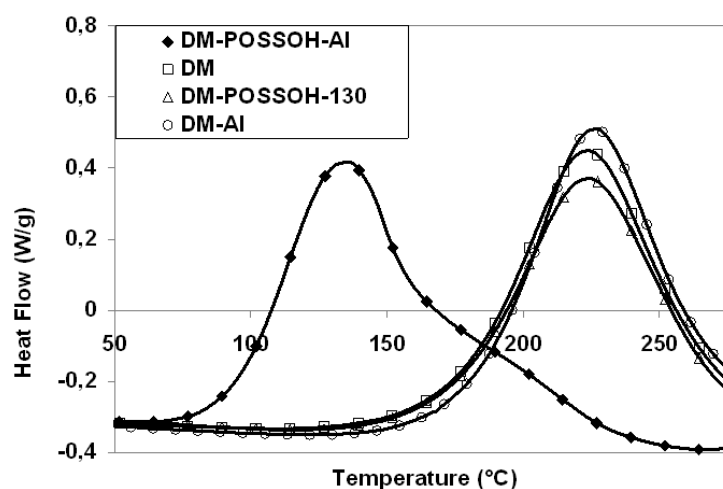


**Figure III-12 Exotherms of reactive DGEBA-based systems (dynamic DSC scan, 10K/min)**

System	Start temp. of exotherm (°C)	Max. temp. of exotherm (°C)	Reaction enthalpy (J/g)
DM	130	223	241
DM-POSSOH	130	223	309
DM-Al	130	227	291
DM-POSSOH-Al	65	136	310

**Table III-2 Temperature and value of enthalpy of reaction of DGEBA-based systems (from DSC)**

Moreover, the exotherm of the DM-POSSOH-Al system presented a shoulder at about 180 °C, which revealed an additional mechanism as compared to the neat system. The same phenomena – the shoulder and the decrease of the exotherm temperature – were observed by Montero et al. [31] for a DGEBA/BSA (4,4'-(1,3-Phenylene)diisopropylidene)bisaniline system containing an isobutyl Aluminium Polyhedral Oligomeric Metallo-Silsesquioxane (POMS) (Figure III-13). The decrease of the exotherm temperature was attributed to the catalytic power of the aluminium atom, activated by the electron withdrawing character of the silicon–oxygen cage. No

further explanation was proposed as concerns the modification of the reaction mechanisms highlighted by the exotherm shoulder.

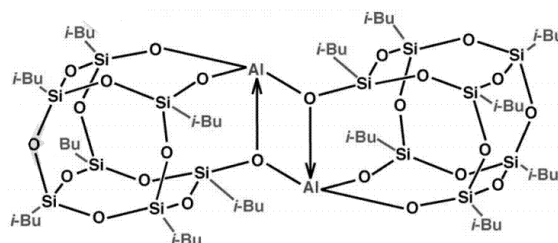


**Figure III-13 Isobutyl Aluminium POMS**

- Investigation of the epoxy-amine kinetics by NIRS

#### ***Experimental protocol and band attribution***

A kinetic study was performed on the DM and DM-POSSOH-Al system at 90 °C by means of NIRS. The aim was to determine in which way the combined presence of POSSOH and Al catalyst modified the epoxy-amine reactions. The Near-Infrared Spectroscopy (NIRS) presents several advantages that made this technique adapted for the present study: (i) the absorption in the NIR domain is less than in the Mid-Infrared (MIR) domain, thus greater sample thicknesses are usable, which simplifies the sampling procedure; (ii) specimens can be observed in their glass container or within glass strips as glass is transparent in the NIR domain; (iii) measurements can be made *in-situ* and are relatively fast; (iv) CO<sub>2</sub> and water vapours bring no interferences; (v) the obtained spectra are simpler than the MIR ones, with less overlapping of the bands. On the other side, attribution of NIR bands is much less documented than for the MIR bands. Hopefully, characteristic bands of DGEBA and MDEA are well-known as they are common compounds for model system studies [83], [111].

Considering the gel times obtained by chemorheology, the times of monitoring were adapted for each system: 15 hours for DM and 5h for DM-POSSOH-Al, with a spectrum collected every 15 minutes and 5 minutes, respectively. The spectrum of a post-cured sample was also collected for each system. The device details, measurement conditions and the post-treatment procedure are given in Appendix A.

Spectra of the DM system before reaction and after post-curing were plotted in Figure III-14. The band attributions are recalled in Table III-3.

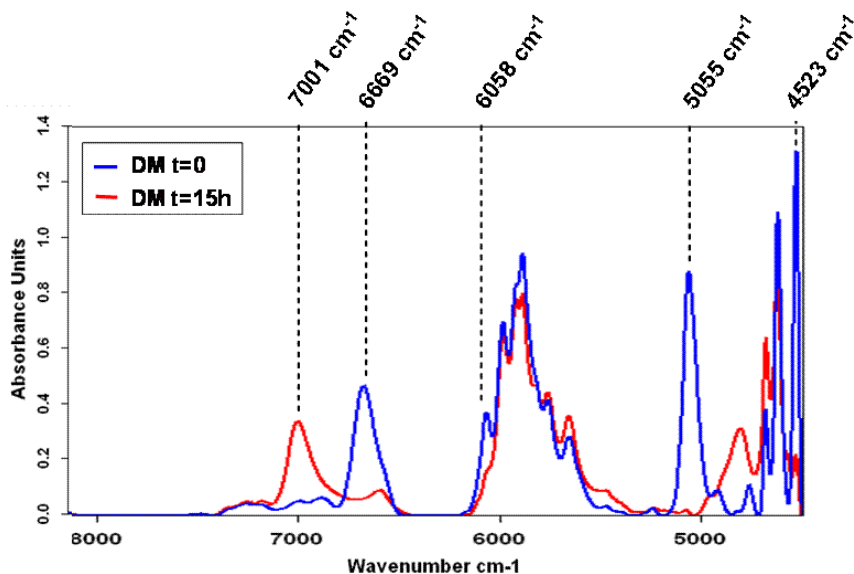


Figure III-14 NIR spectra of DM at t=0 and t=15 hours at 90 °C

Product	Wavenumber (cm <sup>-1</sup> )	Band assignment
DGEBA (Epikote 828)	4523	Epoxy-CH <sub>2</sub> - stretching and deformation
	6058	1 <sup>st</sup> overtone of terminal -CH <sub>2</sub> - stretching
	7001	1 <sup>st</sup> overtone of -OH stretching
MDEA	5055	combination of N-H asymmetric stretching and deformation of the primary amine
	6805-6425	combination of primary and secondary amines first overtone of the N-H stretching

Table III-3 NIR band attribution for DGEBA and MDEA

The NIR spectra of raw products were collected at 90 °C (Figure III-15). The peaks characteristic of the epoxy function of the DGEBA were well defined, although the peak at 4523 cm<sup>-1</sup> was in a zone of high peak concentration, and the peak at 6058 cm<sup>-1</sup> was close to a shoulder. Integrations of such peaks could be sensitive to baseline bias. The intensity of the peak representative of the hydroxyl groups, ca. 7000 cm<sup>-1</sup>, was very low, considering the small concentration of hydroxyl groups in the DGEBA prepolymer.

The spectra of POSSOH revealed different peaks, amongst which one peak at 8756 cm<sup>-1</sup>. This band could possibly be exploited, considering that it was situated out of the peak-concentrated zones of DGEBA and MDEA. However, one must keep in mind that the intensity of this peak was already somehow low when the product was pure, and thus was not likely to be visible in the complete DM-POSSOH-AI system.

The peaks characteristic of MDEA were generally well defined and isolated from other peaks. However the peak at  $6669\text{ cm}^{-1}$  was quite close from the peak of hydroxyl groups from the DGEBA. During curing, this peak will increase while the amine peak will decrease. The amine peak might be disturbed by the hydroxyl peak towards the end of the kinetic study.

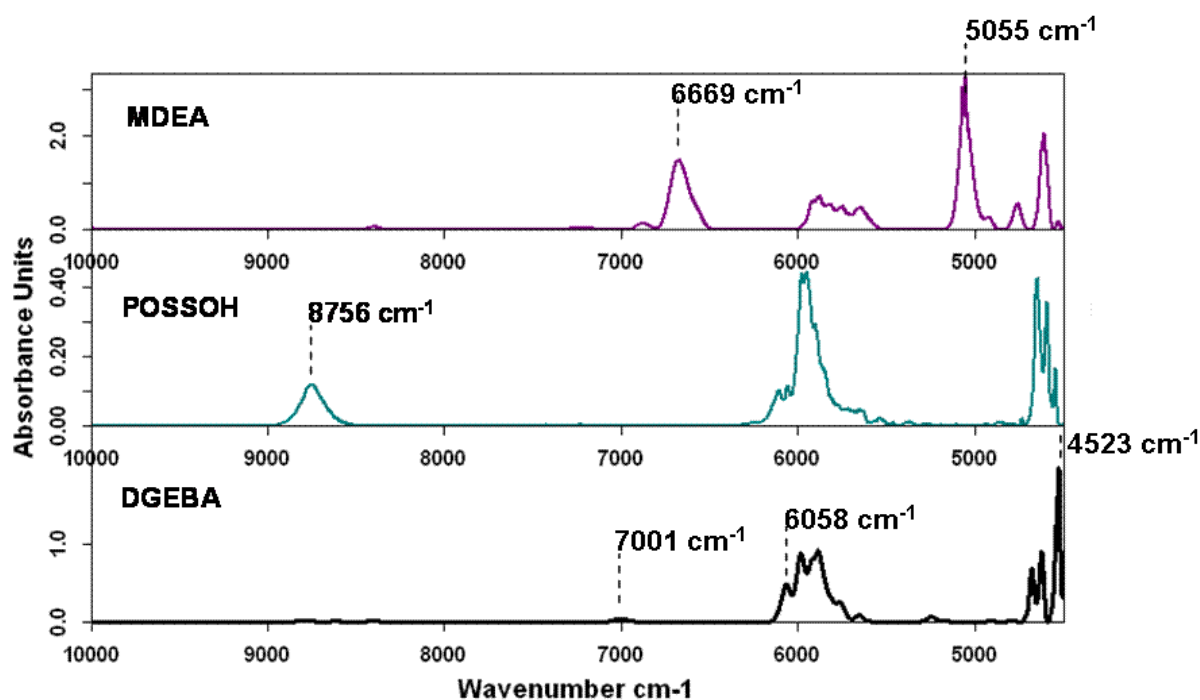


Figure III-15 NIR spectra of raw products at  $90\text{ }^{\circ}\text{C}$

#### ***Procedure for calibration***

Verifying the concentrations of the different functional groups (epoxy, hydroxyl and amine) in the mixtures at the time the first spectra was recorded was mandatory as they served as references in the following kinetic study. The details concerning the calibration procedure are given in Appendix C. The calibration allowed to verify the Beer-Lambert law for all the peaks, and to apply a correction corresponding to the peaks residual intensity for a nil concentration.

Moreover, the intensity of the peaks of post-cured samples was also used for the concentration calculus, and it was verified by DSC that the post-cured samples were fully crosslinked.

#### ***Procedure for concentration calculations during cure***

The same procedure as proposed by Liu et al [83] was implemented. The cure kinetics of the epoxy/amine systems were deduced from the concentrations of the epoxy and amino functional groups. The consumption of epoxy groups were easily followed by monitoring the absorbance of

the peak at 4523 cm<sup>-1</sup> (Figure III-16). The concentration was given by using the first recorded spectrum at t=0, in which the concentration of epoxy functions was known, and the spectrum of the post-cured sample, where the concentration of epoxy groups was assumed to be equal to zero (Equation III-4). In all the equations, the subscripts 't', '0' and 'pc' stand for 'at time t', 'at t=0' and 'in the post-cured sample', respectively.

III-4

$$[EP]_t = [EP]_0 \times \frac{H_{EP,t} - H_{EP,PC}}{H_{EP,0} - H_{EP,PC}}$$

where  $[EP]_t$  is the concentration of epoxy groups at a given time,  $[EP]_0$  is the initial epoxy groups concentration,  $H_{EP,t}$ ,  $H_{EP,pc}$ , and  $H_{EP,0}$  are the absorbance of the peak at 4523 cm<sup>-1</sup> at a given time, of the post-cured sample, and in the first recorded spectrum, respectively.

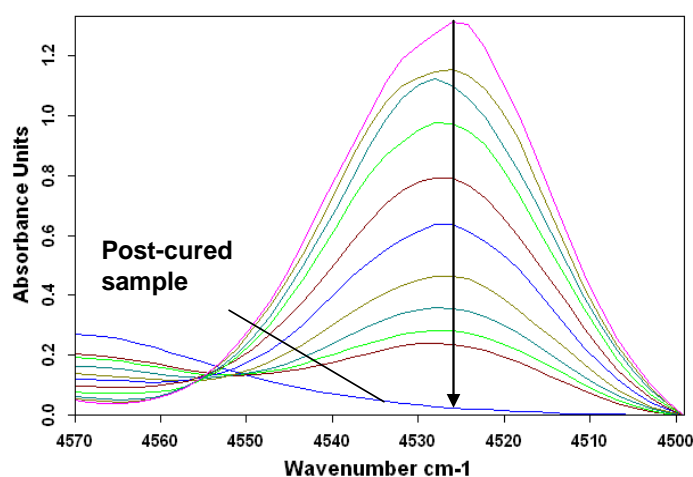


**Figure III-16** Combination band of the CH<sub>2</sub>-epoxy stretching and deformation in the DM system.

The direction of the arrow indicates the evolution of the band with time

Using the peak intensity at 5055 cm<sup>-1</sup> (Figure III-17), the concentration of primary amines was expressed in Equation III-5.

III-5

$$[PA]_t = [PA]_0 \times \frac{H_{PA,t} - H_{PA,PC}}{H_{PA,0} - H_{PA,PC}}$$

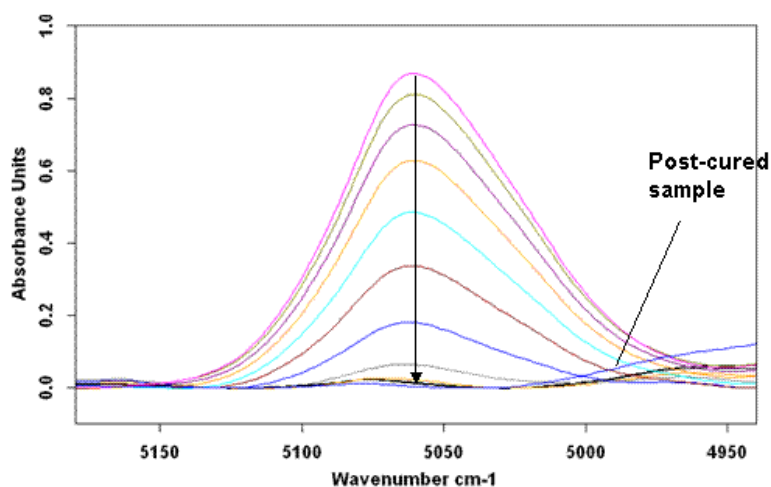


**Figure III-17** Combination band of the N–H asymmetric stretching and deformation of the primary amine in the DM system. The direction of the arrow indicates the evolution of the band with time

The concentration of secondary amines (SA) could be determined indirectly from the band between 6805 and 6425  $\text{cm}^{-1}$ . This band was attributed to the combination of both the PA and the SA (Figure III-18). Liu et al. [83] made the hypothesis that the contribution of each amine to the area of the band could be expressed as a dependence of this area with a linear combination of their concentration (Equation III-6).

III-6

$$A_{PA+SA,t} = a \cdot [PA]_t + b \cdot [SA]_t$$

where  $A_{PA+SA,t}$  corresponds to the area of the peak of interest at a given time  $t$ , and  $a$  and  $b$  are constants.

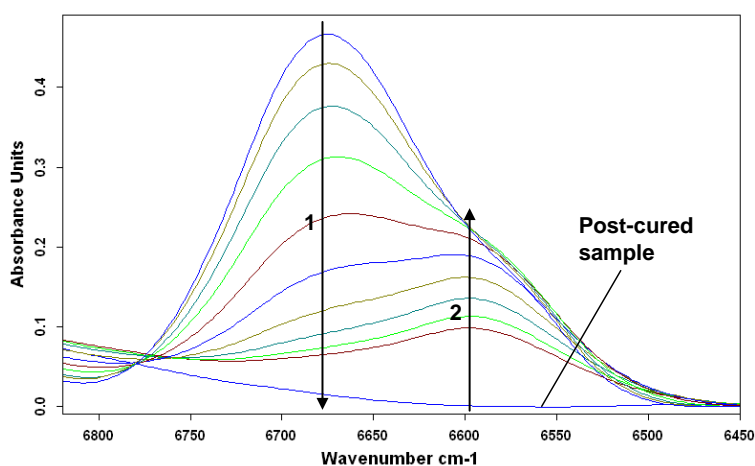


**Figure III-18** Bands characteristic of the PA and SA first overtone (NH stretching). The direction of the arrows 1 and 2 shows the evolution of the contribution of the PA and SA amine, respectively

Knowing the primary amine concentration from the peak at 5055 cm<sup>-1</sup>, the secondary amine concentration could be derived from Equation III-7.

III-7

$$[SA]_t = \frac{A_{PA+SA,t} - a \cdot [PA]_t}{b}$$

A second hypothesis was made by Liu et al., which considered that no reaction of the secondary amine occurred during the first minutes of the study. If the hypothesis was valid, the constants *a* and *b* could be calculated using the first recorded spectra. The validity of the hypothesis will be examined and the *a* and *b* coefficients calculated in the results part.

Finally, the conservation of the overall quantity of amine functions allowed to calculate the concentration of tertiary amines (TA) (Equation III-8), that could not be monitored by NIRS.

III-8

$$[TA]_t = [PA]_0 - ([PA]_t + [SA]_t)$$

The concentration of SA could also be calculated from the concentrations of the epoxy and the amine functions (Equations III-9 to III-11) and compared with the concentration calculated from the band situated between 6450 cm<sup>-1</sup> and 6800cm<sup>-1</sup> (Equation III-9). Those equations were established in the case where homopolymerization was neglected.

III-9

$$[EP]_t = [EP]_0 - ([PA]_0 - [NH_2]_t) - [TA]_t$$

III-10

$$[PA]_0 = [PA]_t + [SA]_t + [TA]_t$$

And by recombining Equations III-9 and III-10 :

III-11

$$[SA]_t = 2 \times ([PA]_0 - [PA]_t) - ([EP]_0 - [EP]_t)$$

### **Results**

The initial concentrations of the functional groups calculated from the calibration are reported in Table III-4 and compared to the theoretical initial concentrations, calculated from the masses of products introduced in the DM and DM-POSSOH-AI systems.

		DM			DM-POSSOH-AI		
		Theoretical	From calibration	Difference (%)	Theoretical	From calibration	Difference (%)
Epoxy	A 4523		3.75	0.3		2.67	25.6
	H 4523	3.76	3.78	0.5	3.59	2.62	27.0
	H 6058		4.00	6.4		3.43	4.5
PA	H 5055	1.88	1.85	1.6	1.81	1.11	38.7

**Table III-4 Comparison of theoretical initial concentrations (mol.kg<sup>-1</sup>) of functional groups and concentrations obtained from the calibration**

In the DM system, the theoretical initial concentrations – i.e. calculated from the masses of products introduced in the medium – and the ones calculated from the calibration corroborated very well, the error being within the technical uncertainty expected for a technique such as the NIRS. This indicated that no reaction occurred before the first spectrum was recorded. In the case of the DM-POSSOH-AI system, the real concentrations – the concentrations calculated from the calibration – were clearly lower than the theoretical ones, indicating that the epoxy amine reaction must have started before the first spectrum was collected, hence the interest of verifying the initial concentration values. Only the value of concentration of epoxies given by the calibration of the peak at 6058 cm<sup>-1</sup> did not corroborate the results given by the peak at 4523 cm<sup>-1</sup>. Considering the value of the initial concentration of PA calculated from the calibration (1.11 mol.kg<sup>-1</sup>) – much lower than the one expected with the theory (1.81 mol.kg<sup>-1</sup>), thus indicating a reaction – the result given by the latter peak seemed the most relevant. In the next step of the study, the area of the peak at 4523 cm<sup>-1</sup> will be used to monitor the epoxy concentration.

For the DM-POSSOH-AI system, the effective conversion at 't=0' – i.e. at the moment the first spectrum of the kinetic study was collected – from either the epoxy concentration or the PA concentration, was calculated according to Equations III-12 and III-13 and reported in Table III-5.

III-12

$$\alpha_{EP} = 100 \times \frac{[EP]_{0,th} - [EP]_{0,r}}{[EP]_{0,th}}$$

III-13

$$\alpha_{PA} = 100 \times \frac{[PA]_{0,th} - [PA]_{0,r}}{2 \times [PA]_{0,th}}$$

where  $\alpha_{EP}$  and  $\alpha_{PA}$  are the conversions (in %) of the epoxy and amine groups, respectively,  $[EP]_{0,th}$  and  $[PA]_{0,th}$  are the theoretical initial concentrations – from the initial products' quantities – of epoxy and amine groups, respectively, and  $[EP]_{0,r}$  and  $[PA]_{0,r}$  the real initial concentrations of functional groups – calculated from the calibration curves (see Table III-4). The factor of 2 in the Equation III-13 accounts for the functionality of 2 of each primary amine group and to compare the value of conversion to the one of the epoxy groups.

The conversion of PA (19.3%) being lower than the one of epoxy groups (ca. 25.6%), this would mean that the epoxy reacted not only with the primary amine groups during the sample preparation, but also with other species, such as the secondary amines created by the previous reaction, the silanols of the POSSOH or the hydroxyl groups born by the DGEBA molecules.

		Conversion (%)
Epoxy	A 4523	25.6
PA	H 5055	19.3

**Table III-5 Conversion of epoxy and primary amine groups at t=0 - defined as the time of the first collected spectrum**

The procedure to calculate the concentrations of functional groups as a function of the time of reaction was detailed in the previous section. However, it remained to determine the  $a$  and  $b$  values allowing to calculate the secondary – and then the tertiary – amine concentration, according to the Equation III-7. To apply this equation, it was also necessary to verify the validity of the hypothesis according which no reaction of the secondary amine occurred during the first minutes of the study. It was validated in the case of the DM system, which allowed to calculate the constants  $a$  and  $b$ , equal to 33.07 and 14.58, respectively. The details of the calculus of  $a$  and  $b$  are given in Appendix C. The concentration of the SA in DM-POSSOH-AI system was then calculated using the value of  $a$  and  $b$  found for the DM system as the same amine compound was used in both systems.

The concentrations of all the functional groups involved in the epoxy-amine reactions were thus determined and the concentration profiles could be plotted as a function of time for both systems (Figure III-19).

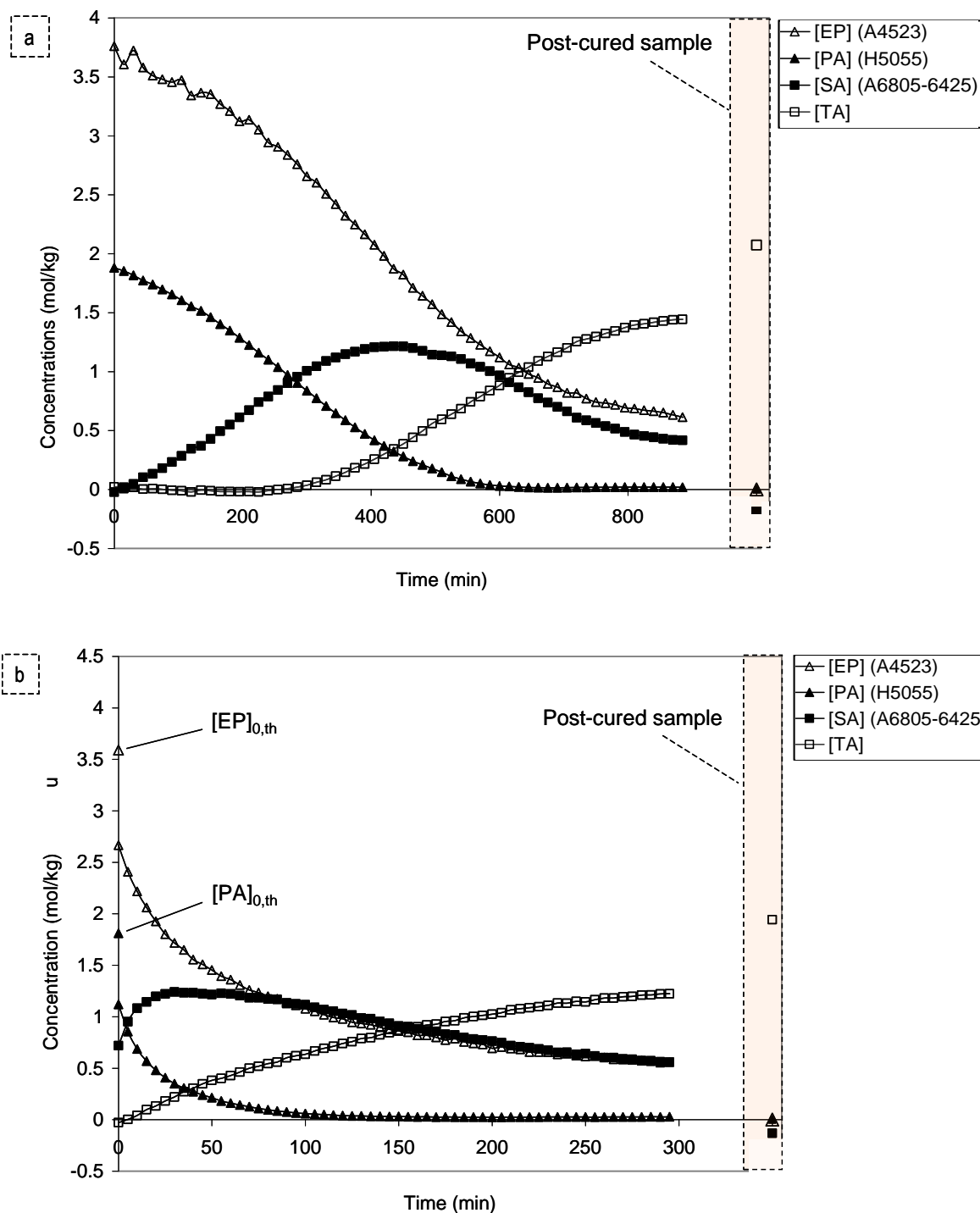


**Figure III-19 Concentration profiles as a function of time of the functional groups in (a) DM and (b) DM-POSSOH-Al systems, during the reaction at 90 °C**

The first observation to draw out of these concentration profiles was that the concentrations of the epoxy groups reached a plateau, indicating that the reactions were complete. However, this did not mean that the systems were fully cured, as indicated by the difference observed with the concentrations of functional groups in the post-cured sample, because the reactions were

limited by the vitrification phenomenon, occurring when the glass transition temperature of the systems neared the temperature of the test, i.e. 90 °C. It could also be observed that the rate of reaction was indeed much higher in the case of the DM-POSSOH-AI system, as previously highlighted by the gel-time measurements. While the DM system presented a classical concentration profile for epoxy/amine system, in the DM-POSSOH-AI the latency time at the beginning was absent.

In the case of the DM-POSSOH-AI system, two phenomena could be observed: (i) the concentration of SA at  $t=0$  was not-nil (equal to  $0.72 \text{ mol.kg}^{-1}$ ) and (ii) the concentration of TA at  $t=0$  was nil. This indicated that while the reaction of consumption of PA, producing SA, had started before  $t=0$ , the reaction of consumption of SA, producing TA, had actually not begun at  $t=0$ . This would have a strong implication as for the effective reaction occurring in the test tube during the NIRS measurement, and by extrapolation in all the samples made of this particular system.

As mentioned before, the epoxy conversion at  $t=0$  (the time at which the first spectrum was collected) was higher than the PA conversion. The fact that no SA was consumed – i.e. the SA conversion at  $t=0$  was nil – implied that the epoxy reacted with other species than the amines. Those species could be (i) the silanol functions born by the POSSOH, according to the mechanism proposed by Liu et al. [86] and not by a condensation reaction as it does not consume an epoxy function, and/or (ii) the hydroxyls of the epoxy monomers, meaning that epoxy homopolymerization actually occurred in this system. Because neither the ether linkage formation nor the evolution of silanol groups could be monitored via NIRS, only hypotheses on this aspect could be expressed.

Calculating the theoretical amount of silanol functions present in the system right after mixing of the components gave a concentration value of  $0.13 \text{ mol.kg}^{-1}$ . It was found before that the theoretical initial concentration of epoxy (calculated from the mass of DGEBA introduced in the mixture) was equal to  $3.59 \text{ mol.kg}^{-1}$ . The value of epoxy concentration calculated from the calibration was of  $2.67 \text{ mol.kg}^{-1}$ , hence a reduction of  $0.92 \text{ mol.kg}^{-1}$ . Similarly, the reduction for SA was equal to  $0.70 \text{ mol.kg}^{-1}$  (see Table III-4), thus leaving  $0.22 \text{ mol.kg}^{-1}$  of ‘inexplicably’ consumed epoxy functions, which was higher than the initial silanol concentration. This would mean that even if the epoxy had reacted with all the silanol functions, a certain amount of homopolymerization actually occurred anyway. Unfortunately, it is not possible to conclude on whether the reaction with the silanol functions did happen or not. Only the epoxy homopolymerization at a more or less high extent, already indicated by the SEC analysis, was confirmed.

If homopolymerization truly occurred in the DM-POSSOH-AI, a residual PA and/or SA concentration could be expected at the end of the reaction – i.e. in the post-cured sample. Considering the concentration profiles of this particular system, it could be observed that the PA and the SA concentrations were equal to zero. This could come from the fact that the PA concentration was artificially set to zero in the post-cured sample, the concentration of PA at any time being corrected by the remaining absorbance of its characteristic peak in the post-cured sample spectrum. As the SA concentration was determined using the PA concentration, it could have suffered from the same artefact. On the other hand, the hypothesis of a complete consumption of the PA, even in presence of a certain amount of homopolymerization, is realistic because the kinetic constant associated with the reaction of the epoxy with the PA is superior to the one related to the reaction of epoxy with the SA in a DGEBA/MDEA system [112], meaning that the PA consumption is favoured as compared to the SA consumption. This means that to have a residual PA concentration, the epoxy homopolymerization must consume more than half of the epoxy groups introduced in the medium.

Finally, the SA concentration was calculated with the epoxy and the primary amine concentrations, according to Equation III-11. The result was plotted in Figure III-20 together with the SA concentration derived from the peak situated between  $6450\text{ cm}^{-1}$  and  $6800\text{ cm}^{-1}$ .

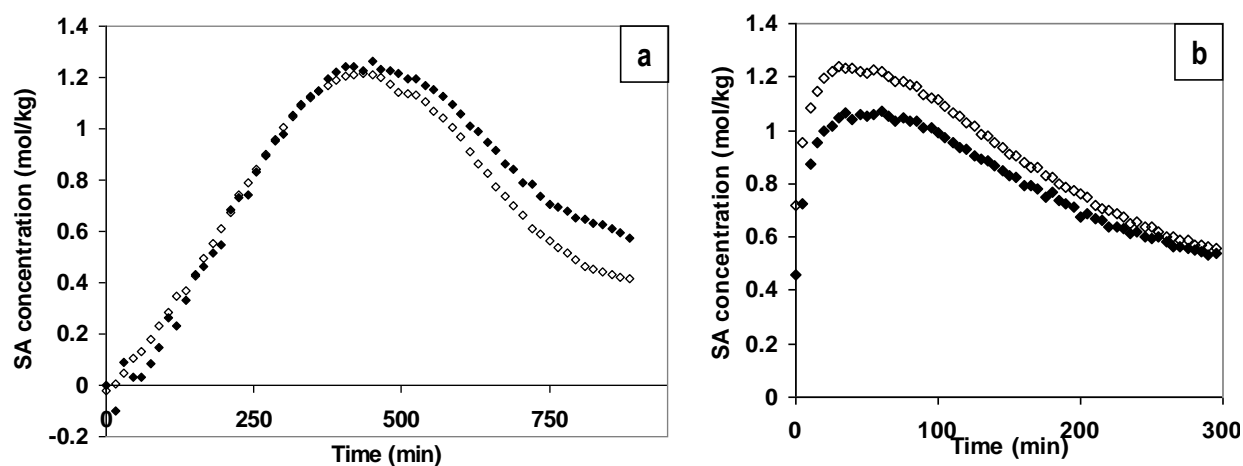


**Figure III-20 SA concentration during curing of the a) DM system and b) DM-POSSOH-AI system at 90 °C, obtained either from the peak between  $6450\text{ cm}^{-1}$  and  $6800\text{ cm}^{-1}$  ( $\diamond$ ), or from the epoxy and the PA concentrations (Equation III-11) ( $\blacklozenge$ ).**

In DM, a reasonable fit was observed between the SA concentrations obtained either from the peak between  $6450\text{ cm}^{-1}$  and  $6800\text{ cm}^{-1}$  or from the epoxy and the PA concentrations,

especially before 500 minutes, where the epoxy and the PA peaks are greater and thus less subjected to measurement and post-treatment bias.

In the case of the DM-POSSOH-AI system, an under-estimation of the SA concentration was observed when calculated from the epoxy and PA concentrations using Equation III-11. In this equation, the homopolymerization was neglected. The SA measured from the peak between  $6450\text{ cm}^{-1}$  and  $6800\text{ cm}^{-1}$  being lower than the calculated one is then consistent with the hypothesis of the occurrence of homopolymerization.

The NIRS study allowed to verify the existence of homopolymerization in the DM system containing both POSSOH and the AI catalyst. However, because of the limit of sensibility of the technique, it was impossible to conclude on which reactions occurred between the epoxies and the POSSOH silanols, or even the occurrence of such reactions.

## **2. POSS-INVOLVING INTERACTIONS IN THE FINAL-STATE NETWORKS**

Investigation of the potential interactions existing between the POSSOH and the DGEBA-MDEA matrix in the final networks was carried out using different techniques. Direct analyses were implemented, such as solid  $^{29}\text{Si}$  NMR, but also indirect methods i.e. thermomechanical analysis of the networks and Size Exclusion Chromatography of solutions in which the networks were left to swell for eventual extraction of soluble compounds, the aim being to extract potentially soluble compounds from the networks.

In this section, focus will be made on POSS interactions in the model networks where POSS were solubilised by heating, with or without the addition of the AI-based catalyst.

### **2.1. DYNAMIC MECHANICAL ANALYSIS (DMA)**

Thermomechanical properties have been assessed by performing DMA for each network. Not only this technique allows to identify the beneficial or detrimental effect of additives in the networks in terms of thermomechanical properties, but it can also provide information on the effect of such an additive on the network structure. The DMA curves ( $G'$  and  $\tan \delta$ ) of the DM-POSSOH-AI together with that of the neat matrix were plotted in Figure III-21. Data extracted from DMA are summarized in Table III-6: the main relaxation temperatures  $T_{\alpha}$  associated with the glass transition phenomenon, given by the temperature of the peak of the loss factor tangent  $\delta$ , the rubbery modulus  $G'_{T_{\alpha}+30^{\circ}\text{C}}$ , measured at  $T_{\alpha}+30\text{K}$  i.e. in the glassy state, and the width of the peak of tangent  $\delta$ ,  $\Delta T_{h=1/2}$ , measured at half the height of the peak.

	$T_g$ (°C)	$\Delta T_{h=1/2}$ (°C)	$G'_{T_g+30^\circ\text{C}}$ (MPa)
DM	157	15	11.2
DM-POSSOH-130	166	15	9.5
DM-POSSOH-AI	159	20	15.6

**Table III-6 DMA data for DGEBA-based networks (1 Hz)**

The introduction of POSSOH did not change much the value of  $T_g$ , the higher variation observed being an increase of 9 °C in DM-POSSOH-130. With the addition of the Al-based catalyst, the width of the glass transition domain was increased, as well as the rubbery modulus, while the POSSOH alone caused the rubbery modulus of the network to decrease slightly.

The widening of the glass transition domain revealed a certain increase in heterogeneity in the network as compared to the reference system, which was consistent with possible residual secondary amine functions due to epoxy homopolymerization. Moreover, the modulus at the rubbery plateau was increased by the addition of POSSOH and Al catalyst. Several origins could be proposed to explain this phenomenon: (i) it could suggest a higher crosslinking density in this network than in the reference matrix, due to the trifunctional POSSOH forming new and compact crosslinking points; (ii) the networks being heterogeneous as seen from morphological characterization (see Figure II-19 in Chapter II), there could be a reinforcing effect from interactions of POSSOH sub-micrometric objects with the epoxy matrix or simply from the contribution of the higher modulus of these partially inorganic objects.

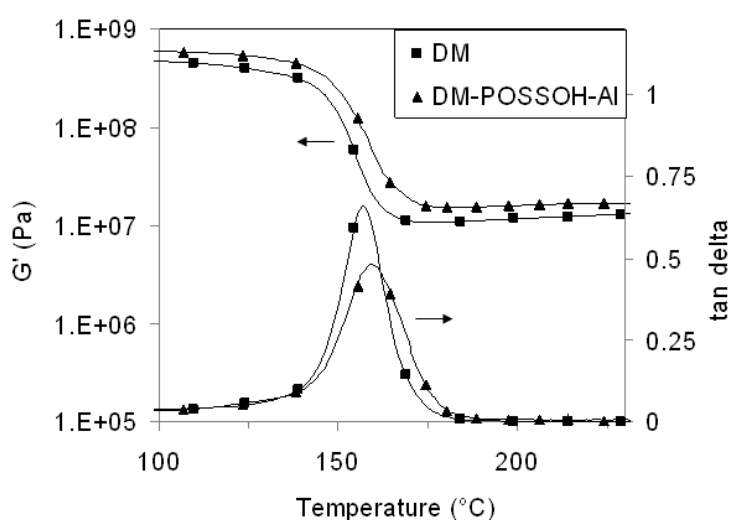


**Figure III-21 Comparison of DMA curves of neat DGEBA-MDEA matrix and DGEBA-based network containing both POSSOH and the Al catalyst (1 Hz)**

## 2.2. INDIRECT ANALYSIS VIA SEC

As highlighted before, the SEC could not be used directly on the epoxy networks as they cannot solubilise in a solvent. They were thus immersed in THF and the solutions were then analysed via SEC. The networks were previously grinded in order to enhance the diffusion of species from the network to the THF. The aim was to determine whether the networks liberated some POSSOH in THF, in which case it would prove that the POSSOH were not attached to the networks.

Looking at the chromatograms corresponding to the DGEBA-based networks (Figure III-22) it could be seen that a certain amount of species with a continuous range of molar masses were liberated by the networks. The positions of characteristic DGEBA and POSSOH peaks were indicated on the spectra by dotted lines. The networks did not liberate DGEBA monomers. The DM-POSSOH-130 network presented a shoulder at 23.1 mL that could be attributed to DGEBA  $n=1$  and/or to POSSOH. Considering that no release of DGEBA  $n=0$  was observed, the shoulder could be reasonably assigned to single POSSOH units, thus indicated that a certain – but low – extent of POSS did not developed covalent interactions in this particular network. In DM-POSSOH-AI no POSSOH seemed to be liberated, at least in the form of single units, highlighting either a reaction of the POSSOH with the matrix or a reaction of POSSOH between themselves. DM-POSSOH-130 released a greater quantity of higher molar mass species than the DM-POSSOH-AI network. These higher molar mass species could be small free network fragments, possibly containing POSSOH. However, even in the DM-POSSOH-130 network, the intensity of the overall signal remained extremely low as compared to the raw products signals for similar analysed solution concentrations, revealing that the overall amount of released species was very limited.

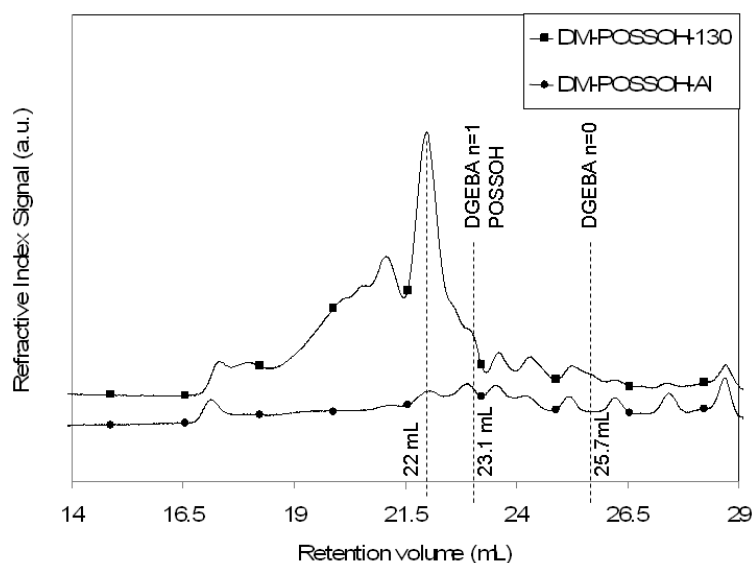


**Figure III-22 SEC chromatograms of THF surfactant solutions of immersed POSSOH-containing DGEBA-based networks**

In conclusion, the occurrence of POSSOH reaction with other species or upon itself in the networks containing both POSSOH and the Al catalyst was confirmed as the great majority of the POSSOH was not extracted. Also the hypothesis supported by the DMA experiments of a higher crosslinking density in these networks was coherent with the present SEC results.

### **2.3. SOLID STATE $^{29}\text{Si}$ NUCLEAR MAGNETIC RESONANCE (NMR)**

The solid state  $^{29}\text{Si}$  NMR is a technique particularly adapted to the issue treated in the present study. However, as many other methods, its sensitivity is limited and considering the low amount of silicon in the networks (less than 1 wt%), an attempt to produce DGEBA-based networks with higher contents of POSSOH was carried out. The issue encountered with this alternative was the poor dissolution of POSSOH when increasing its concentration so that the Si content reached 5 wt% - which is the limit to have an acceptable resolution with the solid state  $^{29}\text{Si}$  NMR. However, the morphology of the networks with higher POSSOH content was verified by SEM and the POSSOH actually adopted the same structure as in the low POSSOH content networks – i.e. nodules of a few microns for DM-POSSOH-130 and of a few hundreds of nanometres for DM-POSSOH-Al. Only, the nodules were more numerous (Figure III-23). It was considered that the interactions developed in these networks were comparable to the ones in the low POSSOH amount networks.

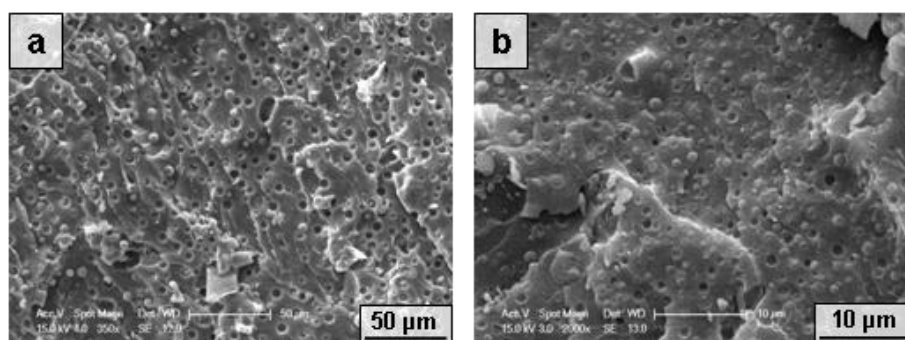


Figure III-23 SEM image of the DM-POSSOH-130 (a) and DM-POSSOH-AI (b) with 5 wt% Si

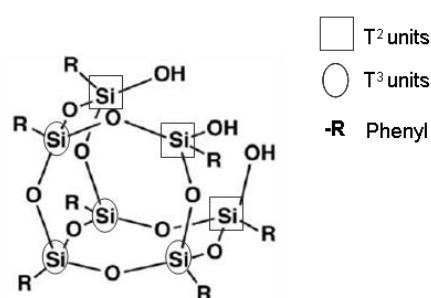


Figure III-24 T<sup>2</sup> and T<sup>3</sup> units in POSSOH structure

The recorded <sup>29</sup>Si Cross Polymerization/Magic Angle Spinning (CP/MAS) NMR spectra (Figure III-25) was analysed bearing in mind the expected structure of POSS building blocks consisting of four fully condensed T<sup>3</sup>(1Ph)(3OSi)(0OH) units and three incompletely condensed groups T<sup>2</sup>(1Ar)(2OSi)(1OH), according to the nomenclature used in <sup>29</sup>Si NMR (circles and squares in Figure III-24, respectively). One has to keep in mind that the CP/MAS NMR is not a quantitative analysis as it depends of the environment of the atom analysed – namely the protons around the atom.

The <sup>29</sup>Si CP/MAS NMR spectrum of the neat POSS was dominated by a set of narrow signals clearly indicating its crystalline state. It is generally accepted that the increase in condensation rate of siloxane units is accompanied by the decrease in <sup>29</sup>Si NMR chemical shift of about 10 ppm. Consequently the fully condensed T<sup>3</sup> units could be attributed to the signals at ca. -78 ppm, while the signals shifted toward higher frequencies -65 and -69 ppm were assigned to the incompletely condensed T<sup>2</sup> groups. The ratio of signal intensities T<sup>2</sup>/T<sup>3</sup>=3.8/3.2 was distorted with respect to the expected value (3.0/4.0) due to the higher efficiency of cross/polarization involving OH protons of T<sup>2</sup> units.

Incorporating POSS units into the polymer matrix caused significant broadening of the <sup>29</sup>Si CP/MAS NMR signals and the dramatic reduction of the ratio of signal intensities of T<sup>2</sup>/T<sup>3</sup>. The observed broadening indicated a loss of crystalline arrangement of POSS units, which

correlated with the results from XRD presented in the last chapter. The ratio of intensities of  $T^2/T^3$  decreased from 3.8/3.2 in the POSSOH, to 2.1/4.9 and 1.4/5.6 in DM-POSSOH-130 and DM-POSSOH-Al, respectively. This reflected a considerable progress in the condensation degree of siloxane units, from  $T^2$  to  $T^3$ . The only reaction able to produce more  $T^3$  units was the self-condensation of POSSOH. A comparison between these ratios could be made considering that the change in the crystalline state of POSSOH did not significantly influence the CP/MAS response for these signals. However, the difference of ratio between both networks was probably too low to affirm with certainty that the extent of self-condensation of POSSOH was higher in the presence of the Al catalyst.

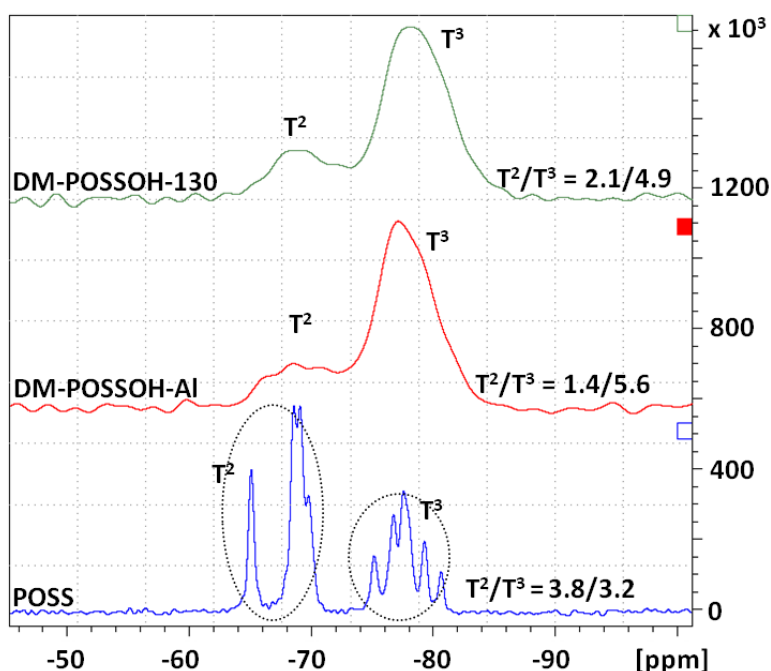


Figure III-25  $^{29}\text{Si}$  CP/MAS NMR spectra of neat POSS and the POSS-containing DGEBA-based networks

### 3. CONCLUSION

The interactions involving functional POSSOH in the model epoxy network based on DGEBA and MDEA were investigated via various analytical methods, either during cure or in the fully-cured networks.

In the case of AmPOSS-containing network, a clear conclusion was reached as for the epoxy-POSS interactions, i.e. the POSS was grafted to the epoxy-amine network. The morphology of the final network, with the absence of POSS domains confirmed this hypothesis.

The systems containing POSSOH are much more complex than the previous one as several reactions, besides the epoxy-amine addition reactions, could possibly occur:

- homopolymerization of epoxy
- epoxy-silanol addition
- hydroxyl-silanol condensation (the hydroxyl coming from the epoxy monomers)
- silanol (self-) condensation

All these reactions were possibly competing with each other, and in the case of the systems containing the  $\text{Al}(\text{acac})_3$ , there was a potential catalytic effect that could activate or modify the reaction mechanisms, including those of the epoxy-amine polymerization.

Namely, the influence of POSSOH and the aluminium-based catalyst on the DGEBA-MDEA model system reactions has been observed and demonstrated through SEC, DSC, chemorheology and NIRS. The silanol-epoxy reaction (POSSOH grafted on the epoxy) could not be evidenced. The low content of POSSOH made it difficult to clearly determine the nature of the interactions in the network.

However, the clear catalytic effect of the combined presence of POSSOH and the Al-based catalyst, demonstrated through the DSC analysis of reactive systems and the measurements of gelation time via chemorheology, validated the hypothesis of the formation of a complex between these two compounds (proposed by Hayase [109]). A certain extent of epoxy homopolymerization was evidenced by the SEC-based study and confirmed by NIRS analyses to the detriment of copolymerization reactions.

The SEC analysis of solutions in which the final networks were immersed proved that the POSSOH could not be extracted from the networks as single units. Moreover, the solid state NMR revealed that the POSSOH was subjected to a certain extent of self-condensation. Finally, the consequences of the various reactions caused or modified by the addition of both POSSOH and  $\text{Al}(\text{acac})_3$  on the thermomechanical properties of the networks were rather limited: a higher rubbery modulus was observed as well as a certain increase in the network heterogeneity as shown by the wider  $\alpha$ -transition.





This chapter is dedicated to the study of the thermal stability and the fire behaviour of the produced epoxy-amine networks. As highlighted in Chapter I, fire retardancy of polymers remain a subject of interest that is still in demand of alternative solutions. Moreover, the fire-retardant mechanisms of these solutions need to be understood, for scientific knowledge contribution, but also to be able to better target efficient fire-retardant solutions.

In this chapter, the model networks – made from either DGEBA or TGDDM epoxy prepolymers with MDEA as crosslinking agent – and the networks based on the commercial MVR444 commercial formulation will be investigated. The effect of the addition of the different POSS presented in Chapter II on the fire retardancy of the model networks will be assessed, and a particular attention will be dedicated to networks – from model or commercial compounds – containing the triSilanolPhenyl POSS.

## **1. PRELIMINARY CONSIDERATIONS ON TECHNIQUES AND DATA TREATMENT**

The thermal stability of the networks was assessed via ThermoGravimetric Analysis (TGA) and their fire behaviour through the UL 94 test and/or cone calorimetry. Details on the techniques and samples are given in Appendix A.

Concerning the TGA experiment, the data collected from the spectra will be gathered in tables presenting the temperature corresponding to a weight loss of 5% ( $T_{5\%}$ ) and of 50% ( $T_{50\%}$ ), as well as the mass residue measured at 700 °C. Theoretical residual weight percentages are displayed in brackets in the tables and were calculated as follows: (i) for the neat POSS it corresponds to either the inorganic content of the molecule in inert atmosphere or the contribution of the potential silica production under oxidative conditions – the air providing the oxygen missing to obtain  $\text{SiO}_2$  from the original  $\text{SiO}_{1.5}$  POSS composition, (ii) for organic/inorganic hybrid networks, it is the sum of the contributions from the pure POSS fraction residue and from the neat epoxy network residue, thus taking into account the experimental residual weights of pure POSS and epoxy matrices, and the composition of the systems (see Chapter II).

Concerning the reaction to fire of the networks, the main parameters taken into account and reported in the present study are:

- for the UL 94 test: the times of flaming ( $t_1$  and  $t_2$  in seconds), the residual weight (in percentage of the initial specimen mass), the flame propagation in some cases (in percentage of the initial specimen length), and the releasing of flaming drops (in number of specimens over the total number of tested specimens);

- for the cone calorimeter: the Time To Ignition (TTI, in seconds), the Total Heat Released (THR, in MJ/m<sup>2</sup>), the peak of Heat Release Rate (pHRR, in kW/m<sup>2</sup>), the Total Smoke Released (TSR, m<sup>2</sup>/m<sup>2</sup>), and the Residual Weight (RW in %).

Representative snapshots of the specimen being tested and HRR curves will come as a support for the tables gathering the data of UL 94 and cone calorimeter, respectively. In certain cases, investigation of the char residues from cone calorimeter samples was carried out.

## **2. THERMAL STABILITY AND FIRE BEHAVIOUR OF EPOXY-AMINE NETWORKS: COMPARISON OF THREE NEAT MATRICES**

The profiles of thermal degradation and fire behaviour of the three different epoxy networks under study – namely the DGEBA-, TGDDM- and MVR444-based networks – were assessed in order to provide a reference for the hybrid networks. It was interesting to first compare the neat matrices between themselves.

- Thermal and thermo-oxidative degradations

The same profiles of thermal degradation were obtained for the three types of epoxy networks (Figure IV-1 and Table IV-1). The one-step degradation in nitrogen atmosphere, which was a purely thermal degradation process, occurred slightly earlier for the TGDDM- and MVR444-based networks, close to 330 °C compared to 370 °C for DGEBA-based networks. The neat epoxy networks decomposed through two competing mechanisms, one producing volatiles, the other producing a residue that cumulates throughout the degradation, resulting in a char stable at least until 700 °C and likely to be a carbon-rich aromatic material possibly containing nitrogen. In the case of neat TGDDM-based network, the residue formation was somewhat less unfavourable than volatilisation as compared to the neat DGEBA-based network, as the residue formed from TM was higher than that obtained from DM. The composition of the TGDDM- and the MVR444-based neat networks was close and the slight differences between the two formulations – additional epoxy prepolymer and different crosslinking agents in the MVR444 network – did not cause significant modifications in the degradation paths. Under air atmosphere, a two-step degradation was observed, the first and second step corresponding to the thermal degradation and the oxidization of the product of the first degradation step, respectively. TGDDM- and MVR444-based networks started degrading at lower temperatures, while the second degradation step occurred at higher temperatures than in DGEBA-based networks. In both cases, no residue at 700 °C was obtained, indicating a total oxidization of the products from the thermal degradation.

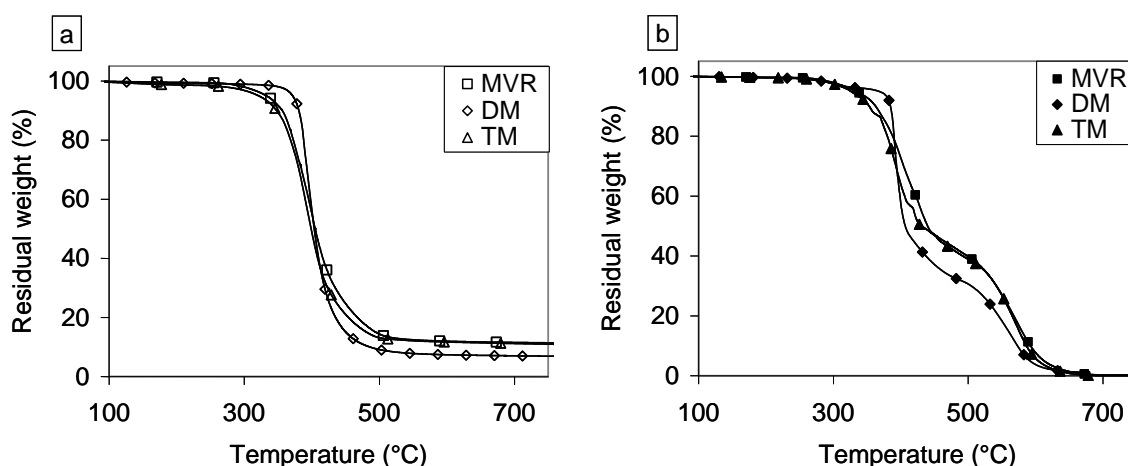


**Figure IV-1 TGA traces of neat epoxy matrices under (a) nitrogen atmosphere or (b) air atmosphere (10K/min)**

	Nitrogen atmosphere			Air atmosphere		
	T <sub>5%</sub> [°C]	T <sub>50%</sub> [°C]	Residual wt. percentage [%]	T <sub>5%</sub> [°C]	T <sub>50%</sub> [°C]	Residual wt. percentage [%]
DM	371	404	6.8	369	404	0.0
TM	323	399	10.8	326	431	0.0
MVR	333	406	14.3	333	440	0.0

**Table IV-1 Characteristic data from TGA analysis of neat epoxy matrices**

While the TGDDM- and MVR444-based matrices yielded more stable chars under inert atmosphere, they started to degrade at lower temperature than the DGEBA-based network. Varley and al. investigated the thermal stability of various epoxy networks – based on DGEBA or TGDDM, and an aromatic isomer mixture of diethyltoluene diamine (DETDA) as the amine crosslinking agent – filled with nanoclays[113]–[115]. As concerns the neat networks, they also reported lower onset temperatures and higher char yields under nitrogen atmosphere for TGDDM-based networks.

- Reaction to fire

From the observation of HRR curves (Figure IV-2), the three types of epoxy neat networks adopted the same kind of fire behaviour. The shape of the HRR curve for neat epoxy matrices, with a shoulder followed by a peak in HRR before the flameout is characteristic for intermediate-thick non-charring samples (see Figure I-10 b in Chapter I), the peak corresponding to the thermal feedback when the pyrolysis zone reached the back of the samples [24].

Hypotheses for the flame retardancy of epoxy networks, based on data obtained from TGA experiments, are often made in the literature. Following this reasoning, one could expect the TGDDM and MVR444 matrices to present a shorter time to ignition (TTI) but a higher residual

char than the DGEBA matrix. This tendency was confirmed for the DM and the TM networks when tested under forced combustion conditions (cone calorimetry), as seen from their HRR curves (Figure IV-2) and cone calorimeter data (Table IV-2). The TTI was shorter of about 10 seconds and the char residue higher of ca. 25% in TM as compared to DM.

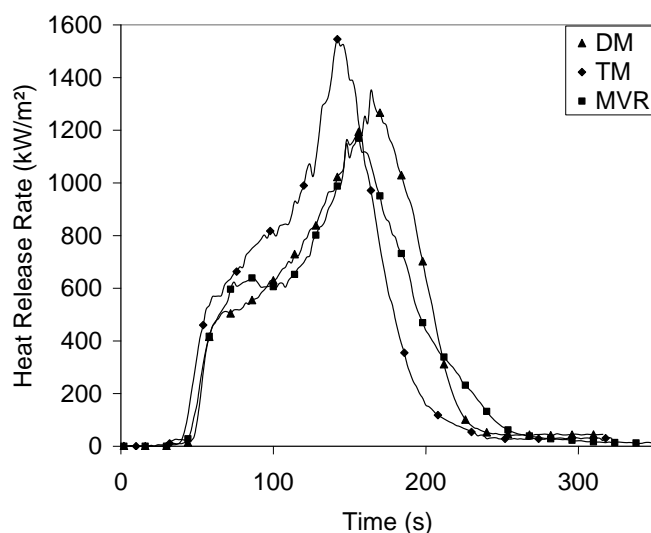


**Figure IV-2 HRR curves of neat epoxy matrices obtained from cone calorimeter experiments (50 kW/m<sup>2</sup>, sample dimensions 100 x 100 x 5 mm)**

System	TTI (s)	THR (MJ/m <sup>2</sup> )	pHRR (kW/m <sup>2</sup> )	TSR (m <sup>2</sup> /m <sup>2</sup> )	RW (%)
DM	54 (2)	127.7 (3.7)	1349 (86)	5695 (156)	9.4 (4.6)
TM	43 (1)	136.8 (7.0)	1535 (184)	6000 (411)	35.5 (0.8)
MVR	45 (3)	121.4 (4.2)	1203 (67)	4813 (258)	5.6 (1.5)

**Table IV-2 Cone calorimeter data of neat epoxy matrices**

However, in the vertical flame ignition scenario (UL 94), the residual weight of the DM network was significantly higher than both the TM and the MVR networks, though for all the matrices the flames reached the clamps and the specimens released flaming drops that were generally able to propagate the fire to the cotton indicator placed below (Figure IV-3 and Table IV-3). One has to note that the UL 94 results presented high standard deviation values, while efforts have been made to keep constant the conditions and parameters during the series of tests. The MVR network yielded the lowest char residue amount in both fire scenarii, though it presented the best performance in terms of pHRR and TSR. The TM matrix presented the most intense pHRR and smoke yield.

Networks	$t_1$ (s)	$t_2$ (s)	Residual weight (%)	Flame propagation (%)	Ignition of cotton via releasing of flaming drops
DM	324 (63)	-	23 (32)	100 (0)	3/6 specimens
TM	267 (32)	-	5 (10)	100 (0)	4/4 specimens
MVR	194 (9)	-	6 (7)	100 (0)	4/4 samples

**Table IV-3 UL 94 features of neat epoxy matrices**

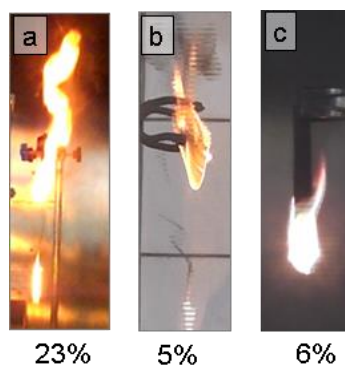


**Figure IV-3 Representative snapshots of UL 94 tests of neat epoxy matrices and their average residual weights after testing: a) DM, b) TM, c) MVR**

As expected, the neat matrices presented a high flammability, confirming the need to find effective solutions for their fire retardancy. The main parameters targeted for a decrease will be the pHRR, which relates to the force of the fire, and the char residue, which gives indications on the structural integrity of the material after a fire. As concerns the UL 94 test, the targeted improvements rely on a self-extinguishment of the sample with reductions of the time of flaming and flame propagation, and no release of flaming drops – or release of non-flaming drops. These parameters are related to the fire propagation. The increase of the residual weight, which is also desired, is more related to the integrity of the polymer under fire conditions.

### **3. THERMAL DEGRADATION AND FIRE BEHAVIOUR OF HYBRID ORGANIC/INORGANIC NETWORKS**

As detailed in Chapter II, the hybrid epoxy networks were produced via the addition of different POSS either by heat solubilisation, high-shear mixing, or heat solubilisation plus the addition of an aluminium-based catalyst. In the networks nomenclature, the process implemented was made explicit by quoting a number corresponding to the temperature of heat solubilisation, or mentioning 'mix' or 'Al' for the high-shear mixing or the catalyst addition processes, respectively. The detailed networks' names and compositions can be found in Table II-2 in Chapter II.

As concerns the morphology of the hybrid networks, the structures developed by the POSS depended on their chemical structure and/or that of the epoxy prepolymer. The iOPOSS formed big aggregates that settled down during curing, both in the DGEBA- and TGDDM-based networks. The AmPOSS achieved a very fine dispersion in the DGEBA-MDEA network, with no visible phase-separated domains from SEM observations. Finally, the POSSOH gave rise to morphologies that were slightly dependent on the dispersion process – the differences being mostly related to the size of the inorganic domains – and much more dependent on the type of epoxy prepolymer the networks were based on. Nodules from a few hundreds of nanometres to a few microns in diameter were observed in the DGEBA-based networks, while intricate structures made of filaments and nodules were discovered in the TGDDM and MVR444-based networks.

### **3.1. NETWORKS CONTAINING POORLY-DISPERSED NON-FUNCTIONAL POSS (iOPOSS)**

- Thermal stability

The residue obtained from the thermal degradation of neat iOPOSS under inert atmosphere (about 6 wt% of initial mass) was much lower than the calculated contribution of the inorganic part of the iOPOSS (39 wt%). The residual weight obtained after heating iOPOSS in oxidative atmosphere (about 44 wt%) was slightly lower than expected, indicating the incomplete oxidative transformation of the initial POSS structure into silica.

Very little changes were observed in the degradation profiles of the iOPOSS-containing epoxy networks as compared to the neat TM and DM matrices. The corresponding TG curves are displayed in Figure IV-4. Under inert atmosphere, the offset degradation temperature ( $T_{5\%}$ ) and the temperature corresponding to a 50% mass loss ( $T_{50\%}$ ) were not modified by the addition of iOPOSS (Table IV-4). The char residues were slightly higher than expected. Under air atmosphere,  $T_{50\%}$  was increased of 20 °C and 40 °C for DM-iOPOSS-205 and TM-iOPOSS-mix, respectively. The effect of iOPOSS was to produce a slightly more stable intermediate char at the end of the first degradation step. This char finally degraded and the second degradation step occurred at the same temperature as in the neat networks. Under air atmosphere, the residues were negligible, indicating an almost complete thermo-oxidation of the POSS-containing networks.

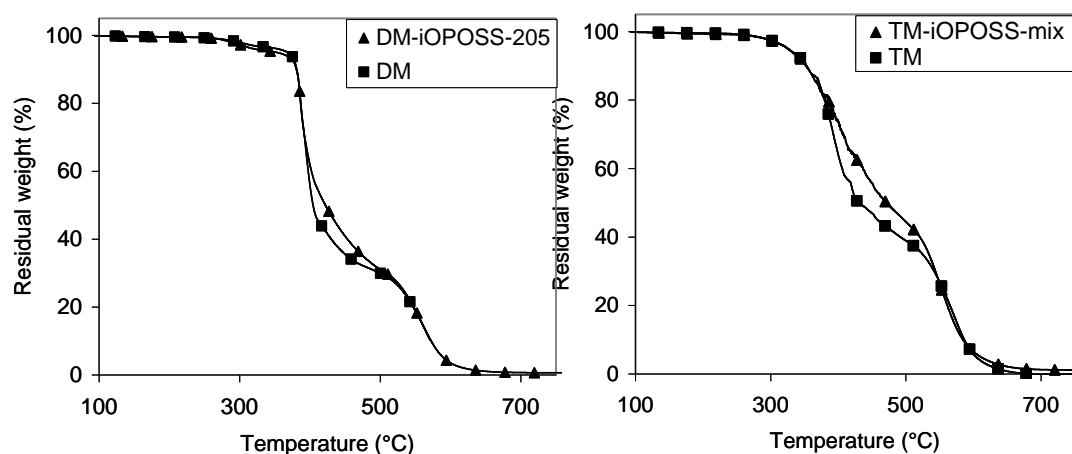


**Figure IV-4 TGA traces of neat matrices and iOPOSS-containing epoxy networks under air atmosphere (10K/min)**

	Nitrogen atmosphere			Air atmosphere		
	T <sub>5%</sub> [°C]	T <sub>50%</sub> [°C]	Residual wt. percentage [%]	T <sub>5%</sub> [°C]	T <sub>50%</sub> [°C]	Residual wt. percentage [%]
iOPOSS	372	422	6.0 (37.0)	364	613	39.0 (44.9)
DM	371	404	6.8	369	404	0.0
DM-iOPOSS-205	377	407	11.1 (6.8)	354	422	0.6 (1.5)
TM	323	399	11.0	326	431	0.0
TM-iOPOSS-mix	326	404	12.3 (10.8)	325	471	1.2 (1.5)

**Table IV-4 Characteristic data from TGA analysis of neat iOPOSS, neat matrices and iOPOSS-containing epoxy networks**

- Fire behaviour

The fire behaviour of the iOPOSS-containing networks was determined through the UL 94 test only, due to the difficulty of producing bigger homogeneous specimens for cone calorimeter experiments. From the UL 94 visual observation (Figure IV-5), it was clear that the iOPOSS decreased spectacularly the flammability of the DGEBA-based network in this vertical small-scale testing configuration. Despite long times of flaming (reported in Table IV-5), the flame was small and its propagation limited. The specimens ended up extinguishing, and after a second ignition the average amount of residue was still as high as 94%, against 23% for the neat DM matrix. This beneficial effect of the POSS could not be predicted by the thermal analysis. Only one specimen over the six tested presented a high flaming behaviour, leading to dripping.

The improvement of the TM matrix via the addition of the iOPOSS was much more limited, with large flaming and dripping. While the specimens self-extinguished, the second ignition led to the

combustion of almost the totality of the sample, the increase in residual weight being only of 30% as compared to the neat TM matrix.

These differences in fire behaviour can be attributed to the chemical composition of the epoxy matrices, more than to the process of dispersion of the POSS – heat solubilisation or high-shear mixing for the DGEBA- or TGDDM-based networks, respectively – which led to similar morphologies. The major segregation of the POSS on the bottom surface of the specimens did not stop the whole DGEBA-based samples to be fire retarded. The macroscopic phase separation could, however, be the reason why one sample behaved differently in this series.

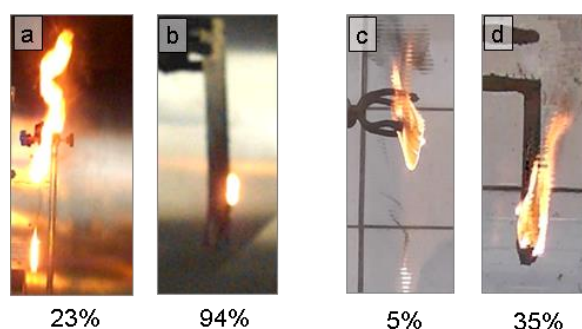


**Figure IV-5 Representative snapshots of UL 94 tests of neat matrices and iOPOSS-containing networks, and their average residual weights after testing: a) DM, b) DM-iOPOSS-205, c) TM, d) TM-iOPOSS-mix**

Networks	$t_1$ (s)	$t_2$ (s)	Residual weight (%)	Ignition of cotton via releasing of flaming drops
DM	324 (63)	-	23 (32)	3/6 specimens
DM-iOPOSS-205	324 (271)	44 (60)	94 (5)	1/6 specimens
TM	267 (32)	-	5 (10)	4/4 specimens
TM-iOPOSS-mix	83 (21)	232 (12)	35 (39)	3/4 specimens

**Table IV-5 UL 94 features of iOPOSS-containing networks and corresponding neat epoxy matrices**

### 3.2. NETWORKS CONTAINING FUNCTIONAL POSS DISPERSED AT A MOLECULAR SCALE (AMPOSS)

- Thermal stability

Data collected from the TGA measurements (Figure IV-6 and Table IV-6) indicated that the neat AmPOSS started degrading at quite low temperature as compared to other neat POSS (340 °C against 364 °C and 482 °C for iOPOSS and POSSOH, respectively), which could be due to the scission of the organic aliphatic bonds of its phenylaminopropyl tethers. The residual char under both inert and air atmospheres were in good agreement with calculated values, indicating that most of the inorganic part was preserved throughout the degradation.

The addition of AmPOSS in the DGEBA-MDEA matrix did not influence the value of the characteristic degradation temperatures of the hybrid network under inert atmosphere, but caused the polymer to yield higher amount of residue than expected (ca. 15% against ca. 8%). Under air atmosphere, the offset degradation temperature was decreased of about 30 °C while the  $T_{50\%}$  increased of ca.30 °C as compared to DM. Indeed, as described earlier for the iOPOSS-containing networks, the intermediate char stability was improved (Figure IV-6).

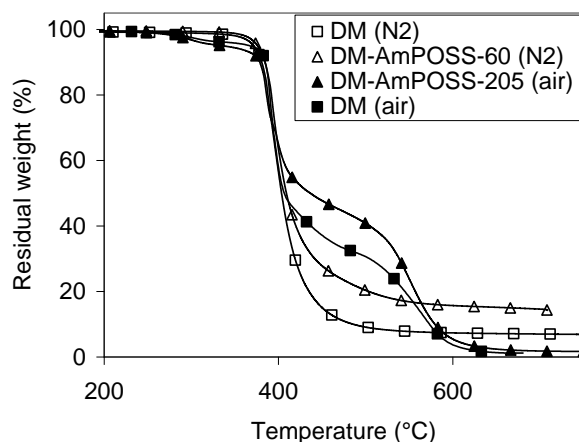


**Figure IV-6 TGA traces of the DGEBA-based matrix and AmPOSS-containing epoxy network under air and nitrogen atmospheres (10K/min)**

	Nitrogen atmosphere			Air atmosphere		
	$T_{5\%}$ [°C]	$T_{50\%}$ [°C]	Residual percentage [%]	$T_{5\%}$ [°C]	$T_{50\%}$ [°C]	Residual percentage [%]
AmPOSS	408	472	26.0 (27.9)	340	456	31.0 (32.1)
DM	371	404	6.8	369	404	0.0
DM-AmPOSS-60	376	409	14.7 (7.8)	337	436	1.7 (1.6)

**Table IV-6 Characteristic data from TGA analysis of neat AmPOSS, DGEBA-based matrix and AmPOSS-containing DGEBA-based network**

- Fire behaviour

The fire behaviour of the AmPOSS-containing network was assessed in the UL 94 vertical configuration. From the visual observation of the test, it was already obvious that no improvement was brought by the addition of AmPOSS in the DM network (Figure IV-7). Indeed, from data collected in Table IV-7, it could be seen that the AmPOSS-60 specimens burnt faster and yielded the same average amount of residue as DM.

Though, as highlighted in Chapter I, correlation between the UL 94 test and the cone calorimeter is generally difficult, the obvious absence of improvement in the vertical configuration could not lead to any significant improvement in the cone configuration – i.e. the

hypothesis was made that the intrinsic flammability of this network, being very high, predominated over the test parameters.

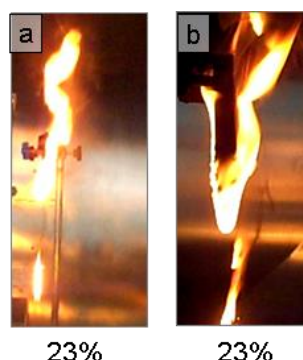


**Figure IV-7 Representative snapshots of UL 94 tests of neat DGEBA-based matrix and AmPOSS-containing network, and their average residual weights after testing: a) DM, b) DM-AmPOSS-60**

Networks	$t_1$ (s)	Residual weight (%)	Ignition of cotton via releasing of flaming drops
DM	324 (63)	23 (32)	3/6
DM-AmPOSS-60	288 (74)	23 (24)	4/5

**Table IV-7 UL 94 features of AmPOSS-containing network and corresponding neat epoxy matrix**

Therefore, no fire-retardant effect of this POSS was observed, while the elements supposed to decrease the flammability of the network – inorganic part, phenyl-containing tethers – were present, as in the iOPOSS-containing DGEBA-based network – presented in the previous section. What varied between these two networks was the chemical structure of the POSS – an alkyl chain separated the silica cage from the phenyl in the tethers, which contained nitrogen atoms – and the morphology of the networks – the AmPOSS was dispersed at molecular scale due to its reaction with the epoxy prepolymer during the polymerization.

As highlighted previously, the alkyl chain of the POSS could break early in the fire scenario, leading to the destruction of crosslinking points, the decrease in viscosity of the network – causing dripping – and the production of volatiles. It would mean that this was predominant as compared to the expected physical fire-retardant effect of the silica and phenyl features of the POSS. Comparison with AminoPhenyl POSS (Figure IV-8) in a DGEBA/*m*-phenylene diamine (mPDA) network revealed that, in absence of the alkyl chain in the POSS tethers, the network with 4.6 wt% POSS – i.e. 1.66 inorganic wt%, against 1.5 wt% in the present work – presented a limited improvement in the UL 94 configuration: no self-extinguishment was observed, but the specimens did not drip [71]. That could be an element to confirm the effect of the breakage of the alkyl chain on the viscosity of the degraded polymer.

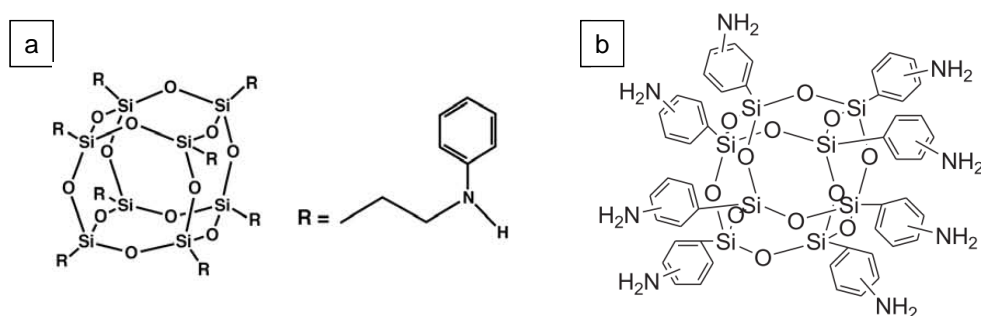


**Figure IV-8 Chemical structure of a) N-phenylaminopropyl POSS (AmPOSS) and and b) aminophenyl POSS**

As for the influence of the POSS dispersion in the DM matrix, while it is generally accepted that the finer the dispersion, the greater the improvement of a wide range of properties – including fire retardancy – the molecular dispersion, given the small amount of POSS, could be detrimental through a simple physical effect of ‘dilution’, thus rendering the POSS inefficient.

### 3.3. THE PARTICULAR CASE OF POSSOH: DEGRADATION AND FIRE BEHAVIOUR OF EPOXY NETWORKS OF DIFFERENT NATURES

#### 3.3.a. Influence of the dispersion process

- Thermal stability

The POSSOH presented a thermal stability much superior to that of the other POSS (Table IV-8). The onset of degradation temperature was close to 500 °C both under inert and air atmosphere. The residue obtained from the thermal degradation of pure POSSOH under inert atmosphere (about 76 wt.% of initial mass) was larger than the calculated contribution of the inorganic part of the POSSOH (35 wt.%). This higher residual weight was likely to arise from the entrapment of carbon in the structure, resulting from phenyl group condensation [116]. On the other hand, the residual weight obtained after heating POSSOH in oxidative atmosphere (about 44 wt.%) was in agreement with the theoretical contribution of silica production arising from the oxidative transformation of the initial POSSOH structure.

TGA curves corresponding to DGEBA-based networks under inert and air atmosphere are displayed in Figure IV-9. The TGDDM-based networks presented similar profiles of degradation. Despite the late degradation of neat POSSOH, no effect resulting from its addition in the epoxy networks was observed on the temperature of degradation under nitrogen or air atmosphere (Table IV-8). Under air atmosphere, the residues of hybrid networks at the end of the first degradation step were greater of up to 10 wt% compared to the ones of the epoxy matrices, which revealed a better oxidative thermal stability conferred by the POSSOH to the networks

until about 500 °C. The effect of POSSOH on the final residues was mainly additional; the values of the theoretical residual weights were generally in good agreement with the experimental values, the TGDDM-based networks yielding slightly lower amount of residue than expected.

Limited changes were thus observed in the networks containing POSSOH as compared to the neat matrices. Based on the thermal analysis of these networks, no improvement should be expected as concerns their fire behaviour.

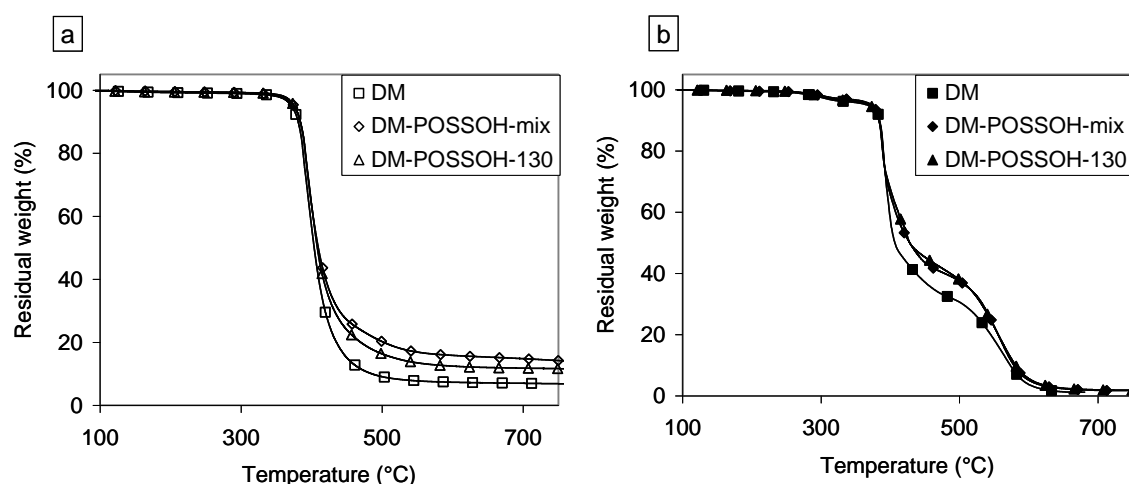


**Figure IV-9 TGA traces of DGEBA-based matrix and POSSOH-containing epoxy networks under nitrogen (a) and air (b) atmospheres (10K/min)**

	Nitrogen atmosphere			Air atmosphere		
	T <sub>5%</sub> [°C]	T <sub>50%</sub> [°C]	Residual percentage [%]	T <sub>5%</sub> [°C]	T <sub>50%</sub> [°C]	Residual percentage [%]
POSSOH	483	-	75.6 (36.6)	482	656	44.1 (45.2)
DM	371	404	6.8	369	404	0.0
DM-POSSOH-mix	375	409	13.9 (10.0)	373	428	1.7 (1.9)
DM-POSSOH-130	375	408	11.6 (10.0)	368	428	1.9 (1.9)
TM	323	399	10.8	326	431	0.0
TM-POSSOH-mix	326	405	12.90 (13.9)	322	474	1.39 (1.9)
TM-POSSOH-130	332	407	11.90 (13.9)	329	473	1.64 (1.9)

**Table IV-8 Characteristic data from TGA analysis of neat POSSOH, neat matrices and POSSOH-containing networks**

- Fire behaviour

The fire behaviour of the networks containing POSSOH dispersed via either high-shear mixing or heat solubilisation was assessed in the UL 94 vertical configuration (Figure IV-10 and Table IV-9). In the DGEBA-based networks, the effect brought by the addition of POSSOH was

obvious. Flame propagation was limited, leading to high amounts of residue and no dripping was observed in most of the samples. The specimens self-extinguished, though the times of flaming were too long for the networks to reach a V-classification. The specimens in which POSSOH was introduced through solubilisation gave better results in terms of residual weight and times of flaming as compared to the specimens where POSSOH was dispersed by high-shear mixing. These large improvements in fire behaviour were not observed in the TGDDM-based networks, where the flame was high and the amounts of residue hardly increased as compared to the neat TGDDM matrix, particularly for the TM-POSSOH-130 network. The TM-POSSOH-mix presented mixed results, with a self-extinguishment but a large flame propagation and flame dripping of half of the specimens tested.

The POSSOH proved to be a good fire retardant solution for the DGEBA-based network in the vertical configuration. The process consisting of heat solubilisation of POSSOH gave better results, though the morphology developed was not very different as compared to the network where POSSOH was introduced by high-shear mixing, the POSS nodules being only slightly smaller in the latter. However, the POSSOH by itself cannot be selected as a 'universal' fire retardant for epoxies in general, as shown by the still high flammability of the TGDDM-based specimens. Two main parameters varied between the DGEBA- and the TGDDM-based networks: (i) the chemical composition of the matrix and its intrinsic flammability, (ii) the morphology and the dispersion of the POSSOH domains, and possibly the interactions they were able to create between them and/or the epoxy matrix. It was however delicate to conclude on the respective part of contribution of these parameters on the differences of fire performance observed between the two types of epoxy networks.

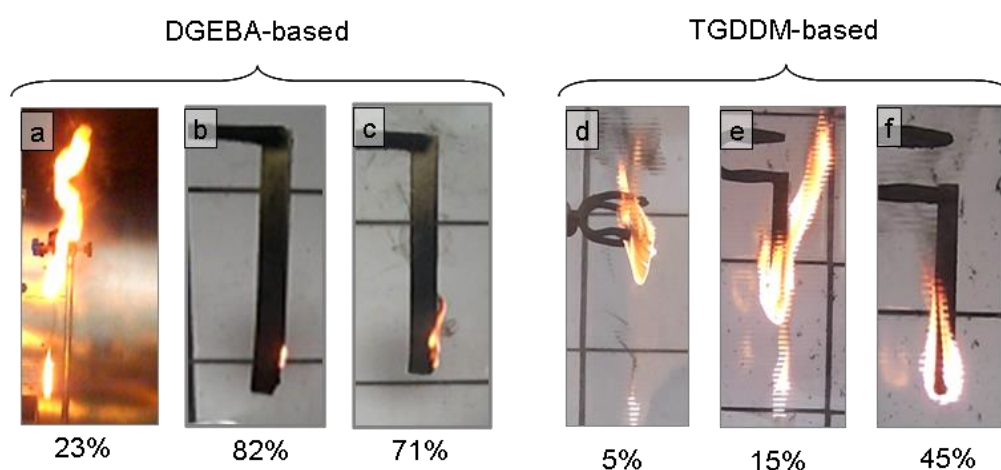


**Figure IV-10 Representative snapshots of UL 94 tests and average residual weights after testing of a) DM, b) DM-POSSOH-130, c) DM-POSSOH-mix, d) TM, e) TM-POSSOH-130, f) TM-POSSOH-mix**

Networks	t <sub>1</sub> (s)	t <sub>2</sub> (s)	Residual weight (%)	Flame propagation (%)	Ignition of cotton via releasing of flaming drops
DM	324 (63)	-	23 (32)	100 (0)	3/6 specimens
DM-POSSOH-mix	146 (145)	74 (108)	71 (42)	52 (35)	1/6 specimens
DM-POSSOH-130	130 (114)	34 (48)	82 (35)	-	1/6 specimens
TM	267(32)	-	5 (10)	100 (0)	4/4 specimens
TM-POSSOH-mix	139 (100)	55 (106)	45 (50)	72 (34)	3/6 specimens
TM-POSSOH-130	234 (21)	-	15 (30)	100 (0)	4/4 specimens

**Table IV-9 UL 94 features of POSSOH-containing networks and corresponding neat epoxy matrices**

### **3.3.b. Influence of the addition of an aluminium-containing catalyst – effect of the nature of the epoxy matrix**

In this section, results of networks based on the model systems, i.e. made from the DGEBA or the TGDDM prepolymer, but also of the epoxy networks based on the commercial MVR444 formulation, will be reported. The networks in which both the POSSOH and the aluminium acetate catalyst were introduced were compared with the reference networks and the ones in which the POSSOH was dispersed via heat solubilisation. The combined presence of the POSSOH and the Al-based catalyst was already shown to significantly modify the kinetics and the reaction mechanisms involved in the epoxy-amine network build-up. Closer investigation of the cone calorimeter chars will be presented in a last part.

- Thermal stability

The addition of the Al-based catalyst to the POSSOH-containing networks did not bring many changes to the thermal degradation profiles. As an example, the TG curves of the DGEBA-based networks – for which the changes are the largest – are displayed in Figure IV-11. For the TGDDM- and MVR-based networks, the degradation profiles were the same as that of the corresponding neat matrices, with only a slightly more stable intermediate char – after the first degradation step – under air atmosphere.

The most significant change in thermal stability was an earlier offset of degradation regarding the DM-POSSOH-Al network through a small mass loss step that was not observed in the DGEBA-based matrix, indicating a different degradation mechanism. Amounts of residue yielded by the networks containing both POSSOH and the Al-based catalyst were systematically higher than expected and higher than that of other epoxy networks (Table IV-10).

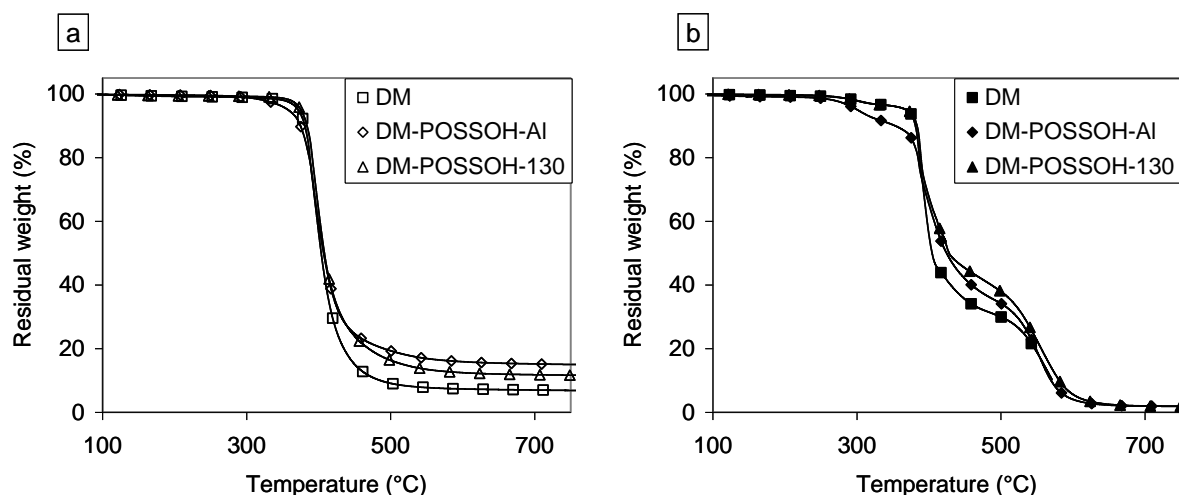


Figure IV-11 TGA traces of DGEBA-based matrix and POSSOH-containing epoxy networks under nitrogen (a) and air (b) atmospheres (10K/min)

	Nitrogen atmosphere			Air atmosphere		
	T <sub>5%</sub> [°C]	T <sub>50%</sub> [°C]	Residual percentage [%]	T <sub>5%</sub> [°C]	T <sub>50%</sub> [°C]	Residual percentage [%]
POSSOH	227	-	75.5 (36.6)	482	656	44.0 (45.2)
DM	371	404	6.8	369	404	0
DM-POSSOH-130	375	408	11.6 (10.0)	368	428	1.9 (1.9)
DM-POSSOH-AI	358	407	14.9 (10.0)	301	425	2.0 (1.9)
TM	323	399	10.8	326	431	0.0
TM-POSSOH-130	332	407	11.9 (13.9)	329	473	1.6 (1.9)
TM-POSSOH-AI	328	406	13.7 (13.9)	320	472	1.9 (1.9)
MVR	333	406	11.5	333	440	0.2
MVR-POSSOH-130	332	413	12.7 (12.5)	327	456	2.0
MVR-POSSOH-AI	324	413	14.3 (12.5)	322	474	2.1

Table IV-10 Characteristic data from TGA analysis of neat POSSOH, neat matrices and POSSOH-containing networks

- Fire behaviour

UL-94 results are displayed in Figure IV-12 and Table IV-11. Introducing POSSOH in combination with the aluminium-based catalyst gave a marked improvement in fire behaviour of the DGEBA- and TGDDM-based networks, as compared to the corresponding neat matrices. The flame spread remained limited and the propagation slow. Not only a fast extinguishment of the flame was reported –  $t_1$  and  $t_2$  were greatly reduced – with no flaming drops being released, but also the residual weight at the end of the test was dramatically increased, especially in the case of the TGDDM-based networks with a rise from 5 to 96%. It is also interesting to note that

these systems showed a particularly stable fire behaviour, with standard deviation values of residual weight and times of flaming greatly decreased compared to other systems. In the particular case of the TM-POSSOH-AI network, a swelling phenomenon with a strong deformation of the sample surface was observed. In the MVR-based network containing both POSSOH and the Al-based catalyst, this swelling effect was also observed but the improvements were much more limited, with an average residual weight of 44% only, releasing of flaming drops and almost total spread of the flame along the specimens.

On the other side, results of UL-94 concerning the networks containing POSSOH only were variable. As highlighted in the previous section, a good improvement was observed in the DGEBA-based system, with results close to those obtained for DM-POSSOH-AI, while POSSOH brought no significant changes in fire behaviour when introduced alone in the TGDDM- or the MVR444-based networks.

A network was also made from the DGEBA-MDEA formulation, in which only the Al-based catalyst was added. This network was subjected to the UL 94 test (Figure IV-12 b.), the aim being to determine whether the catalyst alone could bring significant improvements of the fire behaviour. The test revealed that the DM-AI network actually behaved similarly to the neat DGEBA-MDEA matrix – no self-extinguishment, low residual weight and high flame propagation. This simple verification highlighted the synergistic effect of POSSOH and the Al-based compound in the ‘complete’ network.

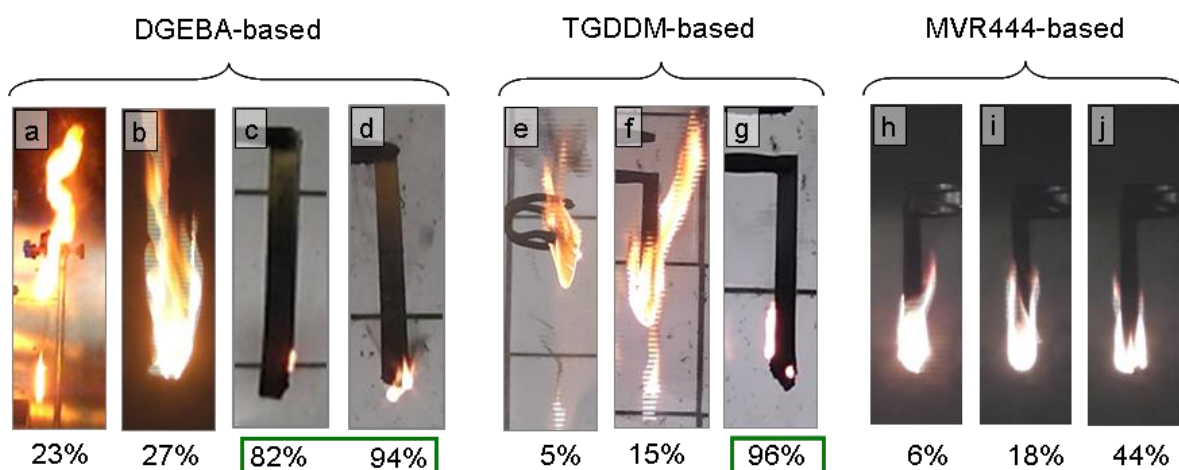


**Figure IV-12 Representative snapshots of UL 94 tests and average residual weights after testing of a) DM, b) DM-AI, c) DM-POSSOH-130, d) DM-POSSOH-AI, e) TM, f) TM-POSSOH-130, g) TM-POSSOH-AI, h) MVR, i) MVR -POSSOH-130, j) MVR -POSSOH-AI**

Networks	t <sub>1</sub> (s)	t <sub>2</sub> (s)	Residual weight (%)	Flame propagation (%)	Ignition of cotton via releasing of flaming drops
DM	324 (63)		23 (32)	100 (0)	3/6 specimens
DM- POSSOH-130	130 (114)	34 (48)	82 (35)	-	1/6 specimens
DM- POSSOH-AI	100 (22)	45 (38)	94 (2)	15 (10)	0/6 specimens
DM-AI	229 (23)	-	27 (21)	90 (11)	4/4 specimens
TM	267 (32)	-	5 (10)	100 (0)	4/4 specimens
TM-POSSOH-130	234 (21)	-	15 (30)	100 (0)	4/4 specimens
TM-POSSOH-AI	33 (14)	13 (1)	96 (4)	12 (4)	0/4 specimens
MVR	194 (9)	-	6 (7)	100 (0)	4/4 samples
MVR-POSSOH-130	186 (13)	-	18 (12)	100 (0)	4/4 samples
MVR-POSSOH-AI	145 (20)	-	44 (33)	98 (4)	4/4 samples

**Table IV-11 UL 94 features of POSSOH-containing networks and the corresponding neat epoxy matrices**

Results from cone calorimeter are reported in Table IV-12 and HRR curves are shown in Figure IV-13. In the case of DGEBA-based materials, the TTI was slightly reduced by the simultaneous addition of POSSOH and Al-based catalyst. The ignition of a material (thickness being kept constant) in the cone calorimeter set-up depends on the concentration of volatiles at the surface, which are the degradation products coming from the material itself. The process of degradation in the cone calorimeter is anaerobic [28]. Granted that the temperature at the surface is related to the time at the beginning of the test for a given thermosetting polymer, the TTI reduction for DM-POSSOH-AI was in good agreement with the tendency observed by thermal analysis under nitrogen, where the offset of degradation of this particular network was slightly shifted to a lower temperature. The shape of HRR curves of hybrid DGEBA-based networks was not clearly modified as compared to neat DGEBA-based epoxy. In both cases the peak of HRR was reduced – 10% and 16% for the DM-POSSOH-130 and the DM-POSSOH-AI networks, respectively – but the reduction lied roughly within the experimental errors for cone calorimeter testing. The Total Heat Released (THR), which is the area under the HRR curve, reflects the size of a fire. The POSSOH when introduced alone in DGEBA-based networks was responsible for a slight decrease of the THR, while in presence of Al catalyst the THR was faintly increased compared to the epoxy matrix. However, the variations were roughly within the standard deviation limits. The presence of POSSOH alone seemed to be sufficient to increase the residual weight, which was then further increased by the presence of Al-based catalyst. The char residues of both networks were quite similar (33 - 36 wt%).

The TTI in TGDDM-based networks was hardly influenced by the presence of POSSOH and/or aluminium acetate catalyst. The same tendencies as in DGEBA-based networks were observed, i.e. the pHRR was reduced by the addition of POSSOH and even more in aluminium acetate catalyst-containing network. Small variations in the range of standard deviations were obtained for the THR parameter. The reduction of pHRR in the TM-POSSOH-130 network was almost equal to that observed for the TM-POSSOH-AI network, which was unexpected when considering the high flammability of this material in the vertical UL 94 configuration. However, the reduction of the residual weight with the addition of POSSOH only in the TGDDM-based matrix was more in agreement with the UL 94 tendency.

MVR444-based networks gave unexpected results, considering their TG and the UL-94 results. No change in TTI was observed with the addition of POSSOH, but the combined presence of POSSOH and the Al-based catalyst did cause the pHRR to decrease dramatically – minus 54% as compared to the neat MVR network – and the residual weight to increase from about 6% to close to 18%. The THR was also decreased of about 25%. The pHRR decrease could be explained by a total change of the profile of HRR of the MVR-POSSOH-AI network (Figure IV-13 c.). The HRR curve did not present any clear peak after the increase of HRR due to the ignition, but rather consisted in a progressive decrease until the extinction of the specimens. This shape is characteristic for intumescent materials [24]: the protective char they produce when burning protects the underlying material for further degradation, thus decreasing the heat released. On the contrary, the MVR-based network containing POSSOH only presented a worsening of most of the quantified parameters.

System	TTI (s)	THR (MJ/m <sup>2</sup> )	pHRR (kW/m <sup>2</sup> )	TSR (m <sup>2</sup> /m <sup>2</sup> )	RW (%)
DM	54 (2)	127.7 (3.7)	1349 (86)	5695 (156)	9.4 (4.6)
DM- POSSOH-130	53 (2)	119.4 (10.8)	1224 (161)	6313 (259)	33.6 (1.6)
DM- POSSOH-AI	47 (1)	137.0 (5.1)	1129 (78)	6530 (254)	36.7 (2.8)
TM	43 (1)	136.8 (7.0)	1535 (184)	6000 (411)	35.5 (0.8)
TM-POSSOH-130	45 (2)	125.5 (6.5)	1221 (74)	5536 (259)	12.0 (1.5)
TM- POSSOH-AI	46 (2)	141.5 (3.6)	1061 (106)	5089 (142)	51.4 (13.9)
MVR	45 (3)	121.4 (4.2)	1203 (67)	4813 (258)	5.6 (1.5)
MVR - POSSOH-130	46 (1)	137.7 (10.7)	1400 (357)	5176 (377)	8.4 (1.2)
MVR - POSSOH-AI	45 (3)	90.9 (2.8)	551 (48)	3169 (88)	17.8 (5.2)

**Table IV-12 Cone calorimeter data of POSSOH-containing networks and the corresponding neat epoxy matrices**

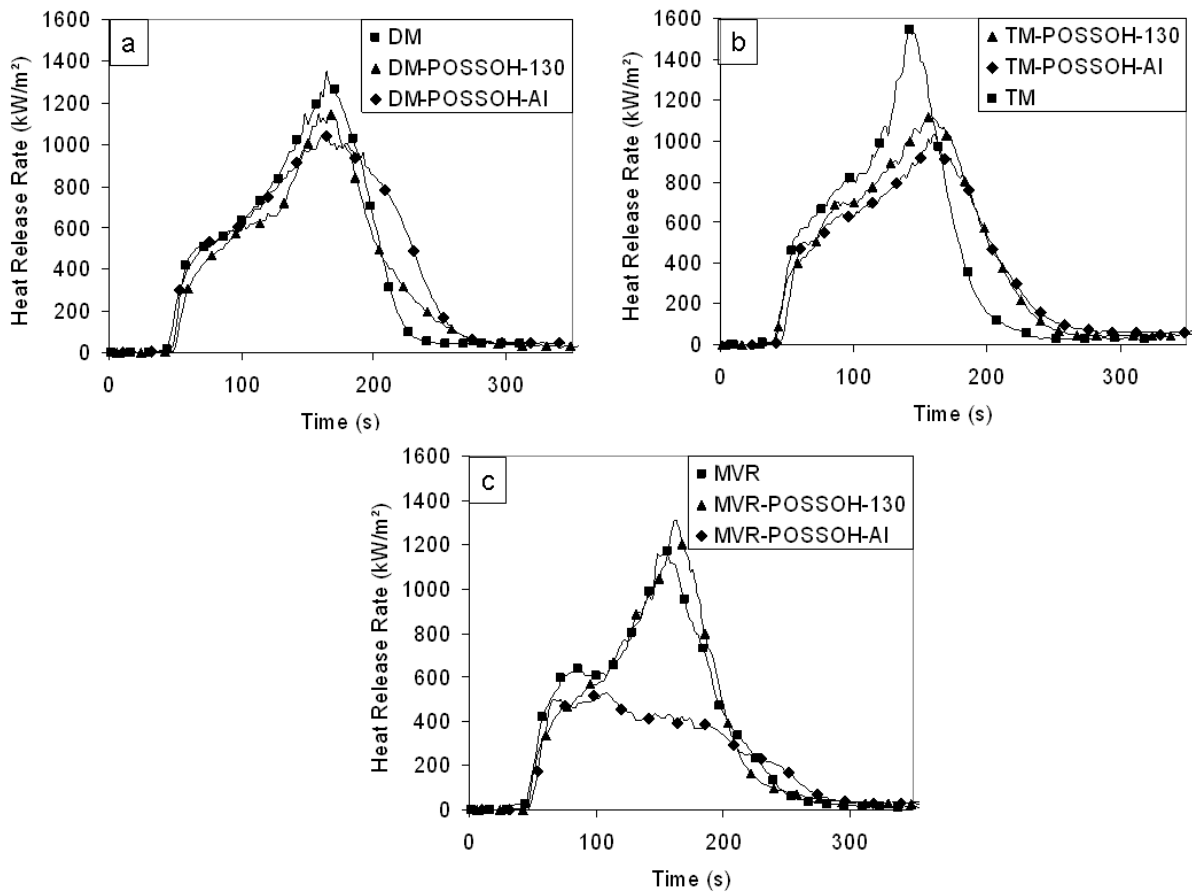


**Figure IV-13 Cone calorimeter HRR curves of a) DGEBA-based networks, b) TGDDM-based networks and c) MVR-based networks**

- Fire retardant mechanism: investigation of char residues

Pictures of char residues obtained after the cone calorimeter experiments are shown in Figure IV-14. As expected from the values of residual weight, the neat epoxy matrices left a small and uncohesive char (Figure IV-14, pictures a), d) and g) on the left). The addition of POSSOH together with the Al-based catalyst in the systems was the most efficient combination in order to obtain a greater and more cohesive char residue. In particular, the TM-POSSOH-Al and MVR-POSSOH-Al samples presented an intumescent behaviour, which caused the char surface to come into contact with the cone electrical resistance and some of the material to fall from the sample holder. The measured residual percentages of 51% and 18%, respectively, were thus underestimated. Although the picture corresponding to TM-POSSOH-130 (Figure IV-14 e.) seemed to display a rather significant char, it was actually a light, flimsy cluster of ashes. In the DGEBA-based networks, the char structures were roughly the same, no intumescent effect being observed with the specimens containing both POSSOH and the Al-based catalyst.

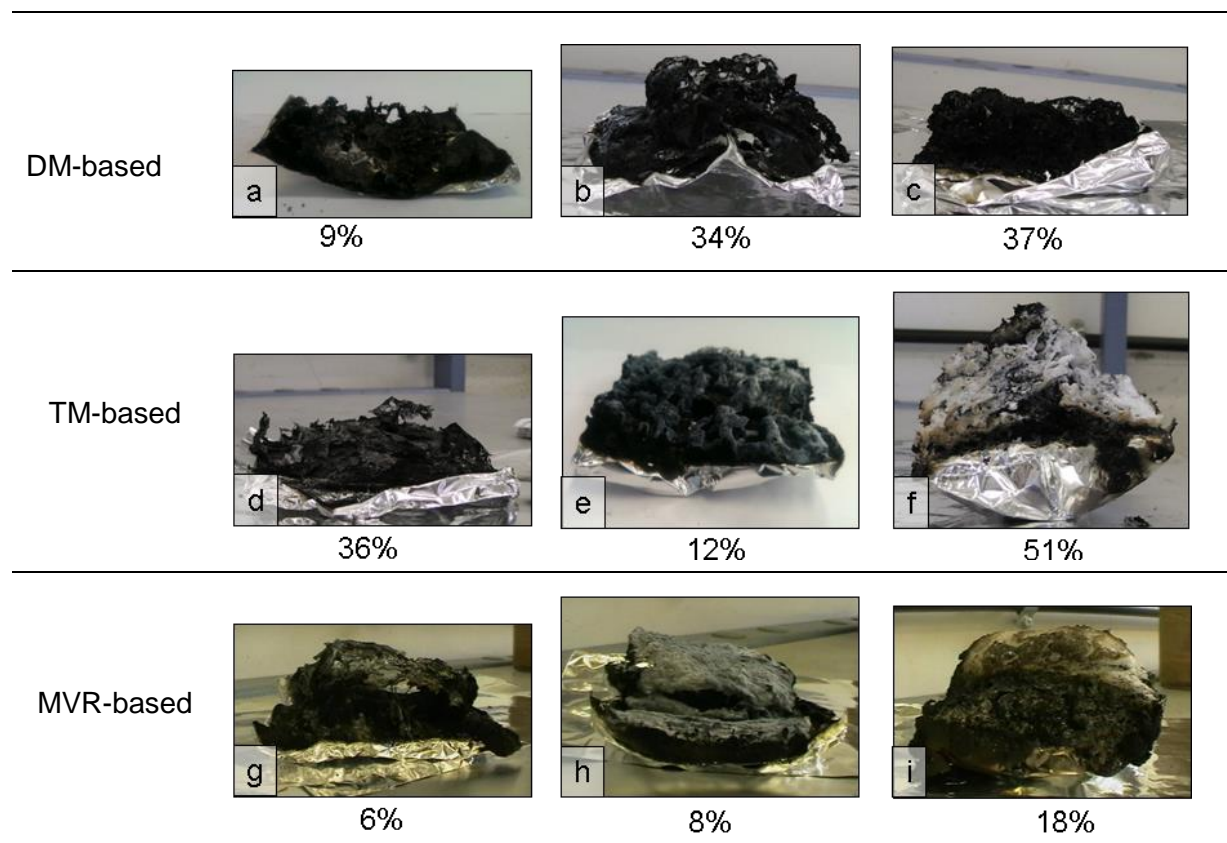


**Figure IV-14 Cone calorimeter residue of a) DM, b) DM-POSSOH-130, c) DM-POSSOH-AI, d) TM, e) TM-POSSOH-130, f) TM-POSSOH-AI, g) MVR, h) MVR-POSSOH-130, i) MVR-POSSOH-AI**

Thus, the addition of POSSOH without or with aluminium acetylacetonate had a different influence on the fire behaviour of the networks, depending on the epoxy-amine formulation they were based on. Though the MVR-based networks were not efficiently fire-retarded in the vertical rectangular-specimen configuration, their fire behaviour was similar to that of the TGDDM-based networks, with the occurrence of intumescence and a poor fire-retardant effect brought by the addition of POSSOH alone. On the contrary, the DGEBA-based networks presented significant improvement of their fire behaviour in the UL 94 configuration even without adding the AI-based catalyst.

Two main different parameters could be identified in the networks that could account for a difference in the combustion mechanisms of the materials:

- The resin formulation: despite some differences in the formulation components, the TGDDM- and MVR444-based materials were mainly based on the same epoxy TGDDM prepolymer and close amine hardeners. Instead, the chemical composition (no N atoms) and functionality of the DGEBA prepolymer were different, leading to distinct network architectures.
- The organisation of POSSOH within the networks: once again, the MVR444- and TGDDM-based networks could be classified together as they presented similar morphologies – a combination of threads and nodules of POSSOH – whereas in the DGEBA-based networks, the POSSOH organised in nodules only.

The finer dispersion of the POSSOH in the DM-POSSOH-AI network could account for this improvement. However, a chemical effect of the aluminium, even at such a low concentration (about 0.09% of aluminium element) is to be taken into account, especially in the TGDDM-based networks where the morphologies in both POSS-modified networks seemed quite similar according to the TEM observations, while the fire behaviours revealed huge differences. The effect of metal-functionalised POSS, in particular with aluminium, was studied by Fina et al. in [117], showing a beneficial effect of the POSS/aluminium combination. However, the study was carried on a polypropylene matrix, at higher contents of POSS and aluminium – i.e. in a significantly different system as the ones under study in the present work. In particular, in propylene systems, fire retardancy cannot be achieved through the graphitisation (formation of aromatic arrays) of the matrix as a result of its aliphatic structure. This would lead to significantly differences as compared to epoxy-based systems, in terms of composition, morphology and thus rheological behaviour of the char during combustion.

The residues from the cone calorimeter experiments of the model epoxy-amine networks – i.e. based on DGEBA or TGDDM – were observed by SEM. Pictures of the char surface are shown in Figure IV-15. The char of the neat epoxy matrices were made of a porous brittle crust. The addition of POSSOH seemed to produce a crust at the surface of the chars with pores of smaller diameter than observed in the neat matrices chars. Bourbigot et al. [118] reported the same effect of POSS on char residues, though they highlighted a certain brittleness of the surface crust, which could also be observed in the present materials. This brittleness could explain the relative reduction of the pHRR because the layer thus formed could not totally fulfil its role of protective barrier towards the underlying material until the end of the test. The char surface of DM-POSSOH-AI seemed further cohesive, with thin cracks instead of circular pores.

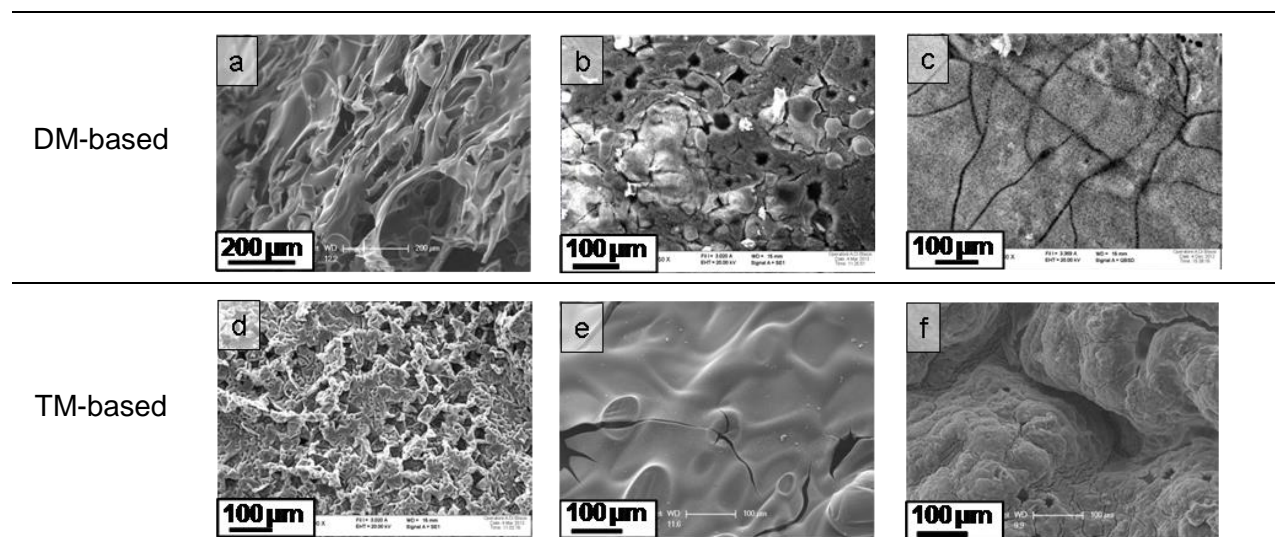


**Figure IV-15 SEM micrographs of cone calorimeter residues a) DM ; b) DM-POSSOH-130 ; c) DM-POSSOH-AI ; d) TM ; e) TM-POSSOH-130 ; f) TM-POSSOH-AI**

The particular cases of TM-POSSOH-AI and MVR-POSSOH-AI, which produced a highly-swollen char, were further investigated by SEM. In Figure IV-16, micrographs of an internal part of the chars are shown. Both residues consisted of well-defined alveolus of a few hundred microns, which walls were made of a thin brittle film. This sponge-like structure certainly contributed in trapping volatiles and thermally insulating the polymer from the flame during the combustion process, enhancing the fire resistance of the structure.

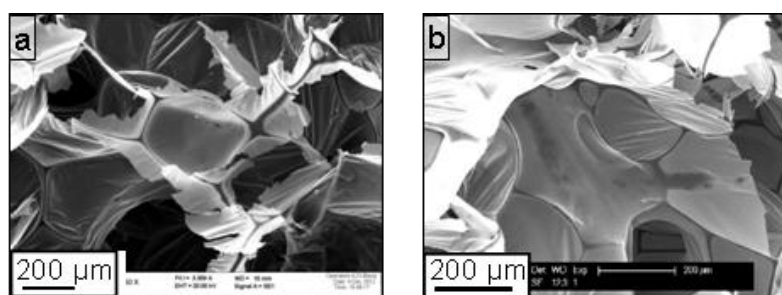


**Figure IV-16 SEM observations of the cone calorimeter residues (intern parts) of a) TM-POSSOH-AI and b) MVR-POSSOH-AI**

Finally, EDX analysis was carried out on the residue of TM-POSSOH-AI (Figure IV-17). Two parts of the samples were analysed: one on the top of the residue, the other inside the residue. The elements found in the residue were principally carbon, oxygen, and silicon, with traces of aluminium, thus corresponding to the composition of a carbonaceous layer containing residues of POSS. It was observed that the concentration of silicon and oxygen was higher at the surface of the residue than inside, where the carbon dominates. This could reveal an accumulation of the POSS towards the surface of the sample during the combustion, leading to a carbonaceous char containing silica or silicon carbide in a greater proportion than inside the sample. The

presence of silica might enforce the char layer at the surface. The structure of the char surface, a crackled crust, seemed more cohesive than inside where the spongy structure made of alveolus of about 500  $\mu\text{m}$  in diameter had formed.

It was also noted the presence of white spherical domains at the surface and inside the char residue. While inside the residue the proportion of elements did not seem to vary, the white spot at the surface contained a higher proportion of oxygen and less carbon for the same proportion of silicon, as compared to its surroundings (Spectrum 1 in Figure IV-17). This could highlight the presence of a higher percentage of silica at this precise point, the silicon being associated to more oxygen than in the surroundings of this domain where it was dispersed in carbon, probably as silicon carbide. This white domain could have been a POSS site before combustion.

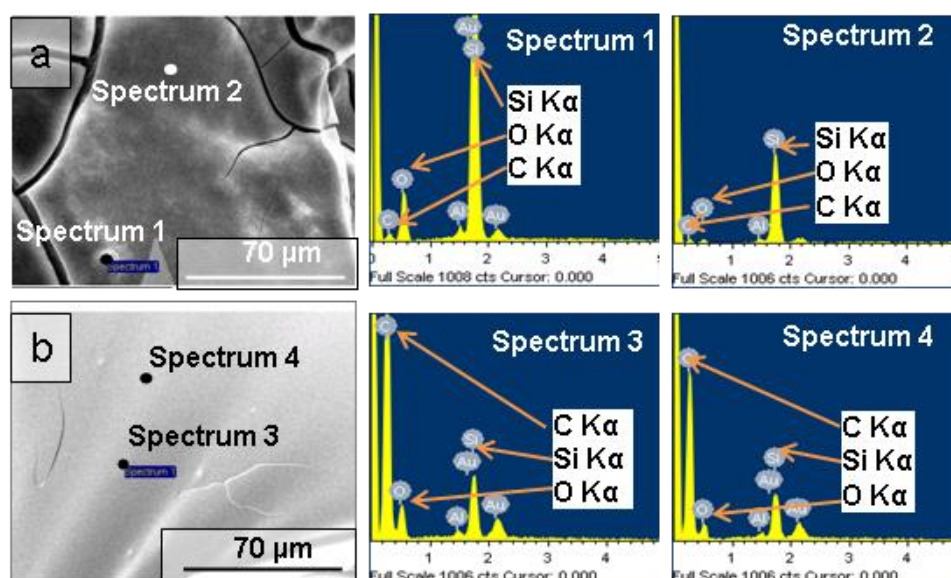


Figure IV-17 SEM pictures and associated EDX spectrum of TM-POSSOH-Al residue; a) surface, b) internal part

#### 4. CONCLUSION

The thermal stability and the fire behaviour of the epoxy-amine networks were assessed by TGA, and through the UL 94 test and the cone calorimeter, respectively. The present study highlighted the influence of the POSS structure on the fire behaviour of the networks they were included in. The POSS bearing phenyl groups have been identified as a generally good fire retardant solution for epoxy materials. As various parameters varied in the systems – POSS and epoxy chemical nature, dispersion of the POSS - the differences in fire behaviour that were observed were complex to interpret and correlate with one or the other parameter. For example, the iOPOSS, with a very low-quality dispersion, was able to fire-retard the DGEBA-based

matrix, while the AmPOSS, molecularly dispersed, brought no improvement in terms of fire retardancy (as assessed via the UL 94 test). In this case, the differences in structure of the POSS had to be taken into account as well.

The more complete study of the POSSOH-containing networks allowed to investigate the influence of other parameters, such as the process of dispersion, the addition of a catalyst – and indirectly the nature of the epoxy-amine network. The influence of the dispersion process – high-shear mixing or heat solubilisation – on the fire behaviour of the epoxy-amine materials was limited. On the contrary, the addition of the Al-based catalyst in combination with POSSOH greatly improved the fire behaviour in the three types of epoxy networks. The introduction of POSSOH alone in the networks was beneficial in the case of the DGEBA-based network only. This led to the conclusion that the efficiency of the POSSOH introduced alone depended on the epoxy resin type, probably due to different developed combustion mechanisms.

The identified mechanism of flame retardancy in the TGDDM- and MVR444-based networks containing both the POSSOH and the Aluminium acetate catalyst was a physical effect of intumescence. However, it is still unclear which role the Al-based catalyst or the morphology developed within this network played in the occurrence of such a mechanism. Also, the combined presence of POSSOH and Al-based catalyst was beneficial in the DM-based network where no intumescence of the samples was observed, leading to the conclusion that intumescence might not be the only protective mechanism. Of course, granted the differences between the chemical structures of the epoxies and the morphologies in the POSS-containing networks, the combustion mechanisms in these two kinds of thermosetting networks were likely to be different. Actually, this could be the reason for the improvement of the fire performance of the DGEBA-based system containing POSSOH only (i.e. without catalyst), while the corresponding MVR444- and TGDDM-based networks showed no enhancement.

The general conclusion of this study was that one particular POSS was unlikely to constitute a 'universal epoxy fire-retardant', i.e. to bring fire retardancy to any kind of epoxy network. However, synergies with other compounds can be found, like it was abundantly reported in the literature with phosphorus-containing compounds ( see Chapter I, section 3.2.d). Here, it was not clear whether the synergy arose from a chemical effect of the 'supplementary' compound on the fire behaviour, similarly to what occurs with phosphorus-containing compounds, or rather from a chemical effect occurring during the network development and which was at the root of a modification of the combustion mechanism of the whole network. In any case, with the combination of POSSOH and the Al-based catalyst, a system was found that was efficient to fire-retard epoxy-amine networks of different natures.



---

**CHAPTER V. CASE STUDY: POSSOH AS A FIRE  
RETARDANT FOR A COMPLEX  
THERMOSET/THERMOPLASTIC  
FORMULATION**

---

A well-proven and established technology for producing affordable, high-performance fibre-reinforced composite parts across a wide range of industrial sectors is the commingling approach [119]. This process involves the spinning of polymer fibres, their commingling with reinforcement fibres, and consolidation with heat and pressure (Figure V-1). This process has originally been developed for the production of thermoplastic-matrix composites because the thermoplastics viscosity can be controlled by temperature and their ability to flow make them suitable for spinning.

The advantages of the commingling process are directly related to the polymer fibres: (i) they allow easy handling: there is no contact with reactive liquid or viscous formulations, the polymer is under the shape of fibres in spools and can thus be handled as reinforcement fibres; (ii) additives – e.g. for fire-retardant materials – can be dispersed in the polymer fibres, allowing high-quality dispersion states of the additives if the commingling process is correctly carried out. It allows to avoid filtration and aggregation of the additives, and high resin viscosity issues usually experienced in the conventional resin transfer processes.

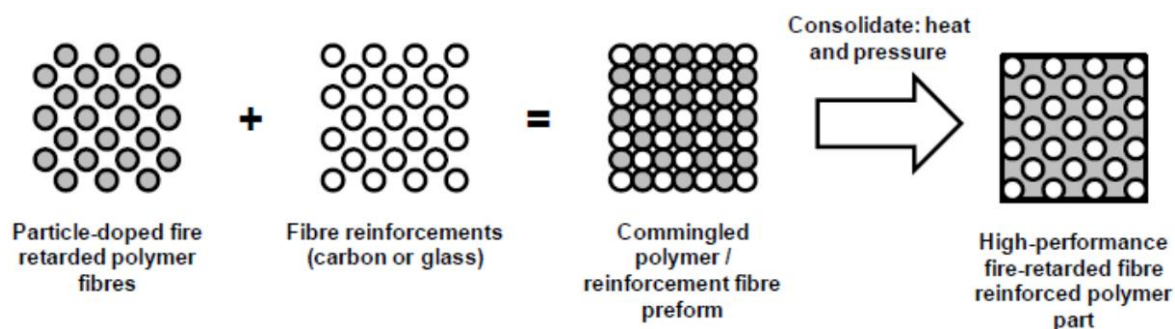


**Figure V-1 Commingling process for fire-retardant composite production**

Production of thermosetting fibres is, however, delicate due to the brittleness of the resulting networks, even at low curing states. Thus, the introduction of a thermoplastic is unavoidable. To reach suitable spinnability, sufficient content of thermoplastic must be added to the thermoset formulation. However, from low contents of thermoplastic (15-20 wt%, depending on the system), there is a phenomenon of inversion of the morphology that leads the final material to acquire thermoplastic properties – this phase inversion phenomenon will be detailed in the following discussion in this chapter. One can thus understand the difficulty to produce a real thermoset, windable fibre. In the framework of the Fire-Resist project, a compromise was found that involved the use of a curative fibre. In practice, the curative fibre contained a certain percentage of thermoplastic in order to be spinable, in which the crosslinking agent was dispersed. The curative fibre was produced by one of the Fire-Resist project partners, Cytac (UK).

The concept of curative fibre (CF) was specifically designed for the production of thermosetting composite materials by the commingling process. The idea was to commingle together the curative fibres and the reinforcement fibres (carbon or glass fibres), in order to produce a preform into which the epoxy resin would be injected. With this solution, one of the advantages of the commingling process was lost, i.e. it required handling of the viscous liquid epoxy prepolymer. Nevertheless, the epoxy and the crosslinking agent were not mixed together as for conventional resin transfer processes, thus there is no problem of shelf-life anymore, nor problems of viscosity during the injection – the epoxy prepolymer could be heated to a suitable temperature and for the time required, providing it does not cause homopolymerization. Above all, the advantage linked to the possibility to disperse additives in the thermoplastic phase of the curative fibres was conserved.

In the present work, the aim was to produce fire-retardant unreinforced epoxy networks using the CF, as a preliminary stage towards production of composite materials. The approach selected for the purpose was to introduce the already presented triSilanolPhenyl POSS (POSSOH). Thus, samples containing a certain fraction of thermoplastic polymer were produced. Introduction of thermoplastics in thermoset networks, in particular in epoxies, constitutes a wide-spread strategy for optimizing several of the networks properties, in particular mechanical properties. One common aim of introducing thermoplastics in inherently brittle epoxy networks is to improve their toughness, as has been widely reported in [120]–[125]. Also, investigating the mechanical properties – fracture toughness, delamination or fatigue resistance [126]–[130] – of composites based on blends of high-performance epoxy and thermoplastic polymers has gathered interest as such systems are usually used in structural parts in the transport sector and thus are subjected to high mechanical stresses. The thermoplastics mainly used are poly (etherimide) (PEI) or poly (ethersulfone) (PES) due to their high thermal resistance. As regards the fire retardancy of these systems, the addition of a high performance thermoplastic could be beneficial as they are intrinsically less flammable than epoxies (Figure V-2). Epoxy/thermoplastic blends fire performance has been scarcely studied up to now. The thermal stability of TGAP-DDS networks with 20 or 30 wt% of poly(ether sulfone) (PES) was improved in terms of char yield, the degradation temperatures being hardly influenced [131]. The same tendency was observed when introducing 20 to 25 wt% of poly(amide-amidic acid) (PAA) in a TGDDM-DDS network, though other PAA levels (from 5 to 30 wt%) proved to be detrimental as compared to the neat TGDDM-DDS network. The LOI measurements showed a slight decrease of the flammability for PAA contents of 20-25 wt%, lower or higher fractions of PAA leading to a worsening of the fire performance of the network [132]. An interesting

approach was the one of Perez et al., who synthesised a flame retardant toughener by introducing phosphorus in poly(sulfone) (P-PSu). They compared their results with common poly(sulfone) (PSu) and reported a dramatic improvement of the fire retardancy – assessed via cone calorimetry – in the networks containing P-PSu, while the toughness was better enhanced by the addition of PSu [133], [134].

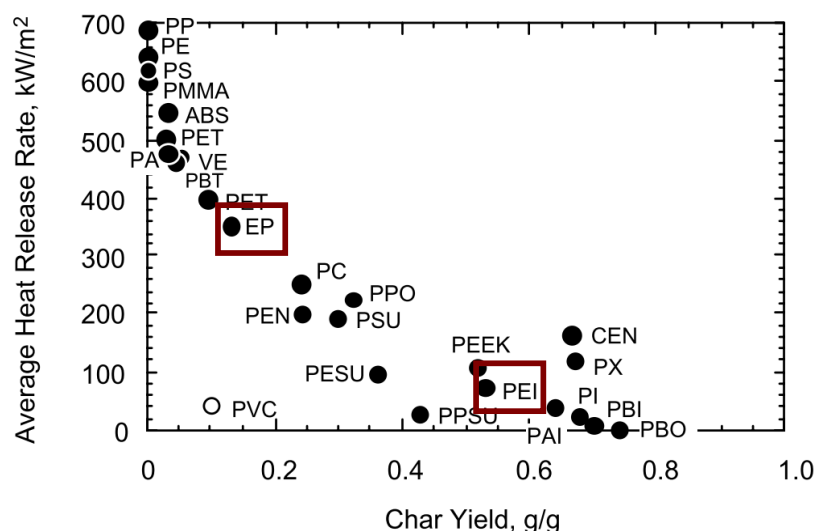


**Figure V-2 Ranking of polymer flammability based on their average flaming HRR from cone calorimeter measurements and char yield [34]**

This chapter will consist of four main sections. A first part will briefly recall the principles of phase separation and phase inversion in thermoset/thermoplastic systems. The second part will deal with the material selection and the process implemented. Then, the morphologies of the cured networks and their thermo-mechanical properties will be analysed. Finally, the fire behaviour of the networks will be presented.

## 1. PROCESS OF PHASE SEPARATION IN A THERMOSET/THERMOPLASTIC BLEND

The phase separation phenomenon has been introduced in Chapter II, as concerns the Reaction-Induced Phase Separation (RIPS) of POSS in the epoxy networks. In the present case, a thermoplastic – poly(etherimide) (PEI), as it will be detailed in the materials part later on in this chapter – was added to the thermosetting polymer through the use of the Curative Fibre and RIPS will occur during the copolymerization of the network. General concepts of the

classical thermoplastic/thermosetting polymer RIPS theory will be presented in the following discussion, based on the enlightening work of Williams et al. [92].

As explained in Chapter II, the RIPS proceeds from the increase in incompatibility between the thermosetting network and the modifier, due the increase in molar masses of the species of the reactive thermosetting system during copolymerization. This will lead to the development of two phases, rich either in the thermosetting polymer, or in the modifier. Thermodynamic models have been developed that are able to describe the RIPS phenomenon. Namely, the Flory-Huggins model can describe qualitatively the RIPS through polymer conversion vs. modifier mass fraction phase diagrams. A first approach of this model consists in considering monodisperse constituents. Binodal and spinodal curves can be determined through the establishment of the Gibbs free energy expression for this simplified model, which can be found in [92]. The binodal and spinodal curves can be plotted in the phase diagram, where they delimit the stable and metastable regions, and the metastable and unstable regions, respectively (see schematic representation in Figure V-3). In the stable region (below the binodal curve), only one phase exists; in the unstable region (over the spinodal curve), the RIPS has started and two phases coexist. In the metastable region, the blend can remain stable under certain conditions, or undergo phase separation. Within this zone, a mechanism of nucleation and growth of the dispersed phase occurs if the phase separation rate is higher than the polymerization rate – the dispersed phase usually taking the shape of spheres as it is the most thermodynamically stable. At the critical point, the two curves are tangent and the metastable zone does not exist. The mechanism of phase separation at this particular point is thus spontaneous – called spinodal demixing – and leads to the formation of co-continuous phases. On the left side of the critical point, the dispersed phase remains rich in the modifier, and when the modifier fraction is higher than the modifier fraction at the critical point ( $\Phi_M > \Phi_{M_{crit}}$ ), the phenomenon of phase inversion occurs: the main phase is rich in the modifier, while the thermosetting network constitutes the dispersed phase.

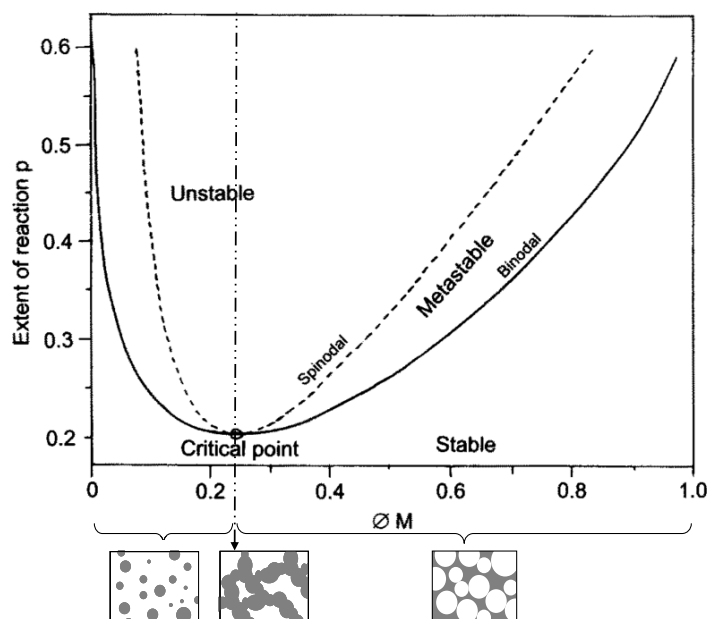


**Figure V-3 Thermosetting conversion vs. modifier fraction schematic phase diagram [92] and characteristic morphologies of the cured network as a function of the modifier fraction ( the white and the grey areas represent the thermosetting- and the modifier-rich phases, respectively)**

The morphology, especially the size of the dispersed phase, will be influenced by various parameters that are related to miscibility, kinetics and/or diffusion concerns. For a thermoplastic/thermosetting system, the miscibility will be controlled by the chemical nature of the polymer and of its chain ends and by its molar mass distribution, as highlighted by Yu et al. for a TGDDM-DDS/PEI system [135]. The temperature will also play a role in the miscibility of the constituents. From a kinetic point-of-view, the parameter describing the influence on the nodule size is the ratio of the RIPS and the polymerization rates: the higher it is, the larger the nodules. Finally, the diffusion is influenced by the viscosity of the medium, which is related to the curing temperature and to the polymerization rate – also dependent on the temperature, and on the presence and concentration of catalysts.

The approach based on monodisperse constituents does not allow to describe the gradients of molar masses in the different phases nor the occurrence of the secondary phase separation phenomenon. In reality, the thermosetting/thermoplastic systems are made of polydisperse species. Due to miscibility concerns, the thermoplastic-rich phase will be enriched in the higher molar mass thermoplastic and the lower molar mass thermosetting species. As a result, local differences of stoichiometry and thus of conversion can exist. In some cases, this can lead to the appearance of the secondary phase phenomenon in the networks where  $\Phi_M > \Phi_{M_{crit}}$  – i.e. the dispersed phase is rich in modifier. After the gelation of the main thermosetting phase, the

phase separation can continue in the dispersed phase where the conversion may be lower, if the curing temperature is higher than the glass transition temperature of the modifier-rich dispersed phase – the molecular mobility being a limiting factor for the development of a second-order morphology. This would lead to the formation of a dispersed thermosetting phase (small nodules) inside the modifier-rich primary dispersed phase.

The morphology of various thermoset/thermoplastic networks based on TGDDM prepolymer and PEI has been investigated as a function of the thermoplastic content [121], [122], [136]. The expected morphologies were obtained and the phase inversion in such systems was usually located between 13 wt% and 18 wt% of PEI. The development of co-continuous phases was usually observed for a range of PEI contents, rather than for a precise value, indicating a progressive change to the inverted morphology. In Figure V-4 are displayed the conventional phase-separated morphologies corresponding to the three conditions  $\Phi_M \ll \Phi_{M_{crit}}$ ,  $\Phi_M \approx \Phi_{M_{crit}}$ , and  $\Phi_M \gg \Phi_{M_{crit}}$ . Cho et al. proposed a mechanism of spinodal demixing for the RIPS within TGDDM-DDS/PEI systems, as they were able to obtain co-continuous phases even at low PEI contents by implementing a low temperature curing cycle [122].

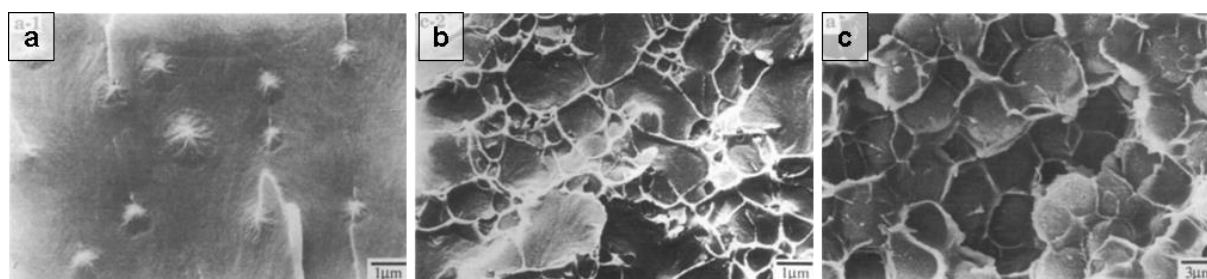


Figure V-4 Morphology of TGDDM-DDS containing PEI (Ultem 1000) a) PEI-rich nodules in an epoxy-rich matrix, b) co-continuous phases, c) epoxy-rich nodules in a continuous PEI-rich phase [122]

## 2. SELECTION OF MATERIALS AND PREPARATION OF PEI-CONTAINING EPOXY NETWORKS

### 2.1. MATERIALS

The networks were based on the TGDDM epoxy prepolymer. The crosslinking agent was introduced in the systems by using the curative fibre EF10007 (CF, Figure V-5), produced and provided by Cytec. The following information on the CF were given by the supplier: (i) the CF was a mixture of 45 wt% of poly (etherimide) (Ultem1010 from Sabic), one or several curing agents, and possibly other compounds whose structure is confidential and Cytec's property; and (ii) the active hydrogen equivalent weight, HEW, was equal to  $140.8 \text{ g.mol}^{-1}$ . The CF was

produced by spinning a few tens of microns in diameter. As concerns the PEI, it is an amorphous thermoplastic with a Tg equal to 218 °C. To measure the Tg of the curative fibre by DSC, it was first melted in order to fit in the small aluminium capsule. A large glass transition was found equal to 24 °C – i.e. close to room temperature – and a small Tg signal was observed at 218 °C, which could be attributed to PEI (Figure V-6). Most of the PEI fraction in the CF was thus very likely to be plasticized by the 55 wt% of other compounds – e.g. crosslinking agent(s) – potentially being small molecules.



Figure V-5 Curative Fibre spool, provided by Cytec

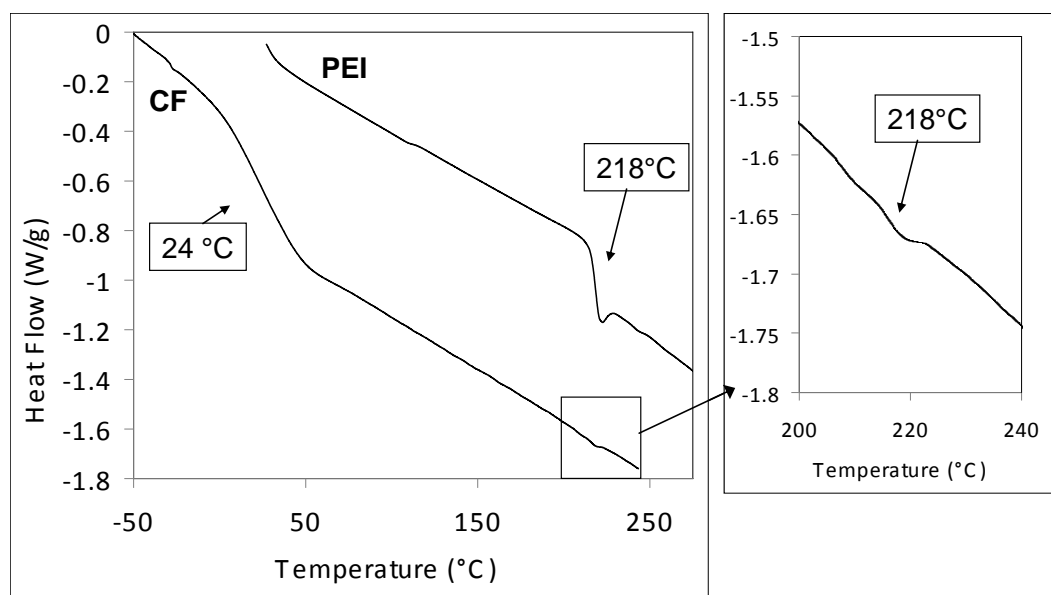


Figure V-6 DSC scans of PEI and the Curative Fibre (CF)

Model networks were produced where the CF was replaced by MDEA as curing agent and a plain ground polyetherimide (PEI) from Aldrich whose grade was similar to the one of CF.

The POSS introduced in some of these networks was the trisilanolPhenyl POSS (POSSOH from Hybrid Plastics). The structure of the materials and abbreviations used for simplification concerns are reported in Table V-1.

Finally, the process implemented required the use of anhydrous dichloromethane from Carlo Erba.

Products	Denomination	EEW or HEW (g/mol)	Schematic structure
Tetraglycidyl(diaminodiphenyl) methane	TGDDM	117-134	
4,4' methylene bis(2,6-diethylaniline)	MDEA	77.6	
Polyetherimide	PEI	-	
Curative Fibre EF10007	CF	140.9	
TrisilanolPhenyl POSS	POSSOH	310.2	
Aluminium triacetylacetonate	Al	-	

**Table V-1 Name and structure of used compounds ; EEW and HEW stand for epoxy equivalent weight and (active) hydrogen equivalent weight, respectively**

## 2.2. PREPARATION OF PEI-CONTAINING EPOXY NETWORKS

### 2.2.a. PEI percentage in the networks and stoichiometric ratio

The CF contained 45 wt% of PEI and the crosslinking agents, thus both the stoichiometric ratio and the quantity of PEI in the final networks were controlled by the CF amount. The following equation links the final weight percentage of PEI – taking into account all the network constituents – to the stoichiometric ratio in the TCF networks (Equation V-1).

V-1

$$\frac{a}{e} = \frac{EEW \times \% PEI}{HEW \times (45 - \% PEI)}$$

Where  $\frac{a}{e}$  is the stoichiometric ratio – i.e. the ratio between the quantity of active hydrogen introduced by the CF, and the quantity of epoxy functions introduced by the TGDDM – and *EEW* and *HEW* are the epoxy equivalent weight of TGDDM and the hydrogen equivalent weight of CF, respectively.

The advice from Cytec was to use a CF content comprised between 80 and 120 phr of TGDDM. As highlighted previously, a reaction-induced phase separation was expected in the thermoset/thermoplastic blends under study. A phase inversion is possible in epoxy-based networks from low contents of PEI. As reported previously, for epoxy networks based on TGDDM-DDS with PEI, the phase inversion phenomenon has been seen to occur from 13 wt% [136]. From all this information, it was decided to study three different cases:

- A case where the CF content was such that the stoichiometry was respected – i.e.  $a/e=1$ ;
- A case where the phase inversion would be avoided, i.e. with a PEI content lower than 13 wt%. The PEI content was settled at 10 wt%;
- An intermediate case, with a PEI content of 17 wt%.

In summary, the values of CF content, which was the varying parameter that controlled the PEI content and the stoichiometric ratio, are reported in Table V-2 below.

CF content (phr)	Final PEI content (wt%)	$a/e$
110	23	1
66	17	0.59
28	10	0.26

**Table V-2 Contents of CF in the networks and consequent PEI content and stoichiometric ratio**

### **2.2.b. Preparation of TGDDM/Curative Fibre-based networks and the reference systems**

- Study of the Curative Fibre dissolution in TGDDM prepolymer

Due to the presence of 45 wt% of PEI within the CF, the issue of the dissolution of the fibre in the TGDDM epoxy prepolymer had to be taken into account. The dissolution of the fibre is the mandatory first step to facilitate the mixing of the two components (epoxy and hardener) prior to curing in order to obtain homogeneously cured networks.

A single CF was thus isolated and introduced in a drop of TGDDM on a glass strip in order to be observed under optical microscopy. A heating device allowed the sample to be subjected to a precise temperature profile. It consisted of heating the sample from 75 °C to 140 °C with dwells of 15 minutes every 5 °C – the heating rate between the dwells being equal to 5 K/min. Pictures were taken at the end of each dwell (except for the picture at  $t=0$  min) and the most significant of them are displayed in Figure V-7.

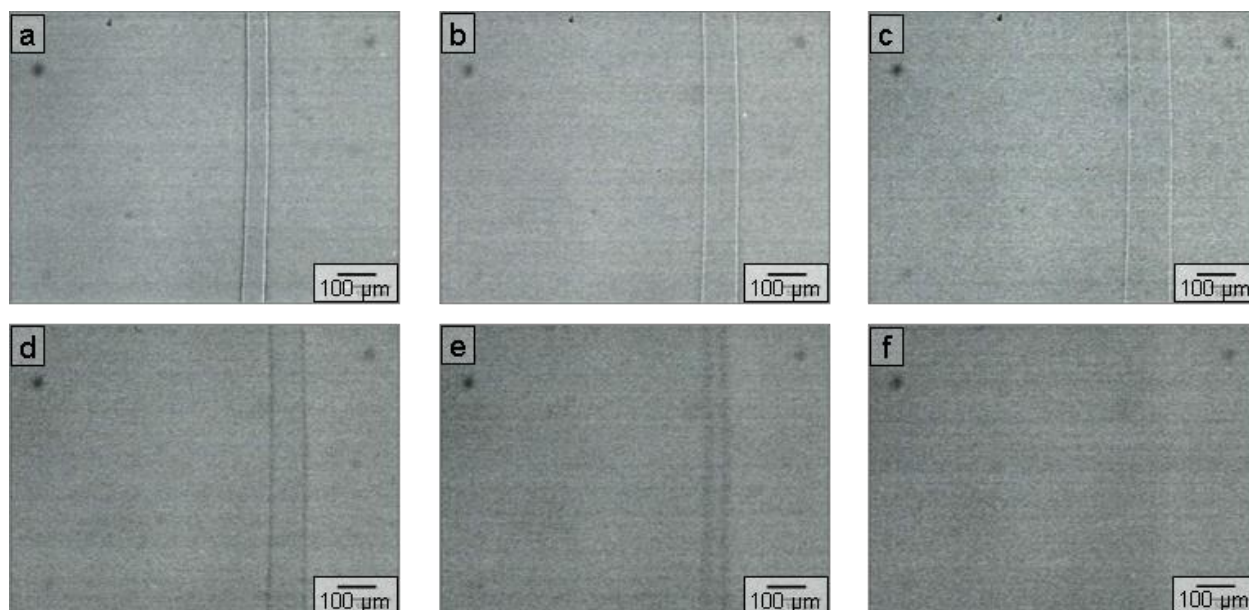


**Figure V-7 Dissolution of the curative fibre in TGDDM by heating through several successive temperature dwells. Images were taken at: a) 75 °C (t=0), and at the end of the dwells at: b) 75 °C ; c) 80 °C ; d) 95 °C ; e) 110 °C ; f) 140 °C**

The initial diameter of the fibre was about 60 µm. After a first dwell of 15 minutes at 75 °C, the diameter increased to 86 µm, while the walls seemed to remain cohesive. It could be assumed that the fibre deformed and expanded with increasing the temperature. It could correspond to the step of swelling of the curing agent-plasticized PEI fibre by the epoxy prepolymer, and the subsequent devitrification of the plasticized PEI when its  $T_g$  equalized the experimental temperature.

The fibre dissolution in TGDDM began from 95 °C – with the fibre walls starting to fade – and seemed complete at 140 °C. The phenomenon of dissolution is likely to be influenced by the polymerisation and thus compete with the reaction-induced phase separation phenomenon, as highlighted by Lestriez et al. [137].

The solubilisation of the CF in TGDDM, in such a proportion as to respect the stoichiometry – i.e. for 110 phr of CF – was attempted with coarsely chopped CF. The ‘mixture’ was mixed while heating at 110 °C for more than half-an hour but the dissolution did not occur and the sample presented macro-phase separation after curing.

- Description and preparation of TGDDM-based networks

Three networks were made for each amount of PEI mentioned in section 2.2.a. :

- A neat network made from TGDDM and CF only: TCF;
- A network containing 4 wt% of POSSOH: TCF-POSSOH;
- A network containing 4 wt% of POSSOH and 0.06 phr of Al catalyst: TCF-POSSOH-Al.

In addition, for the networks with the lowest CF content, reference samples were produced by replacing the CF by MDEA with or without PEI. The PEI content was close to 10 wt% in the final material and the MDEA was introduced in such a quantity so that the stoichiometric ratio was equal to 0.26 – like in the networks with the lowest content of CF. Only neat networks – without POSS or Al catalyst – were produced. The networks' denomination and composition are summarized in Figure V-8.

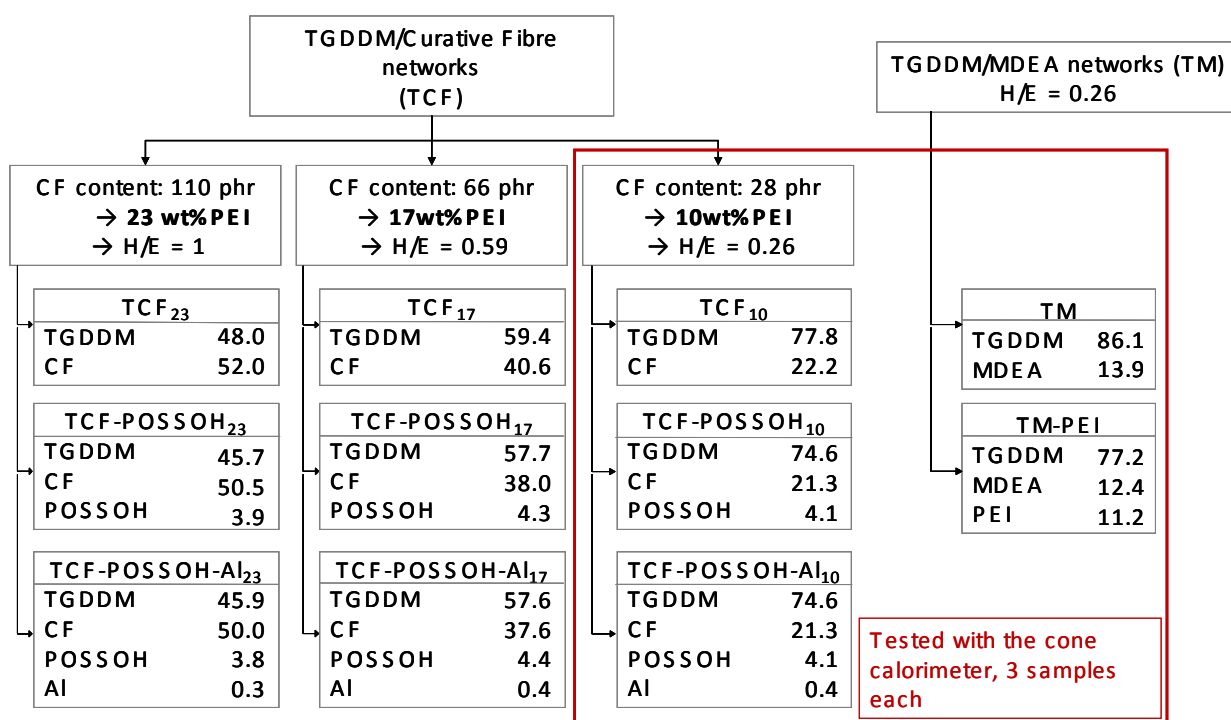


Figure V-8 Actual composition (in wt%) of TCF networks and reference networks based on TGDDM and MDEA

Considering the difficulty to dissolve the CF by heating in the epoxy prepolymer, it was decided to go through a process involving solvent. Various solvents were tested and dichloromethane was finally selected as it was able to dissolve all the components and had a rather low boiling point – equal to 40 °C. Bucknall and Partridge reported that the use of solvent (methylene

chloride) for blending of epoxy prepolymers and PES did not affect the structures nor the properties of the final networks [120].

For each network – neat, with POSSOH and with POSSOH and the aluminium catalyst – two solutions were prepared in flasks with screw caps. One solution contained the CF in dichloromethane, with a mass ratio CF:dichloromethane of about 1:2, the other one consisted of TGDDM – and the POSSOH for the TCF-POSSOH and the TCF-POSSOH-Al networks – in dichloromethane, with a mass ratio TGDDM:dichloromethane of about 1:1. The flasks containing the solutions were sealed with plastic paraffin film and left overnight with magnetic stirring. The aluminium catalyst was added in one of the CF/dichloromethane solutions, which was further left to stir until complete homogenisation of the solution was achieved. The two solutions were then mixed together and the mixture was cast in moulds before curing.

Small rectangular samples were made from silicone-made moulds with dimensions of 20 x 11 mm and were dedicated to thermal characterization and morphological analyses. After casting the solutions, the moulds were directly put in an oven placed under a hood and the samples were cured according to the following curing cycle: a ramp from room temperature to 90 °C with a low heating rate (1K/min) to allow the dichloromethane to slowly evaporate, followed by a dwell of 1 hour at 90 °C, a ramp until 130 °C (1K/min), a dwell at 130 °C for 4 hours, a ramp until 180 °C (1 K/min) and a final dwell at 180 °C for 2 hours before a slow cooling to room temperature. The dwell temperatures and times were advised by Cytec. After curing, the samples were about 1 mm in thickness, and contained small bubbles in the case of TCF and TCF-POSSOH networks. The TCF-POSSOH-Al samples were noticeably darker and their surface was swollen with solidified bubbles.

Cone calorimeter samples were also manufactured in the case of the networks containing 10 wt% of PEI (i.e. 28 phr of CF). Samples were produced in circular aluminium cups of 9 cm in diameter, and they were placed in a vacuum oven for 20 minutes in order to remove most of the dichloromethane prior to curing – the same curing cycle as mentioned above was implemented. Reference samples – TM and TM-PEI – were produced in the cone calorimeter configuration only, by the same process as for the CF-containing networks. After curing, the samples were about 1 mm thick and presented the same aspect as the smaller rectangular samples. The samples were tested with the cone calorimeter directly in their aluminium cups whose edges were trimmed just above the polymer surface. The radiant heat flux was of 35 kW/m<sup>2</sup> instead of the usual 50 kW/m<sup>2</sup>, in order to account for the small thickness of the samples.

### 3. THERMAL AND MORPHOLOGICAL CHARACTERISATION

#### 3.1. INFLUENCE OF THE CURATIVE FIBRE CONTENT ON THE GLASS-TRANSITION TEMPERATURE OF THE TCF NETWORKS

Given that the CF contained both the PEI and the curing agent, the stoichiometric ratio depended on the amount of CF introduced in the networks – see section 2.2.a. Hence, the thermo-mechanical properties were expected to change depending on the CF content. A study of the influence of the stoichiometry on the glass transition temperature of the networks was performed by means of DSC. Each network was subjected to two consecutive heating ramps, from 25 °C to 250 °C at 10 K/min and separated by a controlled cooling ramp at 10 K/min. DSC scans (1<sup>st</sup> ramp) of neat TCF networks for different contents of CF are shown in Figure V-9 for illustration. Data for all the networks and for both heating ramps were collected and plotted as a function of the stoichiometric ratio – PEI content – as displayed in Figure V-10 and Figure V-11.

From Figure V-9, it was clear that the glass transition temperature of the TCF networks depended on the CF content. A reduction of the latter, which meant a reduction of the stoichiometric ratio, resulted in a clear decrease of the glass transition temperature. The maximum of glass transition temperature was obtained for a stoichiometric ratio equal to 1 (PEI content of 23.5 wt%). In this network, a first T<sub>g</sub> was observed at 197 °C that could be assigned to the epoxy network. For comparison, the T<sub>g</sub> of the TGDDM-MDEA network – post-cured at 200 °C – was equal to 216 °C. A second T<sub>g</sub> was observed at 214 °C, attributed to the PEI-rich phase which constituted the matrix as phase inversion occurred in this network. The glass transition of the PEI-rich phase was not observed anymore when the PEI content was decreased to 10 or 17 wt%. For a reduction of the stoichiometric ratio down to 0.26 or 0.59, the T<sub>g</sub> of the TCF network was reduced by about 130 °C or 35 °C, respectively. This was expected as in the great majority of epoxy-amine networks, the maximum of glass transition temperature is observed for a stoichiometric ratio equal to  $a/e=1$  [138]. Liu et al. reported a decrease of T<sub>g</sub> of 5 °C only in a TGDDM-DDS system – from 265 °C to 260 °C – between stoichiometric ratios of 0.9 and 0.6 [139]. For a similar TGDDM-DDS system, Levchik et al. reported greater glass transition temperature decrease, with values of 175 °C and 217 °C for stoichiometric ratios of 0.5 and 0.85, respectively [140]. They highlighted the occurrence of TGDDM homopolymerization at higher temperatures than required for the epoxy/primary amine addition. The small decrease of 5 °C in T<sub>g</sub> reported by Liu et al. could then be attributed to the occurrence of complex cyclisation reactions due to a high temperature of postcuring – 205 °C –

as compared to the curing temperature of 180 °C implemented in Levchik's work, as well as in the present study.

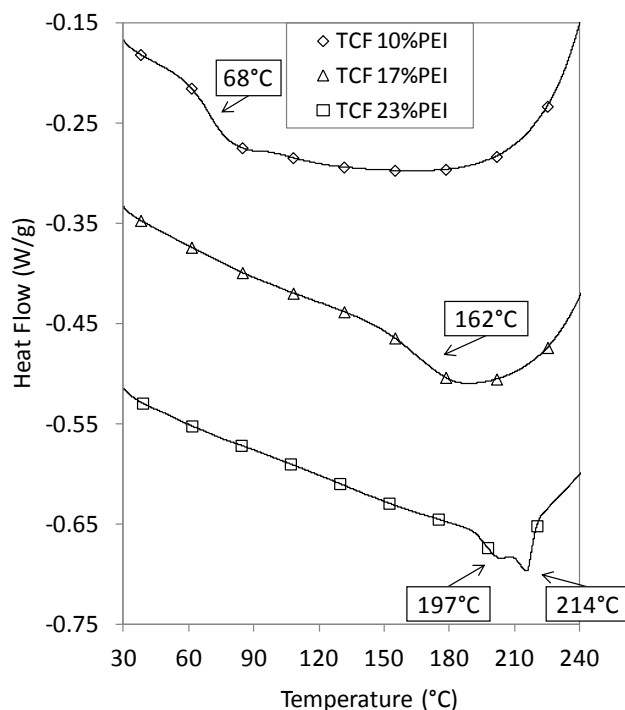


**Figure V-9 DSC scans (first ramp) of neat TCF networks with different contents of CF, i.e. different PEI contents and different stoichiometric ratios**

In Figure V-10 the  $T_g$  of neat TCF networks and TCF networks containing POSSOH±Al – measured during the first ramp of the DSC scans – was plotted as a function of the stoichiometric ratio. The increase of  $T_g$  with the stoichiometric ratio, highlighted earlier in the case of TCF networks, is also valid for TCF-POSSOH and TCF-POSSOH-Al networks, as expected. The influence of POSSOH in the TCF networks on their glass transition temperature was negligible – the TCF-POSSOH ‘curve’ matches the TCF ‘curve’ in Figure V-10. On the contrary, the combined presence of POSSOH and the Al-based catalyst resulted in increasing the  $T_g$  as compared to the neat TCF and the TCF-POSSOH networks, when the stoichiometric ratio was below 1. For a ratio of 0.26 and 0.59, this increase in  $T_g$  was equal to about 75 °C and 20° C, respectively.

No increase in  $T_g$  was observed for a stoichiometric ratio of 1, meaning that the reaction of the epoxies with the active hydrogen functions from the CF reached a maximum during the curing cycle in oven (maximum temperature equal to 180 °C). Most probably, this reaction also reached a maximum in off-stoichiometry samples. Therefore, in these networks, the increase in  $T_g$  observed when introducing both the POSSOH and the aluminium-based catalyst was due to

the activation of TGDDM homopolymerisation – which was already evidenced for the DGEBA/MDEA system, see Chapter III – and/or an epoxy-silanol reaction.

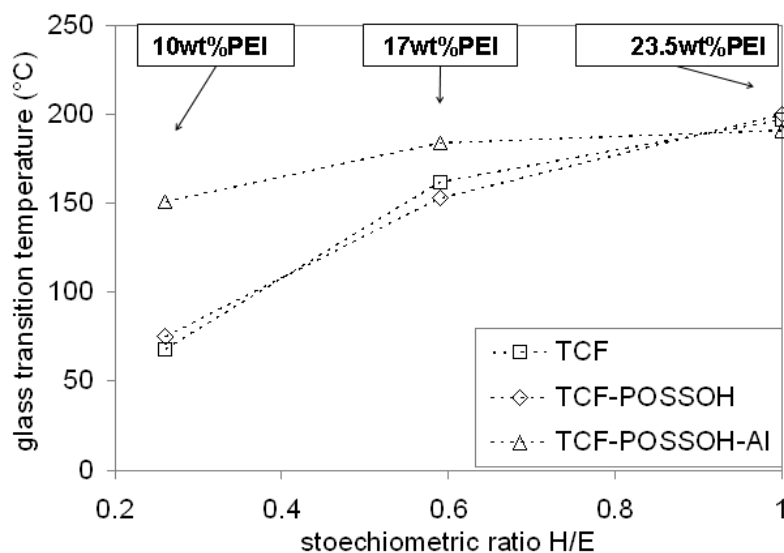


**Figure V-10 Glass transition temperature of TCF-based networks as measured by DSC (1<sup>st</sup> ramp) and as a function of the stoichiometric ratio**

Moreover, an evolution of the glass transition temperature between the two DSC ramps was noticed and highlighted in Figure V-11. Applying a first DSC ramp up to 250 °C caused the Tg of the networks to further increase (value measured during the second ramp), as if they were subjected to postcuring. The increase was all the more important as the stoichiometric ratio was low. At a stoichiometry of 1, the effect of ‘postcuring’ was negligible, confirming the epoxy-hydrogen reaction had reached a maximum through the curing at 180 °C. Thus, further heating to 250 °C during the first DSC ramp caused homopolymerization and/or silanol-epoxy reaction to occur in the off-stoichiometry systems, which caused the observed increase of Tg.

In addition, from Figure V-11c, it could be noticed that after ‘postcuring’, the TCF-POSSOH-Al networks where the stoichiometric ratio was less than 1 reached the same value of Tg as the stoichiometric network. This indicated that a high value of Tg, close to 200 °C, could be reached even in non-stoichiometric conditions, providing that a certain amount of POSSOH and Al catalyst was added to the basic TCF mixture.

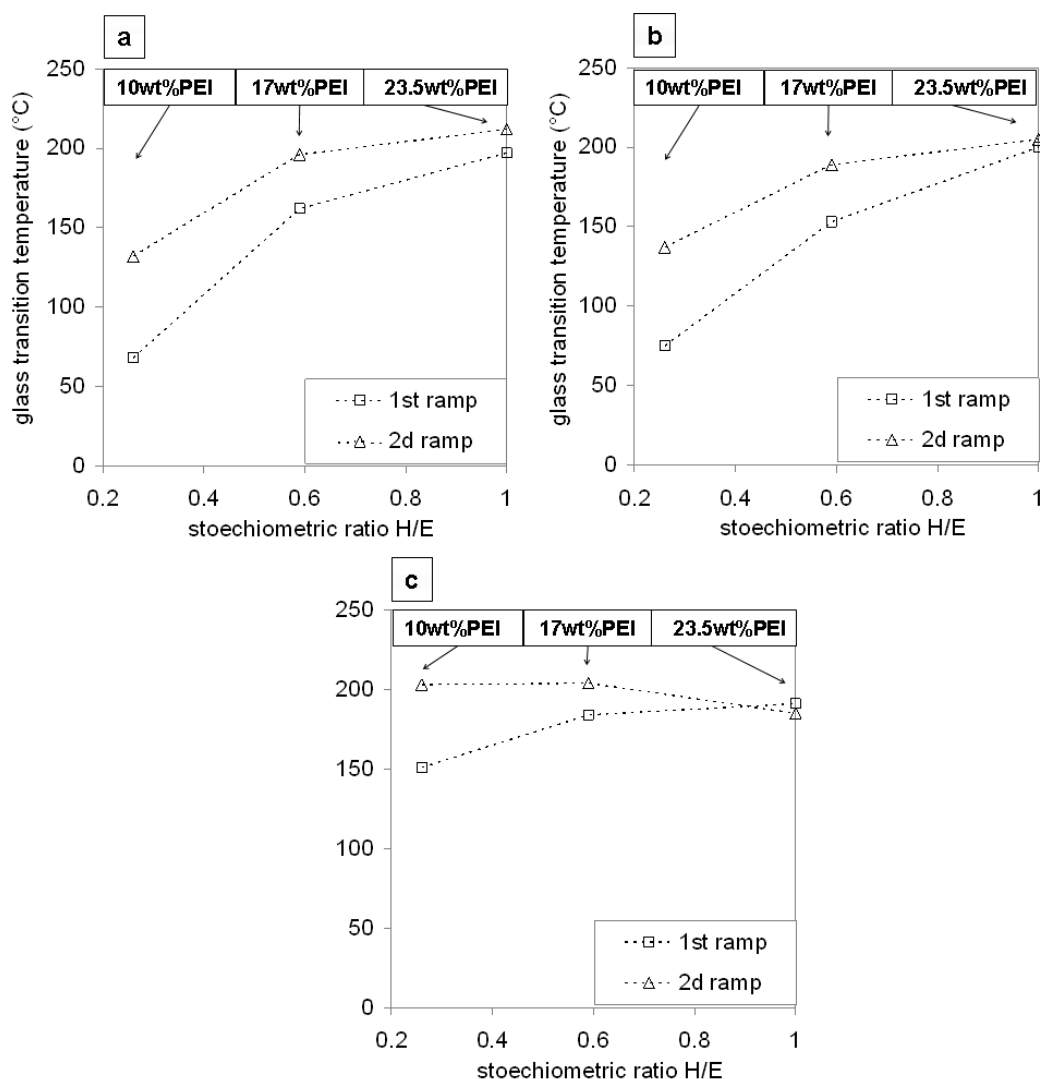


**Figure V-11 Evolution of the T<sub>g</sub> of TCF-based networks between DSC 1<sup>st</sup> ramp (squares) and 2<sup>nd</sup> ramp (triangles). a) TCF; b) TCF-POSSOH; c) TCF-POSSOH-Al**

In conclusion, the combination of POSSOH and the Al-based catalyst favoured the homopolymerization in the off-stoichiometry TCF networks, as it was already observed in the DGEBA-based model system. Similarly, the difference in the reaction kinetics observed in the DGEBA- and the TGDDM-based model systems with the addition of POSSOH and Al(acac)<sub>3</sub> was likely to occur in the TCF-based networks as well. This would possibly have consequences on the final morphology in these networks.

### 3.2. PHASE SEPARATION IN THERMOSET/THERMOPLASTIC BLENDS

In this section, the morphology of the networks will be presented and discussed based on the reaction-induced phase-separation (RIPS) phenomenon presented in the first part of this chapter.

### 3.2.a. Influence of the PEI content on the phase separation and inversion phenomena in PEI-containing epoxy networks

PEI-containing networks, based on the CF were observed via Scanning Electron Microscopy. Pictures of neat TCF networks with different contents of PEI are shown in Figure V-12. The three networks reflected the different possible configurations.

- At low content of PEI (10 wt%), the matrix was an epoxy-rich phase, while the PEI-rich phase was dispersed as nodules of 1  $\mu\text{m}$  or less in diameter. The distribution of the nodules was homogeneous over the sample. While most of the nodules were ejected from the surface when the sample surface was fractured, as shown by the empty half-spherical holes in the matrix, some of the nodules were still visible, and their fracture surface was characteristic of a ductile failure.

- At high content of PEI (23.5 wt%), the phases were inverted. The matrix was made a PEI-rich phase and the epoxy-rich phase was present as nodules of about 700 nm in diameter.

- At an intermediary content of PEI, 17 wt%, the morphology observed under microscope did not allow to distinguish any nodules. The structure was characteristic of thermoset/thermoplastic co-continuous phases, as expected for this PEI content [121], [122], [136].

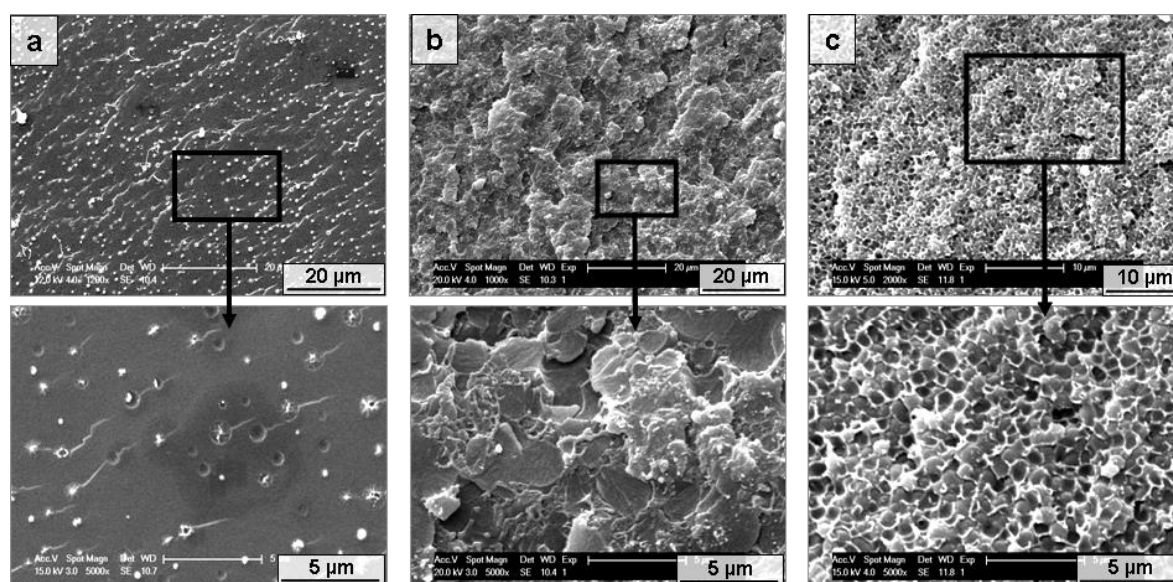


Figure V-12 SEM observation of TCF network with a) 10 wt% PEI ( $a/e=0.26$ ) ; b) 17 wt% PEI ( $a/e=0.59$ ) ; c) 23.5 wt% PEI ( $a/e=1$ )

### 3.2.b. Influence of the introduction of POSSOH and Al catalyst on the phase separation and inversion phenomena in PEI-containing epoxy networks

Several techniques were implemented to investigate the morphology in the networks containing the POSSOH with or without the Al-based catalyst. Considerations about solubility parameters will be presented afterwards together with an overall discussion of the results.

- SEM observations

Introducing other compounds like the POSSOH and the Al-based catalyst in the TCF networks with different contents of PEI could potentially modify the phase separation development and/or generate POSS-rich phases.

In the case of networks containing 10 wt% of PEI, the presence of the POSSOH with or without the aluminium acetate catalyst did not induce significant changes on the morphology: the PEI-rich nodules were evenly dispersed and their size was still about 1  $\mu\text{m}$  in diameter (Figure V-13).

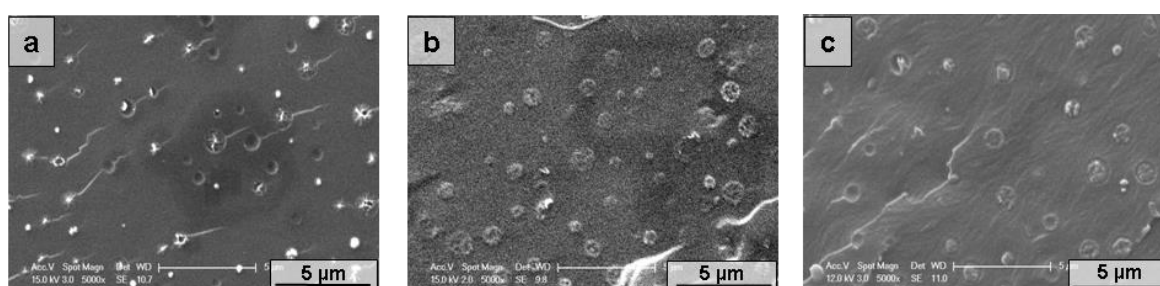
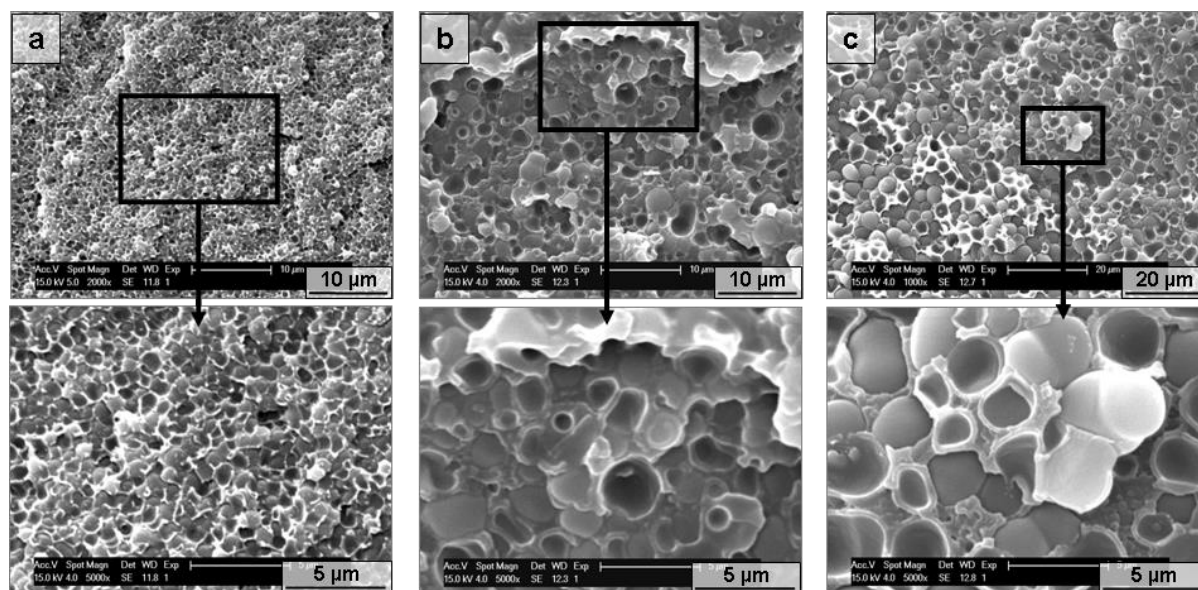


Figure V-13 Morphology of TCF networks containing 10 wt% of PEI ( $a/e=0.26$ ) a) TCF ; b) TCF-POSSOH ; c) TCF-POSSOH-Al

The morphology networks containing 23.5 wt% PEI proved to be slightly influenced by the POSSOH and/or Al-based catalyst presence (Figure V-14). The epoxy-rich nodules were bigger, a few micrometers in diameter, against less than one micrometer in the case of the neat TCF network.



**Figure V-14 Morphology of TCF networks containing 23.5 wt% of PEI ( $a/e=1$ ) a) TCF ; b) TCF-POSSOH ; c) TCF-POSSOH-AI**

The influence of POSSOH±Al introduction was even more obvious in the case of TCF networks containing 17 wt% of PEI (Figure V-15). The TCF-POSSOH and the TCF-POSSOH-AI networks presented phase inversion with epoxy-rich nodules of a few micrometers in diameter, while the neat TCF network was constituted of co-continuous epoxy/PEI phases.

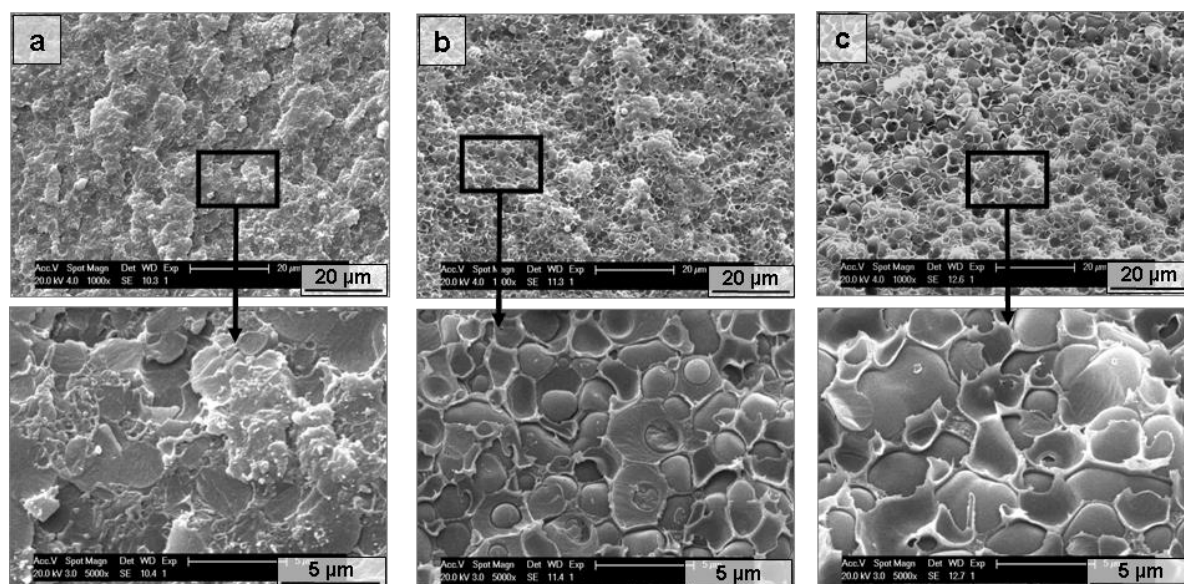


**Figure V-15 Morphology of TCF networks containing 17 wt% of PEI ( $a/e=0.59$ ) a) TCF ; b) TCF-POSSOH ; c) TCF-POSSOH-AI**

From the SEM observations, it was not clear where the POSSOH were located in the phases. Thus, further analyses were necessary in order to investigate deeper the morphology.

- TEM and EDX analyses

TEM observations were carried out on the neat TCF network containing 10 wt% of PEI (Figure V-16), and on the POSSOH-containing networks with 10 or 23 wt% of PEI (Figure V-17 and Figure V-18). The epoxy and PEI phases were clearly observable – the latter being darker than the former – which was not due to the presence of POSSOH in the PEI-rich phase as this natural phase contrast was observed in the neat TCF network containing 10 wt% of PEI as well (Figure V-16). In this network, the nodules of PEI were ellipsoidal, most probably due to the cut during the sample preparation. Their size was comprised between 0.8 and 2  $\mu\text{m}$  and there was no adhesion at the nodule interface as indicated by the thin white zone on one side of the nodules, which could be attributed to a tearing of the matrix under microtoming.

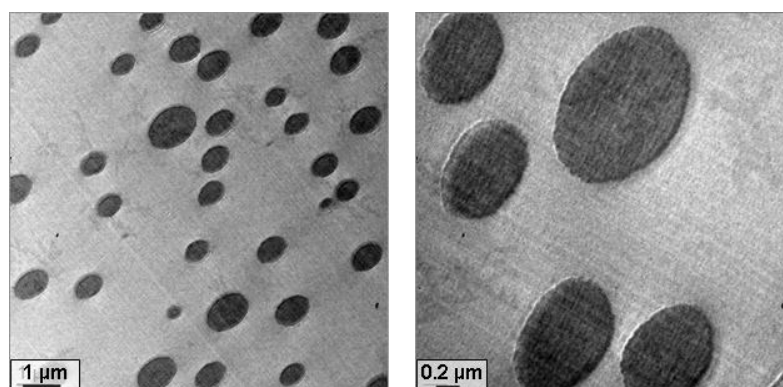


**Figure V-16 TEM images of neat TCF network containing 10 wt% PEI ( $a/e=0.26$ ), the black nodules are the PEI-rich phase, the grey area (matrix) is the epoxy-rich phase**

In the TCF-POSSOH network, nodules as in the neat TCF network described above were observed (size and shape), but there were also some bigger, irregular nodules (Figure V-17). Higher focus on these ones revealed the presence of dark threads and tiny white nodules. The latter were attributed to phase separation within the epoxy-polluted PEI-rich nodules. The former were reminiscent of the morphology observed in the TGDDM-based POSSOH-containing networks, as reported in Chapter II. These dark threads could be reasonably attributed to POSSOH. This implied that some POSSOH was dispersed in the PEI-rich phase. A dispersion of POSSOH in the epoxy matrix could be expected to generate the ‘threads-and-nodules’ morphology as in the stoichiometric TGDDM/MDEA (TM) networks – see Chapter II – though both the type and the ratio of crosslinking agent were different, which should cause significant differences between the phase diagrams of these systems. This special morphology was not observed here, but there was still the possibility to have POSSOH well dispersed in the epoxy matrix, possibly covalently bonded to the network through the reaction of the silanol functions.

The shape of the irregular nodules indicated an out-of-equilibrium morphology, i.e. the phase separation of the PEI-rich nodules containing some POSSOH was stopped by the extent of the polymerization. This would mean that for these irregular nodules, the phase-separation process did not proceed as for the regular ones due to the presence of POSSOH. Irregular, 'splat-like' nodules were observed by Girard-Reydet et al. in an epoxy-amine system containing poly(phenylene ether) (PPE) and a block copolymer PS-*b*-PMMA, which they attributed to the change of interfacial tension of PPE-rich nodules by the block copolymer which separated after the PPE-nodules formation [141]. While the systems investigated in this study were significantly different, an influence of the POSS on the overall interfacial tension of the PEI-rich phase could be an explanation for the irregular shape of the nodules.

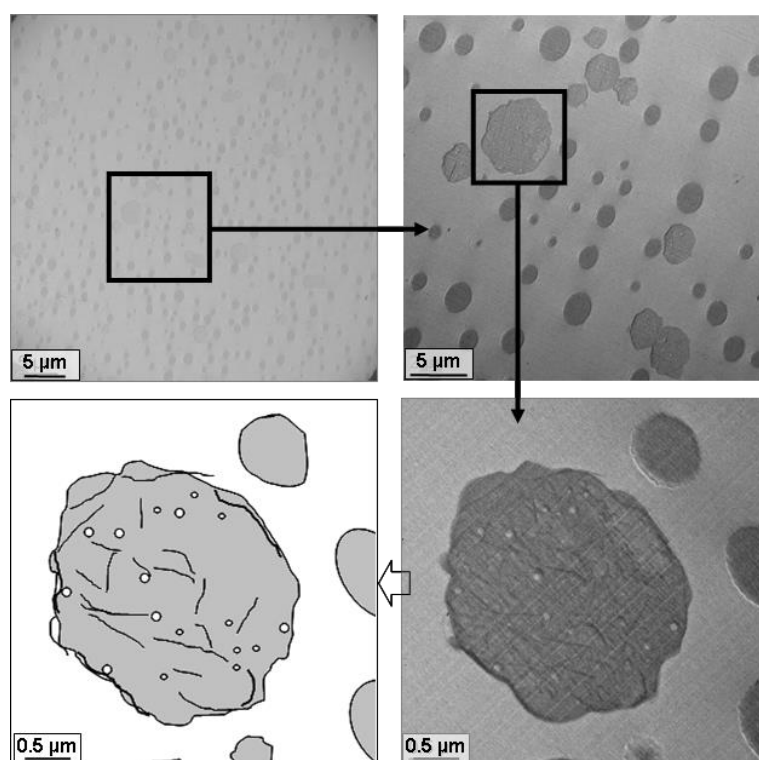


**Figure V-17 TEM images of TCF-POSSOH network containing 10 wt% PEI ( $a/e=0.26$ ) at different magnifications and scheme of an irregular nodule**

The TEM observation at very low magnification of the TCF-POSSOH-Al network revealed a small extent of phase inversion in the sample (Figure V-18), which was not observed by SEM. The predominant morphology however consisted in an epoxy-rich matrix with PEI-rich nodules. These nodules were of the same order of size as in the neat TCF network – with the tiny white nodules already observed in the TCF-POSSOH network – except for bigger nodules presenting sub-structures, i.e. with big epoxy-rich nodules. The partially phase inverted morphology, together with the existence of rather large sub-structures, was an argument to conclude that the

morphology was frozen before reaching an equilibrium, i.e. that the phase-separation was not complete when (i) the epoxy-rich phase reached a degree of crosslinking high enough to impede the diffusion of the species, namely the PEI, and/or (ii) the PEI-rich phase started to vitrify, impeding the diffusion of epoxy-based species.

Also, the dark threads observed in the TCF-POSSOH network were visible nowhere in this network. A good dispersion – finer than the TEM sensitivity, i.e. most probably molecular – was possible and could be due to two phenomena: (i) covalent bonding of the POSSOH to the epoxy-based matrix, possibly enhanced by the presence of the Al-based catalyst, and (ii) fast gelation and vitrification of the system, hindering the phase-separation of the POSSOH. In this case, the POSSOH would separate significantly later than the PEI. In the model systems, the epoxy-amine kinetics were significantly accelerated by the addition of both POSSOH and the Al-based composite which was likely to be the case in the TCF-POSSOH-Al network as well, despite the different crosslinking agent(s) and stoichiometric ratios, as well as the presence of PEI in TCF-POSSOH-Al which could influence the polymerization kinetics.

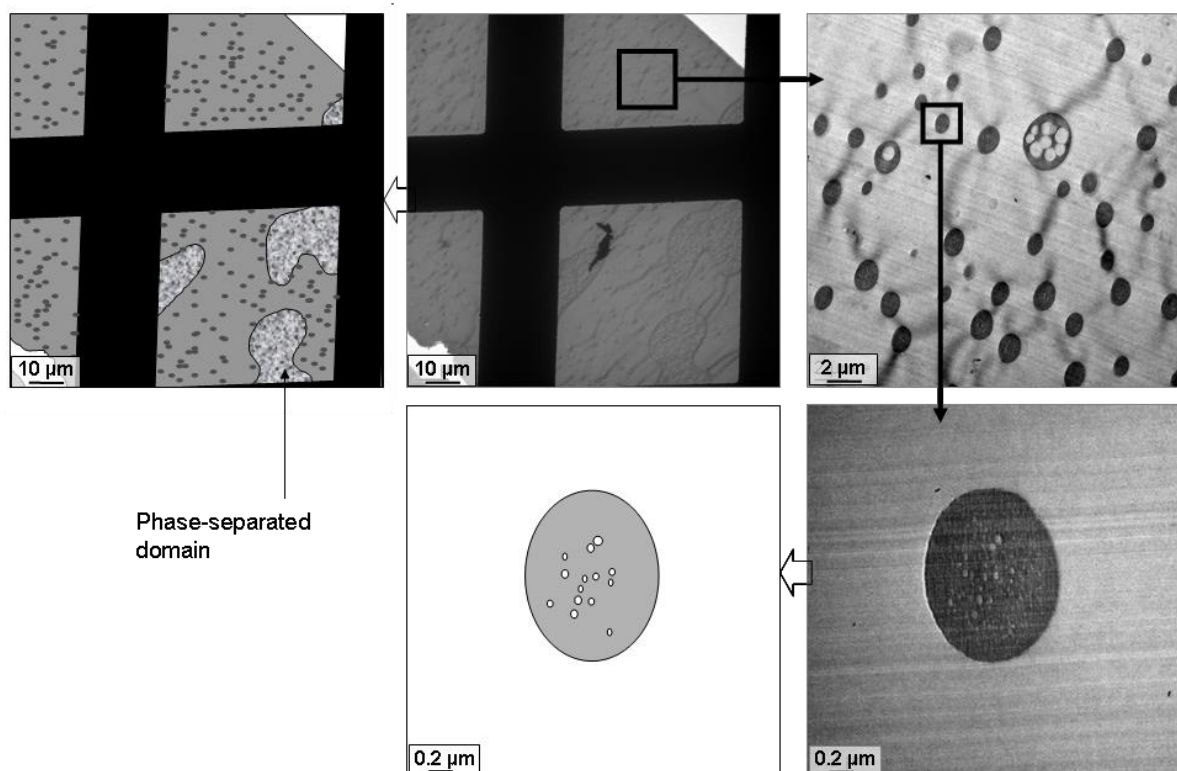


**Figure V-18 TEM images (and schemes) of TCF-POSSOH-Al network containing 10 wt% PEI ( $a/e=0.26$ ) at different magnifications. The black thick lines of the image in the middle top correspond to the grid maintaining the sample, and the black object was a dust on the sample**

In order to investigate the presence of POSSOH in the different phases, EDX analyses were performed during the TEM observation (Figure V-19). In the TCF-POSSOH network, the irregular nodules were targeted and showed an intense peak of silicon (graph b), as compared to the signal obtained for a regular nodule and some of the matrix (graph a). This was assigned to a high concentration of POSSOH in these irregular nodules, confirming the hypothesis established on the basis of the TEM observations. In the TCF-POSSOH-Al network, the silicon peak was significantly more intense when targeting the matrix (graph e) than the nodules (graph d), once again confirming the hypothesis from the TEM images, according which the POSSOH was predominantly present in the epoxy-rich phase – i.e. in the matrix.

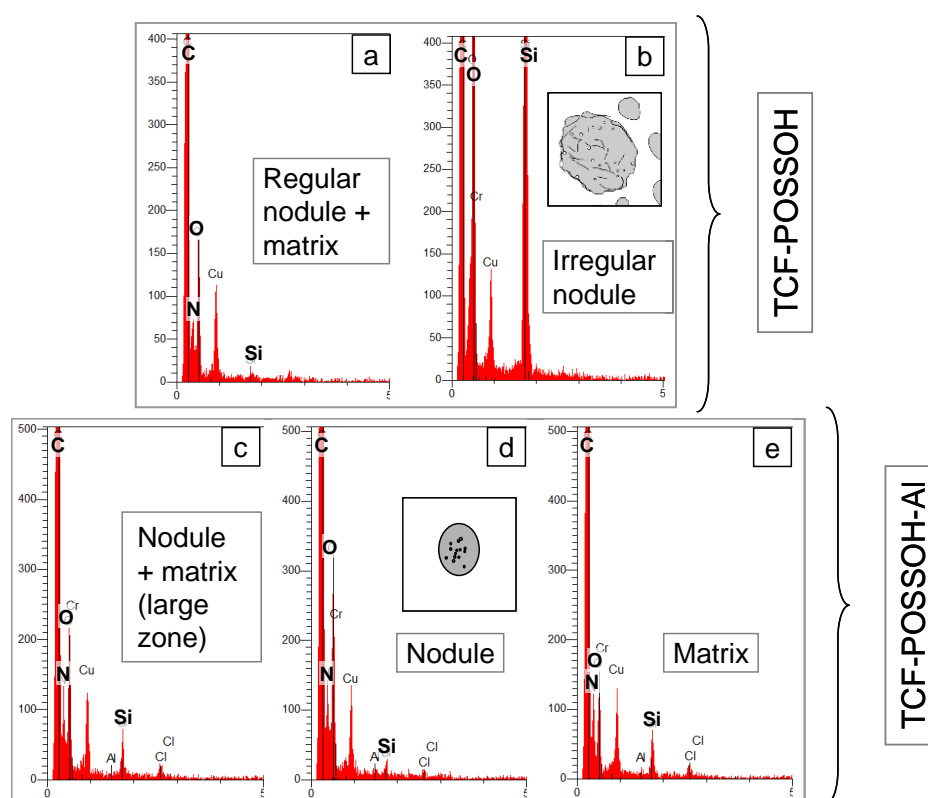


**Figure V-19 EDX analysis of TCF-POSSOH (a,b) and TCF-POSSOH-Al (c, d, e) containing 10 wt% (a/e=0.26) of PEI ; details on the analysed zones: a) zone of 2  $\mu\text{m}$  in diameter, targeting a ‘regular’ nodule and some matrix around, b) zone of 700 nm in diameter, targeting an ‘irregular’ nodule, c) zone of 10  $\mu\text{m}$  in diameter, comprising both matrix and nodules, d) zone of 700 nm in diameter, targeting a nodule, e) zone of 700 nm in diameter, targeting the matrix**

In the stoichiometric networks containing 23 wt% of PEI (Figure V-20), the epoxy-rich nodules (in white) were dispersed in a continuous PEI-rich phase. The nodules’ size in the TCF-POSSOH network ranged around 1  $\mu\text{m}$ . There was greater size dispersion in the TCF-POSSOH-Al network as seen from Figure V-20 b., where the nodule diameter ranged between

0.8 and 6.5  $\mu\text{m}$ . In addition, in both networks the presence of tiny epoxy-rich nodules in the PEI phase – less than 200 nm in diameter – evidenced late phase separation process in these zones which could be due to local variations of the concentration of the components and possibly a fast curing rate. In both networks, the POSSOH could be located neither in the PEI-rich nor in the epoxy-rich phase. Presumably, this meant that the POSSOH was dispersed too finely to be observed under TEM, that is to say POSSOH domain size may be of the order of nanometres – thus probably molecularly dispersed.

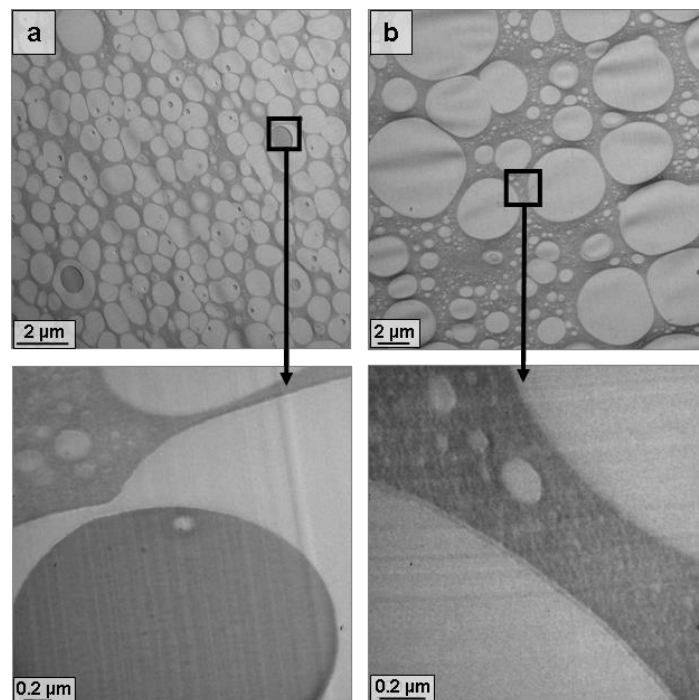


**Figure V-20 TEM observation of networks containing 23 wt% PEI (a/e=1), a) TCF-POSSOH, b) TCF-POSSOH-AI**

The absence of separated POSSOH structures in the TCF-POSSOH-AI network, as in the corresponding network containing 10 wt% of PEI, could be explained by the same hypothesis as before – i.e. POSSOH-epoxy covalent bonding or stop of the phase separation due to a fast curing rate. However, for the TCF-POSSOH networks, there was no obvious reason why the POSSOH should be better dispersed in the network containing 23 wt% of PEI than in the corresponding 10 wt% PEI-containing network. An explanation for the absence of phase-separated POSSOH domains in the PEI-rich phase might be that the POSS was better dispersed in TCF-POSSOH containing 23 wt% of PEI simply due to the higher amount of PEI.

## **4. INVESTIGATION OF THERMAL STABILITY AND FIRE RETARDANCY OF A COMPLEX THERMOSET/THERMOPLASTIC FORMULATION CONTAINING POSS**

### **4.1. INFLUENCE OF THE CURATIVE FIBRE ON THE THERMAL STABILITY AND THE FIRE PERFORMANCE OF EPOXY NETWORKS**

The influence of the presence of PEI in the epoxy networks on their thermal stability and fire behaviour could be highlighted by comparing data obtained for the TGDDM-MDEA network (TM) and the TGDDM-MDEA network in which 10 wt% of PEI has been introduced (TM-PEI). This PEI content was selected as it gave rise to networks where the main phase was the thermoset polymer, while the networks containing 17 or 23 wt% of PEI led to materials presenting a thermoplastic character. One must keep in mind that for the 10 wt% PEI- and 17 wt% PEI-containing networks, the stoichiometric ratio was less than 1.

The influence of the CF composition – apart from the PEI it contained – was revealed by comparing the TM-PEI network and the TCF network containing 10 wt% of PEI introduced by the CF. For such comparisons to be representative, the networks were produced through the same process, they contained the same content of PEI (10 wt%) and the stoichiometric ratio was kept equal in all the networks to the one of the TCF<sub>10%</sub> network, where the CF content imposed a ratio of 0.26.

- Thermal stability : influence of PEI and curative fibre content

The thermal stability of neat PEI, the CF and the networks mentioned earlier was assessed by thermogravimetry. The degradation profiles are shown in Figure V-21 and the related data in Table V-3.

Under nitrogen atmosphere, the PEI started losing weight above 500 °C, and thus was expected to retard the degradation onset in the PEI-containing networks as compared to the neat epoxy-amine network (TM). However, the onset degradation of the PEI-containing networks, TCF and TM-PEI, was decreased of about 10 and 15 °C, respectively, maybe because of the PEI being dispersed as microscopic and sub-microscopic domains. However, the presence of PEI in the epoxy networks almost tripled the residue amount at 700 °C as compared to the neat epoxy-amine network (TM).

The neat CF started degrading early around 230 °C under nitrogen, against more than 300 °C and 500 °C for the thermoset networks and the neat PEI, respectively. This early degradation

onset was due to the curing agents the CF contained which represented 55 wt% of the fibre. It decomposed in two main steps, and left a residue of ca. 25% at 700 °C. The degradation profiles of the TCF and the TM-PEI networks were very similar, indicating that the composition of the CF – hardener(s) and other potential additives – did not influence significantly the degradation pathway of the network, as compared to a TGDDM-based network cured with MDEA.

Under air atmosphere, no or a negligible residue was left after the degradation of the PEI, the CF and the networks. The onset degradation temperatures were slightly lowered in presence of PEI or CF, as under inert atmosphere, and the TCF and TM-PEI networks presented very similar degradation profiles.

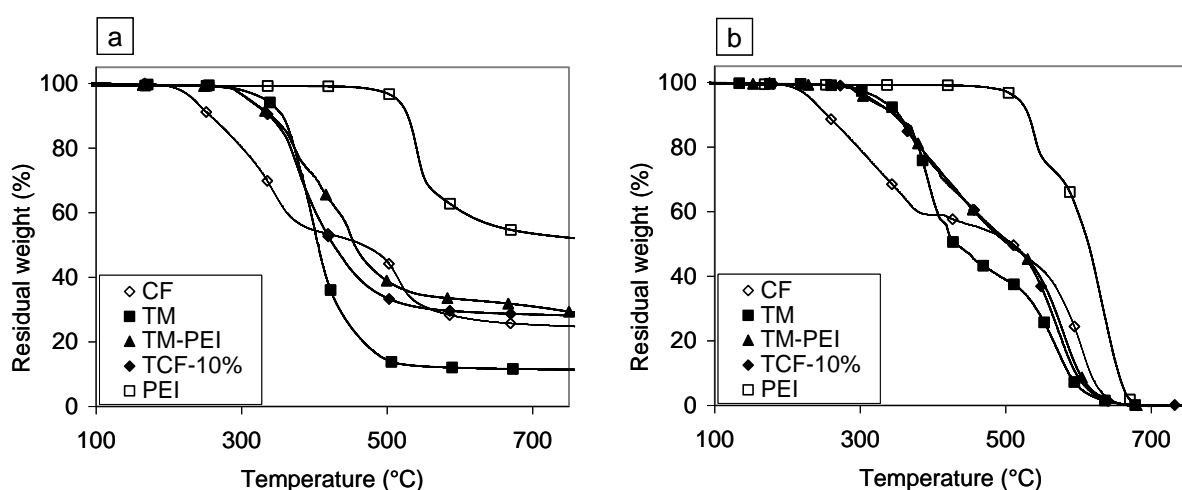


**Figure V-21 TGA curves of the curative fibre (CF) and TGDDM-based matrices, neat or with 10 wt% PEI a) in nitrogen atmosphere and b) in air atmosphere**

	Nitrogen atmosphere			Air atmosphere		
	T <sub>5%</sub> [°C]	T <sub>50%</sub> [°C]	Residual percentage [%]	T <sub>5%</sub> [°C]	T <sub>50%</sub> [°C]	Residual percentage [%]
PEI	514	-	52.3	516	614	0.0
CF	234	466	25.3	232	509	0.0
TM	323	399	10.8	326	431	0.0
TM-PEI	311	455	31.0	309	502	0.0
TCF <sub>10%</sub>	310	427	28.5	315	508	0.1

**Table V-3 TGA data of the curative fibre (CF) and TGDDM-based matrices, neat or with 10 wt% PEI**

In order to highlight the influence of the CF content on the thermal stability of the networks, the characteristic TGA data of TCF systems with different CF contents – i.e. different PEI contents and stoichiometric ratios – were gathered in Table V-4. The TCF networks are designated by

their PEI content, indicated in subscript. The main trend revealed by these data was the increase of the onset degradation temperature when increasing the CF content – i.e. increasing the PEI and curing agent(s) contents. During the ramp-up, the off-stoichiometry networks were likely to be subjected to ‘postcuring’, similarly to what occurred during the DSC ramps (see section 3.1. ), before starting to degrade from about 300 °C. The onset of degradation occurring at lower temperature in these networks, as compared to the stoichiometric TCF<sub>23%</sub>, highlighted the fragility of the bonds formed during ‘postcuring’. Thus, the variations of the degradation onset temperatures could be attributed to the influence of the crosslinking agent, forming more stable covalent bonds with the epoxy, probably due to the presence of heteroatoms, e.g. nitrogen for amine compounds. As concerns the char residue, they were negligible at the end of the degradation under air, and around 25-30% in inert atmosphere. They tended to decrease with the CF increasing, which was unexpected as the higher the CF content, the higher the PEI content – and the higher the residue amount should have been.

	Nitrogen atmosphere			Air atmosphere		
	T <sub>5%</sub> [°C]	T <sub>50%</sub> [°C]	Residual percentage [%]	T <sub>5%</sub> [°C]	T <sub>50%</sub> [°C]	Residual percentage [%]
TCF <sub>10%</sub>	310	427	28.48	315	508	0.10
TCF <sub>17%</sub>	316	431	27.04	320	498	0.18
TCF <sub>23%</sub>	344	447	24.63	345	515	0

**Table V-4 Characteristic data from TCF matrices, with different contents of CF (and thus of PEI)**

- Fire retardancy : networks containing 10 wt% PEI

The TM network and the networks containing 10 wt% of PEI, introduced either by the CF or on purpose, were subjected to the cone calorimeter test. The Heat Release Rate (HRR) curves displayed in Figure V-22 showed that all the networks burnt producing a very sharp and intense HRR peak. This curve shape is representative for thermally thin samples [24], which was the case for these samples – 1 mm in thickness. From the HRR curves, it was clear that the presence of PEI in the thermoset networks did not bring improvements in terms of fire retardancy – comparison between TM and TM-PEI. The data reported in Table V-5 further confirmed it: the Time of Ignition (TTI) and the RW (Residual Weight) were reduced, the peak of HRR and the Total Heat Released (THR) were increased. The only positive point was the reduced smoke yield (TSR). The poor fire performance of the TM-PEI network, as compared to the TM network, was unexpected considering that the intrinsic flammability of PEI was lower than that of epoxy (see chart in Figure V-2). Finally, the TCF gave similar results as the TM-PEI

network, highlighting no positive or detrimental effect of the potentially different crosslinking agent and additives.

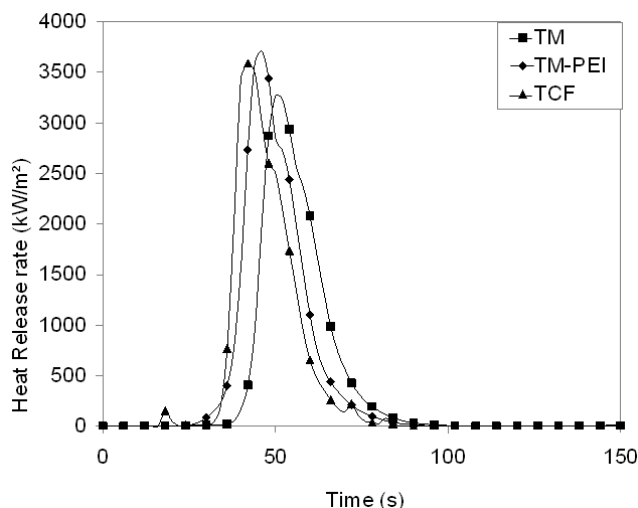


**Figure V-22 Comparison of representative HRR curves of TGDDM-based networks, neat or with 10 wt% of PEI**

System	TTI (s)	THR (MJ/m <sup>2</sup> )	pHRR (kW/m <sup>2</sup> )	TSR (m <sup>2</sup> /m <sup>2</sup> )	RW (%)
TM	41 (4)	60.2 (0.1)	3173 (129)	1242 (145)	19.6 (0.1)
TM-PEI	33 (5)	66.1 (2.9)	3740 (135)	916 (92)	17.2 (0.3)
TCF	33 (6)	62.7 (1.8)	3969 (535)	1061 (21)	14.9 (0.1)

**Table V-5 Cone calorimeter data of TGDDM-based networks, neat or with 10 wt% of PEI**

#### 4.2. INFLUENCE OF ADDITIVES ON THE THERMAL STABILITY AND THE FIRE PERFORMANCE OF EPOXY NETWORKS

- Thermal stability

In Table V-6 are presented the TGA results of the networks containing 10 wt% of PEI, with or without the POSSOH and the aluminium-based catalyst. The data highlighted no influence of the additives, with very similar values of degradation temperatures and residues at 700 °C.

	Nitrogen atmosphere			Air atmosphere		
	T <sub>5%</sub> [°C]	T <sub>50%</sub> [°C]	Residual percentage [%]	T <sub>5%</sub> [°C]	T <sub>50%</sub> [°C]	Residual percentage [%]
TCF	310	427	28.48	315	508	0.10
TCF-POSSOH	314	428	28.58	315	521	2.59
TCF-POSSOH-AI	320	438	28.52	319	512	2.85

**Table V-6 TG data of TCF-based networks containing 10 wt% of PEI**

- Fire behaviour

The HRR curves and cone calorimeter data (Figure V-23 and Table V-7, respectively) speak for themselves. The addition of POSSOH alone resulted in a slight increase of the THR and pHRR, though the TTI, the TSR and the RW were slightly improved. The TCF-POSSOH-AL network displayed an astonishing reduction of the pHRR – minus 86% as compared to the TCF network – but also a reduction in THR, TSR and a large improvement of the residual weight, from about 15% in TCF to close to 42%.

The fact that the POSSOH alone did not enhance the fire performance of the networks was actually very similar to what was observed in the MVR-based networks. In the present case, an explanation could be the preferred location of the POSSOH in the PEI-rich nodules (see section 3.2.b. ), leaving few POSS in the thermoset matrix which gave the final material its properties.

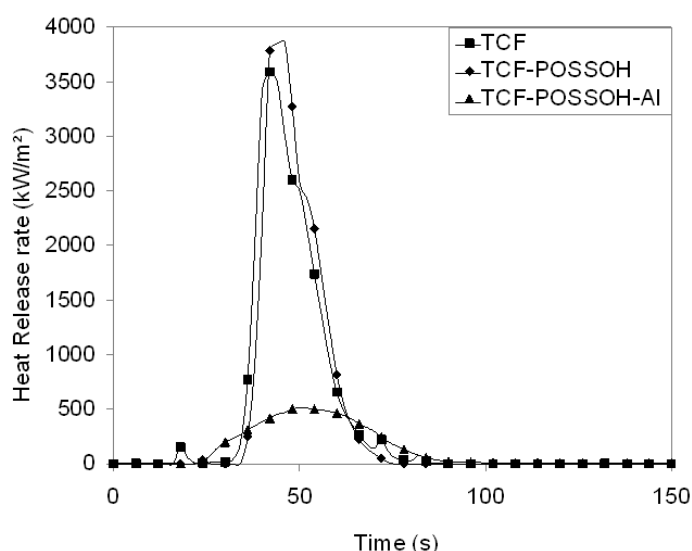


**Figure V-23 Comparison of HRR curves of TCF-based networks with 10 wt% of PEI**

System	TTI (s)	THR (MJ/m <sup>2</sup> )	pHRR (kW/m <sup>2</sup> )	TSR (m <sup>2</sup> /m <sup>2</sup> )	RW (%)
TCF	33 (6)	62.7 (1.8)	3969 (535)	1061 (21)	14.9 (0.1)
TCF-POSSOH	37 (0)	86.5 (22.0)	4281 (378)	946 (122)	15.1 (2.2)
TCF-POSSOH-AI	32 (4)	20.4 (0.8)	564 (75)	926 (94)	41.8 (0.7)

**Table V-7 Cone calorimeter data of TCF-based networks with 10 wt% of PEI**

The char residue pictures are displayed in Figure V-24. The high residual weight obtained for the TCF-POSSOH-AI could be explained by a phenomenon of intumescence, similarly to what was reported for the TGDDM-based networks in Chapter IV. A highly-swollen residue was obtained, while the TCF and TCF-POSSOH networks yielded a thin carbonaceous crackled

crust, as shown in Figure V-24 e and f. A closer look to the TCF-POSSOH-Al residue surface (Figure V-24 g) revealed a crackled crust which let appear a spongy structure that filled the interior of the char. Though the surface was crackled, this thick char layer could play its barrier role, probably through the formation of alveolus trapping the volatiles, as described for the TM-POSSOH-Al network in Chapter IV. The thickness of the layer certainly insulated the material from the radiant heat.

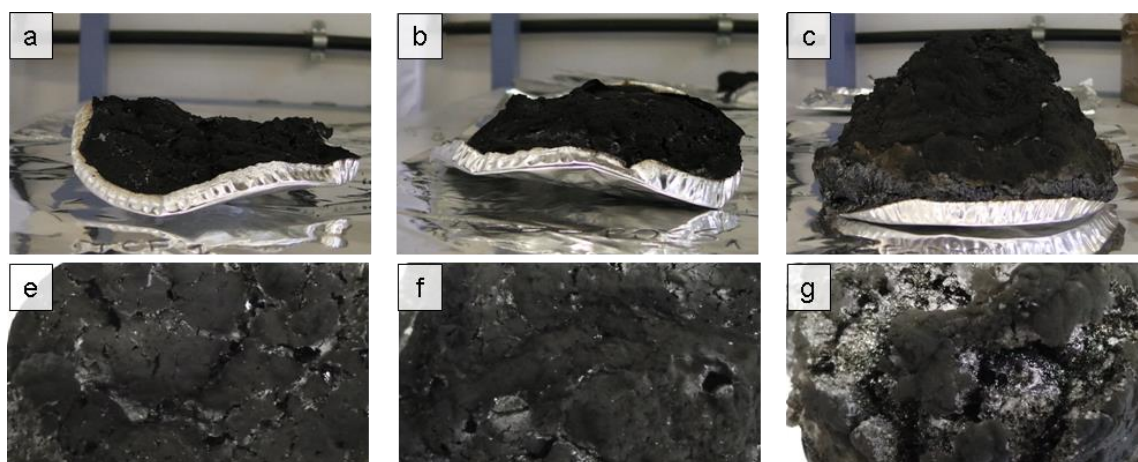


**Figure V-24 Cone calorimeter residues of a) TCF, b) TCF-POSSOH, c) TCF-POSSOH-Al. Photographs e) f) and g) are closer views of the char surface of TCF, TCF-POSSOH and TCF-POSSOH-Al, respectively**

## 5. CONCLUSION

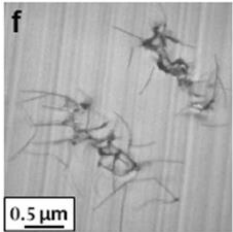
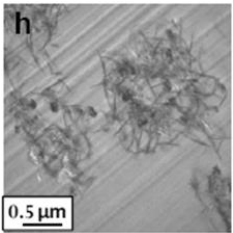
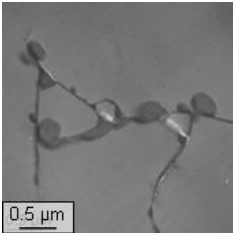
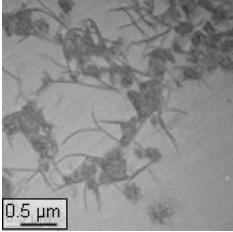
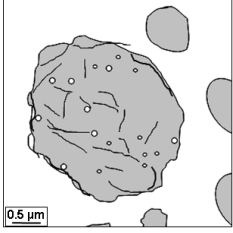
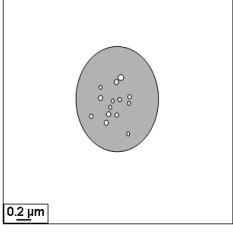
Networks based on a high-performance epoxy prepolymer, TGDDM, and three contents (110, 66 and 28 phr) of a curative fibre containing PEI and the crosslinking agent(s) were produced. The POSSOH, with or without the Al catalyst, was introduced in the 'usual' amount in these systems as a fire retardant.

The phase inversion caused by high PEI fraction was observed and networks with an epoxy matrix were obtained for a CF content such as the PEI content was equal to 10 wt% and the stoichiometric ratio to 0.26. The glass transition logically decreased with the stoichiometric ratio, but in a much lesser extent when adding the POSSOH with the Al catalyst, indicating that their combined presence promoted TGDDM homopolymerization and/or condensation reactions between epoxy and the POSSOH silanol functions. For this particular system, a post-cure at higher temperatures even allowed the system deficient in crosslinking agent to reach the same value of T<sub>g</sub> as the network where the stoichiometry was respected, which was an unexpected and remarkable effect.

The introduction of PEI via the curative fibre did not improve the fire behaviour of the networks, but the combination of POSSOH and the Al catalyst did bring spectacular improvements of the main cone calorimeter measured parameters, through a mechanism of intumescence. Similarly to the TGDDM/MDEA- and the MVR444-based networks, the fire protection mechanism relied on the physical role of barrier and thermal insulation played by the thick spongy char layer. The relationship with the morphology is to be discussed in connection with other TGDDM-based networks. Representative TEM images or schemes of the morphologies of the networks containing POSSOH, with or without the aluminium-based catalyst, were gathered in Table V-8, together with the main features of their fire performance, as assessed via the UL 94 and the cone calorimeter tests. The comments regarding the fire behaviour of the networks are related to that of the reference networks without POSSOH – not included in the table.

In the TCF-POSSOH-Al network, the morphology was totally different than in the TGDDM/MDEA- and the MVR444-based networks, firstly due to the presence of PEI, but also due to POSSOH organisation. In particular, the arrays of filaments and nodules of POSSOH observed via TEM in the TM- and MVR- based networks were not visible in the TCF-POSSOH-Al material. In the latter, the POSSOH was predominantly located in the epoxy-based matrix as indicated by the EDX analysis, and the absence of POSS domains argued in favour of a molecular dispersion, potentially due to POSSOH/epoxy condensation reactions. The presence of the POSSOH in the main epoxy-rich phase, which was predominant in the build-up of the properties of the final material, could then be the reason for the enhanced fire behaviour of this network. It was consistent with the predominant location of the POSS in the PEI-rich phase in the TCF-POSSOH network, which presented poor fire behaviour. The presence of the POSSOH in the matrix could then be a condition *sine qua non* for a good fire behaviour, and the occurrence of intumescence in the TGDDM-based networks.

However, this condition was not sufficient to obtain a fire-retardant material, as seen from the TGDDM/MDEA- and MVR444-based networks containing POSSOH only and which presented a poor fire-retardant behaviour. Indeed, in these networks, the structures developed by the POSSOH were rather similar to those observed in the corresponding materials where the aluminium-based catalyst was introduced in addition to POSSOH. This further underlined the necessity of having both the POSSOH and the catalyst to obtain a consistent improvement in the fire behaviour. It also showed that the morphology adopted by the POSS – phase-separated, as in the TM and MVR networks, or molecularly dispersed, as in the TCF-POSSOH-Al material – might not be that critical for the fire behaviour of the resulting material, at least in the studied systems.

	Morphology (TEM)	Fire behaviour	
	TEM	UL 94	Cone Calorimeter
TM-POSSOH-130		No improvement	Limited reduction in pHRR (-20%)
TM-POSSOH-AI		Remarkable improvements: self-extinguishment, very limited propagation of the flame, high residue amount	Reduction of pHRR (-30%) High amount of swollen char residue with alveoli structure
MVR-POSSOH-130		No improvement	No improvement
MVR-POSSOH-AI		Limited improvements but visible 'intumescing' features (swollen residue)	Remarkable reduction of pHRR (-54%) High amount of swollen char residue with alveoli structure
TCF-POSSOH		-	No improvement
TCF-POSSOH-AI		-	Spectacular reduction of pHRR (-86%), THR, smokes... High amount of swollen char residue

**Table V-8 Summary table : morphology and fire behaviour of TGDDM-based networks containing POSSOH**

Despite the uncertainties in the actual fire behaviour mechanism, the TCF-POSSOH-Al system constitutes a promising alternative for PEI-reinforced epoxy networks and opens great perspectives as concerns composites produced by commingling. The use of a curative fibre containing high-performance thermoplastic, in which additives such as the POSSOH and the Al catalyst could be included, would be an efficient solution both for the improvement of certain mechanical properties and for the enhancement of the fire retardancy.

However, two main issues have to be thought about and finally overcome:

- the fire-retardant effect of the POSSOH and the Al catalyst relying on a physical effect, namely the intumescence of the polymer, the presence of the reinforcement in composite part may hinder the swelling and thus negate the fire-retardant power of these compounds;
- as mentioned in the introduction, the commingling process has to be well set up in order to obtain reliable parts. At the present stage of the Fire-Resist project, the commingling has caused problems due to the fragility of the curative fibre, and no composite parts could be produced.

---

## CONCLUSIONS AND OUTLOOKS

---

The work and reflexion presented herein aimed at giving an insight into the structure and fire behaviour of the hybrid POSS-containing epoxy-amine networks. The initial main objectives were to establish the structure/property relationships existing in such materials and to understand the potential fire retardancy mechanisms. To fulfil these goals, several POSS and various dispersion processes were selected in order to generate POSS-modified epoxy-amine networks with varied morphologies, without losing sight of the main desired goal, i.e. the improvement of the fire-retardancy of the final materials. Low contents of POSS were introduced into the networks, allowing easy processing with no use of solvents. Processes implemented for dispersing the POSS in the epoxy prepolymers were either heat solubilisation or high-shear mixing. However, heat solubilisation involved the breakage of initial POSS-POSS interactions and required sometimes heating at high temperatures, which is not desirable for future applications of the systems.

Through the use of either multi-functional POSS or inert POSS, the objectives were to generate different morphologies which could then be related with the fire behaviour of the networks. However, the structure of the POSS varied as well, and should be taken into account when interpreting the fire behaviour. In this work, the addition of an inert POSS (the isooctylphenyl POSS) into the epoxy-amine matrix gave rise to poorly dispersed POSS-based morphology, while the use of the amine-multifunctional POSS (the N-phenylaminopropyl POSS) resulted in a molecular-scale dispersion through the reaction of the amine functions of the POSS with the epoxies of the network. The associated fire behaviour was either surprisingly enhanced in the former case, leading to self-extinguishment in the UL 94 configuration, or very similar to the fire behaviour of the neat epoxy-amine matrix in the latter case.

An significant effort has been dedicated to the study of an intermediary type of POSS – the triSilanolPhenyl POSS. Such an interest for this particular POSS was first justified by its potential versatility: the initial idea was to diversify the morphologies created by this POSS by

implementing several processes – i.e. high-shear mixing and heat solubilisation with or without the addition of an aluminium-based catalyst. The objective of doing so was to actually understand the role of the morphology on the fire performance, while keeping the same chemical structure of the POSS. The catalyst was supposed to assist in grafting the POSS to the epoxy network, thus creating a molecular dispersion state or at least smaller-scale structures as compared to the systems where the catalyst was not introduced.

The actual observation of the final materials revealed that, more than the process implemented, the type of epoxy prepolymer was the first order parameter governing the final morphology of the networks. While conventional nodule-shaped structures were revealed through the observation of networks based on the most widespread type of epoxy prepolymer (DGEBA), novel structures made of POSS consisting of clusters of filaments' webs with embedded nodules were discovered in the networks based on an epoxy prepolymer for high performance composite materials (TGDDM). The observation of the evolution of the morphology during curing showed that the formation of such structures occurred before gelation, starting from POSS aggregates with the filaments developing afterwards. This potentially implied a condensation of POSS upon itself, which was also suggested by the results from solid-state  $^{29}\text{Si}$  NMR for the DGEBA-based networks.

However, the process implemented, and in particular, the addition or not of an aluminium-based catalyst, proved to be determinant as concerns (i) the kinetics of the epoxy-amine polymerization and (ii) the fire behaviour of the final networks. On a kinetic and reactivity point of view, the addition of combined POSS and aluminium-based catalyst has proved to significantly accelerate the epoxy-amine polymerization, and even favour epoxy homopolymerization. This presented an interest as it could allow to obtain fast-curing or off-stoichiometry systems with similar or close final thermal properties as the neat matrices – see TGDDM/curative fibre-based networks in Chapter V.

Despite little changes in morphology – examined via SEM, TEM and EDX – when introducing the aluminium-based catalyst in addition to the POSS, fire retardancy was subjected to a systematic large improvement when both compounds were present. The mechanism involved in the fire protection also depended on the epoxy prepolymer nature: an intumescent phenomenon was observed in the TGDDM-based network that did not occur in the DGEBA-based material, despite the important fire retardant potential observed in this network as well. Investigation of the residues after combustion revealed their alveolar structure, which is at the origin of a physical barrier mechanism, impeding both volatile and heat transfers. This physical phenomenon was likely to be caused by a chemical mechanism occurring only in presence of

both the POSS and the aluminium-based catalyst, but which also required a specific chemical structure of the epoxy prepolymer.

From the comparison of the different networks based on the TGDDM prepolymer, in particular with the PEI-containing epoxy materials, clues could be brought out as concerns the fire behaviour-morphology relationship. It seemed that the presence of POSSOH in the main epoxy phase could be a mandatory – but not sufficient – condition in order to obtain improvements in the fire retardancy of the materials.

The present work thus does not allow to reach a complete and general conclusion on a potential structure-property relationship as concerns the fire behaviour of epoxy networks, but it does provide an interesting two-component fire retardant that is potentially applicable to a range of epoxy formulations. It has been validated not only on simple model epoxy-amine systems, but also on a commercial formulation and a complex system involving a thermoset/thermoplastic blend. The study of this particular case also demonstrated the nil fire-retardant power of PEI in the epoxy-amine network, despite the intrinsic lower flammability of the thermoplastic polymer.

As concerns the application targeted within the Fire-Resist project, namely the production of light-weight, high-performance fire retardant composites, two of the developed POSSOH-containing, epoxy-based formulations were selected for production of carbon or glass fibre-reinforced composite panels by infusion – Appendix D. The introduction of a reinforcement brought additional considerations as concerns: *(i)* the development of potential interactions between the POSS and the fibres and the consequences on the generated morphologies and interfaces, and *(ii)* the effect of the reinforcement on the fire-retardant mechanism as compared to the non-reinforced networks. In particular, the presence of the fibres proved to be an obstacle to the development of the fire retardant mechanism by hindering the development of intumescence in the MVR444-based composites.

As concerns the present study, it remains to evidence and understand the mechanism by which intumescence occurs in certain networks. In particular, the role of the aluminium catalyst and of the nature of the epoxy prepolymer is still to be understood. A thorough molecular analysis of the char, giving information about the char structure and composition, could be a first step towards an explanation of the phenomenon. Another strategy would be to test different catalyst concentrations and various metal-based compounds in order to bring out a potential influence of the catalyst nature on the fire behaviour of the final material.

There is also a real need to understand the development of the particular morphology observed in TGDDM-based networks, and even to clearly identify the structures and the interactions. The difficulty to be overcome here consists of finding an experimental technique sensitive enough to detect changes induced by the low quantity of POSS introduced in the networks. In a first phase, working on incomplete systems – as was attempted in the work presented in Chapter III – or with mono-functional compounds could allow to perform liquid-state NMR. However, greater quantities of POSS would still be required in order to be within the detection limits, which adds considerations about the solubility of the POSS in the epoxy. Another possible track to follow would be the in-situ monitoring of infra-red absorption during polymerization, especially of bands attributed to bonds involving the silicon element. However, there is still the issue of the sensitivity limit of the technique, and the high peak concentration of infrared spectra does not help detecting very small peak variations. As concerns the development of the morphology, even if it may not allow to actually provide information about POSS-involving interactions, investigation of the networks by in-situ Small Angle X-Ray Scattering technique (SAXS) could be of interest.

The particular issue of a potential relationship between morphology and fire behaviour could probably be better investigated by producing networks in which the only varying parameter would be the morphology – i.e. with no variation in composition. The morphologies should then be well-controlled, but also present significant changes in order to highlight a potential influence on the fire behaviour of the final material. This was what was targeted originally, but the study demonstrated that more thorough means of control should be implemented to obtain the desired morphology, for example by introducing additional POSS/epoxy pre-reaction steps with validation procedures in order to check for the effective implementation of the desired reactions. Controlling the kinetics of polymerization, via the curing temperatures and heating rates, could also allow to design the morphology, to a certain extent, by controlling the reaction-induced phase separation phenomenon.

The Silsesquioxanes proved to be compounds of interest for the fire-retardancy of epoxy-based networks. The diversified range of Silsesquioxanes, not limited to the ligand nature of POSS, allows a number of configurations to be investigated such as silsesquioxanes with other geometries – e.g. linear structures with the synthesis of POSS copolymers, or random, network structures with the introduction of a sol-gel organic-inorganic glass in the epoxy-amine networks. As highlighted in Chapter I, the interest and potential of synergistic combinations of Silsesquioxanes with other elements, in particular phosphorus, is not to be neglected as it could constitute a good compromise allowing to counter the sometimes-not-efficient-enough fire

retardant potential of silsesquioxanes. Finally, the effect of the concentration of additives deserves to be investigated in order to select the optimum content for a material with good balance of properties – not only with an improved fire retardancy. In all cases, the study of the morphology should be carried out as it presents a real interest on the scientific point of view, but also for future applications, as concerns for example the compatibility with certain processing requirements.



---

## APPENDIX A – EXPERIMENTAL TECHNIQUES

---

### 1. SIZE EXCLUSION CHROMATOGRAPHY (SEC)

Size Exclusion Chromatography, used to assess purity of the POSS powders and for the reaction kinetic studies, was performed in tetrahydrofuran (THF), with a flow rate of 1mL/min. Columns were Waters ultrastryragel HR0.5, HR1, and HR2. Detection was done using a refractive index detector (Shimadzu RID 10A). The spectra were always normalised by the concentration of the sample solutions when they were used for comparison.

### 2. GEL TIME

The gel times of the reactive systems were determined via chemorheology and the parallel-plates method. Six frequencies were implemented (1, 5, 10, 20, 30 and 40 Hz); the gelation time was given by the point of crossing of the  $\tan\delta$ -vs-time curves at the different frequencies as (Chambon & Winter criteria, [142]). The gel time were measured either at 90 °C or 135 °C.

### 3. DIFFERENTIAL SCANNING CALORIMETRY (DSC)

DSC analysis was performed using a DSC Q20 or DSC Q10 from TA Instruments under inert atmosphere (nitrogen), the scan rate being of 10K.min<sup>-1</sup> and the temperature range of 25-250 °C. The middle point of the glass transition domain, as given by the analysis tool of Universal Analysis (TA Instruments software), was taken as the value of glass transition temperature. In certain cases, the heat capacities  $C_p$  before and after the glass transition were also measured.

### 4. NEAR INFRARED SPECTROSCOPY (NIRS)

A FT-NIR Equinox 55 spectrophotometer from Bruker and the associated OPUS software were used for recording spectra between 4500 cm<sup>-1</sup> and 10,000 cm<sup>-1</sup>. A heating cell designed for glass tubes of 5 mm of external diameter was mounted in the spectrometer. It was set at 90 °C and let to stabilize for at least one hour before starting the experiment. The gain was set at a value of 2 and the filter used was a grid. The resolution was set to 4 cm<sup>-1</sup>, and 32 scans were

collected for each measurement. The backgrounds were performed on an empty glass tube in the same conditions as for the experiment.

After collection, all the spectra were subjected to a concave elastic baseline correction. The integration methods were varied according to the shape of the peaks and their environment.

## **5. VISCOSITY MEASUREMENTS**

An Anton Paar rheometer Physica MCR 301 was used to determine the viscosity of reactive systems (results presented in Appendix D). The configuration used was the cone-plate geometry (50 mm in diameter, 4°) with a constant shear rate of 5 s<sup>-1</sup> and at a given temperature, controlled by the heating plate. The viscosity was measured every 30 seconds.

## **6. DYNAMIC MECHANICAL ANALYSIS (DMA)**

The dynamic thermo-mechanical behaviour of the networks was characterized using a Rheometric Dynamic Analyser (RDAII) in the rectangular torsion configuration. The rectangular samples (30x5x5 mm) have been submitted to a constant torsion at a frequency of 1 Hz and over a range of temperature of 25-250 °C with a rate of 3 K.min<sup>-1</sup>.

## **7. WIDE ANGLE X-RAY DIFFRACTION (WAXS)**

Wide Angle X-ray Diffraction was performed using Bruker D8 advance X-ray diffractometer, operated at 33 mV and 45 mA and CuK $\alpha$  radiation. The step size and the step time were 0.02° and 67.04s, respectively. Both the POSS powders and the POSS-containing networks were analysed. In the case of the networks, the plates produced had a smooth surface. Therefore, squared specimens (15 mm edge) were cut from these plates and directly analysed by XRD.

## **8. SCANNING ELECTRON MICROSCOPE (SEM)**

Scanning Electron Microscopy examinations were carried on using a Jeol JSM 6400 microscope and a FEI Quanta 250, at an acceleration voltage ranging from 5 to 20kV, on samples fractured in liquid nitrogen and coated with gold, carbon or a gold/palladium mixture.

## **9. TRANSMISSION ELECTRON MICROSCOPY (TEM)**

Transmission Electron Microscopy observations were carried out using a Philips CM120 at an acceleration voltage of 80kV. The samples were trimmed using a ultramicrotome machine at room temperature, except if specified otherwise.

## 10. ENERGY DISPERSIVE X-RAY SPECTROSCOPY (EDX)

The EDX analyses were carried out during either the SEM or the TEM observations.

## 11. CLOUD-POINT MEASUREMENTS

In this study, the experimental apparatus for cloud-point measurements consisted of a visible light source emitting a ray that passes through the sample test tube, which is placed in an oven controlled by feedback from the system temperature (Figure A-1). The transmitted light is then quantified by a receptor at the exit of the oven. Isothermal measurements were carried out. The light was attenuated when the phase separation occurred as a result of the difference of the refractive index of both phases.

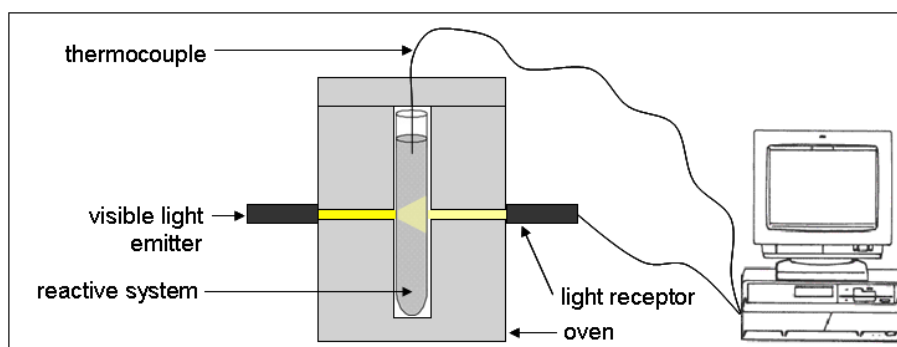


Figure A-1 Schematic diagram of the device used for the cloud-point measurement

## 12. SOLID $^{29}\text{Si}$ NMR

The  $^{29}\text{Si}$  cross-polarization magic-angle spinning (CP/MAS) NMR spectra were measured at 11.7 T using a BrukerAvance III HD 500 US/WB NMR spectrometer (Karlsruhe, Germany, 2013). The finely powdered samples were placed into the 4-mm  $\text{ZrO}_2$  rotors and the spinning frequency was always 12 kHz. Duration of cross-polarization contact time was 3 ms and the number of scans was ranging from 1024 to 2048 to reach acceptable signal-to-noise ratio.

## 13. THERMOGRAVIMETRIC ANALYSIS (TGA)

TGA analyses were performed with a TGA Q500 from TA Instruments, under air or inert atmosphere. The temperature range was of 20 to 800 °C, the ramp rate of 10 °C/min. The specimens were placed in a platinum holder.

## **14. UL 94 TEST**

The UL-94 test was performed according to the standard ASTM D3801 (ref). A blue flame of 20 mm was applied during ten seconds on the rectangular specimens (13x125x4.2 mm<sup>3</sup>). If the specimen extinguished, a second ignition was performed. The times of afterflame were measured, as well as the residual mass of the tested specimens. Visual observation provided information on the eventual presence of flaming drops and ignition of the cotton placed under the specimen. The tests were filmed for a better visual observation, and pictures extracted from the videos. Five to six specimens were tested in this way for each system.

## **15. CONE CALORIMETER**

The cone calorimeter experiments were performed in Politecnico of Torino in Alessandria. Apart from systems presented in Chapter V, square samples of 100 mm by 100 mm were made out of the bigger manufactured plates and their edges were polished. The heat flow used during the test was of 50 kW.m<sup>-2</sup>. Four specimens were tested for each system.

---

## APPENDIX B – COMPLEMENTARY RESULTS RELATED TO TGDDM-BASED NETWORKS

---

### 1. TGDDM/MDEA-BASED NETWORKS CONTAINING POSSOH

#### 1.1. GEL TIMES

Gel times of TM-based systems are given in Table B-1. As for DM-based systems, the presence of both POSSOH and the Al catalyst accelerates the gelation. However, at 90 °C, the gelation took more time than the scheduled dwell step at 90 °C of 2 hours in the curing cycle of the networks. Thus, the gelation should occur during the dwell at 135 °C.

Temperature	System	Gelation time
135 °C	TM	1h 43min
	TM-POSSOH	1h 42min
	TM-Al	1h 28min
	TM-POSSOH-Al	40 min
90 °C	TM-POSSOH-Al	> 4h

**Table B-1 Gel times of TGDDM-based systems**

#### 1.2. DSC OF REACTIVE SYSTEMS

Reactive TGDDM-based mixtures were subjected to dynamic DSC scans (Figure B-1). The same effects as for the reactive DM-based systems were observed: the presence of POSSOH alone did not lower the temperature of exotherm but increased the specific exothermic energy. Combined presence of POSSOH and Al catalyst significantly decreased the temperature of exotherm, revealing a clear catalytic effect.

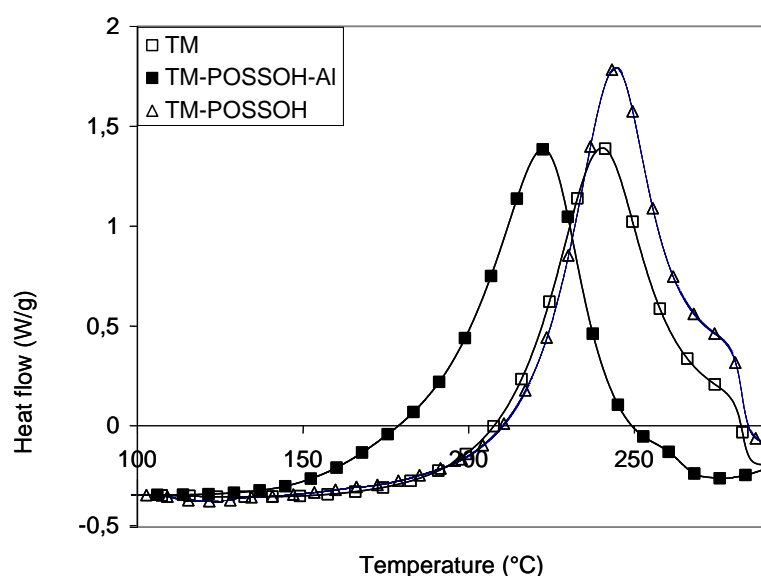


Figure B-1 Exotherms of reactive TGDDM-based systems (dynamic DSC scan, 10 °C/min)

### 1.3. DYNAMIC MECHANICAL ANALYSIS

Data extracted from the DMA measurements performed on the TGDDM-based networks are presented in Table B-2. The glass transition was decreased and significantly widened by the simultaneous addition of POSSOH and Al catalyst, while the rubbery modulus was increased.

Networks	$T_{\alpha}$ (°C)	$\Delta T_{h=1/2}$ (°C)	$G'_{T_{\alpha}+30^{\circ}\text{C}}$ (MPa)
TM	210	13	10.1
TM-POSSOH-130	209	15	12.5
TM-POSSOH-AI	197	21	13.7

Table B-2 DMA data of TGDDM-based networks

## 2. COMPLEMENTARY RESULTS RELATED TO MVR444-BASED SYSTEMS

### 2.1. MORPHOLOGY

In the MVR444-based networks, the morphology was assessed by means of Scanning and Transmission Electron Microscopies (SEM, TEM), displayed in Figure B-2 and Figure B-3, respectively. The structures developed by the POSSOH in the MVR networks are very similar to those present in the TGDDM-based networks. Observing by SEM revealed small nodules and aggregates of a few microns in size, and the TEM technique finally revealed the nature of these aggregates, i.e. arrays of filaments and nodules embedded in the epoxy matrix. The structures

developed in the Al-containing network were significantly better defined and smaller than the objects present in the network containing POSSOH only.

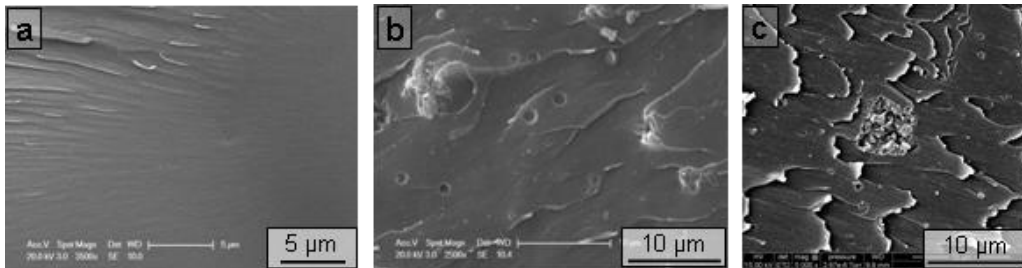


Figure B-2 SEM images of a) MVR, b) MVR-POSSOH-130, c) MVR-POSSOH-AI

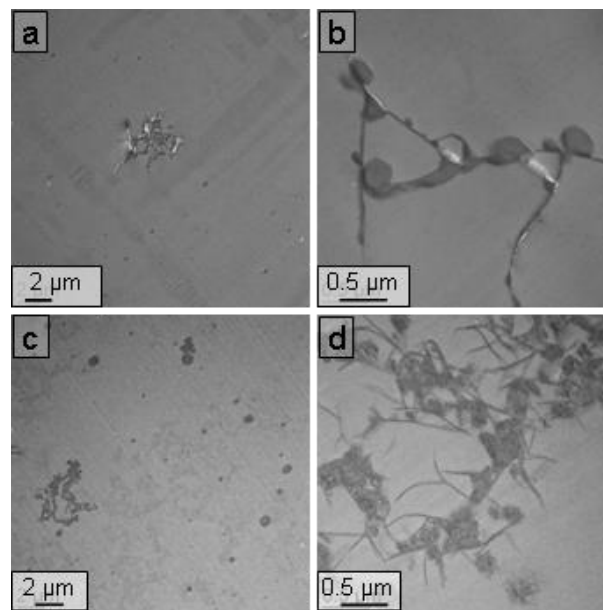


Figure B-3 TEM images of a), b) MVR-POSSOH-130 and c), d) MVR-POSSOH-AI

## 2.2. DYNAMIC MECHANICAL ANALYSIS

DMA were performed on MVR444-based networks and data are gathered in Table B-3. The most remarkable fact was the decrease of the glass transition width of the network containing both POSSOH and the Al catalyst. In the networks based on other types of epoxy, an increase of this value was observed, suggesting a more heterogeneous network in terms of molar mass of the segments between crosslinking points and chain end amount.

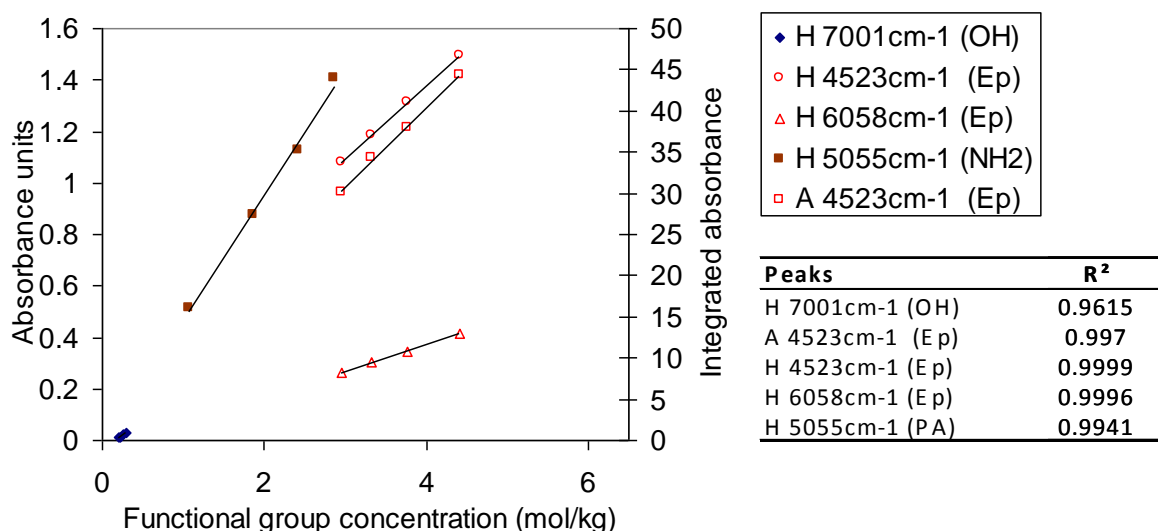
Networks	$T_{\alpha}$ (°C)	$\Delta T_{h=1/2}$ (°C)	$G'_{T_{\alpha}+30^{\circ}\text{C}}$ (MPa)
MVR	224	27	11.0
MVR-POSSOH-130	223	27	9.7
MVR-POSSOH-AI	205	18	7.7

Table B-3 DMA data of MVR444-based networks

## APPENDIX C – CALIBRATION AND COMPLEMENTARY RESULTS RELATED TO THE NIRS PRESENTED IN CHAPTER III

### 1. CALIBRATION PROCEDURE

Several mixtures of different proportions of DGEBA and MDEA were thus prepared and their NIR spectra recorded. The values of intensity or integrals of the various bands were plotted as a function of the concentration of the functional groups they are characteristic of in Figure V-25. These concentrations were calculated from the masses of products introduced in each mixture. The hydroxyl concentration, from the few oligomers existing in the epoxy prepolymer, was calculated from the Epoxy Equivalent Weight value provided by the supplier.



**Figure V-25 Dependence of the intensity and/or the area of various absorption peaks in the DGEBA/MDEA systems with the concentration of the functional groups (calculated). H stands for Height and A for Area. In the table is given the coefficient of determination (R<sup>2</sup>) from the linear regression associated to each peak.**

All the peaks verified the Beer-Lambert law (Equation C-1) by showing a clear proportionality between their intensity and/or their area with the products concentration and thus the concentration of the functional group they are characteristic of.

**C-1**

$$A = \varepsilon \ell c$$

where  $A$  is the absorbance,  $\varepsilon$  is the molar extinction coefficient,  $\ell$  is the pathlength, and  $c$  the concentration of the monitored species.

However, for most of the peaks, the relationship was not purely linear – i.e. a nil concentration gave a non-zero intensity or area of the peak – indicating a certain intensity bias introduced by the baseline, which had to be taken into account in the calculus of the concentrations at  $t=0$ .

In the case of the peak at  $7001\text{cm}^{-1}$ , which is characteristic of the  $-\text{OH}$  groups, the coefficient of determination for the linear regression was low, due to the fact that the concentration of the  $-\text{OH}$  groups in the non-crosslinked mixtures was very low. Thus, the intensity of the characteristic peak was low and likely to be biased by small measurements and baseline uncertainties. Given that, considering these uncertainties, the hydroxyl concentration provided no reliable information as concerns the epoxy-amine kinetics, the data from the peak at  $7001\text{cm}^{-1}$  won't be treated in the next parts of the study.

The initial concentrations of the functional groups of interest were thus calculated using the linear regression equations obtained from this calibration. They will be reported in the results part later on in this section.

The concentrations of the epoxy and primary amine groups in the post-cured samples were supposed equal to zero. The hypothesis according which the post-cured sample was fully crosslinked was verified by performing a DSC scan on these samples, with two successive heating ramps, which are plotted in Figure V-26. The glass transition temperature of the post-cured networks not increasing between the first and the second heat ramps indicated that the sample was already fully crosslinked, thus validating the hypothesis made on the concentrations of functional groups in the post-cured sample.

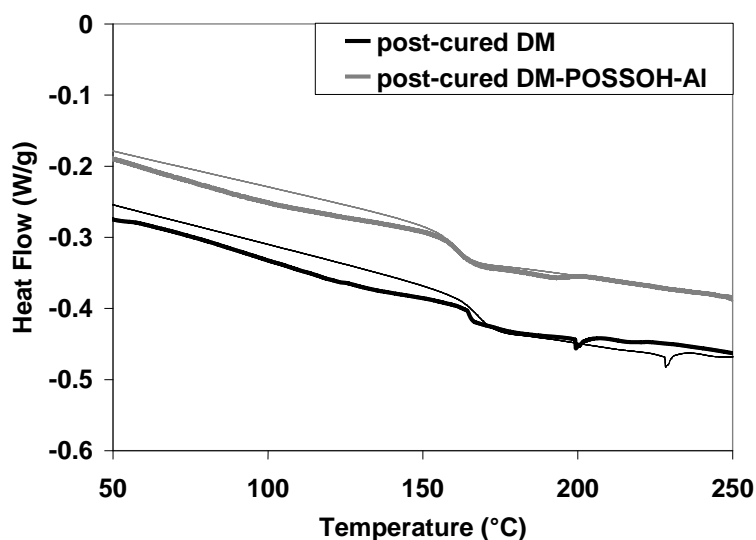


Figure V-26 Evolution of the glass transition temperature of DM and DM-POSSOH-AI post-cured samples between the first DSC heat ramp (thick line) and the second DSC heat ramp (thin line)

## 2. DETERMINATION OF THE SECONDARY AMINE CONCENTRATION

The procedure to calculate the concentrations of functional groups as a function of the time of reaction was detailed in Chapter III. In order to calculate the secondary – and then the tertiary – amine concentration according to the following equation, the constants  $a$  and  $b$  must be determined:

C-2

$$[SA]_t = \frac{A_{PA+SA,t} - a \cdot [PA]_t}{b}$$

where  $[SA]_t$  and  $[PA]_t$  are the concentrations of the secondary and the primary amine, respectively,  $A_{PA+SA,t}$  corresponds to the area of the peak of interest at a given time  $t$ , and  $a$  and  $b$  are constants.

This equation was based on the hypothesis that no reaction of the secondary amine occurred during the first minutes of the study. In the case of the DM-POSSOH-AI system, this hypothesis was not valid as it was shown by calculating the conversion of epoxy and PA at  $t=0$  using the calibration curves. In the case of the DM system, the hypothesis was verified by plotting the PA concentration as a function of the epoxy concentration (Figure V-27). Indeed, if the epoxy reacted only with the PA, the slope of such a curve should be equal to one. The time from which the hypothesis was not valid anymore – meaning that the SA were not only produced but also

started to be consumed – could be determined from the point where the curve started to diverge from the tangent to the curve at the first points. In the present study, such a point gave a time limit of 300 minutes for the DM system, leaving 21 data sets for determining best fitted values of the coefficients  $a$  and  $b$ , equal to 33.07 and 14.58, respectively. Considering that in DM and DM-POSSOH-AI systems, the same amine was used,  $a$  and  $b$  constants should be equal in both systems. The concentration of the SA in DM-POSSOH-AI system was then calculated using the value of  $a$  and  $b$  found for the DM system.

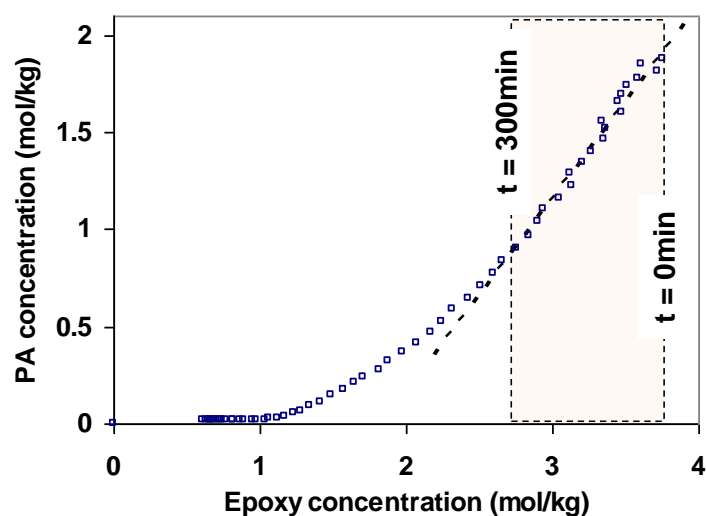


**Figure V-27 PA concentration as a function of the epoxy concentration for the DM system. The dashed line (slope of 1) represents the tangent to the first points of the curve. The zone represents the domain where the hypothesis was valid – i.e. no SA was consumed.**

---

## **APPENDIX D – RESULTS RELATED TO COMPOSITES BASED ON EPOXY FORMULATIONS**

---

In the framework of the Fire-Resist project, aim of which was to propose new fire-retardant solutions for high-performance composites, some of the epoxy formulations presented in the main body of this manuscript were selected for production of flat glass or carbon reinforced-composites. A preliminary study of the viscosity of the uncured mixtures was carried out in order to assess the feasibility of infusion with these reactive systems. The composites were studied in terms of morphology, thermo-mechanical and mechanical properties, and fire behaviour. The results are presented here.

### **1. MATERIALS AND PROCESS**

Composite panels were produced out of selected formulations developed within this study, namely:

- the DGEBA/MDEA system containing 4 wt% of POSSOH (DM-POSSOH), and the corresponding reference (DM);
- the MVR444-based system with both POSSOH and the Al-based catalyst (MVR-POSSOH-Al) and the reference (MVR). The MVR444 resin was a commercial formulation containing several epoxy prepolymers and hardeners, among which TGDDM and MMIPA (see Chapter II).

Two types of reinforcement were used each time:

- carbon: 3 layers of a triax 700 gr and 1 layer of twill 200 gr
- glass: 3 layers of biax 700 gr and 1 layer of twill 200 gr

The formulations were prepared at IMP@INSA-Lyon and shipped to one of the Fire-Resist project partners, APC (Sweden), where the composite panels were produced by vacuum bag infusion. They were square plates of 300 mm and about 3 mm thick. The curing cycle implemented at APC was the same as for the non-reinforced networks, i.e.:

- 4 hours at 135 °C and 4 hours at 190 °C for the DGEBA-based composites
- 4 hours at 130 °C and 2 hours at 180 °C for the MVR composites. For mixtures containing the POSSOH and the Al-based catalyst, 2 hours at 90 °C + 2 hours at 130 °C were performed instead of the first 4 hour dwell.

The final volume fraction of fibres within the composites comprised between 56 and 60%.

Visual observations before and during testing revealed a certain amount of defects probably due to issues related to the infusion process: wettability (dry fibres, voids) and/or insufficient curing. Cyttec indeed reported some resin flowing during the DMA testing, which can only suggests uncured zones in the composite panels. Such an observation was not reported as concerns the non-reinforced networks. It could reveal a severe demixing of the epoxy prepolymer and the hardener before infusing, leading to locally largely off-stoichiometry zones, though APC took care to stir and degas the mixtures before infusing.

## 2. VISCOSITY OF THE REACTIVE SYSTEMS

The viscosity of the epoxy-based formulations as a function of time and temperature is of major interest for the infusion process. Infusing the resin must be performed at an acceptable temperature, within a reasonable time – depending of course of the size of the part – and the gelation of the system during the infusion must be avoided. The advice given by APC who performed the infusion was to target a temperature between 30 °C and 80 °C, and to keep the viscosity between 200 mPa.s<sup>-1</sup> and 1 Pa.s<sup>-1</sup> as long as possible. The viscosity will depend on both the temperature and the time through two competing mechanisms: the fluidizing as the interactions between the molecules weaken, and the polymerization, which rate depends on the temperature. A compromise on the temperature must then be found that allows the viscosity to decrease enough by fluidizing, while keeping the polymerization slow.

In Figure C-1 and Figure C-2 are presented the viscosity curves of the DM and MVR systems that were used in the composite materials, respectively, at different temperatures and as a function of time. Addition of POSSOH in the DM formulation resulted in an increase of the viscosity of a few tens of MPa. It did not cause the viscosity to increase faster than in the DM system, confirming the non-catalytic effect of the POSSOH alone. The infusion was possible from 60 °C. In the MVR system, the addition of both the POSSOH and the Al catalyst had qualitatively the same effect. Though the combined presence of Al catalyst and POSSOH was thought to increase the polymerization rate, which would result in a faster increase of the viscosity, this catalytic effect was observed neither at 60 °C nor at 80 °C. The viscosity of MVR-

POSSOH-AI at 60 °C was close to the limit viscosity of 1 Pa.s<sup>-1</sup>, so the infusion was performed at 80 °C.

A comparison could be made with the DM system where both the POSSOH and the AI catalyst were introduced. The viscosity curves of such a formulation are given in Figure C-3. The catalytic effect of the combined presence of both compounds could be observed, which clearly depended on the temperature. The higher the temperature, the faster the viscosity increased, leaving at the best about 22 minutes at 60 °C.

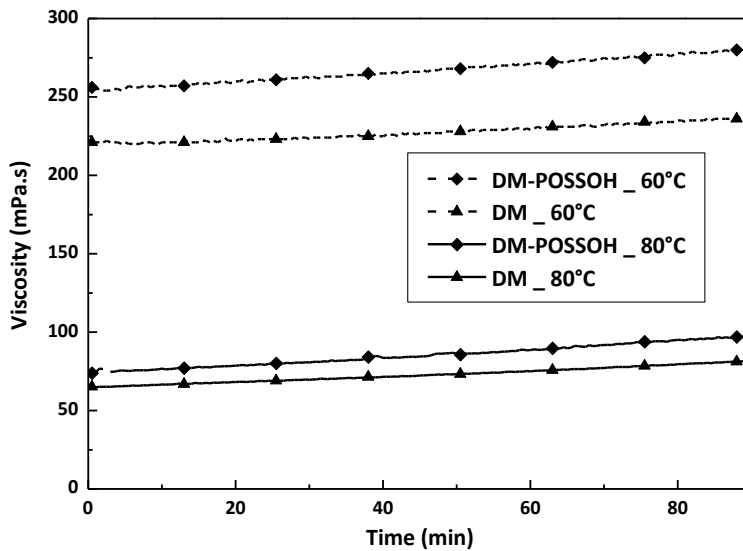


Figure C-1 Viscosity as a function of time of the DM-based systems, at different temperatures

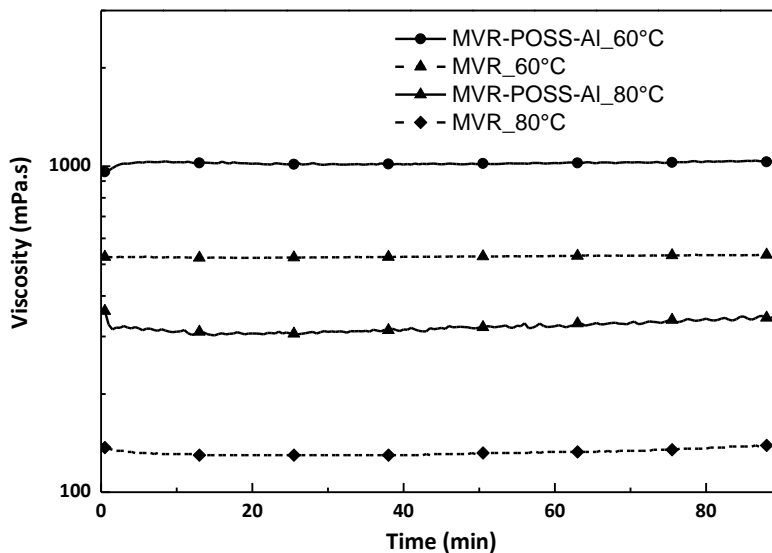


Figure C-2 Viscosity as a function of time of the DM-based systems, at different temperatures

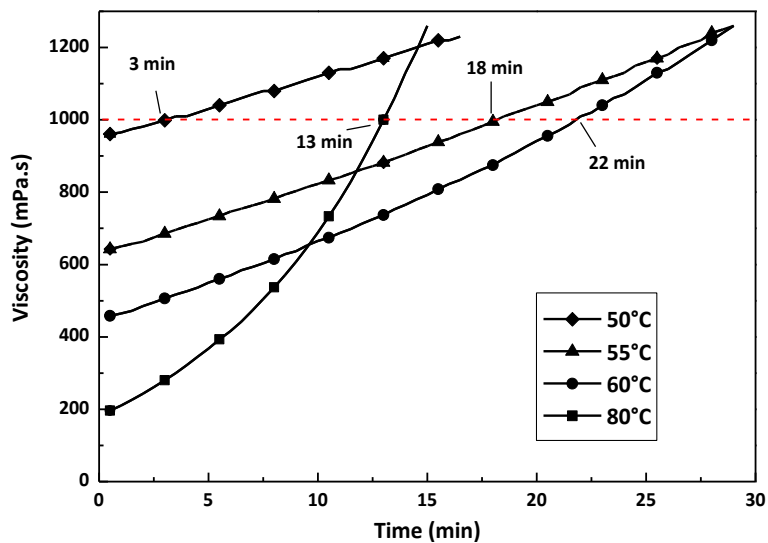


Figure C-3 Viscosity as a function of time of the DM-POSSOH-Al system, at different temperatures. The dotted line represents the limit viscosity of  $1\text{Pa}\cdot\text{s}^{-1}$

### 3. MORPHOLOGY OF THE COMPOSITES CONTAINING POSSOH

The morphology of composites, cut at room temperature, was investigated by SEM. Representative pictures of glass reinforced samples are displayed in Figure C-4. The POSSOH arranged in the shape of nodules, of bigger diameter in the MVR-POSSOH-Al composite – few microns against less than  $1\ \mu\text{m}$  in diameter in DM-POSSOH composite. Due to the difficulty to have clean and neat fracture surface, no conclusions could be drawn about the overall nodules dispersion in the thickness sample or about the fibre-matrix interface. The morphologies of composites were quite similar to those developed in the non-reinforced networks as observed by SEM (Figure C-5 a and c), but the structures revealed by the TEM in the MVR-POSSOH-Al network without reinforcement – the arrays of filaments and nodules in Figure C-5 d – could not be observed by SEM in the composites. Observation of the composites via TEM was not performed as it was not possible to obtain consistent microtomed layers.

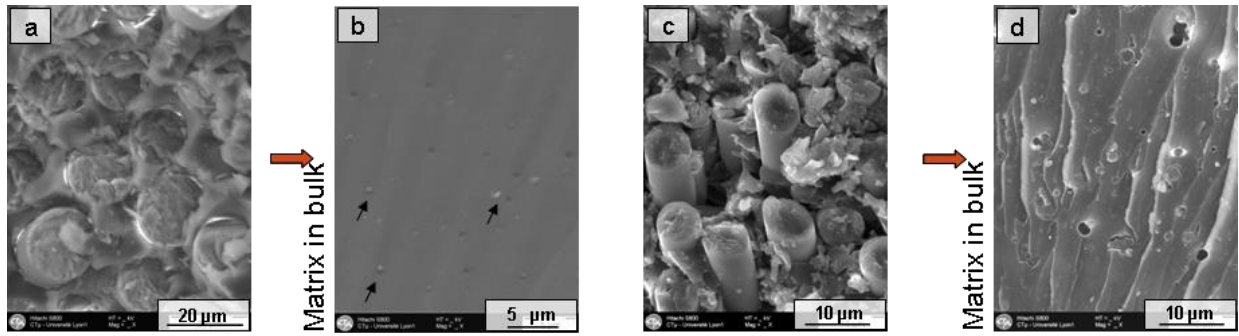


Figure C-4 Representative SEM photographs of a), b) DM-POSSOH-glass and c), d) MVR-POSSOH-Al-glass. Reinforcement fibres were visible in a) and c), while pictures b) and d) focused on matrix zones in between the fibres. In picture b), the arrows point at the POSSOH nodules

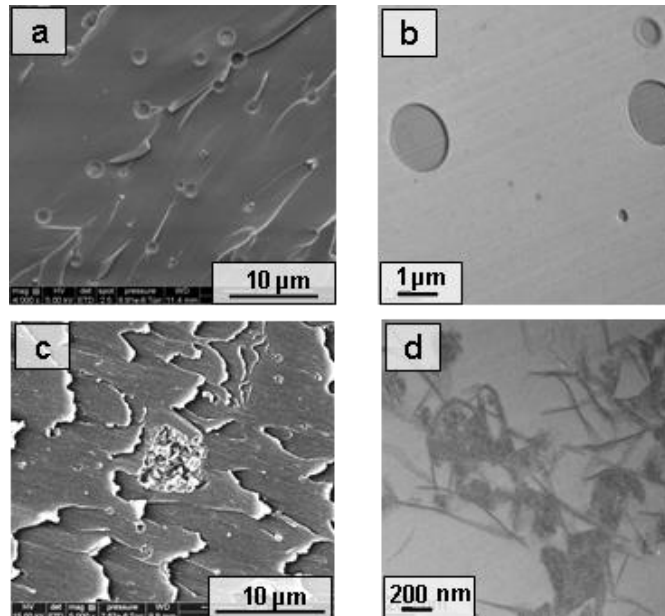


Figure C-5 Representative micrographs of a), b) non-reinforced DM-POSSOH-Al network and c), d) non-reinforced MVR-POSSOH-Al network. Images a) and c) were taken with SEM, images b) and d) with TEM

#### 4. THERMO-MECHANICAL AND MECHANICAL PROPERTIES

The thermo-mechanical properties of the composites were assessed via DMA, performed at Cytec (UK). The mechanical tests, also performed at Cytec, were the Interlaminar Shear Strength (ILSS), tensile and flexural tests, which allowed to determine the flexural and tensile moduli, the ILSS, flexural and tensile strength, the ultimate tensile strain and the Poisson's ratio for each material.

#### 4.1. THERMO-MECHANICAL PROPERTIES

The Table C-1 below gathers the DMA data of the composites, obtained from Cytec, as well as the T<sub>g</sub> value of the corresponding unreinforced networks, measured by DMA at INSA. The visual observations suggested a low curing of the composite matrices, which was supported by the appearance of two successive relaxations (see illustration in Figure C-6): the DMA testing may have been postcuring the samples, leading to the appearance of an immediate second higher T<sub>α</sub>. The DMA of the unreinforced networks actually showed the same tendency, in a much lesser extent: only a shoulder in the tan δ peak was visible (Figure C-7). This was probably due to a too low curing temperature and/or a too short last curing dwell.

	DM-based				MVR444-based			
	neat		POSSOH		neat		POSSOH-AI	
T <sub>α</sub> networks (°C)	157		166		224		205	
	glass	carbon	glass	carbon	glass	carbon	glass	carbon
T <sub>α</sub> composites (°C)	142	150	142	145	173 (215)	182 (210)	180 (201)	189
ΔT <sub>h1/2</sub> (°C)	17	17	18	17	83	70	60	55

**Table C-1 DMA data of composites panels (from Cytec) and T<sub>g</sub> of corresponding unreinforced networks for comparison**

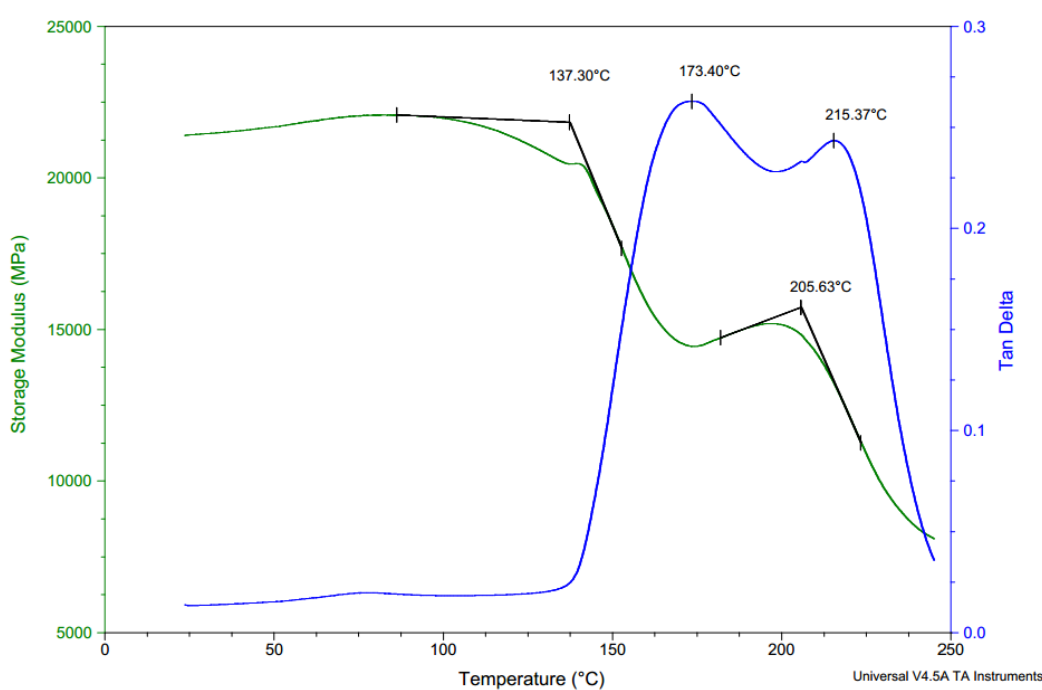


**Figure C-6 DMA curves (storage modulus and tan delta) of the MVR-glass composite**

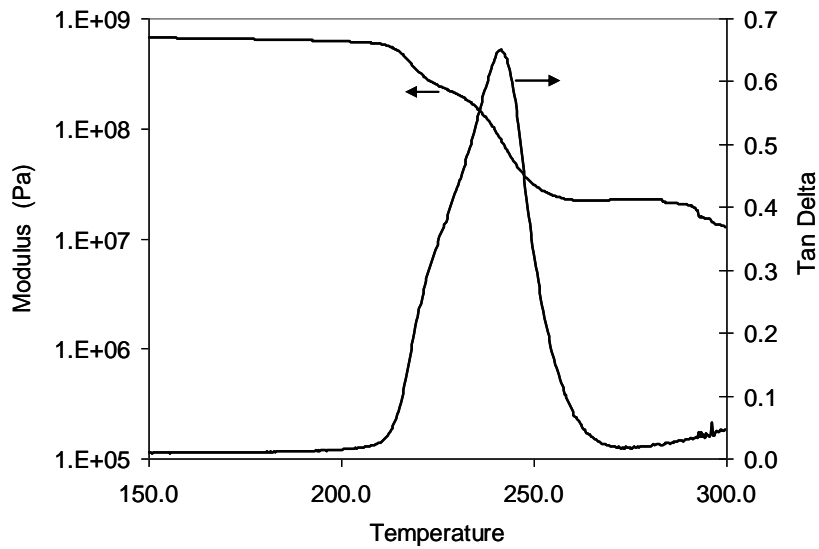


Figure C-7 DMA curves (storage modulus and tan delta) of the unreinforced MVR network

#### 4.2. MECHANICAL PROPERTIES

The results from mechanical testing of composite parts are given in Table C-2 and Table C-3. In the DM-based composites, the mechanical properties were generally increased by the addition of POSSOH, even the fibre-dominated properties, whereas the POSSOH, being dispersed in the matrix, should not significantly influence those properties. No trend was observed, a property enhanced in a glass-reinforced composite could be lowered in the carbon-reinforced material, as it was the case for the ILSS strength.

	DM/glass	DM-POSSOH/ glass	Diff. (%)	DM/carbon	DM-POSSOH/ carbon	Diff. (%)
ILSS (MPa)	34 (2)	37 (2)	+8.4	22 (1)	21 (1)	-7.6
0° FS (MPa)	495 (21)	607 (40)	+22.8	349 (70)	394 (37)	+13.0
0° FM (GPa)	12 (1)	21 (1)	+72.0	15 (1)	15 (1)	-4.4
0° TS (MPa)	347 (6)	356 (14)	+2.7	234 (14)	480 (65)	+105.4
0° TM (GPa)	21 (1)	20 (0)	-0.8	35 (1)	32 (2)	-8.2
0° TPR	0.12 (0.00)	0.12 (0.01)	+2.8	0.05 (0.02)	0.06 (0.02)	+6.3
0° TUS (%)	1.7 (0.0)	1.8 (0.1)	+3.7	0.7 (0.0)	1.5 (0.1)	+122.6

Table C-2 Results from mechanical testing on DGEBA-based composites. Abbreviations meaning: 'ILSS': 'ILSS 0° strength', '0° FS': '0° Flexural Strength', '0° FM': '0° Flexural Modulus', '0° TS': '0° Tensile Strength', '0° TM': '0° Tensile Modulus', '0° TPS': '0° Tensile Poisson's Ratio', '0° TUS': '0° Tensile Ultimate Strain'. Values in brackets are the standard deviations

In the MVR-based glass-reinforced composites, the flexural properties were significantly decreased by the addition of POSSOH and the Al catalyst, a trend that was not observed in the carbon-reinforced composites.

	MVR/glass	MVR-POSSOH-Al/glass	Diff. (%)	MVR/carbon	MVR-POSSOH-Al/carbon	Diff. (%)
ILSS (MPa)	44 (2)	41 (2)	-6.8	31.3 (4.0)	36 (3)	+16.1
0° FS (MPa)	686 (55)	502 (43)	<b>-26.8</b>	542 (58)	674 (57)	+24.3
0° FM (GPa)	24 (1)	12 (1)	<b>-47.8</b>	20 (2)	22 (2)	+10.4
0° TS (MPa)	340 (31)	335 (19)	-1.5	228 (37)	698 (3)	+206.1
0° TM (GPa)	21 (1)	21 (1)	+0.2	37 (1)	36 (1)	-2.6
0° TPR	0.13 (0.01)	0.13 (0.01)	-2.6	0.05 (0.01)	0.06 (0.01)	+12.5
0° TUS (%)	1.6 (0.1)	1.6 (0.2)	-2.8	0.6 (0.1)	1.9 (0.1)	+214.8

**Table C-3 Results from mechanical testing on MVR-based composites. Abbreviations meaning: 'ILSS': 'ILSS 0° strength', '0° FS': '0° Flexural Strength', '0° FM': '0° Flexural Modulus', '0° TS': '0° Tensile Strength', '0° TM': '0° Tensile Modulus', '0° TPS': '0° Tensile Poisson's Ratio', '0° TUS': '0° Tensile Ultimate Strain'. Values in brackets are the standard deviations**

## 5. FIRE BEHAVIOUR

The cone calorimeter experiments were performed at SP, Sweden, with two radiative heat fluxes – 35 kW/m<sup>2</sup> and 70 kW/m<sup>2</sup>. In Figure C-8 are represented the HRR curves of the composites subjected to a radiative heat flux of 35kW/m<sup>2</sup>, and the corresponding cone calorimeter data were gathered in Table C-4. There was a general slight tendency to improvement on all the cone calorimeter data with the addition of POSSOH in the systems, which however stayed within the uncertainty limits of the technique. The only significant improvement – i.e., a decrease of the pHRR – was observed in the case of the MVR-based glass reinforced composites. The slight tendency to improvement observed for tests at het flux of 35kW/m<sup>2</sup> was attenuated at 70 kW/m<sup>2</sup> (results not shown here). Thus, the addition of POSSOH did not allow to significantly enhance the fire retardancy of the composites.

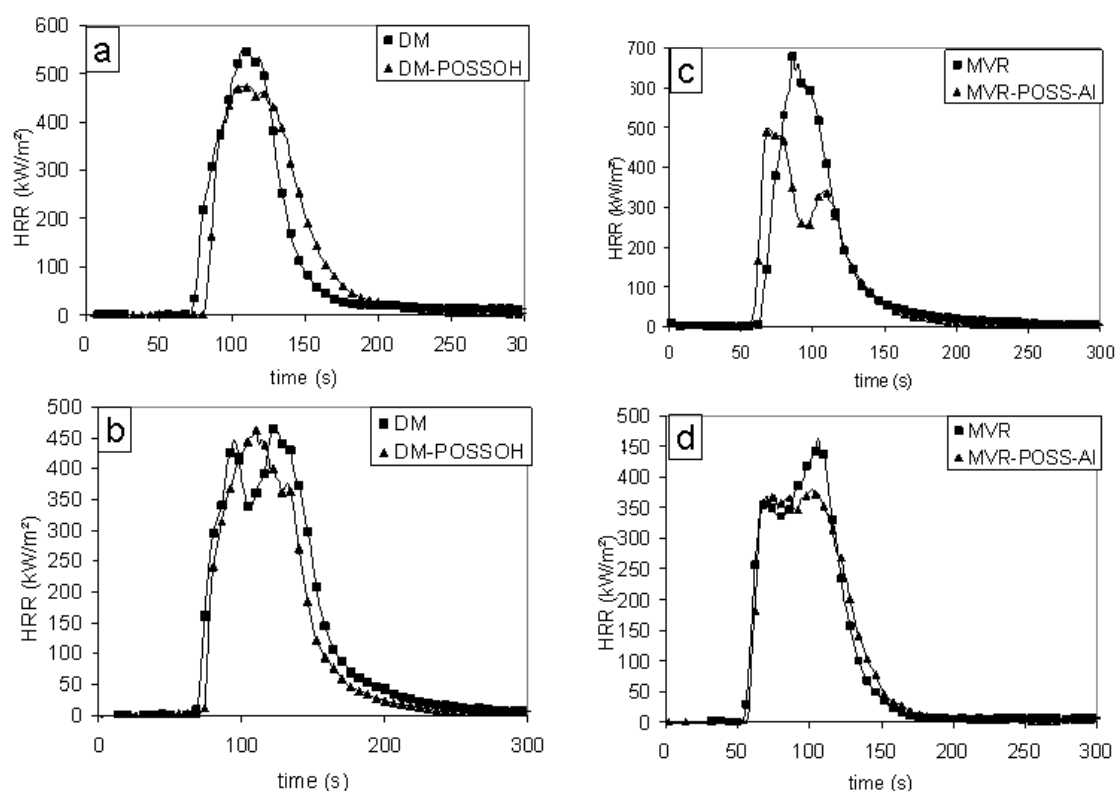


**Figure C-8 HRR curves obtained by cone calorimetry (at SP, Sweden) of a) DM-based glass reinforced composites, b) DM-based carbon reinforced composites, c) MVR-based glass-reinforced composites, d) MVR-based carbon-reinforced composites. Radiative heat flux of 35 kW/m<sup>2</sup>**

System	TTI (s)	THR (MJ/m <sup>2</sup> )	pHRR (kW/m <sup>2</sup> )	TSR (m <sup>2</sup> /m <sup>2</sup> )	RW (%)
DM glass	72 (0)	32.3 (1.9)	518 (42)	1452 (269)	66.8 (1.3)
DM-POSSOH glass	80 (0)	28.0 (3.6)	488 (19)	1319 (99)	69.7 (2.0)
DM carbon	68 (0)	32.9 (3.0)	484 (70)	1464 (182)	51.5 (3.8)
DM-POSSOH carbon	72 (0)	29.4 (0.8)	438 (37)	1278 (74)	55.0 (0.1)
MVR glass	57 (7)	31.2 (0.4)	611 (93)	1441 (90)	67.8 (0.3)
MVR-POSSOH-Al glass	50 (8)	26.8 (1.3)	481 (22)	1387 (95)	71.1 (1.1)
MVR carbon	59 (7)	28.2 (1.4)	454 (13)	1224 (28)	55.5 (1.7)
MVR-POSSOH-Al carbon	56 (0)	26.9 (0.9)	394 (22)	1297 (37)	59.1 (0.5)

**Table C-4 Cone calorimeter data of POSSOH-containing reinforced-composites and the corresponding reference epoxy composites, heat flux: 35kW/m<sup>2</sup>**

In the case of MVR-POSSOH-Al composites, a phenomenon of intumescence providing a protective layer for the underlying material was expected, according to the study of the non-reinforced networks (see Chapter IV). Side views of the samples after testing are displayed in Figure C-9. The reference MVR composites, with carbon and glass reinforcement (Figure C-9 a

and b, respectively), show a certain extent of delamination, higher in the carbon reinforced residue. The delamination was visibly reduced in the samples containing both POSSOH and the Al-based catalyst, which was unexpected as they were more likely to intumesce, and thus cause more delamination. Instead, it seemed that the effect of POSSOH in combination with the Al-based catalyst changed in presence of the reinforcement, which brought no enhancement in terms of Heat Release Rate, but provided more cohesive residues with possibly slightly better residual mechanical performance as compared to the reference MVR composites.

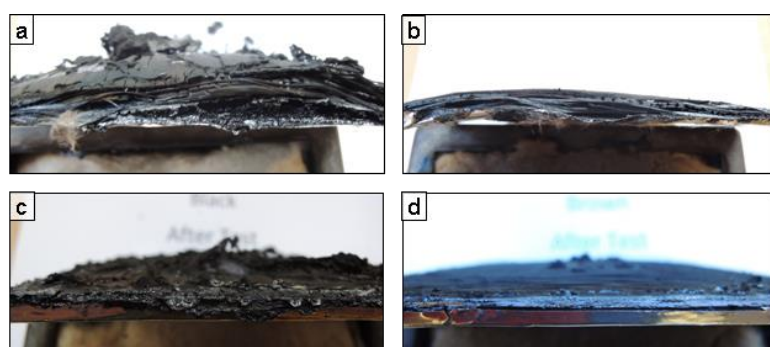


**Figure C-9 Side views of residues of samples after cone calorimeter testing at 35 kW/m<sup>2</sup> a) MVR carbon, b) MVR glass, c) MVR-POSSOH-Al carbon, d) MVR-POSSOH-Al glass**



---

## EXTENDED ABSTRACT IN FRENCH

---

Les matériaux polymères se sont démocratisés au cours du siècle dernier et sont à présent utilisés dans un très large champ d'applications. En particulier, les polymères thermodurcissables, et notamment les systèmes epoxy-amine, sont utilisés pour répondre à de nombreuses problématiques, comme par exemple celles du secteur des transports où ils servent de matrices pour matériaux composites structuraux. Malgré leurs hautes performances au niveau mécanique, chimique et thermique, ces polymères ont l'inconvénient d'être hautement inflammables, ce qui pose des problèmes en termes de sécurité et coûts économiques liés aux dégâts humains et matériels qu'impliquent les incendies.

Les retardateurs de flamme conventionnels, tels que les monomères halogénés ou phosphorés, ou des additifs inertes inorganiques, sont généralement efficaces mais posent souvent les problèmes suivants : (i) parfois nécessaires en grandes quantités, ils peuvent modifier significativement les propriétés du matériau final ; (ii) certains retardateurs de flamme, notamment les composés halogénés, peuvent diffuser dans l'environnement au cours de la phase d'utilisation du matériau, et les fumées dégagées par de tels matériaux lors d'un incendie sont souvent toxiques et corrosives. Ce dernier point est la raison pour laquelle les régulations européennes, notamment la directive REACH [48], tendent à limiter voire interdire l'utilisation de telles substances. Il y a donc un besoin d'alternatives en termes d'ignifugation, respectueuses de la santé et de l'environnement, efficaces en petites quantités et économiques. Ce domaine d'investigation fait l'objet d'une recherche scientifique intensive, dont la préoccupation est de comprendre les mécanismes impliqués dans la combustion des matériaux polymères, ainsi que leur modification induite par la présence de retardateurs de flamme.

Les composés à base de silicium ont notamment été identifiés comme des alternatives prometteuses aux retardateurs de flamme conventionnels. Les nano-argiles, composés inorganiques, ont été massivement étudiés dans l'optique d'améliorer la tenue au feu des polymères. Leur mécanisme de protection est basé sur l'agrégation de ces nano-charges durant la combustion et la production en surface d'une couche inorganique protectrice [64]. En ce qui concerne les systèmes epoxy, il semble cependant qu'il faille introduire ces objets en

quantité importante (10 à 20 % en masse) pour avoir un effet significatif sur la tenue au feu des matériaux finaux [60]–[64]. Une autre voie de recherche consiste à introduire des objets « vitreux » à base de silicium, soit inorganiques comme des particules de nano-silices, soit partiellement organiques comme les polysilsesquioxanes, qui sont des assemblages 2D ou 3D contenant un squelette à base de silice sur lequel sont attachés des groupements organiques. Ces structures organiques/inorganiques présentent un intérêt pour la tenue au feu des polymères epoxy, qui semble cependant dépendre des caractéristiques physiques de ces « verres » [65]–[68]. Le potentiel de ces matériaux n'a cependant pas été suffisamment étudié pour confirmer cet intérêt et déterminer les paramètres influant dans le caractère ignifugeant de tels composés. Enfin, un certain type de polysilsesquioxanes, les Polyhedral Oligomeric Silsesquioxanes (POSS) possédant une structure cubique, sont des solutions intéressantes pour augmenter la tenue au feu des polymères epoxy-amine. En particulier, les POSS possédant des groupements phenyl se sont révélés efficaces même en faible quantité (moins de 5% en masse) [60]. Ces molécules – les POSS – sont d'autant plus intéressantes que la variété des groupements organiques attachés aux atomes de silicium – nature, réactivité – permettent d'obtenir des structures très diverses. Dans l'étude présente, l'objectif de l'étude a également consisté à mettre en évidence une potentielle relation structure/propriétés feu dans les systèmes epoxy-amine hybrides. Les caractéristiques des POSS ont donc justifié le choix de ce type de molécules pour améliorer la tenue au feu de ces systèmes.

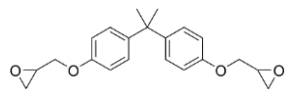
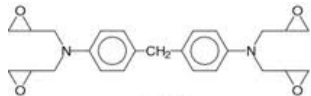
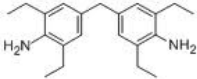
Ce travail s'inscrit dans le cadre d'un projet européen, Fire-Resist, portant sur le développement de matériaux composites résistants au feu pour le secteur des transports. L'étude présentée ici se place dans la phase de développement du projet, ciblant ainsi les matrices polymères pour application aux matériaux composites. Cette position, relativement en amont de l'application finale, justifie notamment le choix des tests utilisés pour caractériser le comportement au feu des matériaux finaux : l'UL 94 et le cone calorimètre. Il s'agit de deux tests de réaction au feu, dont l'un repose sur l'observation visuelle (UL 94) tandis que l'autre permet d'obtenir des données quantitatives. Ils sont relativement faciles à mettre en œuvre, ne nécessitent pas de grandes quantités de matériaux et sont largement employés dans la communauté scientifique. Ces tests correspondent à deux scénarii de combustion différents, et les corrélations existantes entre les résultats de ces tests restent limitées [26]–[28]. Dans l'étude, l'analyse thermogravimétrique a également été employée pour caractériser la stabilité thermique des réseaux, mais là encore le scénario de dégradation reste très différent de celui de combustion. Il faut donc considérer l'ATG comme une analyse complémentaire, ne permettant pas de conclure sur le comportement au feu des matériaux, comme c'est parfois le cas dans la littérature scientifique.

Ce manuscrit de thèse se compose de cinq parties principales, la première traitant de l'état de l'art dans le domaine de la tenue au feu des systèmes polymères à base d'époxy, les quatre suivantes étant consacrées aux résultats expérimentaux et à leur interprétation. Les morphologies des systèmes, l'étude des réactions dans les systèmes complexes, le comportement au feu des réseaux, et le cas particulier de systèmes thermodurs/thermoplastiques sont abordés dans ces parties et synthétisés dans ce résumé en langue française.

## 1. RÉSEAUX EPOXY: PROCÉDÉS ET MORPHOLOGIES

### 1.1. PRODUCTION DES RÉSEAUX

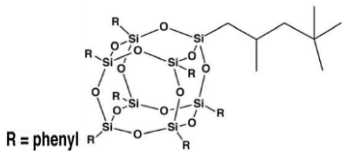
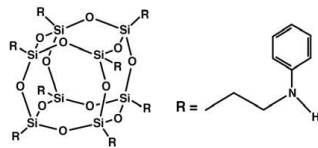
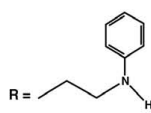
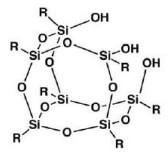
L'étude a porté sur deux systèmes modèles différents, dont les composants sont présentés dans le Tableau 1. Un système basé sur une formulation commerciale destinée aux composites structuraux produits par infusion, la MVR444, mélange de prépolymères epoxy (dont la TGDDM) et de durcisseurs amines aromatiques, a également été choisi. La sélection des matériaux s'est justifiée par : (i) la forte utilisation du prépolymère DGEBA, tant dans l'industrie que pour les études scientifiques, (ii) les hautes propriétés des réseaux à base de TGDDM et de MVR444, compatibles avec l'application aéronautique, (iii) la faible réactivité de la diamine aromatique MDEA (agent de réticulation) permettant le contrôle de la polymérisation.

Composé	Abréviation	Fonctionnalité	Structure
Diglycidyl Ether of Bisphenol A (Epon 828, Momentive)	DGEBA	2	
Tetraglycidyl(diaminodiphenyl) methane (MY9512, Huntsman)	TGDDM	4	
4,4' methylene bis(2,6-diethylaniline) (Lonza)	MDEA	4	

**Tableau 1 Composants de base (monomères époxy et durcisseur) des systèmes modèles**

Trois POSS contenant des groupements phenyls ont été sélectionnés (Tableau 2), dont l'un est non-réactif (l'isooctylphenyl POSS) et deux autres possèdent des groupements fonctionnels (le N-phenylaminopropyl POSS et le trisilanolphenyl POSS). De par ces différents groupements organiques, ils sont susceptibles de mener à des structures différentes au sein des réseaux. En particulier, dans le cas du trisilanolphenyl POSS, un sel d'aluminium (aluminium acetylacetonate, Figure 1) a été ajouté, pouvant potentiellement catalyser le greffage des POSS

au réseau. Les POSS ont été dispersés dans les prépolymères epoxy par solubilisation à différentes températures, ou par mélange à cisaillement élevé (2000 rpm pendant une heure).

Produit	Abréviation	Funcionnalité	Structure	T <sub>sol</sub>
isooctylphenyl POSS	iOPOSS	0	 R = phenyl	205 °C
N-phenylaminopropyl POSS	AmPOSS	8	 R = 	60 °C
trisilanolphenyl POSS	POSSOH	3	 R = phenyl	130 °C

**Tableau 2 Les différents POSS et la température T<sub>sol</sub> à laquelle ils ont été solubilisés dans les prépolymères epoxy**

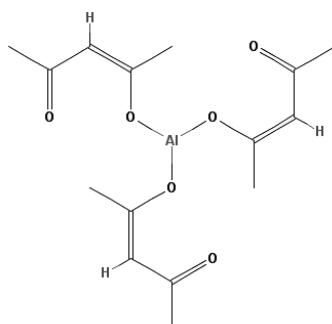


**Figure 1 Structure du tri(acetylacetonate) d'aluminium Al(acac)<sub>3</sub>**

Le Tableau 3 résume :

- la composition des systèmes, en pourcentages massiques. La quantité de POSS a été fixée en terme de pourcentage massique inorganique (quantité représentée par le cœur de silice des molécules de POSS) ;
- les abréviations associées à chaque réseau. L'indication chiffrée en fin d'appellation correspond à la température de solubilisation du POSS, alors que « mix » désigne un système dans lequel le POSS a été introduit par mélange à cisaillement élevé ;
- Les cycles de cuisson. Le palier à plus basse température dans les systèmes contenant Al(acac)<sub>3</sub> se justifie par une polymérisation visiblement plus – trop – rapide à 135 °C.

	Compositions des systèmes				Curing cycle
	POSS		durcisseur	Epoxy	
	[inorg. wt%]	[wt%]	[wt%]	[wt%]	
DM	/	/	29.2	70.8	
DM-AmPOSS-60	1.5	5.2	26.3	68.5	
DM-iOPOSS-205	1.5	3.9	28.0	68.1	4h @ 135 °C + 4h @ 190 °C
DM-POSSOH-mix	1.5	4.1	28.0	67.9	
DM-POSSOH-130	1.5	4.1	28.0	67.9	
DM-POSSOH-AI	1.5	4.1	27.9	67.7	2h @90 °C + 2h @ 135 °C + 4h @ 190 °C
TM	/	/	38.2	61.8	
TM-iOPOSS-mix	1.5	3.9	36.7	59.4	4h @ 135 °C + 3h @ 200 °C
TM-POSSOH-mix	1.5	4.1	36.6	59.3	
TM-POSSOH-130	1.5	4.1	36.6	59.3	
TM-POSSOH-AI	1.5	4.1	36.5	59.0	2h @90 °C + 2h @ 135 °C + 3h @ 200 °C
MVR	/	/	36.7	63.3	4h @ 130 °C + 2h @180 °C
MVR-POSSOH-130	1.5	4.1	35.2	60.7	
MVR-POSSOH-AI	1.5	4.1	35.1	60.5	2h @ 90 °C + 2h @ 130 °C + 2h @180 °C

**Tableau 3 Compositions des systèmes, abréviations et cycles de cuisson – la quantité de sel d'aluminium dans les réseaux en contenant s'élève à 0.4 %m**

## 1.2. MORPHOLOGIES DES RÉSEAUX

Les réseaux de référence présentent au microscope électronique à balayage (MEB) une surface homogène. Dans les réseaux contenant les POSS, une morphologie avec des domaines isolés riches en POSS est attendue, car les POSS peuvent être sujets à une séparation de phase induite par la réaction de polymérisation des systèmes. Cette séparation dépend de nombreux facteurs et peut notamment être entravée par des possibles réactions entre les POSS et les comonomères formant le réseau.

L'observation MEB du réseau DM-AmPOSS-60, ne permet pas de détecter des domaines séparés de POSS, indiquant une dispersion des POSS à l'échelle au moins sub-micronique.

L'observation MEB des réseaux contenant le POSS non-fonctionnel, l'iOPOSS, a démontré sa forte tendance à l'agglomération avec même une certaine sédimentation du POSS vers la surface inférieure des matériaux (par rapport à l'orientation des moules lors de la cuisson). Ce phénomène est illustré en Figure 2 pour les réseaux à base de DGEBA, les morphologies étant similaires dans les réseaux à base de TGDDM.

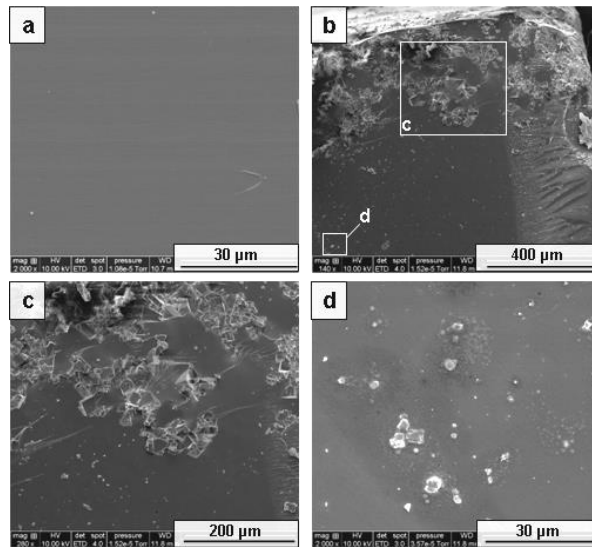


**Figure 2 Images MEB des surfaces de DM (a) et DM-iOPOSS-205 (b,c,d) où: b) image de la surface inférieure et c) et d) forts grossissements des zones correspondantes de b)**

L'observation au microscope électronique à transmission (MET) a révélé une séparation de phase « classique », en forme de nodules, dans les systèmes à base de DGEBA contenant le POSSOH (Figure 3), sans qu'il soit cependant possible de conclure à l'absence de POSSOH dans la matrice epoxy-amine. Une morphologie similaire a été observée par MEB dans les réseaux où le POSS avait été dispersé par mélange à cisaillement élevé. L'ajout du sel d'aluminium a pour influence de réduire la taille des nodules, passant de quelques microns à quelques centaines de nanomètres.

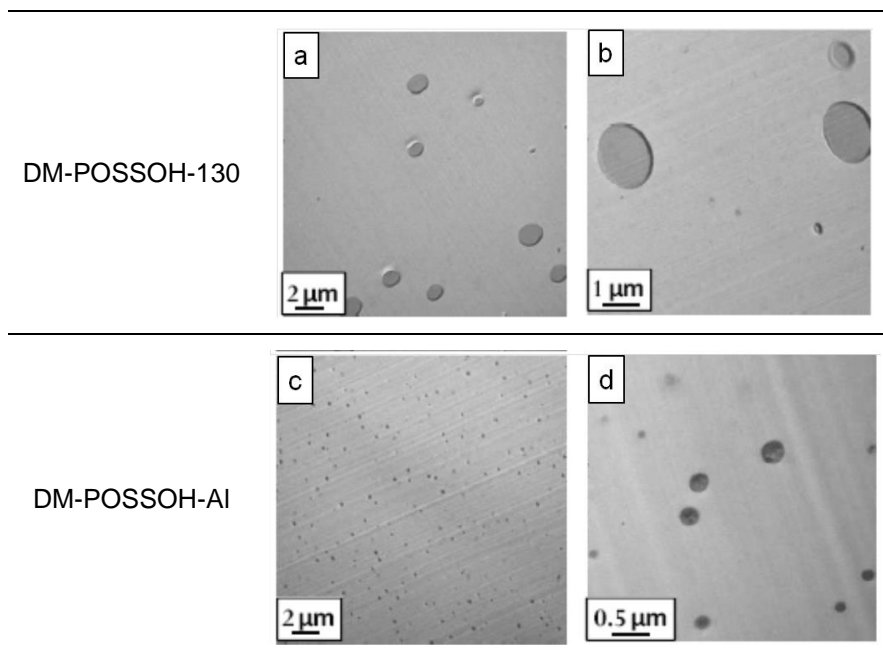


**Figure 3 Images MET de DM-POSSOH-130 (a, b) et DM-POSSOH-AI (c, d); b) et d) sont de forts grossissements de a) and c), respectivement**

En revanche, des morphologies très différentes et jamais rapportées dans la littérature ont été observées dans les réseaux à base de TGDDM et de MVR444 et contenant le POSSOH. Les structures formées par les POSS, et révélées uniquement par le MET (le MEB montrant des agrégats ainsi que des nodules), sont composées de filaments, mieux définis dans le réseau contenant le sel d'aluminium, où ces fils sont organisés en toiles dans lesquelles sont inclus quelques nodules. Dans TM-POSSOH-Al, l'épaisseur des filaments est d'une dizaine de nanomètres, ce qui pourrait correspondre à la largeur de quelques unités POSS, groupements organiques compris. Une hypothèse plausible serait l'assemblage des POSS, possiblement via des liaisons covalentes issues de réactions de condensations entre les POSS eux-mêmes, menant à ces structures « poly-POSS ».

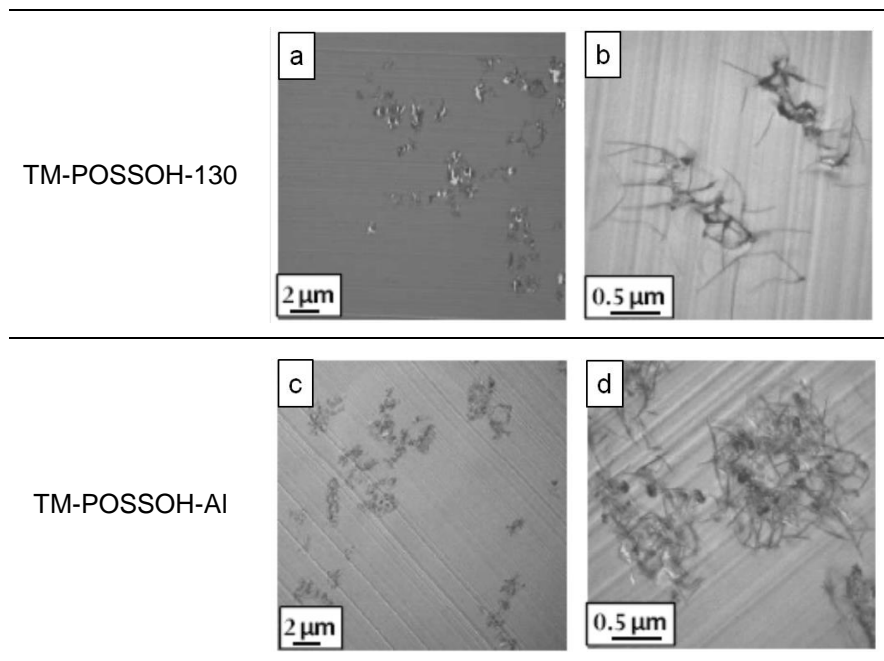


**Figure 4 Images MET de TM-POSSOH-130 (a, b) et TM-POSSOH-Al (c, d); b) et d) sont de forts grossissements de a) and c), respectivement**

Une étude visant à répondre à la question du développement de ces morphologies complexes au cours du cycle de cuisson a été menée sur le système TM-POSSOH-Al. Des échantillons ont été soumis au cycle de cuisson et retiré puis immédiatement trempés à divers temps pendant la cuisson. Ces échantillons, conservés à -20 °C, ont par la suite été observés au MET, dont les images ont été regroupées dans la Figure 5. La morphologie ne semble plus évoluer significativement après la gélification, située aux environs de 40 minutes à 135°C. Les structures passent ainsi d'agrégats mal définis au début du palier à 135°C, aux structures en filaments et nodules, ce qui indique que les filaments se développent de manière progressive pendant la polymérisation.

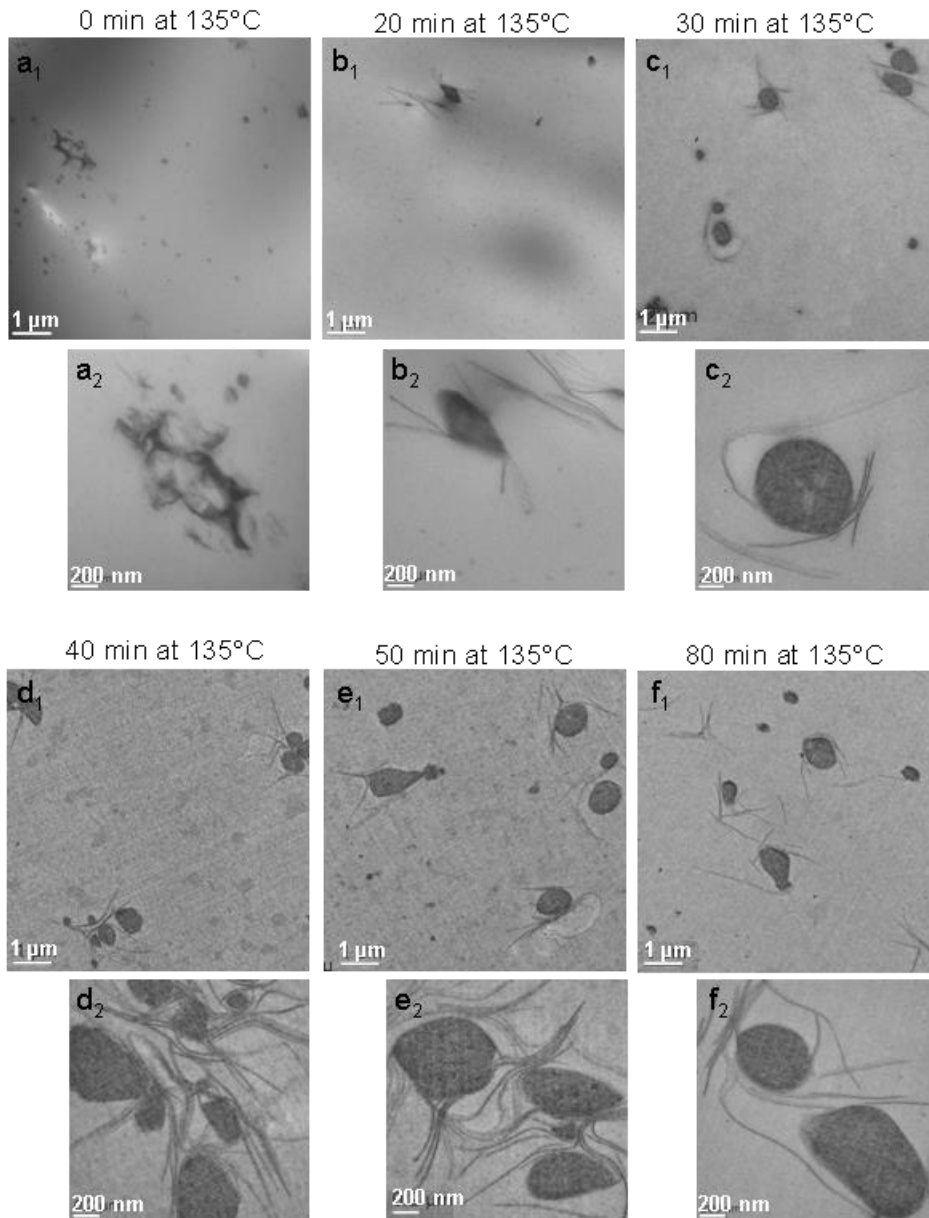


**Figure 5 Images TEM du système TM-POSSOH-Al à différents temps durant le deuxième palier du cycle de cuisson (135 °C) ; les images dénotées  $x_2$  montrent des détails de la morphologie générale (images  $x_1$ )**

La nature du prépolymère epoxy constitue donc l'élément clé contrôlant les types de structures formées par les POSS dans les réseaux, l'ajout d'un sel d'aluminium permettant de réduire la taille des objets ou de les affiner sans en modifier significativement ni la forme ni l'organisation et la dispersion globale dans le réseau.

## **2. RÉACTIONS DANS LES SYSTÈMES A BASE DE DGEBA CONTENANT DES POSS FONCTIONNELS**

Comme évoqué dans la partie précédente, le phénomène de séparation de phase, et donc les morphologies des réseaux, sont très dépendants des réactions à l'œuvre dans les systèmes pendant le cycle de cuisson. Dans tous les systèmes se déroulent les réactions de polymérisation epoxy-amine (addition nucléophile de l'amine primaire puis de l'amine secondaire sur le cycle epoxy), et éventuellement des réactions d'homopolymérisation des epoxy dans certaines conditions. Mais dans les systèmes contenant les POSS, et notamment les POSS portant des groupes fonctionnels, ces réactions peuvent être modifiées au niveau des mécanismes et/ou des cinétiques, et d'autres réactions peuvent avoir lieu. Des études ont été menées sur les systèmes à base de DGEBA.

### **2.1. SYSTÈME CONTENANT LE N-PHENYLAMINOPROPYL POSS**

Dans ce système, un phénomène possible est la réaction des groupements amines secondaires de l'AmPOSS avec l'époxy de la DGEBA, auquel cas ce POSS participerait à la formation du réseau, possiblement en tant qu'agent de réticulation. Pour étudier la possibilité d'avoir cette réaction dans le milieu, une étude cinétique par DSC et SEC a été menée sur le système binaire DGEBA-AmPOSS (sans agent durcisseur MDEA), et dans lequel le POSS a été introduit en quantité telle que le rapport stœchiométrique entre les fonctions amine et epoxy est respecté. La réaction DGEBA-AmPOSS a ainsi été mise en évidence et la conversion en fonction du temps a été calculée. D'autre part, il a été montré que la réactivité du POSS vis-à-vis de la DGEBA était supérieure à celle de la MDEA, toujours vis-à-vis de la DGEBA (Figure 6), permettant de conclure que, dans le système ternaire contenant le POSS et la MDEA, le POSS réagissait probablement en premier avec la DGEBA. Ceci permettrait en outre d'expliquer la dispersion submicronique des POSS dans le réseau, ceux-ci étant lié aux monomères epoxy avant que ne commence la séparation de phase induite par la progressive gélification du système DGEBA-MDEA.

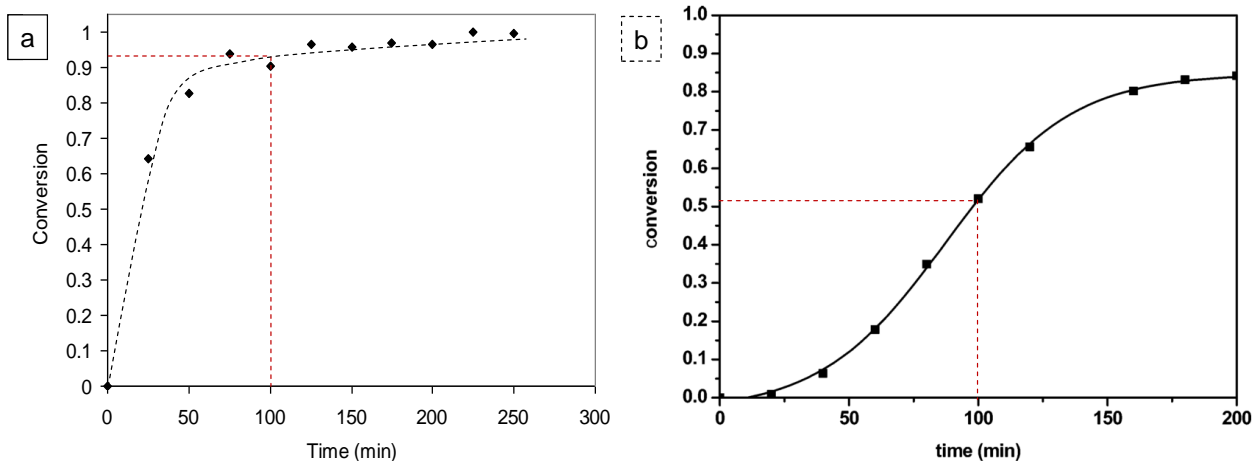


**Figure 6 Évolution de la conversion dans les systèmes a) DGEBA-AmPOSS pendant la cuisson à 135 °C (calculée d'après les données de DSC et la relation modifiée de DiBenedetto) et b) DM (obtenue par DSC isotherme) [93]**

## 2.2. SYSTÈMES CONTENANT LE TRISILANOLPHENYL POSS ET/OU LE TRI(ACÉTYLACÉTATE) D'ALUMINIUM

Ce système est relativement complexe étant donné que :

- La présence des silanols pourrait catalyser les réactions de polymérisation epoxy-amine ;
- La présence combinée de POSSOH et du sel d'aluminium pourrait également catalyser les réactions de polymérisation, mais également d'homopolymérisation [106,109] ;
- Une réaction d'addition des silanols portés par les POSSOH sur le cycle epoxy pourrait avoir lieu [86], formant ainsi des liaisons Si-O-C et modifiant la stœchiométrie du système ;
- Une réaction de condensation des POSSOH avec les groupements OH portés par les monomères époxy est possible, formant également des liaisons Si-O-C ;
- Une réaction de condensation des POSSOH sur eux-mêmes via leurs groupements silanol est également à considérer, formant ainsi des chaînes voire des réseaux de POSS.

Un effet catalytique flagrant de la présence combinée du POSSOH et de  $Al(acac)_3$  sur la polymérisation des systèmes complets à base de DGEBA (mais également à base de TGDDM) a été mis en évidence expérimentalement. L'étude des temps de gel, mesurés par chimiorhéologie, a montré une accélération spectaculaire du phénomène de polymérisation exclusivement constatée en présence des deux composés. Similairement, les exothermes de réaction, obtenus par DSC, montrent une diminution significative de la température d'exotherme de réaction (Figure 7).

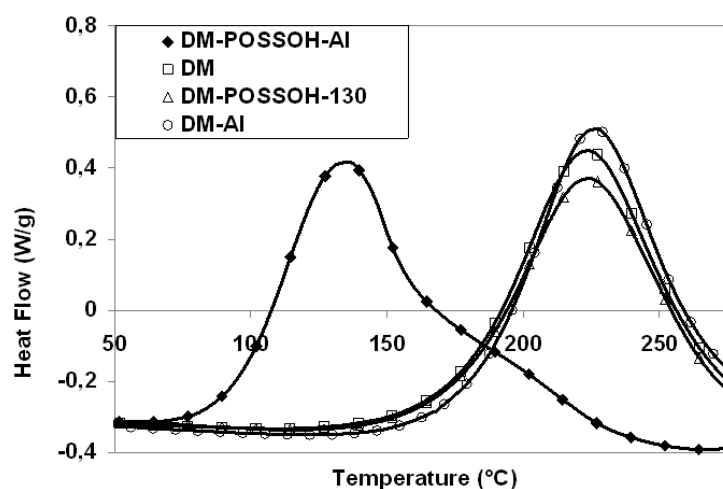


**Figure 7 Exothermes des systèmes réactifs à base de DGEBA (scans DSC dynamiques, 10K/min)**

Une étude comparative des systèmes DM et DM-POSSOH-AI par spectroscopie proche infrarouge (PIRS) a permis de donner des éléments de réponse sur l'influence du couple POSSOH/AI(acac)<sub>3</sub> sur le système DGEBA-MDEA. Outre la confirmation d'une accélération de la polymérisation, l'étude a mis en évidence la présence d'homopolymérisation, sans toutefois pouvoir la quantifier. Cela a été confirmé par une étude SEC sur le système privé de l'agent durcisseur (MDEA). Toutefois, ces techniques ne sont pas adaptées pour détecter l'évolution des groupements silanol portés par le POSSOH, notamment à cause de leur manque de sensibilité face à une quantité de fonctions très faible.

Dans les réseaux réticulés, les réactions/interactions impliquant les POSS ont été examinées par DMA, SEC (méthodes indirectes) et RMN solide du <sup>29</sup>Si. La DMA révèle quelques changements limités apportés par la présence de POSSOH, notamment un élargissement du domaine de transition vitreuse, mais ne permet pas de conclure de manière catégorique sur l'organisation des POSS et leur potentielle participation au réseau. L'extraction d'espèces « libres » des réseaux, broyés et immergés dans le THF, et l'analyse SEC de ces solutions, a révélé l'absence de relargage de POSSOH à l'état d'unité, permettant de conclure à une réaction des POSS avec une autre espèce, soit eux-mêmes, soit un composant de la matrice.

L'étude RMN a porté sur les réseaux DM-POSSOH-130 et DM-POSSOH-AI, dans lesquels la quantité de POSSOH avait été largement augmentée pour obtenir une quantité de silicium d'environ 5 %m. Cette augmentation a posé des problèmes de solubilisation du POSS dans le prépolymère epoxy, mais l'observation MEB de ces réseaux a montré une morphologie similaire aux réseaux moins chargés. L'expérimentation a montré une augmentation de l'état de condensation des atomes de silicium, comparé à l'état de condensation dans le POSSOH pur, ce qui ne peut provenir que de la condensation des POSS sur eux-mêmes.

### 3. DÉGRADATION ET COMPORTEMENT AU FEU DES RÉSEAUX HYBRIDES ORGANIQUES/INORGANIQUES

Chaque réseau a subi des tests de dégradation et de combustion : l'analyse thermogravimétrique (ATG) sous air ou sous azote et des tests de réaction au feu, l'UL 94 et le cône calorimètre. Les trois matrices traitées dans cette partie, à base de DGEBA, de MDEA ou de MVR444, présentent toutes des comportements au feu peu satisfaisants, avec la présence d'une grande flamme et de gouttes enflammées, ainsi qu'une faible masse résiduelle dans le cas de l'UL 94, et notamment d'un fort pic de taux de dégagement calorifique, pHRR (pour « peak of Heat Release Rate ») au cône calorimètre.

En ce qui concerne la dégradation thermique des réseaux, l'ajout de POSS amène peu de changements en ce qui concerne les températures de dégradation et les masses résiduelles en fin de dégradation, avec des profils thermogravimétriques assez similaires à ceux des systèmes de référence, comme l'illustre la Figure 8.

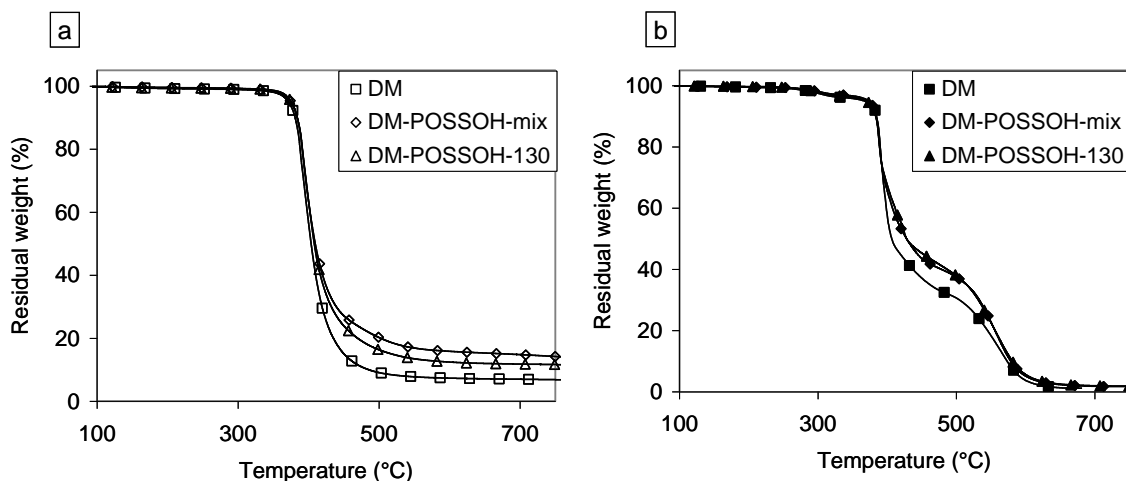


Figure 8 Spectres ATG des systèmes à base de DGEBA sous azote (a) et air (b) (10K/min)

En revanche, ces résultats d'ATG ne présagent pas de la réaction au feu des matériaux hybrides. Dans le cas du système DM-AmPOSS-60, l'ajout du POSS n'a pas permis d'améliorer la réaction au feu du réseau, comme l'a montré le test de l'UL 94, et ce malgré (i) la présence des groupements phényle du POSS et (ii) son état de fine dispersion.

Au contraire, l'ajout du POSS non réactif, l'iOPOSS, amène de fortes améliorations du comportement au feu du réseau à base de DGEBA dans le cadre du test UL 94, avec une limitation de la propagation de la flamme, l'absence de gouttes enflammées sur la quasi-totalité des échantillons, et une masse résiduelle de 94% contre 23% pour le système de référence. Les longs temps d'inflammation ne permettent cependant pas à ce matériau d'accéder à une

classification selon les critères du test. L'effet bénéfique du POSS n'est en revanche pas retrouvé dans le cas du réseau à base de TGDDM, soulignant l'importance de la matrice dans l'étude du comportement au feu.

Les systèmes à base de DGEBA et contenant le trisilanolphenyl POSS ont présenté une nette amélioration de la tenue au feu, caractérisée par l'UL 94 (Figure 9), qui est plus nette lorsque le sel d'aluminium est ajouté en plus du POSS. Cette amélioration est inexistante en présence du sel d'aluminium seulement, soulignant l'effet synergique de ces deux composés sur la tenue au feu. Cette synergie est d'ailleurs bien plus visible dans le cas des réseaux à base de TGDDM, pour lesquels l'ajout de POSSOH seulement est inefficace alors que la présence combinée des deux composés résulte en une amélioration spectaculaire. En ce qui concerne les réseaux à base de MVR444, l'ajout de POSSOH, même en combinaison du sel d'aluminium, ne permet pas d'améliorer significativement la réaction au feu des réseaux dans le scénario de l'UL 94.

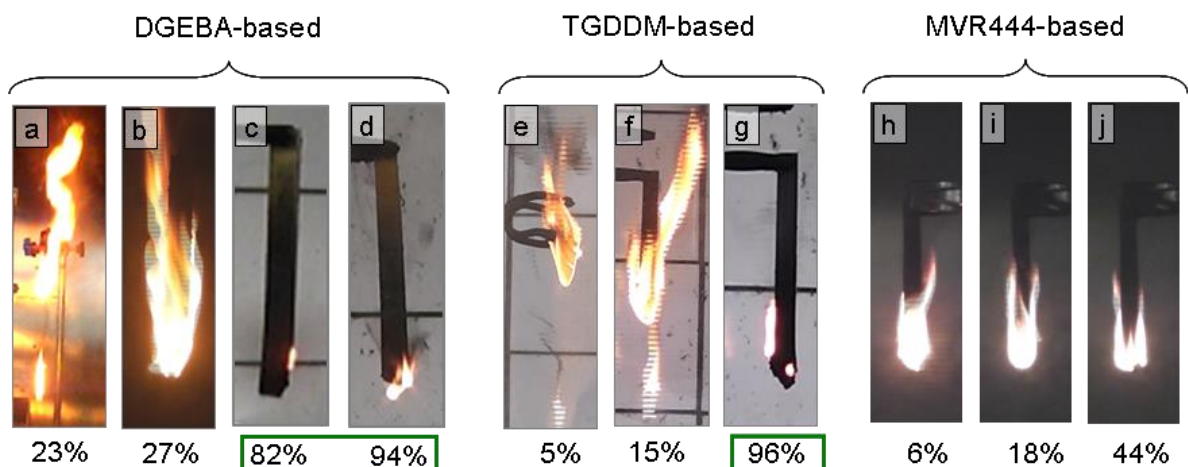


**Figure 9** Instantanés représentatifs, acquis pendant les tests d'UL 94, et masse résiduelle moyenne de a) DM, b) DM-AI, c) DM-POSSOH-130, d) DM-POSSOH-AI, e) TM, f) TM-POSSOH-130, g) TM-POSSOH-AI, h) MVR, i) MVR-POSSOH-130, j) MVR-POSSOH-AI

En revanche, les résultats obtenus via le test du cône calorimètre, mené sur des échantillons carrés de 10 cm de côté à 50 kW/m<sup>2</sup>, présentent des tendances sensiblement différentes de celles révélées par le test de l'UL 94. En effet, en ce qui concerne les réseaux à base de DGEBA, les courbes HRR présentent une amélioration limitée, en terme de pHRR notamment, alors que les réseaux à base de TGDDM contenant le POSSOH présentent une réduction de près de 30% du pHRR comparé à la référence, mais il n'y a quasiment pas de différence entre les réseaux TM-POSSOH-130 et TM-POSSOH-AI. Pour les réseaux à base de MVR444, l'amélioration spectaculaire (-54% sur le pHRR) observée pour le réseau MVR-POSSOH-AI est d'autant plus remarquable que l'UL 94 ne laissait en aucun cas présager d'une telle amélioration. Cela confirme l'effet synergique des deux composés – le POSS et le sel

métallique – qui ne semble toutefois s’exprimer ou être efficace que dans certaines conditions de scénario au feu et de nature du prépolymère epoxy.

L’étude des résidus de cône donne également des informations sur le mécanisme de protection au feu dans certains cas (Figure 11), notamment dans le cas des réseaux TM-POSSOH-AI et MVR-POSSOH-AI, qui présentent un fort gonflement qui se développe durant la combustion et persiste jusqu’à l’extinction de l’échantillon. L’intérieur de ces résidus se caractérise par une structure alvéolée, bien définie, inexistante dans les autres matériaux. Ce phénomène de gonflement est connu sous le nom d’intumescence, souvent présent dans les matériaux comportant des composés phosphorés, et est associé à un mécanisme de protection physique basé sur l’isolation thermique et l’inhibition des transferts de gaz entre le matériau et la zone de flamme.

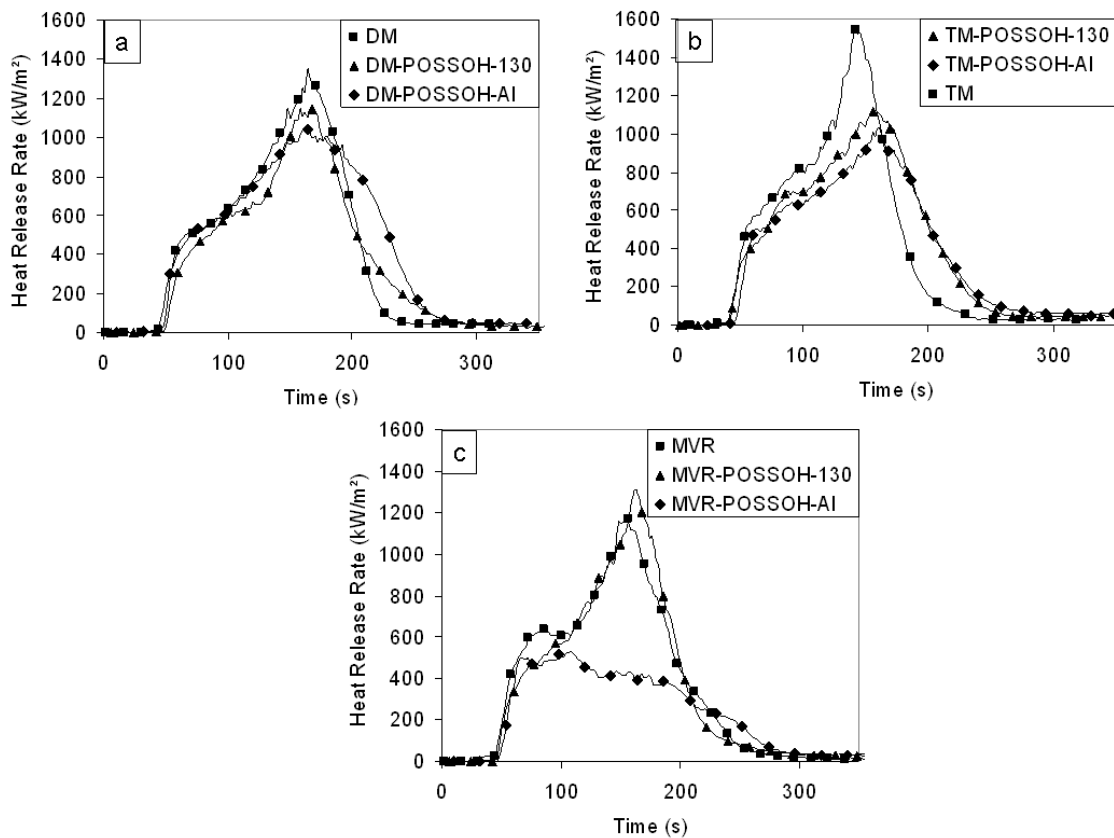


**Figure 10 Courbes HRR de cône calorimètre des réseaux à base de a) DGEBA, b) TGDDM et c) MVR444**

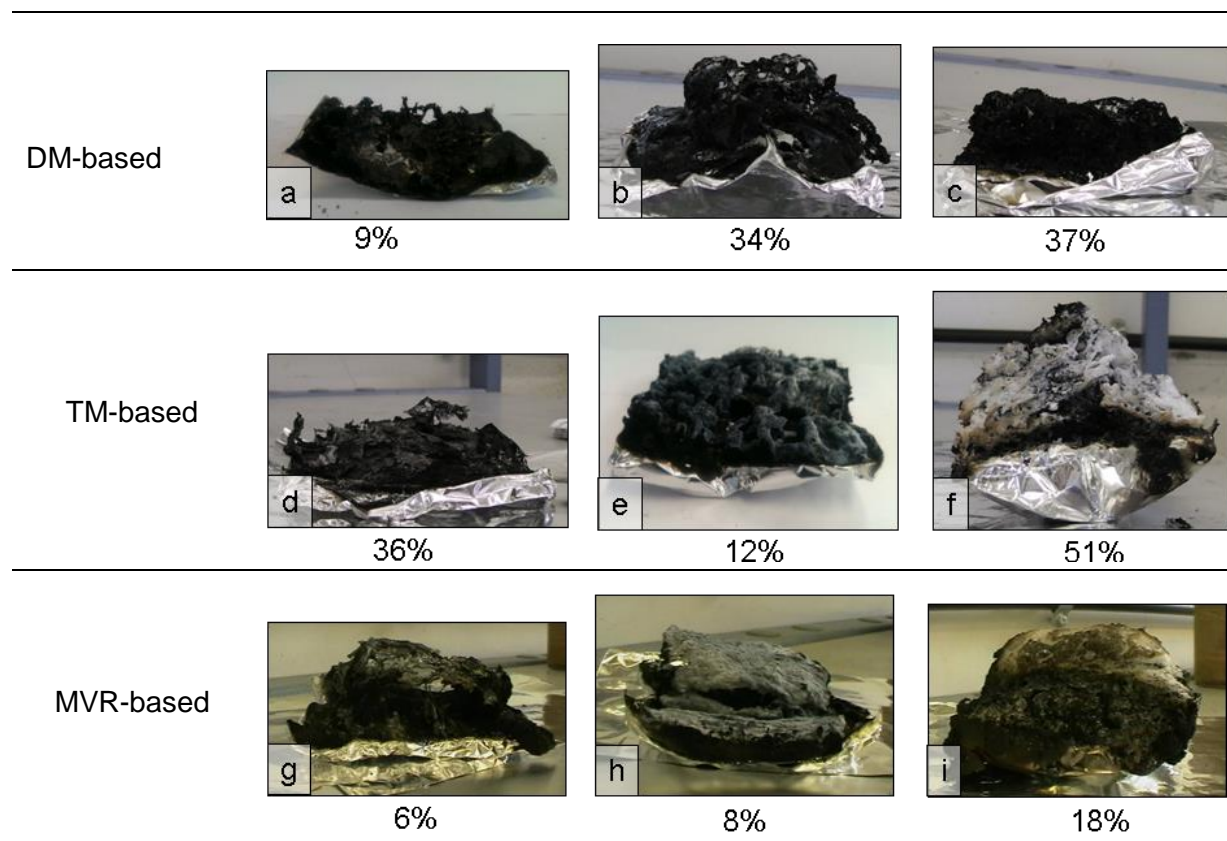


**Figure 11** Résidus de cône calorimètre de a) DM, b) DM-POSSOH-130, c) DM-POSSOH-AI, d) TM, e) TM-POSSOH-130, f) TM-POSSOH-AI, g) MVR, h) MVR -POSSOH-130, i) MVR -POSSOH-AI

Faire le lien entre le comportement au feu et la morphologie des systèmes avant combustion est finalement difficile, car pour des systèmes pour lesquels la morphologie ne change pas fondamentalement (TM-POSSOH-130 vs TM-POSSOH-AI), le comportement au feu peut être radicalement différent. Si la nature du prépolymère est effectivement le paramètre clé contrôlant la morphologie, elle influe aussi sur le comportement au feu des réseaux, mais également sur l'influence des additifs sur les propriétés feu.

Il est également délicat de comparer des systèmes dans lesquels des POSS de différentes natures ont été introduits, sur la base seule des morphologies générées par ces POSS. Par exemple, le très bon état de dispersion de l'AmPOSS n'a pas permis d'obtenir une amélioration de la réaction au feu du réseau dans lequel il a été introduit, au contraire de l'iOPOSS, à l'état d'agrégats dans le matériau final.

#### 4. LE POSSOH COMME RETARDATEUR DE FLAMME DANS DES MÉLANGES THERMODURS/THERMOPLASTIQUES

Un des objectifs du projet européen dans lequel s'est inscrit ce travail a été la production de matériaux composites résistants au feu par le procédé d'entremêlement. Celui-ci consiste à

entrelacer des fibres de polymère, possiblement dopé, avec des fibres de renfort, puis à soumettre la pièce à un cycle de pression et de température afin de former la matrice polymère. Dans le cadre des matériaux thermodurcissables, l'introduction de polymère thermoplastique est inévitable pour obtenir un matériau filable.

Un des partenaires du projet, Cytec, a proposé l'utilisation d'une fibre à base de polymère thermoplastique, le polyetherimide (PEI), et contenant l'agent durcisseur. Le procédé consisterait donc à entremêler ces fibres avec les fibres de renfort, et injecter par la suite le prépolymère epoxy. L'intérêt d'une telle stratégie serait la dispersion d'additifs ignifugeants dans ces fibres à base de polymère, ce qui permettrait de s'affranchir de l'effet de filtration par le renfort souvent expérimenté lors de la production de composites chargés par le procédé d'infusion. D'autre part, l'ajout de thermoplastique dans les réseaux thermodurs est une solution pour l'amélioration de certaines propriétés mécaniques telles que la ténacité.

Les mélanges thermodurs/thermoplastiques sont soumis à un phénomène de séparation de phase bien connu. Au-delà d'une certaine quantité de thermoplastique dans le système, une inversion de phase apparaît, caractérisée par des nodules riches en epoxy dans une matrice à dominante thermoplastique (Figure 12). Dans le cas des systèmes à base de TGDDM et PEI (comme dans le cas présent), l'inversion de phase a été observée pour un taux de thermoplastique aussi bas que 13 %m [136] – le point d'inversion de phase dépendant de plusieurs paramètres, notamment de la masse molaire du thermoplastique.

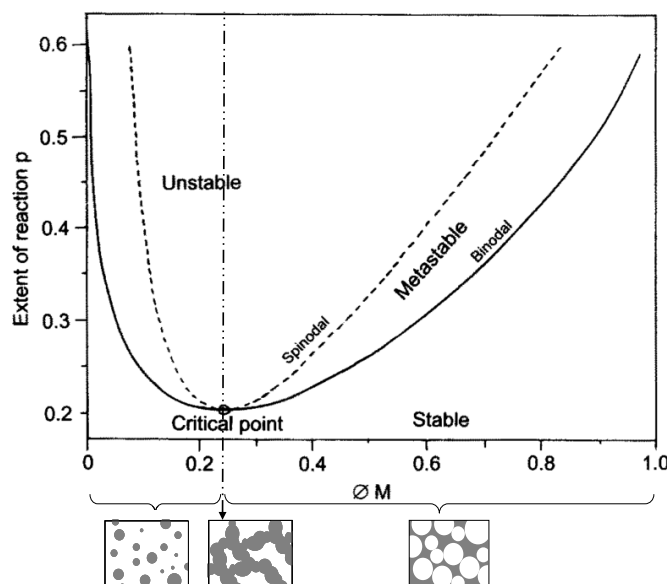


**Figure 12 Diagramme de phase schématisant conversion-pourcentage de thermoplastique [92] et morphologies caractéristiques des matériaux finaux ( les zones blanches et grises représentent les phases riches en polymères thermodurcissable et thermoplastique, respectivement)**

## 4.1. MATÉRIAUX, MORPHOLOGIES ET TEMPÉRATURES DE TRANSITION VITREUSE

### 4.1.a. Matériaux

Les réseaux sont basés sur la TGDDM, l'(les) agent(s) de réticulation étant amené(s) par la fibre EF 10007, fournie par Cytec (« Curative Fibre », CF). Cette fibre contenant 55 %m de PEI (Ultem 1010, Sabic), son utilisation contrôle non seulement le rapport stœchiométrique, mais également la quantité de thermoplastique présent dans le matériau final.

Trois cas ont été étudiés (Tableau 4) :

- Un cas pour lequel le rapport stœchiométrique est respecté –  $a/e=1$  ;
- Un cas pour lequel l'inversion de phase est évitée, avec une quantité de thermoplastique de 10 %m ;
- Un cas intermédiaire, avec une quantité de thermoplastique de 17 %m.

CF content (phr)	Final PEI content (wt%)	a/e
110	23	1
66	17	0.59
28	10	0.26

**Tableau 4 Quantité de CF dans les réseaux, et, en conséquence, quantité de PEI et ratio stœchiométrique**

Pour chacun de ces 3 cas, 3 réseaux ont été produits, donnant un total de 9 réseaux :

- Un réseau de référence : TGDDM/CF, appelé TCF
- Un réseau contenant 4 %m de POSSOH : TCF-POSSOH
- Un réseau contenant 4 %m de POSSOH et 0.4 %m d'  $Al(acac)_3$  : TCF-POSSOH-Al

La fibre contenant le thermoplastique étant difficilement soluble dans la TGDDM, tous les composants des réseaux ont été préalablement solubilisés dans le dichlorométhane. Des échantillons destinés au cône calorimètre ont été produits pour les trois réseaux avec 10 %m de PEI.

### 4.1.b. Morphologies et séparation de phase

Les matériaux finaux ont été observés au MEB, dans un premier temps. Comme attendu, les réseaux de référence contenant 10 %m et 23%<sub>m</sub> de PEI présentent une matrice riche en epoxy et PEI (inversion de phase), respectivement (Figure 13). Le système TCF comprenant 17 %m

de PEI présente quant à lui une structure en phases co-continues, signifiant que cette quantité de PEI se situe proche du point critique (cf Figure 12).

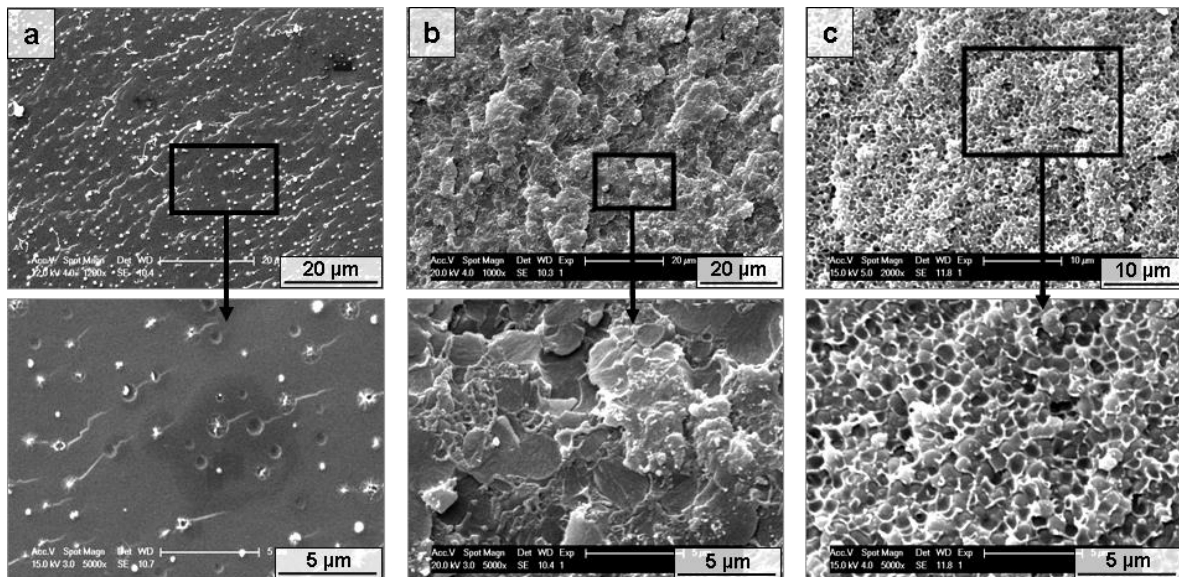


**Figure 13 Observation MEB des réseaux TCF avec a) 10 %m PEI ( $a/e=0.26$ ) ; b) 17 %m PEI ( $a/e=0.59$ ) ; c) 23.5 %m PEI ( $a/e=1$ )**

L'ajout du POSS avec ou sans le sel d'aluminium a potentiellement une influence sur la morphologie, pouvant résulter de la modification des cinétiques de réactions, de la miscibilité des composants des systèmes, etc – modifiant ainsi le phénomène de séparation de phase. L'effet est différent suivant la quantité de CF introduite dans les systèmes :

- Systèmes contenant 10 %m de PEI : l'ajout de POSS avec ou sans  $Al(acac)_3$  n'a pas d'effet notoire sur la morphologie ;
- Systèmes contenant 17 %m de PEI : la morphologie en phases co-continues passe, avec l'ajout de POSSOH (avec ou sans  $Al(acac)_3$ ), à une structure d'inversion de phase, majoritairement ;
- Systèmes contenant 23 %m de PEI : l'ajout de POSSOH avec ou sans le sel d'aluminium cause une augmentation des nodules riches en epoxy au sein de la matrice PEI.

L'observation MEB ne permettant pas de distinguer des domaines riches en POSS, l'observation MET, couplée à une analyse EDX, a été menée sur les réseaux contenant des POSS. En terme de structure, l'effet le plus notable consiste en l'apparition de nodules de PEI irréguliers dans le réseau TCF-POSSOH comportant 10 %m de PEI (Figure 14), et la présence de filaments noirs – faisant penser aux structures observées dans les réseaux à base de TGDDM – dans ces nodules seulement. Dans le réseau TCF-POSSOH-Al (10 %m PEI), les

nodules de PEI sont tous réguliers, avec parfois des sous-structures (des nodules riches en epoxy dans les phases de PEI), et aucun filament noir n'a été observé.

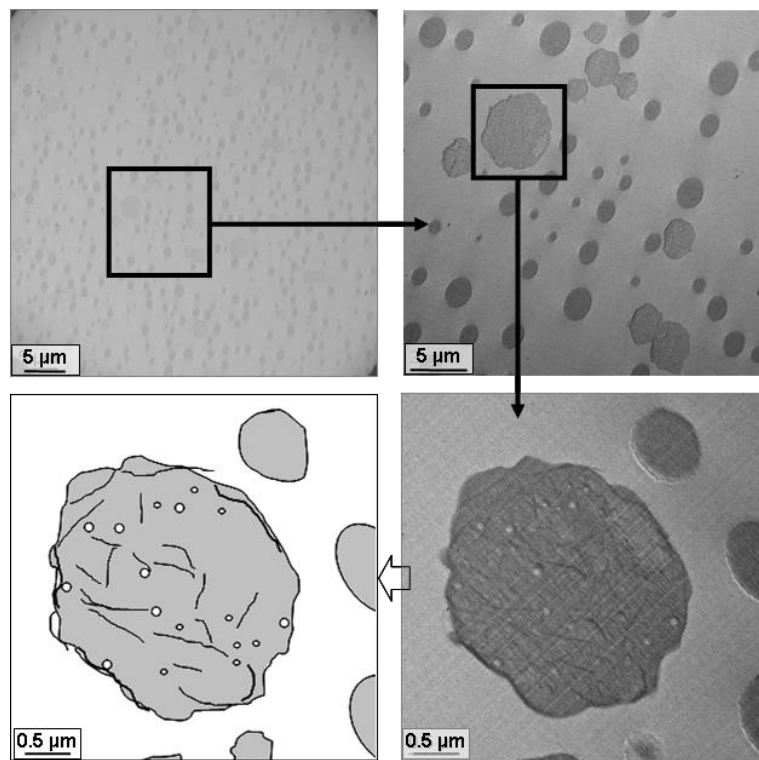


**Figure 14 Images MET du réseau TCF-POSSOH contenant 10 %m de PEI ( $a/e=0.26$ ) à différent grossissements et schéma d'un nodule irrégulier**

L'analyse EDX (Figure 15), indiquant un fort taux de silicium dans les nodules irréguliers du système TCF-POSSOH, confirme la présence de POSSOH dans ces nodules et la nature des filaments noirs. Dans le réseau TCF-POSSOH-AI, la quantité de silicium détectée est significativement plus importante dans la matrice que dans les nodules. L'absence de domaines séparés dans la matrice riche en epoxy indique la dispersion à l'état nanométrique, donc moléculaire, du POSSOH.

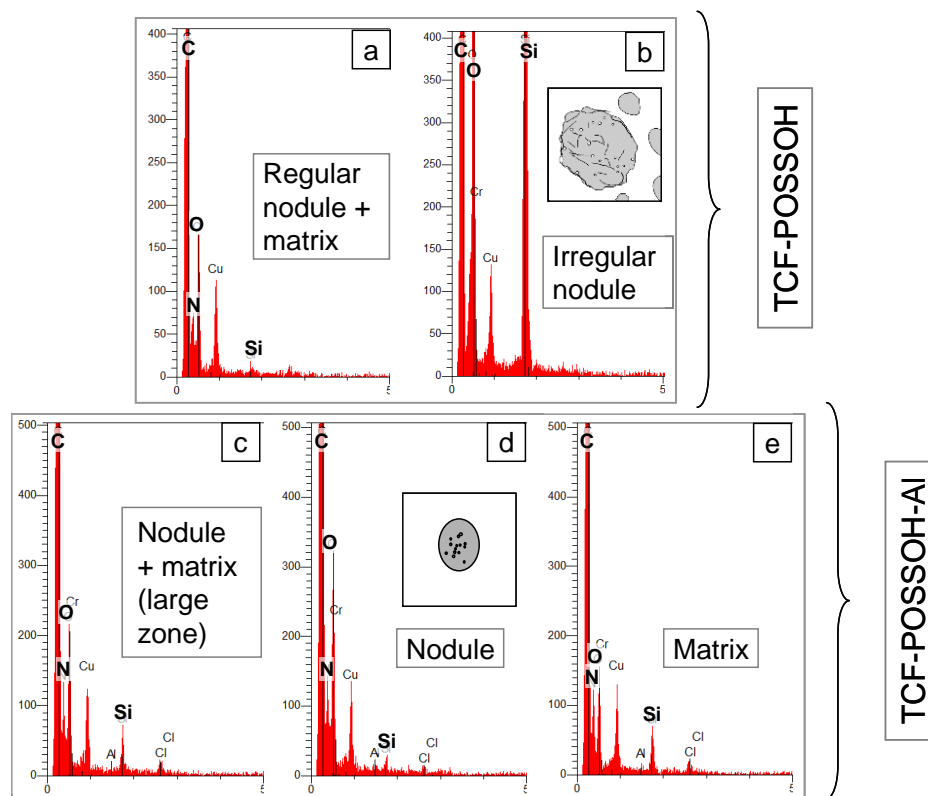


**Figure 15 Analyse EDX des réseaux TCF-POSSOH (a,b) et TCF-POSSOH-AI (c, d, e) contenant 10 %m de PEI (a/e=0.26) ; détails des zones analysées : a) zone de diamètre 2  $\mu\text{m}$ , ciblant un nodule régulier et la matrice environnante, b) zone de diamètre 700 nm, ciblant un nodule irrégulier, c) zone de diamètre 10  $\mu\text{m}$ , comprenant la matrice et des des nodules, d) zone de diamètre 700 nm, ciblant un nodule, e) zone de diamètre 700 nm, ciblant la matrice**

#### **4.1.c. Températures de transition vitreuse**

Etant donné que la quantité de fibre CF contrôle le rapport stœchiométrique et également la nature de la phase principale des matériaux polymères. Une analyse par DSC comportant 2 rampes de montée en température (jusqu'à 250 °C, 10 K/min) a permis d'étudier l'influence des additifs sur la température de transition vitreuse, mais également sur son évolution entre les deux rampes en températures.

La première rampe en température révèle, comme il était attendu, que la température de transition vitreuse ( $T_g$ ) est la plus élevée pour un rapport stœchiométrique de 1. En revanche, pour les réseaux hors-stœchiométrie contenant le POSSOH et le sel d'aluminium, la  $T_g$  est bien plus élevée que pour les réseaux correspondants de référence et avec seulement le POSS.

D'autre part, la  $T_g$  des réseaux pour lesquels le rapport stœchiométrique vaut 1 n'augmente pas ou très peu entre les deux rampes de température (Figure 16), ce qui implique que la réaction epoxy-agent de réticulation est complète. Au contraire, l'augmentation de la  $T_g$  d'une

rampe de température à l'autre pour les réseaux hors-stœchiométrie révèle un effet de post-cuisson de la première rampe de montée en température, qui peut être attribuée à une réaction d'homopolymérisation en la présence d'un excès d'époxy. D'autre part, cette augmentation est plus importante dans les réseaux hors-stœchiométrie contenant le POSSOH et l'Al(acac)<sub>3</sub>. La présence combinée de ces deux composés promeut donc cette réaction d'homopolymérisation – comme il l'avait d'ailleurs été montré pour des réseaux à base de DGEBA/MDEA.

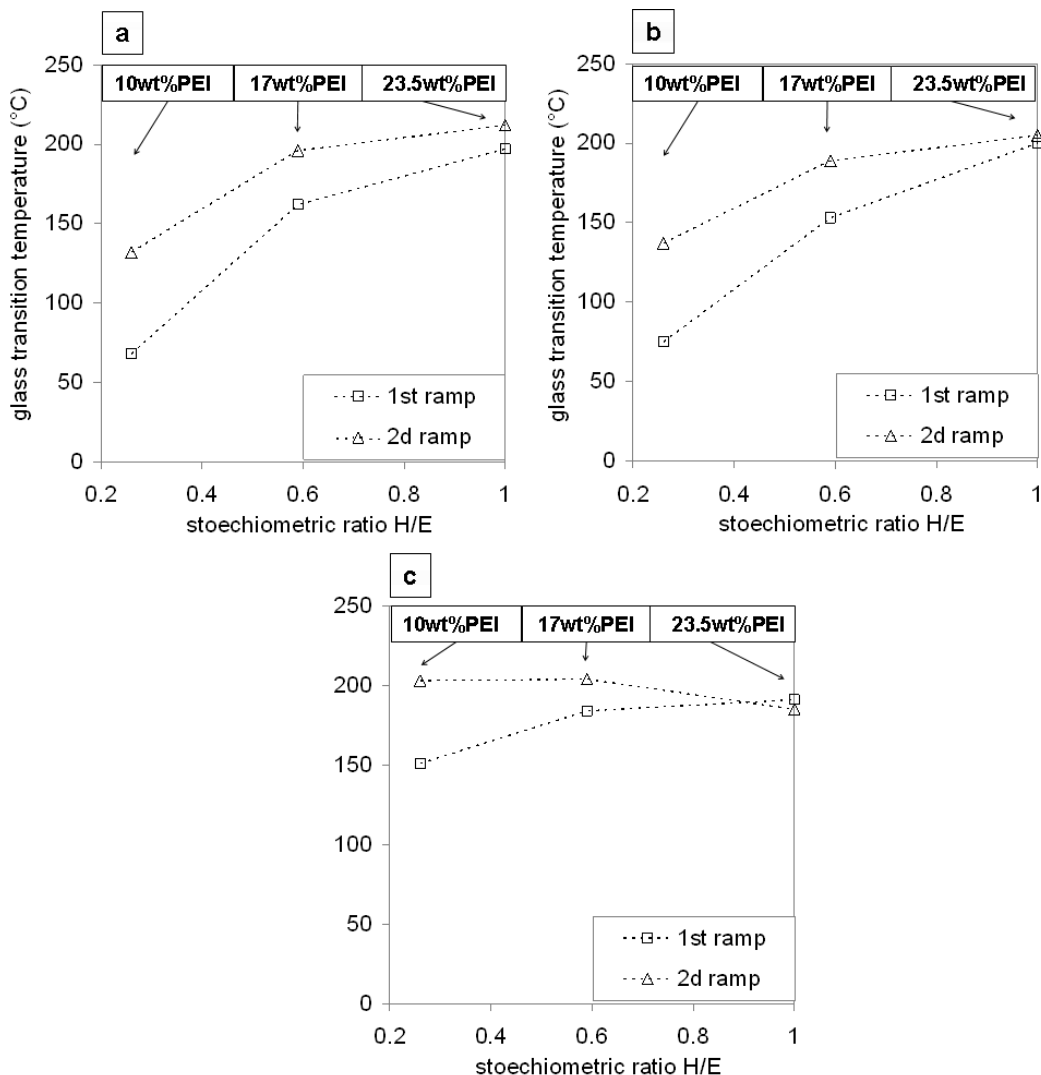


**Figure 16 Evolution de la Tg des réseaux à base de TGDDM et CF entre la 1<sup>ère</sup> rampe DSC (carrés) et la 2<sup>de</sup> rampe (triangles). a) TCF; b) TCF-POSSOH; c) TCF-POSSOH-Al**

#### 4.2. COMPORTEMENT AU FEU DES RÉSEAUX CONTENANT 10 %M DE PEI

Les courbes HRR obtenues pour les systèmes TCF contenant 10 %m de PEI parlent d'elles-mêmes (Figure 17). Une diminution de 84% du pHRR est obtenue par l'ajout du POSSOH en combinaison avec le sel d'aluminium. Les autres paramètres relatifs au cône – dégagement

calorifique total, quantité de fumées – sont également significativement réduits. En revanche, l'ajout de POSSOH seulement ne permet pas d'obtenir la moindre amélioration du comportement au feu, évalué par le cône calorimètre. Ici encore, une synergie entre les deux composés – également responsable d'un phénomène d'intumescence – est observée.

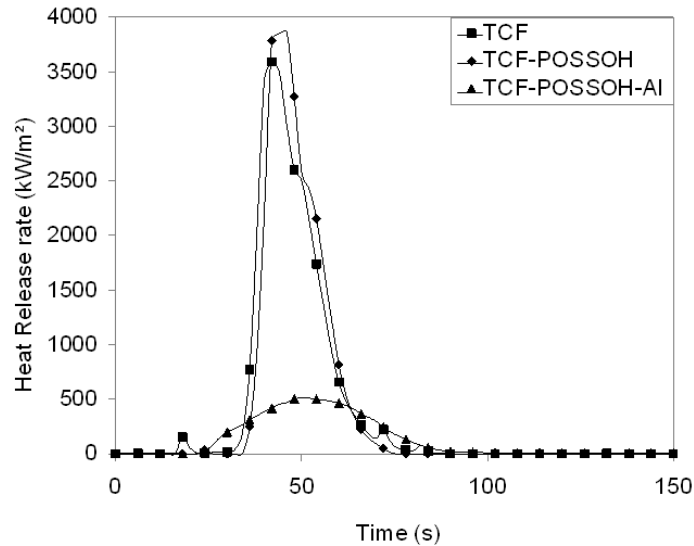


Figure 17 Comparaison des courbes HRR des réseaux TCF avec 10 %m de PEI

## 5. CONCLUSION

Dans ce travail, l'influence de POSS de différentes natures sur le comportement au feu de réseaux thermodurs basés sur différents prépolymères epoxy a été étudiée. La question de l'influence de la morphologie sur cette propriété macroscopique – qui n'est pas seulement intrinsèque au matériau, mais dépend bien de nombreux paramètres externes – a été traitée en faisant varier les POSS ainsi que leur procédé de dispersion.

L'une des conclusions majeures de cette étude, en ce qui concerne la morphologie des matériaux finaux, est que le paramètre clé qui la contrôle reste la nature du prépolymère epoxy – de laquelle dépend la structure chimique du réseau mais aussi les mécanismes et les cinétiques de polymérisation. Un arrangement inédit des POSS ayant des fonctions silanol a notamment été observé dans les réseaux à base de TGDDM, qui découle probablement de la condensation des POSS sur eux-mêmes dans ces systèmes. Un système particulier, comprenant l'addition combinée de POSSOH et d'un sel d'aluminium, a montré une forte accélération de la cinétique de polymérisation, s'accompagnant peut-être d'un changement dans les mécanismes de réaction.

En ce qui concerne le comportement au feu des réseaux ainsi élaborés, il est au final délicat de discriminer l'effet des différentes variables : la nature des POSS eux-mêmes, évidemment, mais

également, dans le cas particulier du POSSOH, la nature du prépolymère epoxy et le type de morphologie – qui varie avec la nature de l'epoxy. Il semble que le mode de dispersion des POSS dans le prépolymère, dans le cas présent, n'ait pas eu une influence significative sur le comportement au feu. D'autre part, une synergie a été mise en évidence par l'ajout combiné du POSSOH avec l' $\text{Al}(\text{acac})_3$ , qui se manifeste dans tous les types de réseaux epoxy – mais entraîne des phénomènes différents suivant la nature du prépolymère.

Des résultats intéressants et prometteurs ont été dégagés dans cette thèse, avec de nombreuses questions qui restent parfois en suspens, telles que le mécanisme d'action du couple POSSOH/ $\text{Al}(\text{acac})_3$  sur la combustion des réseaux, ou l'origine des différences en termes de morphologie et de réaction au feu entre les réseaux basés sur différents types d'epoxy. Une des limitations rencontrées dans cette étude a notamment été le manque de sensibilité de certaines techniques de caractérisation, considérant les petites quantités d'additifs introduites dans les systèmes. L'utilisation d'autres techniques ou l'étude de systèmes modèles pourraient éventuellement permettre d'obtenir des éléments sur les mécanismes de réaction à l'œuvre dans ces systèmes complexes. Faire varier les concentrations d'additifs et la nature du sel métallique pourrait également être une stratégie pour acquérir des éléments de compréhension.



---

## REFERENCES

---

- [1] EFRA, "The Reality / Statistics." [Online]. Available: [www.cefic-efra.com](http://www.cefic-efra.com). Accessed: 2014.
- [2] European Parliament and Council of European Union, "Directive 95/28/EC of the European Parliament and of the Council of 24 October 1995 relating to the burning behaviour of materials used in the interior construction of certain categories of motor vehicle," *Official Journal L 281*. [Online]. Available: <http://eur-lex.europa.eu/legal-content/EN/ALL/?jsessionid=4tvITRQfQ22nW0jQXGyXXQcML1kXXgv5V345hN2KznHGTXvc3znJl-67492056?uri=CELEX:31995L0028>. Accessed: 2014.
- [3] European Flame Retardants Association, "Frequently Asked Questions on Flame Retardants." [Online]. Available: [http://www.flameretardants-online.com/images/userdata/pdf/168\\_DE.pdf](http://www.flameretardants-online.com/images/userdata/pdf/168_DE.pdf). Accessed: 2014.
- [4] D. M. Marquis and É. Guillaume, "Modelling Reaction-to-fire of Polymer-based Composite Laminate," in *Nanocomposites with Unique Properties and Applications in Medicine and Industry*, D. J. Cuppoletti, Ed. InTech, 2011, pp. 175–204.
- [5] C. Beyler and M. Hirschler, "Thermal decomposition of polymers," in *SFPE Handbook of Fire Protection Engineering, 3rd ed.*, NFPA, Ed. Quincy, MA (USA), 2002, pp. 110–131.
- [6] T. Kashiwagi, "Polymer combustion and flammability—role of the condensed phase," in *Symposium (International) on Combustion, 25th*, 1994, pp. 1423–1437.
- [7] A. Factor, "Char formation in aromatic engineering polymers," in *Fire and Polymers*, G. L. Nelson, Ed. Washington, DC (USA): American Chemical Society, 1990, pp. 274–287.
- [8] D. E. Stuetz, A. H. DiEdwardo, F. Zitomer, and B. P. Barnes, "Polymer combustion," *J. Polym. - Polym. Chem. Ed.*, vol. 13, no. 3, pp. 585–621, 1975.
- [9] S. K. Brauman, "Polymer degradation during combustion," *J. Polym. Sci. - Part B Polym. Phys.*, vol. 26, no. 6, pp. 1159–1171, 1988.
- [10] D. E. Stuetz, A. H. DiEdwardo, F. Zitomer, and B. P. Barnes, "Polymer flammability. I," *J. Polym. - Polym. Chem. Ed.*, vol. 18, no. 3, pp. 967–985, 1980.
- [11] D. E. Stuetz, A. H. DiEdwardo, F. Zitomer, and B. P. Barnes, "Polymer flammability. II," *J. Polym. - Polym. Chem. Ed.*, vol. 18, no. 3, pp. 987–1009, 1980.

- [12] T. Kashiwagi and T. J. Ohlemiller, "A study of oxygen effects on nonflaming transient gasification of PMMA and PE during thermal irradiation," *Symp. Combust.*, vol. 19, no. 1, pp. 815–823, 1982.
- [13] T. R. Hull and A. A. Stec, "Polymers and Fire," in *Fire Retardancy of Polymers: New Strategies and Mechanisms*, T. R. Hull and B. K. Kandola, Eds. Cambridge, UK: Royal Society of Chemistry, 2009, pp. 1–14.
- [14] W. Zhang, X. Li, L. Li, and R. Yang, "Study of the synergistic effect of silicon and phosphorus on the blowing-out effect of epoxy resin composites," *Polym. Degrad. Stab.*, vol. 97, no. 6, pp. 1041–1048, 2012.
- [15] C. Gérard, G. Fontaine, S. Bellayer, and S. Bourbigot, "Reaction to fire of an intumescent epoxy resin: Protection mechanisms and synergy," *Polym. Degrad. Stab.*, vol. 97, no. 8, pp. 1366–1386, 2012.
- [16] ASTM International, "D3801-00 Standard Test Method for Measuring the Comparative Burning Characteristics of Solid Plastics in a Vertical Position," 2000.
- [17] W. Kaufmann, F. H. Prager, and H. W. Schiffer, *Electrical engineering: international plastics flammability Handbook*. Munich: Hanser Publishers, 1990, pp. 344–378.
- [18] G. You, Z. Cheng, H. Peng, and H. He, "The synthesis and characterization of a novel phosphorus-nitrogen containing flame retardant and its application in epoxy resins," *J. Appl. Polym. Sci.*, vol. 131, no. 22, p. to be published in Nov. 2014, 2014.
- [19] V. Babrauskas, "Development of the cone calorimeter—A bench-scale heat release rate apparatus based on oxygen consumption," *Fire Mater.*, vol. 8, no. 2, pp. 81–95, 1984.
- [20] ISO, "ISO 5660-1:2002 Reaction-to-fire tests -- Heat release, smoke production and mass loss rate -- Part 1: Heat release rate (cone calorimeter method)," 2002.
- [21] V. Babrauskas, "The Cone Calorimeter," in *Heat Release in Fires*, S. J. Grayson, Ed. Barking: Elsevier Science Publishers LTD, 1992, pp. 61–92.
- [22] V. Babrauskas and R. Peacock, "Heat release rate: the single most important variable in fire hazard," *Fire Saf. J.*, vol. 18, no. 3, pp. 255–272, 1992.
- [23] W. Liu, R. J. Varley, and G. P. Simon, "Understanding the decomposition and fire performance processes in phosphorus and nanomodified high performance epoxy resins and composites," *Polymer (Guildf.)*, vol. 48, no. 8, pp. 2345–2354, 2007.
- [24] B. Scharrel and T. Hull, "Development of fire-retarded materials—Interpretation of cone calorimeter data," *Fire Mater.*, vol. 31, no. 5, pp. 327–354, 2007.
- [25] B. Scharrel, M. Bartholmai, and U. Knoll, "Some comments on the use of cone calorimeter data," *Polym. Degrad. Stab.*, vol. 88, no. 3, pp. 540–547, 2005.
- [26] A. Morgan and M. Bundy, "Cone calorimeter analysis of UL-94 V-rated plastics," *Fire Mater.*, vol. 31, no. 4, pp. 257–283, 2007.

- 
- [27] R. E. Lyon, "Ignition resistance of plastics," in *BCC Conference Proceedings: Recent advances in flame retardancy of polymeric materials*, 2002.
- [28] R. E. Lyon, "Plastics and Rubber," in *Handbook of Building Materials for Fire Protection*, C. A. Harper, Ed. New York (USA): McGraw-Hill, 2004, pp. 1–51.
- [29] M. F. Mustafa, W. D. Cook, T. L. Schiller, and H. M. Siddiqi, "Curing behavior and thermal properties of TGDDM copolymerized with a new pyridine-containing diamine and with DDM or DDS," *Thermochim. Acta*, vol. 575, pp. 21–28, 2014.
- [30] A. Gu and G. Liang, "Thermal degradation behaviour and kinetic analysis of epoxy/montmorillonite nanocomposites," *Polym. Degrad. Stab.*, vol. 80, no. 2, pp. 383–391, 2003.
- [31] B. Montero, R. Bellas, C. Ramírez, M. Rico, and R. Bouza, "Flame retardancy and thermal stability of organic–inorganic hybrid resins based on polyhedral oligomeric silsesquioxanes and montmorillonite clay," *Compos. Part B Eng.*, vol. 63, pp. 67–76, 2014.
- [32] G. Camino, L. Costa, E. Casorati, G. Bertelli, and R. Locatelli, "The oxygen index method in fire retardance studies of polymeric materials," *J. Appl. Polym. Sci.*, vol. 35, no. 7, pp. 1863–76, 1988.
- [33] R. Walters and R. Lyon, "Molar group contributions to polymer flammability," *J. Appl. Polym. Sci.*, vol. 87, no. 3, pp. 548–563, 2003.
- [34] R. E. Lyon and M. L. Janssens, "Polymer Flammability," Springfield, Virginia (USA), report, 25p, 2005.
- [35] A. B. Morgan and J. Gilman, "An overview of flame retardancy of polymeric materials: application, technology, and future directions," *Fire Mater.*, vol. 37, no. 4, pp. 259–279, 2013.
- [36] G. Camino and L. Costa, "Performance and mechanisms of fire retardants in polymers—A review," *Polym. Degrad. Stab.*, vol. 20, no. 3–4, pp. 271–294, 1988.
- [37] J. Troitzsch, "Overview of flame retardants," *Chem. today*, vol. 16, pp. 18–24, 1998.
- [38] E. Papazoglou, "Flame retardants for plastics," in *Handbook of building materials for fire protection*, C. Harper, Ed. New York: Professional, McGraw-Hill, 2004, pp. 1–88.
- [39] R. Debdatta, "Epoxy Composites: Impact Resistance and Flame Retardancy," *Rapra Rev. Reports*, vol. 16, no. 5, pp. 23–26, 2005.
- [40] M. Alaei, P. Arias, A. Sjödin, and A. Bergman, "An overview of commercially used brominated flame retardants, their applications, their use patterns in different countries/regions and possible modes of release.," *Environ. Int.*, vol. 29, no. 6, pp. 683–9, 2003.
- [41] C. Gérard, G. Fontaine, and S. Bourbigot, "New Trends in Reaction and Resistance to Fire of Fire-retardant Epoxies," *Materials (Basel)*, vol. 3, no. 8, pp. 4476–4499, 2010.

- [42] S. Kemmlein, D. Herzke, and R. J. Law, "Brominated flame retardants in the European chemicals policy of REACH-Regulation and determination in materials.," *J. Chromatogr. A*, vol. 1216, no. 3, pp. 320–33, 2009.
- [43] L. S. Birnbaum and D. F. Staskal, "Brominated Flame Retardants: Cause for Concern?," *Environ. Health Perspect.*, vol. 112, no. 1, pp. 9–17, 2003.
- [44] Y. Liu, G. Hsiue, R. Lee, and Y. Chiu, "Phosphorus-Containing Epoxy for Flame Retardant . III : Using Phosphorylated Diamines as Curing Agents," *J. Appl. Polym. Sci.*, vol. 63, no. 7, pp. 895–901, 1996.
- [45] P. M. Hergenrother, C. M. Thompson, J. G. Smith, J. W. Connell, J. a. Hinkley, R. E. Lyon, and R. Moulton, "Flame retardant aircraft epoxy resins containing phosphorus," *Polymer (Guildf.)*, vol. 46, no. 14, pp. 5012–5024, 2005.
- [46] S. Levchik and G. Camino, "Epoxy resins cured with aminophenylmethylphosphine oxide 1: Combustion performance," *Polym. Adv. Technol.*, vol. 7, no. 11, pp. 823–830, 1996.
- [47] S. Levchik, A. Piotrowski, E. Weil, and Q. Yao, "New developments in flame retardancy of epoxy resins," *Polym. Degrad. Stab.*, vol. 88, no. 1, pp. 57–62, 2005.
- [48] European Parliament and Council of European Union, "Corrigendum to Regulation (EC) No 1907/2006 of the European Parliament and of the Council of 18 December 2006 concerning the Registration, Evaluation, Authorisation and Restriction of Chemicals (REACH), establishing a European Chemicals Agency, amending D," *Official Journal L* 136/3, 2007. [Online]. Available: <http://eur-lex.europa.eu/LexUriServ/LexUriServ.do?uri=OJ:L:2007:136:0003:0280:EN:PDF>. Accessed: 2014.
- [49] European Parliament and Council of European Union, "DIRECTIVE 2003/11/EC OF THE EUROPEAN PARLIAMENT AND OF THE COUNCIL of 6 February 2003 amending for the 24th time Council Directive 76/769/EEC relating to restrictions on the marketing and use of certain dangerous substances and preparations (pentabromodip," *Official Journal L* 42/45, 2003. [Online]. Available: <http://eur-lex.europa.eu/LexUriServ/LexUriServ.do?uri=OJ:L:2003:042:0045:0046:EN:PDF>. Accessed: 2014.
- [50] European Commission, "Communication from the Commission on the results of the risk evaluation and the risk reduction strategies for the substances: sodium chromate, sodium dichromate and 2,2',6,6'-tetrabromo-4,4'-iso- propylidenediphenol (tetrabromobisphenol A)," *Official Journal C* 152/11, 2008. [Online]. Available: <http://eur-lex.europa.eu/LexUriServ/LexUriServ.do?uri=OJ:C:2008:152:0011:0020:EN:PDF>. Accessed: 2014.
- [51] European Commission, "Nanomaterials: Impact assessment on transparency measures for nanomaterials on the market," *European Commission website*. [Online]. Available: [http://ec.europa.eu/enterprise/sectors/chemicals/reach/nanomaterials/index\\_en.htm](http://ec.europa.eu/enterprise/sectors/chemicals/reach/nanomaterials/index_en.htm). Accessed: 2014.
- [52] C. A. May, Ed., *Epoxy resins-chemistry and technology*. New York (USA): Marcel Dekker, Inc., 1988.

- [53] D. Ratna, "Epoxy Resins," in *Handbook of thermoset resins*, Shawbury (UK): iSmithers Rapra Publishing, 2009, pp. 155–186.
- [54] Hybrid Plastics Company, "POSS User's Guide." [Online]. Available: <http://www.hybridplastics.com/docs/user-v2.06.pdf>. Accessed: 2014.
- [55] M. F. Roll, M. Z. Asuncion, J. Kampf, and R. M. Laine, "Para-Octaiodophenylsilsesquioxane, [p-IC<sub>6</sub>H<sub>4</sub>SiO<sub>1.5</sub>]<sub>8</sub>, a Nearly Perfect Nano-Building Block," *ACS Nano*, vol. 2, no. 2, pp. 320–326, 2008.
- [56] C. Zhang, T. J. Bunning, and R. M. Laine, "Synthesis and Characterization of Liquid Crystalline Silsesquioxanes," *Chem. Mater.*, vol. 13, no. 10, pp. 3653–3662, 2001.
- [57] R. M. Laine, "Nanobuilding blocks based on the [OSiO<sub>1.5</sub>]<sub>x</sub> (x= 6, 8, 10) octasilsesquioxanes," *J. Mater. Chem.*, vol. 15, no. 35–36, pp. 3725–3744, 2005.
- [58] Hybrid Plastics Company, "Nanostructured POSS chemicals," 2013. [Online]. Available: <http://www.hybridplastics.com/products/catalog.htm>. Accessed: 2014.
- [59] S. Bizet, "Nanomatériaux hybrides organique/inorganique par copolymérisation de polysilsesquioxanes polyédriques (POSSTM) avec des monomères méthacrylate," Thesis, INSA Lyon, 338 p.
- [60] E. Franchini, "Structuration of Nano-Objects in Epoxy-based Polymer Systems," Thesis, INSA-Lyon, 260 p.
- [61] G. Camino, G. Tartaglione, A. Frache, C. Manfredi, and G. Costa, "Thermal and combustion behaviour of layered silicate–epoxy nanocomposites," *Polym. Degrad. Stab.*, vol. 90, no. 2, pp. 354–362, 2005.
- [62] C. Kaynak, G. I. Nakas, and N. A. Isitman, "Mechanical properties, flammability and char morphology of epoxy resin/montmorillonite nanocomposites," *Appl. Clay Sci.*, vol. 46, no. 3, pp. 319–324, 2009.
- [63] C. Katsoulis, E. Kandare, and B. K. Kandola, "The effect of nanoparticles on structural morphology, thermal and flammability properties of two epoxy resins with different functionalities," *Polym. Degrad. Stab.*, vol. 96, no. 4, pp. 529–540, 2011.
- [64] M. Lewin and E. Pearce, "Nanocomposites at elevated temperatures: migration and structural changes," *Polym. Adv. Technol.*, vol. 17, no. 4, pp. 226–234, 2006.
- [65] G. Wu, B. Schartel, M. Kleemeier, and A. Hartwig, "Flammability of layered silicate epoxy nanocomposites combined with low-melting inorganic ceepree glass," *Polym. Eng. ...*, vol. 52, no. 3, pp. 507–517, 2012.
- [66] G. M. Wu, "Quantitative Assessment and Optimization of Flame Retardancy by the Shielding Effect in Epoxy Nanocomposites," MSc. thesis, Universität Berlin, 111 p.
- [67] D. Yu, M. Kleemeier, G. M. Wu, B. Schartel, W. Q. Liu, and A. Hartwig, "A low melting organic-inorganic glass and its effect on flame retardancy of clay/epoxy composites," *Polymer (Guildf.)*, vol. 52, no. 10, pp. 2120–2131, 2011.

- [68] G. M. Wu, B. Schartel, D. Yu, M. Kleemeier, and a. Hartwig, "Synergistic fire retardancy in layered-silicate nanocomposite combined with low-melting phenylsiloxane glass," *J. Fire Sci.*, vol. 30, no. 1, pp. 69–87, 2011.
- [69] W. Zhang, X. Li, Y. Jiang, and R. Yang, "Investigations of epoxy resins flame-retarded by phenyl silsesquioxanes of cage and ladder structures," *Polym. Degrad. Stab.*, vol. 98, no. 1, pp. 246–254, 2013.
- [70] E. Franchini, J. Galy, J.-F. Gérard, D. Tabuani, and A. Medici, "Influence of POSS structure on the fire retardant properties of epoxy hybrid networks," *Polym. Degrad. Stab.*, vol. 94, no. 10, pp. 1728–1736, 2009.
- [71] W. Zhang, X. Li, H. Fan, and R. Yang, "Study on mechanism of phosphorus–silicon synergistic flame retardancy on epoxy resins," *Polym. Degrad. Stab.*, vol. 97, no. 11, pp. 2241–2248, 2012.
- [72] H. Yang, X. Wang, B. Yu, L. Song, Y. Hu, and R. K. K. Yuen, "Effect of borates on thermal degradation and flame retardancy of epoxy resins using polyhedral oligomeric silsesquioxane as a curing agent," *Thermochim. Acta*, vol. 535, pp. 71–78, 2012.
- [73] Q. Wu, C. Zhang, R. Liang, and B. Wang, "Combustion and thermal properties of epoxy/phenyltrisilanol polyhedral oligomeric silsesquioxane nanocomposites," *J. Therm. Anal. Calorim.*, vol. 100, no. 3, pp. 1009–1015, 2009.
- [74] K. Wu, L. Song, Y. Hu, H. Lu, B. K. Kandola, and E. Kandare, "Synthesis and characterization of a functional polyhedral oligomeric silsesquioxane and its flame retardancy in epoxy resin," *Prog. Org. Coatings*, vol. 65, no. 4, pp. 490–497, 2009.
- [75] T. Lu, T. Chen, and G. Liang, "Synthesis, thermal properties, and flame retardance of the epoxy-silsesquioxane hybrid resins," *Polym. Eng. Sci.*, vol. 47, no. 3, pp. 225–234, 2007.
- [76] K. Wu, B. Kandola, and E. Kandare, "Flame retardant effect of polyhedral oligomeric silsesquioxane and triglycidyl isocyanurate on glass fibre-reinforced epoxy composites," *Polym. Compos.*, vol. 32, no. 3, 2011.
- [77] C. Gérard, G. Fontaine, and S. Bourbigot, "Synergistic and antagonistic effects in flame retardancy of an intumescent epoxy resin," *Polym. Adv. Technol.*, vol. 22, no. 7, pp. 1085–1090, 2011.
- [78] S. Bourbigot, M. Le Bras, S. Duquesne, and M. Rochery, "Recent Advances for Intumescent Polymers," *Macromol. Mater. Eng.*, vol. 289, no. 6, pp. 499–511, 2004.
- [79] W. Zhang, X. Li, and R. Yang, "Novel flame retardancy effects of DOPO-POSS on epoxy resins," *Polym. Degrad. Stab.*, 2011.
- [80] W. Zhang, X. Li, and R. Yang, "Blowing-out effect in epoxy composites flame retarded by DOPO-POSS and its correlation with amide curing agents," *Polym. Degrad. Stab.*, vol. 97, no. 8, pp. 1314–1324, 2012.
- [81] W. Zhang, X. Li, and R. Yang, "The degradation and charring of flame retarded epoxy resin during the combustion," *J. Appl. Polym. Sci.*, vol. 130, no. 6, pp. 4119–4128, 2013.

- [82] B. Ellis, *Chemistry and Technology of Epoxy resins*. London: Blackie Academic & Professional, 1993, p. 332.
- [83] H. Liu, A. Uhlherr, R. J. Varley, and M. K. Bannister, "Influence of substituents on the kinetics of epoxy/aromatic diamine resin systems," *J. Polym. Sci. Part A Polym. Chem.*, vol. 42, no. 13, pp. 3143–3156, 2004.
- [84] J.-P. Pascault and R. J. J. Williams, "General Concepts about Epoxy Polymers," in *Epoxy Polymers: New Materials and Innovation*, J.-P. Pascault and R. J. J. Williams, Eds. Wiley-VCH Verlag GmbH & Co. KGaA, 2010, pp. 1–12.
- [85] J. Zhao, Y. Fu, and S. Liu, "Polyhedral Oligomeric Silsesquioxane (POSS)-modified Thermoplastic and Thermosetting Nanocomposites: A Review," *Polym. Polym. Compos.*, vol. 16, no. 8, pp. 483–500, 2008.
- [86] H. Liu, S. Zheng, and K. Nie, "Morphology and thermomechanical properties of organic-inorganic hybrid composites involving epoxy resin and an incompletely condensed polyhedral oligomeric silsesquioxane," *Macromolecules*, vol. 38, no. 12, pp. 5088–5097, 2005.
- [87] J. Carroll, A. Waddon, H. Nakade, and V. Rotello, "'Plug and play' polymers. Thermal and X-ray characterizations of noncovalently grafted polyhedral oligomeric silsesquioxane (POSS)-Polystyrene nanocomposites," *Macromolecules*, vol. 36, no. 17, pp. 6289–6291, 2003.
- [88] Y. Ni, S. Zheng, and K. Nie, "Morphology and thermal properties of inorganic-organic hybrids involving epoxy resin and polyhedral oligomeric silsesquioxanes," *Polymer (Guildf.)*, vol. 45, no. 16, pp. 5557–5568, 2004.
- [89] Z. Wang, W. Liu, C. Hu, and S. Ma, "Study on the Modification of Epoxy Resin by a Phosphorus- and Silica-Containing Hybrid," 2011.
- [90] L. Song, Q. He, Y. Hu, H. Chen, and L. Liu, "Study on thermal degradation and combustion behaviors of PC/POSS hybrids," *Polym. Degrad. Stab.*, vol. 93, no. 3, pp. 627–639, 2008.
- [91] L. Matejka, A. Strachota, J. Plestil, P. Whelan, M. Steinhart, and M. Slouf, "Epoxy Networks Reinforced with Polyhedral Oligomeric Silsesquioxanes. Structure and Morphology," *Macromolecules*, vol. 37, no. 25, pp. 9449–9456, 2004.
- [92] R. J. J. Williams, B. A. Rozenberg, J. Pascault, and I. National, "Reaction-Induced Phase Separation in Modified Thermosetting Polymers," in *Polymer analysis Polymer Physics*, Springer Berlin Heidelberg, 1997, pp. 95–156.
- [93] I. A. Zucchi, J. Galante, R. J. J. Williams, E. Franchini, J. Galy, and J.-F. Gérard, "Monofunctional Epoxy-POSS Dispersed in Epoxy - Amine Networks: Effect of a Prereaction on the Morphology and Crystallinity of POSS Domains," *Macromolecules*, vol. 40, no. 4, pp. 1274–1282, 2007.
- [94] A. Strachota, P. Whelan, J. Kříž, J. Brus, M. Urbanová, M. Šlouf, and L. Matějka, "Formation of nanostructured epoxy networks containing polyhedral oligomeric silsesquioxane (POSS) blocks," *Polymer (Guildf.)*, vol. 48, no. 11, pp. 3041–3058, 2007.

- [95] M. J. Abad, L. Barral, D. P. Fasce, and R. J. J. Williams, "Epoxy Networks Containing Large Mass Fractions of a Monofunctional Polyhedral Oligomeric Silsesquioxane (POSS)," *Macromolecules*, vol. 36, no. 9, pp. 3128–3135, 2003.
- [96] D. Verchere, H. Sautereau, J. P. Pascault, S. M. Moschiar, C. C. Riccardi, and R. J. J. Williams, "Miscibility of epoxy monomers with carboxyl-terminated butadiene acrylonitrile random copolymers," *Polymer (Guildf)*, vol. 30, no. 1, pp. 107–115, 1989.
- [97] D. Verchere, H. Sautereau, J.-P. Pascault, C. C. Riccardi, S. M. Moschiar, and R. J. J. Williams, "Buildup of epoxycycloaliphatic amine networks. Kinetics, vitrification and gelation," *Macromolecules*, vol. 23, no. 3, pp. 725–731, 1990.
- [98] J. Flory, "Molecular Size Distribution in Three Dimensional Polymers. I. Gelation," *J. Am. Chem. Soc.*, vol. 63, no. 11, pp. 3083–3090, 1941.
- [99] J. P. Pascault and R. J. J. Williams, "Glass transition temperature versus conversion relationships for thermosetting polymers," *J. Polym. Sci. Part B Polym. Phys.*, vol. 28, no. 1, pp. 85–95, 1990.
- [100] J. Livage and C. Sanchez, "Sol-gel chemistry," *J. Non. Cryst. Solids*, vol. 145, pp. 11–19, 1992.
- [101] S.-T. Lin and S. K. Huang, "Study of Curing Kinetics of Siloxane-Modified DCEBA Epoxy Resins," *J. Appl. Polym. Sci.*, vol. 62, no. 10, pp. 1641–1649, 1996.
- [102] S. Sobhani, "Effect of molecular weight and content of PDMS on morphology and properties of silicone-modified epoxy resin," *J. Appl. Polym. Sci.*, vol. 123, no. 1, pp. 162–178, 2012.
- [103] A. K. Manna, D. K. Tripathy, and D. G. Peiffer, "Bonding Between Precipitated Silica and Epoxidized Natural Rubber in the Presence of Silane Coupling Agent," *J. Appl. Polym. Sci.*, vol. 74, no. 2, pp. 389–398, 1998.
- [104] K. Sengloyluan, K. Sahakaro, W. K. Dierkes, and J. W. M. Noordermeer, "Silica-reinforced tire tread compounds compatibilized by using epoxidized natural rubber," *Eur. Polym. J.*, vol. 51, pp. 69–79, 2014.
- [105] S. Murai, S. Fujieda, and S. Hayase, "A novel latent initiator for cationic polymerizations of epoxides: Composite catalysts containing aluminum complexes phase-separated in epoxides," *J. Appl. Polym. Sci.*, vol. 83, no. 5, pp. 1046–1053, 2002.
- [106] S. Hayase, T. Ito, S. Suzuki, and M. Wada, "Polymerization of Cyclohexene Oxide with Al(acac)<sub>3</sub>-silanol catalyst," *J. Polym. Sci. - Polym. Chem. Ed.*, vol. 19, no. 9, pp. 2185–2194, 1981.
- [107] S. Hayase, S. Suzuki, M. Wada, Y. Inoue, and H. Mitui, "Polymerization of Epoxide with Aluminium Complex-Silanol catalyst. VII. Thermal and Electrical Properties of Epoxy Resin Cured with the New Catalyst," *J. Appl. Polym. Sci.*, vol. 29, no. 1, pp. 269–278, 1984.

- [108] S. Hayase, T. Ito, S. Suzuki, and M. Wada, "Polymerization of Cyclohexene Oxide with Aluminium Complex-Silanol catalysts. III. Dependence of Catalytic Activity on Bulkiness of Silanol and Its Intramolecular Hydrogen Bond.pdf," *J. Polym. Sci. - Polym. Chem. Ed.*, vol. 19, no. 11, pp. 2977–2985, 1981.
- [109] S. Hayase, Y. Onishi, K. Yoshikiyo, and S. Suzuki, "Polymerization of Cyclohexene Oxide with Aluminium Complex-Silanol Catalysts. III. Dependence on Aluminium Chelate Structure," *J. Polym. - Polym. Chem. Ed.*, vol. 20, no. 11, pp. 3155–3165, 1982.
- [110] S. Hayase, Y. Onishi, S. Suzuki, and M. Wada, "Polymerization of Cyclohexene Oxide with Aluminium Complex/Silanol Catalyst. VI. Oligomer and Polymer Effect," *J. Polym. - Polym. Chem. Ed.*, vol. 21, no. 2, pp. 467–477, 1983.
- [111] M. Pramanik, S. K. Mendon, and J. W. Rawlins, "Determination of epoxy equivalent weight of glycidyl ether based epoxides via near infrared spectroscopy," *Polym. Test.*, vol. 31, no. 5, pp. 716–721, 2012.
- [112] E. Girard-Reydet, C. C. Riccardi, H. Sautereau, and J.-P. Pascault, "Epoxy-Aromatic Diamine Kinetics. Part 1. Modeling and Influence of the Diamine Structure," *Macromolecules*, vol. 28, no. 23, pp. 7599–7607, 1995.
- [113] M. Hussain, R. Varley, Z. Mathys, Y. B. Cheng, and G. P. Simon, "Effect of organo-phosphorus and nano-clay materials on the thermal and fire performance of epoxy resins," *J. Appl. Polym. Sci.*, vol. 91, no. 2, pp. 1233–1253, 2004.
- [114] W. Liu, R. J. Varley, and G. P. Simon, "Phosphorus-containing diamine for flame retardancy of high functionality epoxy resins. Part II. The thermal and mechanical properties of mixed amine systems," *Polymer (Guildf.)*, vol. 47, no. 6, pp. 2091–2098, 2006.
- [115] O. Becker, R. J. Varley, and G. P. Simon, "Thermal stability and water uptake of high performance epoxy layered silicate nanocomposites," *Eur. Polym. J.*, vol. 40, no. 1, pp. 187–195, 2004.
- [116] A. Fina, D. Tabuani, F. Carniato, A. Frache, E. Boccaleri, and G. Camino, "Polyhedral oligomeric silsesquioxanes (POSS) thermal degradation," *Thermochim. Acta*, vol. 440, no. 1, pp. 36–42, 2006.
- [117] A. Fina, H. C. L. Abbenhuis, D. Tabuani, and G. Camino, "Metal functionalized POSS as fire retardants in polypropylene," *Polym. Degrad. Stab.*, vol. 91, no. 10, pp. 2275–2281, 2006.
- [118] S. Bourbigot, T. Turf, S. Bellayer, and S. Duquesne, "Polyhedral oligomeric silsesquioxane as flame retardant for thermoplastic polyurethane," *Polym. Degrad. Stab.*, vol. 94, no. 8, pp. 1230–1237, 2009.
- [119] M. Ijaz, M. Robinson, P. N. H. Wright, and A. G. Gibson, "Vacuum Consolidation of Commingled Thermoplastic Matrix Composites," *J. Compos. Mater.*, vol. 41, no. 2, pp. 243–262, 2007.
- [120] C. B. Bucknall and I. K. Partridge, "Phase separation in crosslinked resins containing polymeric modifiers," *Polym. Eng. Sci.*, vol. 26, no. 1, pp. 54–62, 1986.

- [121] C. Bucknall and A. Gilbert, "Toughening tetrafunctional epoxy resins using polyetherimide," *Polymer (Guildf)*, vol. 30, no. 2, pp. 213–217, 1989.
- [122] J. Cho, J. Hwang, K. Cho, J. An, and C. Park, "Effects of morphology on toughening of tetrafunctional epoxy resins with poly (ether imide)," *Polymer (Guildf)*, vol. 34, no. 23, pp. 4832–4836, 1993.
- [123] D. J. Hourston, J. M. Lane, and H. X. Zhang, "Toughening of Epoxy Resins with Thermoplastics: 3. An Investigation into the Effects of Composition on the Properties of Epoxy Resin Blends," *Polym. Int.*, vol. 42, no. 4, pp. 349–355, 1997.
- [124] J. Jang and S. Shin, "Toughness improvement of tetrafunctional epoxy resin by using hydrolysed poly (ether imide)," vol. 36, no. 6, pp. 1199–1207, 1995.
- [125] J. M. Lane and P. Centre, "The toughening of epoxy resins with thermoplastics: 1. Trifunctional epoxy resin-polyetherimide blends," vol. 33, no. 7, pp. 1–5, 1992.
- [126] D. J.-P. Turmel and I. K. Partridge, "Heterogeneous phase separation around fibres in epoxy/PEI blends and its effect on composite delamination resistance," *Compos. Sci. Technol.*, vol. 57, no. 8, pp. 1001–1007, 1997.
- [127] D. W. Y. Wong, L. Lin, P. T. McGrail, T. Peijs, and P. J. Hogg, "Improved fracture toughness of carbon fibre/epoxy composite laminates using dissolvable thermoplastic fibres," *Compos. Part A Appl. Sci. Manuf.*, vol. 41, no. 6, pp. 759–767, 2010.
- [128] K. Jang, W. Cho, and C. Ha, "Influence of processing method on the fracture toughness of thermoplastic-modified, carbon-fiber-reinforced epoxy composites," *Compos. Sci. Technol.*, vol. 59, no. 7, pp. 995–1001, 1999.
- [129] C. B. Bucknall and I. K. Partridge, "Effects of morphology in the epoxy/PES matrix on the fatigue behaviour of uniaxial CFRP," *Composites*, vol. 15, no. 2, pp. 129–133, 1984.
- [130] M. Naffakh, M. Dumon, and J. Gerard, "Study of a reactive epoxy–amine resin enabling in situ dissolution of thermoplastic films during resin transfer moulding for toughening composites," *Compos. Sci. Technol.*, vol. 66, no. 10, pp. 1376–1384, 2006.
- [131] B. K. Kandola, B. Biswas, D. Price, and a. R. Horrocks, "Studies on the effect of different levels of toughener and flame retardants on thermal stability of epoxy resin," *Polym. Degrad. Stab.*, vol. 95, no. 2, pp. 144–152, 2010.
- [132] H. Chen, R. Lv, P. Liu, H. Wang, Z. Huang, T. Huang, and T. Li, "An investigation of cure and thermal stability of poly(amide-amidic acid) modified tetraglycidyl 4,4'-diaminodiphenylmethane/4,4'-diaminodiphenylsulfone," *J. Appl. Polym. Sci.*, vol. 128, no. 3, pp. 1592–1600, 2013.
- [133] U. Braun, U. Knoll, B. Schartel, T. Hoffmann, D. Pospiech, J. Artner, M. Ciesielski, M. Döring, R. Perez-Graterol, J. K. W. Sandler, and V. Altstädt, "Novel Phosphorus-Containing Poly(ether sulfone)s and Their Blends with an Epoxy Resin: Thermal Decomposition and Fire Retardancy," *Macromol. Chem. Phys.*, vol. 207, no. 16, pp. 1501–1514, 2006.

- 
- [134] R. M. Perez, J. K. W. Sandler, V. Altstädt, T. Hoffmann, D. Pospiech, M. Ciesielski, M. Döring, U. Braun, A. I. Balabanovich, and B. Schartel, "Novel phosphorus-modified polysulfone as a combined flame retardant and toughness modifier for epoxy resins," *Polymer (Guildf)*., vol. 48, no. 3, pp. 778–790, 2007.
- [135] Y. F. Yu, J. Cui, W. J. Chen, and S. J. Li, "Studies on the Phase Separation of Polyetherimide Modified Tetrafunctional Epoxy Resin. II. Effects of the Molecular Weight," *J. Macromol. Sci. Part A*, vol. 35, no. 1, pp. 121–135, 1998.
- [136] C. Su and E. Woo, "Cure kinetics and morphology of amine-cured tetraglycidyl-4, 4'-diaminodiphenylmethane epoxy blends with poly (ether imide)," *Polymer (Guildf)*., vol. 36, no. 15, pp. 2883–2894, 1995.
- [137] B. Lestriez, J. Chapel, and J. Gérard, "Gradient interphase between reactive epoxy and glassy thermoplastic from dissolution process, reaction kinetics, and phase separation thermodynamics," *Macromolecules*, vol. 34, no. 5, pp. 1204–1213, 2001.
- [138] J. Galy, A. Sabra, and J. Pascault, "Characterisation of Epoxy Thermosetting Systems by Differential Scanning Calorimetry," *Polym. Eng. Sci.*, vol. 26, no. 21, pp. 1514–1523, 1986.
- [139] H. Liu, A. Uhlherr, and M. K. Bannister, "Quantitative structure–property relationships for composites: prediction of glass transition temperatures for epoxy resins," *Polymer (Guildf)*., vol. 45, no. 6, pp. 2051–2060, 2004.
- [140] S. Levchik, G. Camino, and M. Luda, "Mechanistic study of thermal behaviour and combustion performance of epoxy resins . II . TGDDM / DDS system," *Polym. Degrad. Stab.*, vol. 48, no. 3, pp. 359–370, 1995.
- [141] E. Girard-Reydet, J. Pascault, and H. Brown, "Splat: A nonequilibrium morphology on the way to a microemulsion," *Macromolecules*, vol. 34, no. 15, pp. 5349–5353, 2001.
- [142] H. Winter and F. Chambon, "Analysis of linear viscoelasticity of a crosslinking polymer at the gel point," *J. Rheol.*, vol. 30, no. 2, pp. 367–382, 1986.





## FOLIO ADMINISTRATIF

### THESE SOUTENUE DEVANT L'INSTITUT NATIONAL DES SCIENCES APPLIQUEES DE LYON

NOM : Laik	DATE de SOUTENANCE : 12 décembre 2014	
Prénoms : Suzanne		
NATURE : Doctorat	Numéro d'ordre : 2014ISAL0126	
Ecole doctorale : Matériaux de Lyon		
Spécialité : Matériaux Polymères et Composites		
TITRE : Etude des Silsesquioxanes Oligomériques Polyédriques (POSS) pour l'Amélioration de la Tenue au Feu de Systèmes Polymères Hybrides à base d'Epoxy		
RESUME :		
<p>Les matériaux composites à matrice polymère thermodurcissable interviennent dans de nombreux domaines d'application, parmi lesquels le secteur des transports. Ils présentent toutefois une faible tenue au feu qui limite leur utilisation pour des raisons évidentes de sécurité. De par les restrictions de plus en plus exigeantes de la Commission Européenne (REACH), il existe un réel besoin de se tourner vers des solutions alternatives. Des études récentes ont prouvé l'intérêt des Silsesquioxanes Oligomériques Polyédriques (POSS) comme agents ignifuges, et particulièrement les POSS portant des ligands phényl. L'objectif de ce travail a été d'étudier comment la tenue au feu de réseaux hybrides époxy-amine pouvait être améliorée par l'ajout de POSS dans ces matériaux. En faisant varier la nature des comonomères époxydes et amines, ainsi que la structure des POSS sélectionnés, des éléments de réponse ont pu être apportés à la question : existe-t-il une relation structure-propriété en ce qui concerne le comportement au feu des réseaux époxydes ? Des POSS fonctionnels et inertes ont été choisis pour cette étude, et une attention particulière a été portée sur le trisilanolphényl POSS (POSSOH), pour lequel différents procédés de dispersion ont été mis en œuvre.</p>		
ABSTRACT :		
<p>Thermoset polymer composite materials are used in a number of application domains, amongst which the transports sector, but they suffer from poor fire resistance which limits their use for obvious safety and security issues. With the increasingly demanding restrictions from the European Commission, there is a real need to seek for alternative solutions. Recent studies have found the Polyhedral Oligomeric Silsesquioxane (POSS) compounds interesting as fire retardant agents, particularly the POSS bearing phenyl ligands. The present work aimed at investigating how the fire retardancy of hybrid epoxy networks can be improved by incorporating Polyhedral Oligomeric Silsesquioxanes (POSS).</p> <p>In this study, the nature of the epoxy-amine comonomers was varied, as well as the POSS structure. An inert POSS and two multifunctional POSS were selected in order to generate various morphologies. The aim was to answer the question: does a structure-property relationship exist as concerns the fire behaviour of epoxy networks? Particular attention was dedicated to systems containing the trisilanolphenyl POSS (POSSOH) for which different processes of dispersion were implemented.</p>		
MOTS-CLES : polymères, epoxy, tenue au feu, POSS, cone calorimètre, intumescence, catalyseur polymer, epoxy, fire retardancy, POSS, cone calorimeter, intumescence, catalyst		
Laboratoire (s) de recherche : IMP@INSA		
Directeur de thèse: Dr Jocelyne Galy Co-directeur de thèse : Prof. Jean-François Gérard		
Président de jury : Prof. Giovanni Camino		
Composition du jury :		
<i>Rapportrice</i>	Ivana Partridge	Professeure, Faculty of Engineering, University of Bristol (UK)
<i>Rapportrice</i>	Sophie Duquesne	Professeure, UMET, Université de Lille (France)
<i>Examinateur</i>	Giovanni Camino	Professeur, Politecnico di Torino – Sede di Alessandria (Italy)
<i>Examinatrice</i>	Sophie Cozien-Cazuc	Docteur, Far-UK Ltd, Nottingham (UK)
<i>Directrice de thèse</i>	Jocelyne Galy	Directrice de recherches, IMP UMR CNRS 5223, INSA Lyon (France)
<i>Co-directeur de thèse</i>	Jean-François Gérard	Professeur, IMP UMR CNRS 5223, INSA Lyon (France)